Title

Transition metal complexes with multidentate phosphorous/nitrogen ligands. Synthesis, characterization and reactivity.

Author

Rozenel, Sergio Santiago

Publication Date

2011

Peer reviewed|Thesis/dissertation

Transition metal complexes with multidentate phosphorous/nitrogen ligands. Synthesis, characterization and reactivity.

by

Sergio Santiago Rozenel

A dissertation submitted in partial satisfaction of the

requirements for the degree of

Doctor of Philosophy

in

Chemistry

in the

Graduate Division

of the

University of California, Berkeley

Committee in charge:

Professor John Arnold. Chair
Professor Jeffrey R. Long
Professor Clayton J. Radke

Fall 2011

Abstract

Transition metal complexes with multidentate phosphorous/nitrogen ligands.
Synthesis, characterization and reactivity.

By
Sergio Santiago Rozenel
Doctor in Philosophy in Chemistry
University of California, Berkeley
Professor John Arnold, Chair

Chapter 1: Chromium complexes supported by the multidentate monoanionic ligand $[N_2P_2]$ {$H[N_2P_2]$ = $^tBuN(H)SiMe_2N(CH_2CH_2P^iPr_2)_2$} are presented, and the activity of these complexes towards ethylene oligomerization/polymerization is examined. The complexes $[N_2P_2]CrCl_2$ (**1**) and $[N_2P_2]CrCl$ (**2**) polymerized ethylene after activation with MAO. Derivatives of **1** and **2** were synthesized in order to gain insights about the active species in the ethylene oligomerization/polymerization processes. The alkyl complexes $[N_2P_2]CrMe$ (**3**), $[N_2P_2]CrCH_2SiMe_3$ (**4**) and $[N_2P_2]Cr(Cl)CH_2SiMe_3$ (**5**), the cationic species $\{[N_2P_2]CrCl\}BF_4$ (**7**), $\{[N_2P_2]CrCl\}BPh_4$ (**8**) and $\{[N_2P_2]CrCH_2SiMe_3\}BF_4$ (**9**), and the Cr(II) complex $[N_2P_2]CrOSO_2CF_3$ (**11**) were not active ethylene oligomerization/polymerization catalysts in absence of an activator. Reaction of **1** with two equivalents of MeLi led to reduction to **3**. However, with one equivalent of MeLi the stable mixed alkyl-halide derivative $[N_2P_2]Cr(Cl)Me$ (**6**) was obtained. Reaction of **2** with Red-Al® produced the hydride $([N_2P_2]Cr)_2(\mu\text{-}H)_2$ (**10**), which reacted with CO to produce the Cr(I) complex $[N_2P_2]Cr(CO)_2$ (**12**). Reduction of **2** with KC_8 in the presence of *p*-tolyl azide produced the dimeric cis μ-imido $([N_2P_2]Cr)_2(\mu\text{-}NC_7H_7)_2$ (**13**). A similar reduction in the presence of ethylene resulted in the isolation of the Cr(III) metallacyclohexane compound $[N_2P_2]CrC_4H_8$ (**14**).

Chapter 2: A series of Co, Ni and Cu complexes with the ligand $HN(CH_2CH_2P^iPr_2)_2$ (HPNP) has been isolated and their electrochemical behavior investigated by cyclic voltammetry. The nickel complexes [(HPNP)NiOTf]OTf and $[(HPNP)NiNCCH_3](BF_4)_2$ display reversible reductions, as does the related amide derivative $(NP_2)NiBr$. Related copper(I) and cobalt(II) derivatives were isolated and characterized. Addition of piperidine to $[(HNP_2)NiNCCH_3](BF_4)_2$ led to the formation of the new species $[(HPNP)Ni(N(H)C(CH_3)NC_5H_{10})](BF_4)_2$. Nucleophilic addition of piperidine to acetonitrile to produce $HN{=}C(CH_3)NC_5H_{10}$ was catalyzed by $[(HPNP)NiNCCH_3](BF_4)_2$.

Chapter 3: A series of bimetallic ruthenium complexes $[HPNPRu(N_2)]_2(\mu\text{-}Cl)_2](BF_4)_2$ (**2**), $[(HPNPRu(H_2)Cl)_2(\mu\text{-}Cl)_2](BF_4)_2$ (**3**), $[(HPNPRu)_2(\mu\text{-}H_2NNH_2)(\mu\text{-}Cl)_2](BF_4)_2$ (**4**), $[(HPNPRu)_2(\mu\text{-}Cl)_2(\mu\text{-}HNNPh)](BF_4)_2$ (**5**), $[HPNPRu(NH_3)(\eta^2\text{-}N_2H_4)](BF_4)Cl$ (**6**), $[(HNP_2Ru)_2(\mu\text{-}Cl)_2(\mu^2\text{-}OSO_2CF_3)]OSO_2CF_3$ (**7**), $[HPNPRu]_2(\mu\text{-}Cl)_3]BPh_4$ (**8**) and $[HPNPRu]_2(\mu\text{-}Cl)_3]BF_4$ (**9**) were isolated and characterized in the course of reactions aimed at studying the reduction of N_2 and hydrazine. Complex **4** produces ammonia catalytically from hydrazine, and complex **2** generates ammonia upon reaction with $Cp_2Co/HLuBF_4$. DFT

calculations support the idea that the diazene complex formed is more stable than the expected Chatt-type intermediate.

Chapter 4: The reduction chemistry of cobalt complexes with the PNP ligand was explored. Reaction of (HPNP)$CoCl_2$ (**1**) with *n*-BuLi generated the deprotonated Co(II) product (PNP)CoCl (**2**), and the Co(I) reduced species (HPNP)CoCl (**3**). The reaction of complex **2** with KC_8 was investigated, where it was found that the products obtained depended upon the inert gas used to carry out the reaction: (PNP)CoN_2 (**4**) under N_2, bimetallic complex $[(PNP)Co]_2$ (**5**) under Ar, and (HPNP)$Co(H)_3$ (**8**) under H_2. Complex **5** reacted with H_2 to generate the bimetallic complex $[(PNP)CoH]_2$ (**6**). With H_2, H_3SiPh and $AgBPh_4$ complex **3** generated the species (HPNP)$CoCl(H)_2$ (**9**), (HPNP)$CoCl(H)SiH_2Ph$ (**10**) and $[(HPNP)CoCl]BPh_4$ (**11**) respectively. DFT calculations were performed to gain insights about the transformations observed.

Transition metal complexes with multidentate phosphorous/nitrogen ligands.
Synthesis, characterization and reactivity.

Table of Contents

Acknowledgements

First and foremost I have to thank John for opportunity to work in his group, for teaching me how to think about chemistry, and for his support during the Ph.D. As a freshly unpacked Mexican barely speaking English (I like to think I have improved), and trying to understand what was going on around me, finding the Arnold group was the best thing that could have happened to me at Berkeley. The chemistry presented in this thesis would not be possible without his constant advice and insights. I also have to acknowledge his approach to chemistry that allowed me to take research paths not directly related to the group goals.

I cannot finish this stage of my life without thanking Hugo Torrens, my undergraduate adviser and the person who developed in me my love for inorganic chemistry. It has been almost ten years since I start working with him and I will be grateful for his support and friendship all my life.

Of the plethora of people that helped me during this period as a Graduate student, I have to especially thank Antonio DiPasquale, Fred Hollander, and Chris Canlas. Their help and infinite patience in X ray crystallography and NMR, make this work possible.

The Arnold group would not have been such a good place without the people working there, former and current members. I am especially thankful with Pete La Pierre and Wayne Chomitz. Having conversations with Pete always pushed my understanding of chemistry and my own project, making me a better chemist. I wish you the best of luck pursuing your research goals and I am confident that I will hear from the great chemistry you will develop. Wayne thought me how to work in the lab, with a patience that deserves special recognition. I also have to thank Dan and Ashleigh, Heather and Thomas, for making the lab a lot more enjoyable place (except for the music). Being part of the Long Johns has been one of the most fun things that have happened to me at Berkeley.

I have to thank my family, my father, my mother and my sister, for their love and support and for being the most influential people during my entire life. For teaching me the love for studying and for being the example to follow.

Finally, I want to thank the most fantastic person in this world, the love of my life, my wife Tania. This Ph.D. is as much as mine as it is hers. Without you I could not have complete this goal, not only because I probably would have died of starvation, but because having you by my side is the best thing that has ever happened to me. No success in live is worthy if you do not have someone to share it with, and I am happy to say that I have you. I love you and I wish I would be better with words to express all you mean to me.

Curriculum Vitae

Sergio Santiago Rozenel

Education

Ph.D. Inorganic Chemistry Department of Chemistry, **University of California, Berkeley.**
B. S., Chemistry, Facultad de Química, **Universidad Nacional Autónoma de México (UNAM).**

Research and work experience

Reactivity and mechanistic studies of chromium catalysts for ethylene trimerization/polymerization. ***Arnold Group. UC Berkeley***. *2006 - 2009*
Coordination chemistry and activation of small molecules with reduced metal centers. ***Arnold Group. UC Berkeley***. *2008 – present.*

Synthesis and characterization of transition metal complexes for electrocatalytical oxidation of hydrogenated organic substrates. ***Arnold Group, UC Berkeley and Kerr Group, LBNL.*** *2009 – 2011.*

Analyst. Quality Control and Products Development Department. ***BONAPLAST SA de CV***. Los Reyes La Paz, Estado de México. 2005.

Synthesis of platinum complexes with thiofluorated ligands for C – F bond activation. ***Torrens Group, UNAM.*** *2003 – 2004.*

Synthesis of thiofluorated polymers for precious metals coordination. ***Torrens Group, UNAM.*** *2002 – 2003.*

Mechanism studies of calcium ionic channels in cell membranes. ***Cereijido Group, CINVESTAV***. *2001.*

Distinctions

2008-2009 Outstanding Graduate Student Instructor Award. UC Berkeley.
Thesis and professional exam for *B.S. in Chemistry*, with Honors, UNAM.
Second best GPA in the Chemistry major, Class 1999, UNAM.
One of the three best GPA´s in the Chemistry major during 2001, UNAM.
One of the three best GPA´s in the Chemistry career during 1999, UNAM.

Publications

Rozenel, Sergio S.; Kerr, J. B.; Arnold, J. "Metal complexes of Co, Ni and Cu with the pincer ligand $HN(CH_2CH_2P^iPr_2)_2$: preparation, characterization and electrochemistry". *Dalton Trans*. **2011**. 10397.

Rozenel, Sergio S.; Chomitz, Wayne A.; Arnold, J. "Chromium Complexes Supported by the Multidentate Monoanionic N_2P_2 Ligand: Reduction Chemistry and Reactivity with Ethylene". *Organometallics*. **2009**. *28*. 6243 – 6253.

Kazhdan, Daniel.; Hu, Yung-Jin.; Kokay, Akos.; Levi, Zerubba.; Rozenel, Sergio S.; (2,2-Bipyridyl)bis(η^5-pentamethylcyclopentadienyl) strontium(II). *Acta Cryst.* **2008**. E64. m1134.

Thesis: Platinum complexes with thiofluorated ligands (Carbon-Fluorine bond activation). UNAM. **2004**.

Seminars

"Chromium complexes supported by the multidentate monoanionic ligand N_2P_2: Reduction chemistry and reactivity with ethylene". Presented at the 239th ACS National Meeting, San Francisco, CA, March, 2010.

Chapter 1:

Chromium Complexes Supported by the Multidentate Monoanionic N_2P_2 Ligand: Reduction Chemistry and Reactivity with Ethylene

Introduction

Chromium catalysts are widely used industrially for the polymerization of ethylene: Phillips-type catalysts (Cr/SiO_2) are responsible for the production of one third of the polyethylene sold worldwide.[1] In comparison to Ziegler-Natta catalysts, chromium catalysts have the advantage of producing a wide variety of polyethylenes and can be used without an activator.[2] Though Phillips-type catalysts have been known for more than 50 years, the active species, as well as the mechanism of the transformation, remain topics of interest. [1-5]

The selective oligomerization of ethylene to 1-hexene and 1-octene is of special interest due to the use of these co-monomers in the production of LLDPE.[3-12] Chromium is the most commonly used metal for this transformation due to its high activity and selectivity,[13] although other metals have also been used.[14-16]

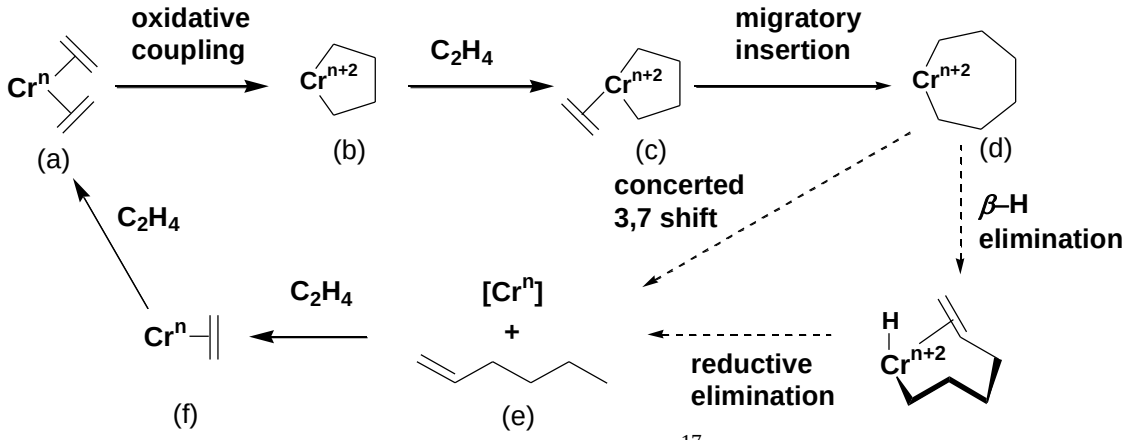

Scheme 1. Proposed ethylene trimerization mechanism.[17]

The currently accepted mechanism for ethylene trimerization involves a metallacycle intermediate (Scheme 1),[4, 17, 18] which is formed following the oxidative coupling of two ethylene molecules.[17-20] Ethylene tetramerization is also thought to go through a metallacyclic intermediate where the steric effects of the ligand favor the expansion of the seven-membered metallacycle ring to form a nine-membered metallacycle intermediate.[21, 22]

The oxidation state of the chromium species participating in olefin oligomerization remains ambiguous.[23] Although the majority of reports attribute the catalytic activity to the Cr(I)/Cr(III) couple, Gambarotta and co-workers have proposed that Cr(III) is reduced by the alkyl aluminum activator to Cr(II) in the early stages of the catalytic cycle and oxidative coupling of two ethylene molecules produces a Cr(IV) metallacycle.[5] McGuinness and co-workers, studying Cr(II) and Cr(III) species supported by the ligands $Ph_2PCH_2CH_2NHCH_2CH_2PPh_2$ and $^tBuSCH_2CH_2NHCH_2CH_2S^tBu$, favor a mechanism consistent with the cationic Cr(II)/Cr(IV) couple over the neutral Cr(I)/Cr(III) couple, given that MAO is normally thought to form cationic metal centers. [23]

In the course of expanding the scope of $[N_2P_2]$ coordination chemistry,[24-30] it was found that the ligand supported both $[N_2P_2]$Cr(II) and $[N_2P_2]$Cr(III) derivatives. Facile access to both oxidation states allowed us to investigate the activity of each towards ethylene oligomerization/polymerization and to compare the influence of the oxidation state of the metal center on reactivity.

Results and Discussion

In an earlier paper, we reported the synthesis of the Cr(III) starting material $[N_2P_2]CrCl_2$ (**1**); [27] the corresponding Cr(II) analogue was prepared by reaction of $Li[N_2P_2]$ and $CrCl_2(THF)$, from which $[N_2P_2]CrCl$ (**2**) was isolated as light blue needle-like crystals in 58% yield (Scheme 2).

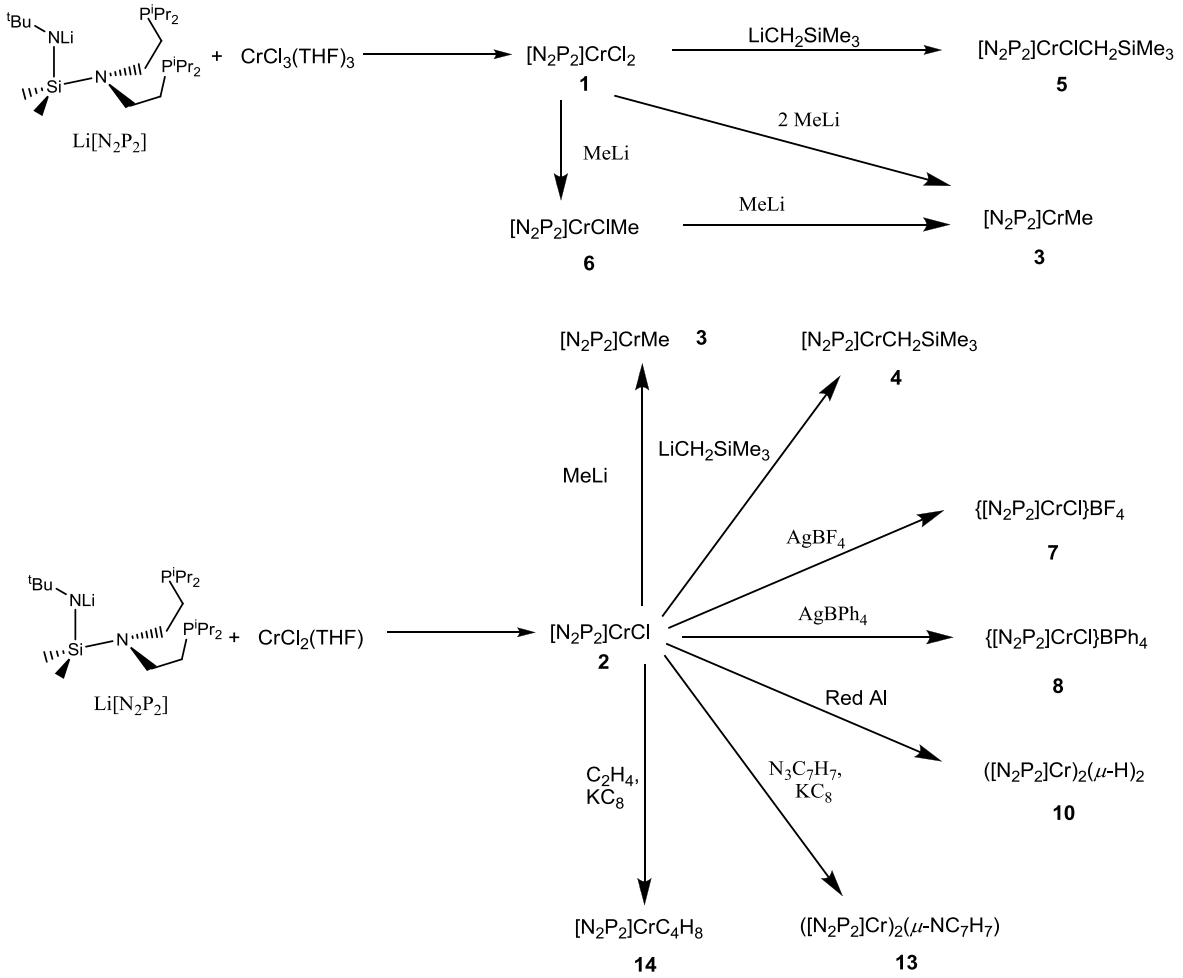

Scheme 2. Reactions performed with $[N_2P_2]Cr$ complexes.

Recrystallization of **2** from toluene gave crystals suitable for an X-ray diffraction study. Selected bond distances and angles are shown in Table 2, and an ORTEP diagram is provided in Figure 1.

Complex **2** displays a distorted trigonal bipyramidal geometry in the solid-state with the $[N_2P_2]$ ligand bound κ^4-N_2P_2 to the metal. Little distortion along the axial direction (Cl1-Cr1-N2 179.41(8)°) is observed, though the equatorial positions are distorted from the expected value of 120° (P1-Cr1-P2 105.09(5)°, P1-Cr1-N1 120.34(13)° and P2-Cr1-N1 125.61(14)°), likely due to steric constraints. The Cr1-Cl1 (2.3459(15) Å), Cr1-N1 (2.044(3) Å) and Cr1-N2 (2.191(3) Å) bond distances are close to those found in the related complexes $\{[(Ph_2P)_2NMe]_2Cr(\mu\text{-}Cl)AlMe_3\}^+$ (Cr-Cl 2.3682(19) Å, 2.3199(13) Å),[13] $[(Ph_2PCH_2CH_2)_2NH]CrCl_2$ (Cr-N 2.168(4) Å),[10] and $[N(SiMe_2CH_2PPh_2)_2]CrMe$ (Cr-N

2.117(3) Å).[10] The Cr1-P1 distances in **2** (2.5902(17) Å and 2.5253(17) Å) correspond well with the distances found in the chromium di(isopropyl)phosphine compound (dippe)Cr(CH_2CMe_3)$_2$ (2.556(2) Å).[31] The solution magnetic susceptibility (μ_{eff}) for complex **2** was found to be 4.7 μ_B, consistent with four unpaired electrons.

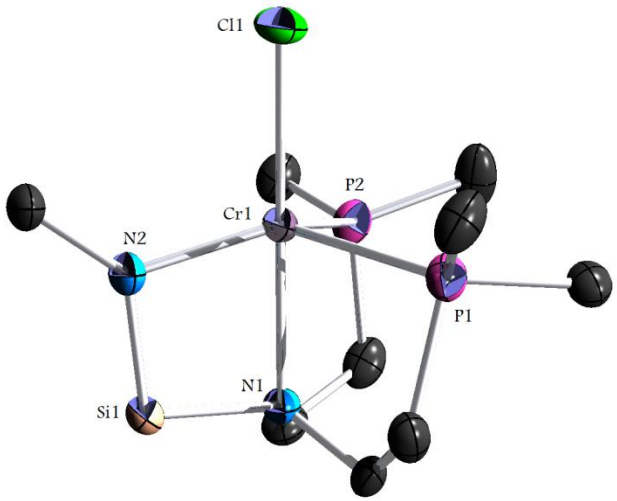

Figure 1: Thermal ellipsoid (50%) plot of **2**. Hydrogen atoms, methyl and iso-propyl groups have been omitted for clarity.

Table 2: Selected bond distances and angles for Cr(II) complexes **2**, **3** and **4**.

	2 [a]	**3** [b]	**4** [b]
Cr1 – X	2.3459(15) Å	2.127(3) Å	2.122(3) Å
Cr1 - P1	2.5902(17) Å	2.5530(10) Å	2.4614(8) Å
Cr1 - P2	2.5253(17) Å	2.5337(9) Å	-
Cr1 – N1	2.191(3) Å	2.259(2) Å	2.224(2) Å
Cr1 – N2	2.044(3) Å	2.069(2) Å	2.001(2) Å
X – Cr – P1	98.36(6)°	97.75(9)°	98.70(8)°
X – Cr – P2	96.09(5)°	98.19(9)°	-
X – Cr – N1	179.41(8)°	178.80(11)°	164.68(10)°
X – Cr – N2	104.58(8)°	106.00(10)°	109.74(11)°
P1 – Cr – P2	105.09(5)°	105.79(3)°	-
P1 – Cr – N2	120.34(13)°	119.15(7)°	145.01(7)°
P1 – Cr – N1	81.19(11)°	81.06(6)°	81.58(6)°
P2 – Cr – N2	125.61(14)°	124.31(7)°	-
P2 – Cr – N1	83.66(10)°	82.22(6)°	-
N1 – Cr – N2	76.00(10)°	74.61(8)°	76.26(9)°

[a] X = Cl, [b] X = C.

The reaction of **2** with MeLi in THF at -78 °C resulted in a color change of blue to brown. Warming of the reaction mixture to room temperature, followed by evaporation of the solvent under vacuum, extraction with hexane, and cooling at -40 °C, resulted in the isolation

of $[N_2P_2]CrMe$ (**3**) as a purple solid in 38% yield. Recrystallization from hexane at -40 °C afforded crystals suitable for a X-ray diffraction study. Selected bond distances and angles are shown in Table 2, and an ORTEP diagram is provided in Figure 2. The solid-state structures of **2** and **3** are similar with the replacement of a methyl group for a chloride. The Cr1-C1 bond distance (2.127(3) Å in **3**) is close to that found in $(dippe)Cr(CH_2CMe_3)_2$ (2.149(8) Å) and in $(dippe)Cr(CH_2SiMe_3)_2$ (2.128(4) Å).[31] The solution magnetic susceptibility (μ_{eff}) for complex **3** was found to be 4.5 μ_B, lower than the theoretical value (4.89 μ_B) but consistent with the presence of four unpaired electrons as in the case of **2**.

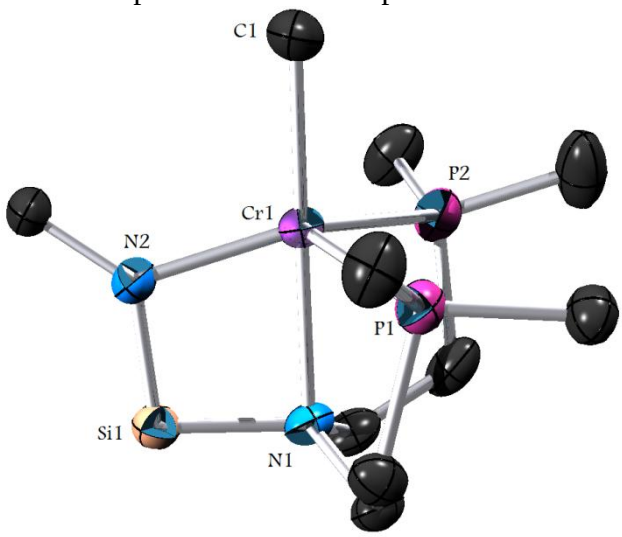

Figure 2: Thermal ellipsoid (50%) plot of **3**. Hydrogen atoms, methyl and iso-propyl groups have been omitted for clarity.

Addition of $LiCH_2SiMe_3$ to a solution of **2** in toluene at room temperature resulted in a color change of the solution from blue to purple. Following evaporation of the solvent under vacuum, extraction with hexane, and cooling at -40 °C, $[N_2P_2]CrCH_2SiMe_3$ (**4**) was isolated as a purple solid in 53% yield. An X-ray diffraction study was undertaken (an ORTEP diagram is provided in Figure 3), and selected bond distances and angles are shown in Table 2. The chromium atom lies in a highly distorted tetrahedral geometry (C1-Cr1-N1 164.68(10)°, C1-Cr1-N2 109.74(11)° and C1-Cr1-P1 98.70(8)°) with the ligand bound κ^3-N_2P to the metal. The Cr1-N1, Cr1-N2 and Cr1-P1 bond distances of 2.224(2) Å, 2.001(2) Å and 2.4614(8) Å, respectively, show a constriction in comparison with **3**. The Cr1-C1 distances in both complexes, however, are equivalent within error (2.127(3) Å for **3** and 2.122(3) Å for **4**), suggesting the change in coordination mode is likely due to steric rather than electronic effects. The μ_{eff} of complex **4** is 4.4 μ_B, consistent with the presence of four unpaired electrons.

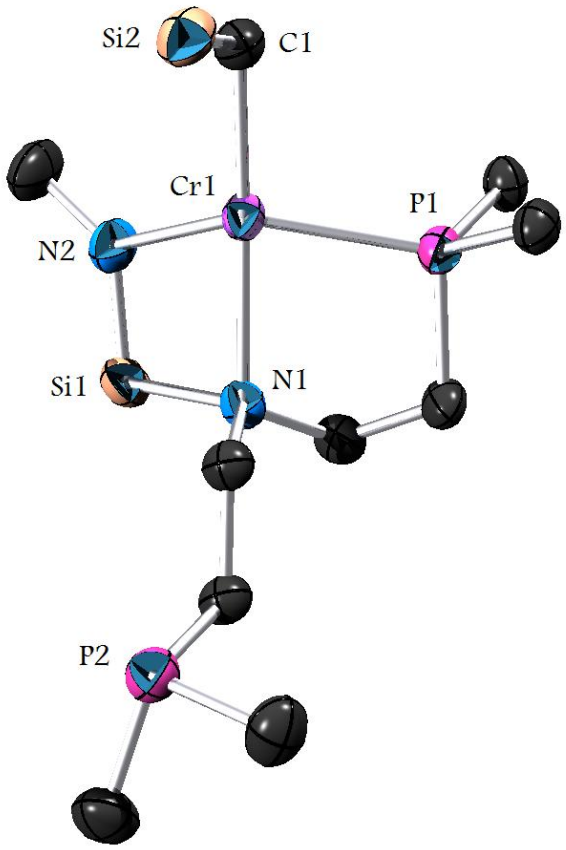

Figure 3: Thermal ellipsoid (50%) plot of **4**. Hydrogen atoms, methyl and iso-propyl groups have been omitted for clarity.

The metathesis reaction of **1** with one equivalent of $LiCH_2SiMe_3$ in toluene at room temperature gave a dark blue solution, which yielded $[N_2P_2]CrClCH_2SiMe_3$ (**5**) as a purple solid in 57% yield after work-up and crystallization from hexane. An ORTEP diagram of **5** is shown in Figure 4 with selected bond distances and angles provided in Table 3. Complex **5** crystallizes with one molecule of diethyl ether for every two molecules of **5** in the unit cell. It displays a trigonal bipyramidal geometry in the solid-state with the $[N_2P_2]$ ligand bound κ^3-N_2P to the metal center. The Cr1-C1 (2.066(6) Å), Cr1-Cl1 (2.3157(17) Å), Cr1-N1 (2.202(4) Å), Cr1-N2 (1.939(4) Å) and Cr1-P1 (2.5176(19) Å) metal-ligand bond distances are consistent with distances found in the related Cr(III) complexes $[(Ph_2PCH_2SiMe_2)_2N]CrClCH_2SiMe_3$ (Cr-C 2.110(6) Å, Cr-Cl 2.315(2) Å, Cr-N_{amide} 2.022(4) Å, Cr-P 2.525(2) Å and 2.442(2) Å);[32] $[\eta^3$-$(^iPrNCH_2)_3]CrCl(CH_2SiMe_3)_2$ (Cr-C 2.086(5) Å and 2.080(6) Å, Cr-Cl 2.316(1) Å, Cr-N_{amine} 2.292(4) Å, 2.298(4) Å and 2.181(4) Å);[33] and $\{(Me_2PCH_2CH_2)_2N\}_2CrCl$ (Cr-Cl 2.401(1) Å, Cr-N_{amide} 2.017(2) Å and 1.996(2) Å, Cr-P 2.435(1) Å, 2.444(1) Å and 2.429(1) Å).[34] Comparison of the solid-state structure of **5** with **1** showed consistent distances around the metal center. The μ_{eff} for complex **5** was found to be 3.9 μ_B, in accord with three unpaired electrons.

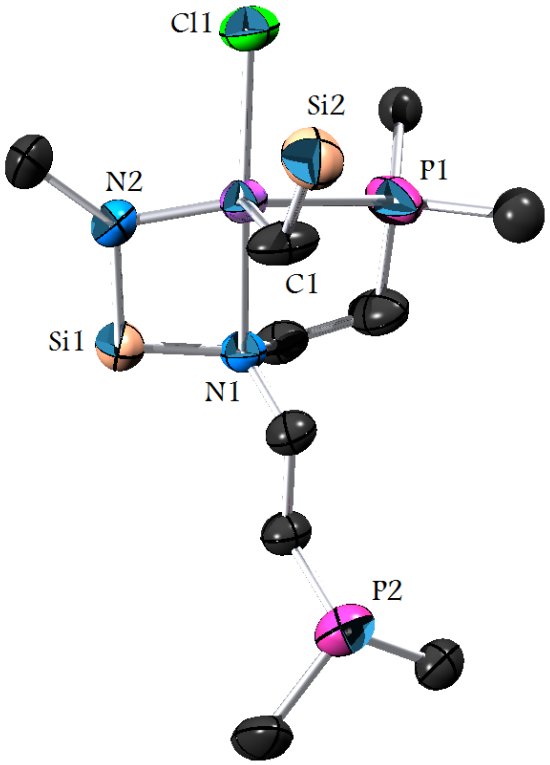

Figure 4: Thermal ellipsoid (50%) plot of **5**. Hydrogen atoms, methyl, iso-propyl groups and diethyl ether have been omitted for clarity.

In an attempt to synthesize a Cr(III) dialkyl derivative, two equivalents of MeLi were added to a solution of **1** in diethyl ether. Upon addition, the reaction mixture changed color from purple to brown. After evaporation of the solvent, extraction with hexane, concentration, and cooling at -40 °C, brown crystals were obtained. Analysis of the crystalline material by mass spectrometry showed signals consistent with complex **3** (m^+/z = 500). The spectrum also showed peaks at 564 and 508 that could not be assigned, but no peak corresponding to $[N_2P_2]CrMe_2$ (m^+ = 515) was observed. The identity of **3** was also confirmed by X-ray crystallography. The reduction of chromium complexes by alkylating reagents during ethylene polymerization/oligomerization has been proposed as a key step in the initiation of chromium catalysts. [5, 6]

The reaction path to **3** likely involved the formation of $[N_2P_2]Cr(Cl)Me$ from the reaction of **1** and MeLi, followed subsequently by reduction by a second equivalent to give the product. To test whether $[N_2P_2]Cr(Cl)Me$ was a viable intermediate, the reaction of **1** and one equivalent of MeLi was undertaken. Following the addition of MeLi to a THF solution of **1**, a deep purple solution was formed which gave purple crystals of $[N_2P_2]Cr(Cl)Me$ (**6**) in 68% yield following crystallization from diethyl ether. The composition of **6** is supported by mass spectrometry (m^+ = 535, m^+- Me = 520) and elemental analysis. Complex **6** is paramagnetic with three unpaired electrons (μ_{eff} = 3.8), and the ^{31}P-NMR spectrum shows one broad resonance peak at 45.65 ppm.

Table 3: Selected bond distances and angles for Cr(III) complexes **5, 9** and **10**.

	5 [a]	**13** [b]	**14** [c]
Cr1 – X	2.3157(17) Å	1.856(3) Å	2.081(4) Å
Cr1 – Y	2.066(6) Å	1.870(3) Å	2.102(4) Å
Cr1 – P1	2.5176(19) Å	-	2.5203(14) Å
Cr1 – N1	2.202(4) Å	2.174(3) Å	2.245(3) Å
Cr1 – N2	1.939(4) Å	1.900(3) Å	1.959(3) Å
Cr1 – Cr2	-	2.6325(8) Å	-
X – Cr1 – P1	90.62(6)°	-	95.64(12)°
X – Cr1 – N1	164.78(12)°	125.35(12)°	176.57(14)°
X – Cr1 – N2	102.07(13)°	126.66(10)°	106.74(15)°
X – Cr1 – Y	99.67(16)°	90.08(11)°	83.83(16)°
P1 – Cr1 – N2	137.99(15)°	-	135.53(10)°
Y – Cr1 – P1	102.75(18)°	-	104.58(19)°
Y – Cr1 – N1	94.45(18)°	115.09(10)°	115.46(15)°
N1 – Cr1 – N2	77.01(16)°	77.96(11)°	76.37(13)°

[a] X = Cl, Y = C; [b] X = N3, Y = N4; [c] X = C1, Y = C2.

Two chromium(III) cationic complexes were obtained by the oxidation of **2** with silver salts. Addition of $AgBF_4$ to **2** in THF produced a green solution and precipitation of silver metal. Filtration of the solution followed by concentration and cooling to -40 ºC gave the cationic complex $\{[N_2P_2]CrCl\}BF_4$ (**7**) as green blocks in 64% yield. Analogous oxidation with $AgBPh_4$ produced $\{[N_2P_2]CrCl\}BPh_4$ (**8**) in 29% yield as dark green, block-like, crystals. The μ_{eff} for these complexes are 3.8 μ_B, and 3.9 μ_B, respectively, confirming an oxidation state change of Cr(II) to Cr(III). Crystals suitable for X-ray diffraction studies were grown from concentrated THF solutions cooled at -40 ºC.

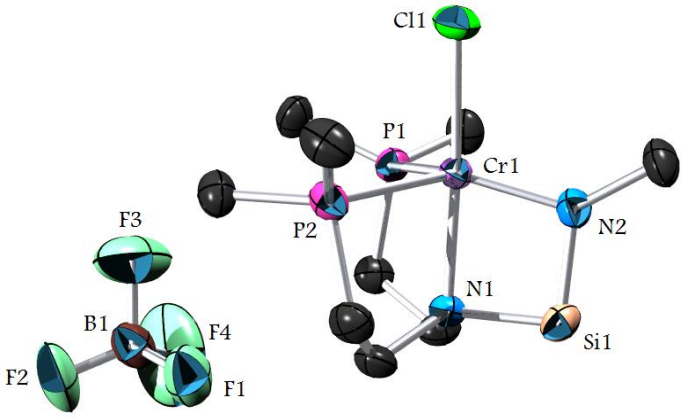

Figure 5: Thermal ellipsoid (50%) plot of **7**. Hydrogen atoms, methyl and iso-propyl groups and THF molecule have been omitted for clarity.

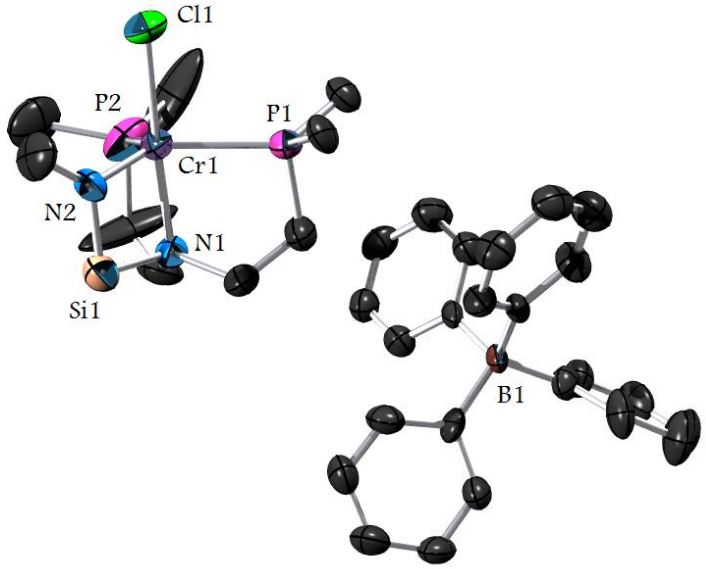

Figure 6: Thermal ellipsoid (50%) plot of **8**. Hydrogen atoms, methyl and iso-propyl groups and THF molecule have been omitted for clarity.

An X-ray diffraction study was performed for **7** and **8** (Figures 5 and 6). Complex **7** exhibits significant disorder around the BF_4 anion. The cationic moiety $\{[N_2P_2]CrCl\}^+$ in **7** showed slightly larger distances around the metal center (Cr1-Cl1 2.2965(14) Å, Cr1-N1 2.150(2) Å, Cr1-N2 1.898(2) Å, Cr1-P1 2.4691(12) Å and Cr1-P2 2.4554(13) Å) than in **8** (Cr1-Cl1 2.272(3) Å, Cr1-N1 2.139(7) Å, Cr1-N2 1.889(7) Å, Cr1-P1 2.465(4) Å and Cr1-P2 2.436(4) Å).

Table 4: Selected bond distances and angles for Cr(III) complexes **7** and **8**.

	7	**8**
Cr1 – Cl1	2.2965(14) Å	2.272(3) Å
Cr1 - P1	2.4691(12) Å	2.465(4) Å
Cr1 - P2	2.4554(13) Å	2.436(4) Å
Cr1 – N1	2.150(3) Å	2.139(7) Å
Cr1 – N2	1.898(2) Å	1.889(7) Å
Cl1 – Cr – P1	95.98(3)°	94.37(12)°
Cl1 – Cr – P2	93.53(9)°	96.10(12)º
Cl1 – Cr – N1	176.36(6)°	177.5(2)°
Cl1 – Cr – N2	104.09(7)°	103.1(3)°
P1 – Cr – P2	104.77(5)°	107.72(11)º
P1 – Cr – N2	123.83(7)°	127.8(2)°
P1 – Cr – N1	83.70(5)°	83.2(2)°
P2 – Cr – N2	123.83(7)°	118.5(2)º
P2 – Cr – N1	83.07(6)°	84.0(3)º
N1 – Cr – N2	78.95(8)°	79.0(3)°

Although the Cr atoms in **7** and **8** are in the same ligand environment as in **2**, a constriction in the distances around the metal center is observed as expected due the higher oxidation state of the chromium atoms in **7** and **8**. The biggest difference is observed in the Cr1-N2 bond distance, approximately 0.15 Å smaller in the Cr(III) species.

The reaction of $AgBF_4$ with **4** in THF at room temperature produced a purple solution and a silver mirror. Evaporation of the solvent, followed by extraction with diethyl ether and crystallization at -40 ºC gave $\{[N_2P_2]CrCH_2SiMe_3\}BF_4$ (**9**) as purple blocks in 60% yield. Single crystals suitable for X-ray crystallography of 9 could not be obtained, but the ^{1}H-NMR and IR spectra, elemental analysis and the magnetic susceptibility (μ_{eff} = 3.7 μ_B, three unpaired electrons) are consistent with the proposed formulation.

Reactions of **2**, **3**, **4**, and **5** were carried out with alkyl aluminum reagents ($AlMe_3$, $AlMe_2Cl$, $AlEt_2Cl$ and MAO). These were generally unproductive, yielding starting materials or intractable mixtures. However, the reaction of **2** with KC_8 in THF at -78 ºC in the presence of $AlMe_3$ (3 eq) produced a dark green solution after warming to room temperature, from which the alkylated Cr(II) species **3** (see above) was obtained in 29% yield.

Chromium-hydride derivatives have been postulated as intermediates formed following β-hydride elimination of the hepta- or nonametallacycle, prior to elimination of 1-hexene or 1-octene (Scheme 1). McGuinness and co-workers suggested that Cr-dihydride species are formed in side-chain reactions during the tetramerization process.[35] In order to explore the stability of these kinds of complexes, we targeted a $[N_2P_2]$Cr-hydride derivative.

The reaction of **2** with 1.1 eq. of Red-Al® (3.5 M in toluene) in THF produced a brown solution. Following extraction with hexane, concentration, and cooling at -40 °C, the product $([N_2P_2]Cr)_2(\mu\text{-}H)_2$ (**10**) was isolated as brown crystals in 84% yield. Crystals suitable for an X-ray diffraction study were obtained by recrystallization of **10** from a concentrated solution of HMDSO at -35 °C. An ORTEP diagram is provided in Figure 7 and selected bond distances and angles are shown in Table 1. Complex **10** crystallizes as a dimer with bridging hydrides and with one $[N_2P_2]$ ligand bound κ^3-N_2P to each metal center. The geometry around each metal atom is distorted square pyramidal with the axial position occupied by the phosphine ligand. The Cr1-N1 and Cr1-N2 distances (2.2158(19) Å and 2.0437(19) Å) are similar with those found in **2**, **3** and **4**, while the Cr1-P1 distance (2.5810(8) Å) is slightly longer. The Cr1-Cr2 distance of 2.6268(9) Å is consistent with that found in the two other structurally characterized hydride bridged chromium dimers: $[((MeC(N(2,6\text{-}Me_2Ph)_2)CH_2C(N(2,6\text{-}Me_2Ph)_2)Me)Cr)_2(\mu\text{-}H)_2]$ (2.6207(7) Å)[36] and $\{[(Ph_2PCH_2CH_2SiMe_2)_2N]Cr\}_2(\mu\text{-}H)_2$ (2.641(1) Å).[37] In **10,** the hydride H atoms were located in the Fourier map and refined. The Cr-H distances found (1.84(2) Å and 1.85(2) Å) may be compared to those reported above by Theopold (1.77(3) Å and 1.77(3) Å) and Fryzuk (1.78(3) Å and 1.76(3) Å).

The solution magnetic susceptibility data indicate a μ_{eff} of 1.6 μ_B/Cr at 293 K. This value is close to the single spin value (1.73 μ_B) and is inconsistent with a d^4 metal center, implying an interaction between the chromium atoms in **10**. Similar results have been observed for $\{[(Ph_2PCH_2CH_2SiMe_2)_2N]Cr\}_2(\mu\text{-}H)_2$ (1.6 μ_B/Cr), and $[((MeC(N(2,6\text{-}Me_2Ph)_2)CH_2C(N(2,6\text{-}Me_2Ph)_2)Me)Cr)_2(\mu\text{-}H)_2]$ (1.2 μ_B/Cr).

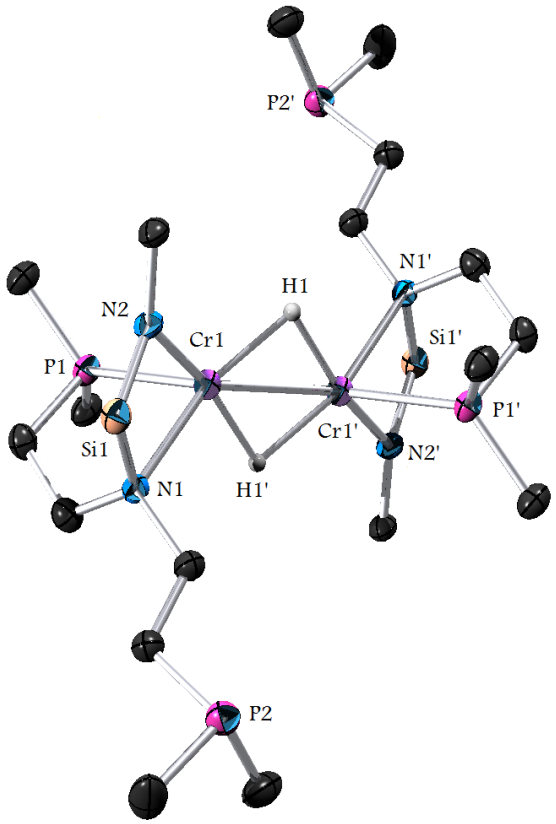

Figure 7: Thermal ellipsoid (50%) plot of **10**. Hydrogen atoms, methyl and iso-propyl groups have been omitted for clarity.

The reaction of the chromium-hydride **10** with silver triflate (2 equiv.) in refluxing THF overnight, followed by evaporation of the solvent, extraction with toluene, and crystallization at -40 ºC, gave $[N_2P_2]CrOSO_2CF_3$ (**11**) as blue needles in 39% yield. Crystals suitable for an X-ray diffraction study were grown from a concentrated toluene solution at -40 ºC. The μ_{eff} for **11** was 4.6 μ_B, consistent with four unpaired electrons.

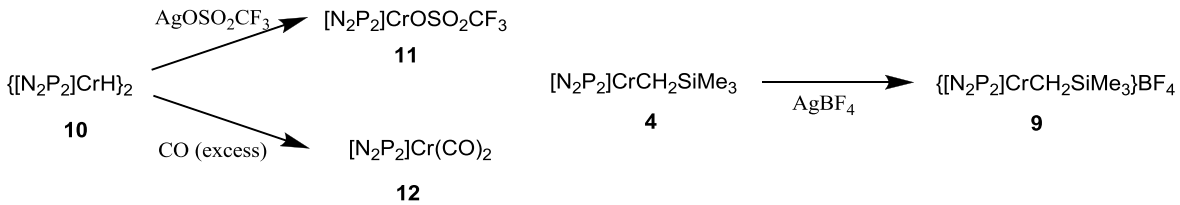

Scheme 3: Reactivity of **10**, synthesis of $[N_2P_2]CrOSO_2CF_3$ (**11**) $[N_2P_2]Cr(CO)_2$ (**12**).

Table 2: Selected bond distances and angles for Cr(II) complexes **10** and **11**.

	10 [a]	**11** [b]
Cr1 – X	1.84(2), 1.85(2) Å	2.029(5) Å
Cr1 - P1	2.5810(8) Å	2.567(3) Å
Cr1 - P2	-	2.596(3) Å
Cr1 – N1	2.2158(19) Å	2.142(6) Å
Cr1 – N2	2.0437(19) Å	2.032(6) Å
Cr1 – Cr2	2.6268(9) Å	-
X – Cr – P1	119.9(7)°	97.3(2)°
X – Cr – P2	-	102.57(17)°
X – Cr – N1	99.8(6)°	174.0(2)°
X – Cr – N2	156.0(7)°	100.0(3)°
P1 – Cr – P2	-	107.87(8)°
P1 – Cr – N2	91.98(6)°	125.4(2)°
P1 – Cr – N1	84.03(6)°	83.0(2)°
P2 – Cr – N2	-	117.9(2)°
P2 – Cr – N1	-	82.92(18)°
N1 – Cr – N2	74.97(7)°	75.1(3)°

[a] X = H, [b] X = O.

The structure of **11** showed distorted trigonal bipyramidal geometry very similar to that of **2**, with the ligand fully bound to the metal center and the axial positions being occupied by the triflate and the amine nitrogen of the N_2P_2 ligand (selected bond distances and angles are shown in Table 2). In **11**, the $\{OSO_2CF_3\}^-$ anion is coordinated to the chromium atom (An ORTEP diagram for is shown in Figure 8). The bond distances around the metal center are very similar to those found in **2** (Cr1-N1 2.142(6) Å, Cr1-N2 2.032(6) Å, Cr1-P1 2.596(3) Å and Cr1-P2(2.567(3) Å) but with a small contraction in the Cr1-N1 distance of almost 0.05 Å, to compensate for the weaker binding of triflate compared to chloride. The Cr1-O1 distance of 2.029(5) Å is consistent with that found in $Cp^*Cr(NO)_2OSO_2CF_3$ (2.030(2) Å).[38]

Reaction of **10** with excess CO in hexane at -78 °C, followed by warming to room temperature, produced a dark red solution with concomitant precipitation. Following work-up and cooling at -40 °C, $[N_2P_2]Cr(CO)_2$ (**12**) was isolated as brown crystals in 53% yield. An X-ray diffraction study of **12** was undertaken, and an ORTEP diagram is provided in Figure 9 (selected bond distances and angles are shown in Table 5). The chromium atom sits in a distorted trigonal bipyramidal geometry, with the $[N_2P_2]$ ligand bound κ^3-N_2P to the metal. The axial positions are occupied by the basal nitrogen and one CO ligand. To form **12**, the metal center was reduced from Cr(II) to Cr(I) by the liberation of H_2 (observed by ^{1}H-NMR). The magnetic susceptibility of the molecule (1.8 μ_B), indicates one unpaired electron, consistent with a low spin conformation.

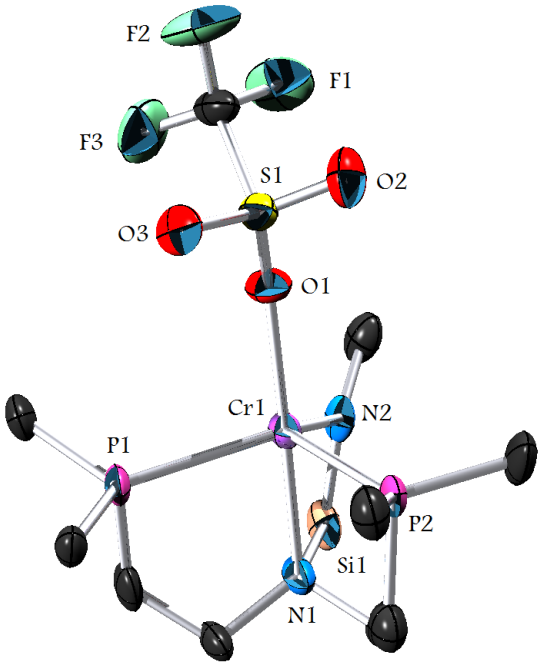

Figure 8: Thermal ellipsoid (50%) plot of **11**. Hydrogen atoms, methyl and iso-propyl groups have been omitted for clarity.

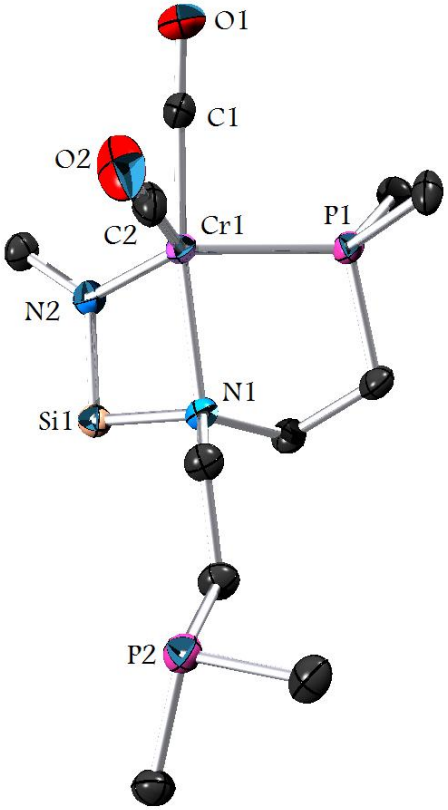

Figure 6: Thermal ellipsoid (50%) plot of **12**. Hydrogen atoms, methyl and iso-propyl groups have been omitted for clarity.

The Cr-C and C-O distances in **12** (1.816 (3) Å, 1.830 (3) Å and 1.176 (4) Å, 1.175 (4) Å) are consistent with those found in other Cr(I)-CO complexes such as $CpCr(CO)_2PPh_3$ (Cr-C: 1.826(3) Å and 1.816(4) Å; C-O: 1.16(12) Å and 1.16(12) Å).[39] A considerable amount of π-back bonding from the metal to the CO ligands is reflected in the low values observed in the IR spectrum for ν_{CO} (1742 and 1872 cm^{-1}).

Table 5: Selected bond distances and angles for **12**.

	12
Cr1 – C1	1.816(3) Å
Cr1 – C2	1.830(3) Å
Cr1 – P	2.3471(9) Å
Cr1 – N1	1.922(2) Å
Cr1 – N2	2.200(2) Å
C1 – O1	1.176(4) Å
C2 – O2	1.175(4) Å
C1 –Cr1 – C2	76.89(14)°
C1 – Cr1 – P	90.51(10)°
C1 – Cr1 – N1	106.28(12)°
C1 – Cr1 – N2	173.13(11)°
P1 – Cr1 – N1	133.95(8)°
C2 – Cr1 – P1	103.15(10)°
C2 – Cr1 – N1	105.80(12)°

Several attempts to isolate a $[N_2P_2]Cr(I)$ derivative by reduction of **2** gave intractable mixtures. In an attempt to trap a Cr(I) intermediate, **2** was reduced with KC_8 in the presence of *p*-tolyl azide in THF at -78 °C, with gas evolution being observed immediately. Following evaporation of the solvent under vacuum, extraction with diethyl ether and cooling at -40 °C, the bimetallic complex $([N_2P_2]Cr)_2(\mu\text{-}NC_7H_7)_2$ (**13**) was isolated in 44% yield as brown blocks.

Recrystallization from diethyl ether at -40 °C afforded crystals suitable for X-ray diffraction. Selected bond distances and angles are shown in Table 3; an ORTEP diagram is provided in Figure 10. Complex **13** is dimeric with two bridging imido ligands. Remarkably, the $[N_2P_2]$ ligand is bound κ^2-N_2 in the solid-state, providing the first example of an $[N_2P_2]$ complex without a metal-phosphine bond. The geometry around the chromium atom is pseudo-tetrahedral with N3-Cr1-N4 (90.08(11)°), N1-Cr1-N2 (77.96(11)°), N1-Cr1-N4 (115.09(10)°) and N1-Cr1-N3 (125.35(12)°). The Cr1-N3 and Cr1-N4 distances (1.856(2), 1.870(3), 1.853(2) and 1.873(3) Å) are slightly shorter than the Cr1-N2 and Cr2-N6 distances (1.900(2) and 1.904(2) Å). These values are consistent with those found in $[Cp^*Cr(\mu\text{-}NR)]_2$ (R = 2,6-$^{i}Pr_2C_6H_3$) (Cr1-N1: 1.886(2) Å and Cr1-N2: 1.861(2) Å) and $[Cp^*Cr(\mu\text{-}NR)]_2$ (R = 2,4,6-$^{t}Bu_3C_6H_2$) (Cr1-N1: 1.888(2) Å and Cr1-N2: 1.905(2) Å).[40] Complex **13** is diamagnetic with the ^{31}P-NMR showing a sharp singlet (4.76 ppm), implying that the phosphine arms are equivalent in solution.

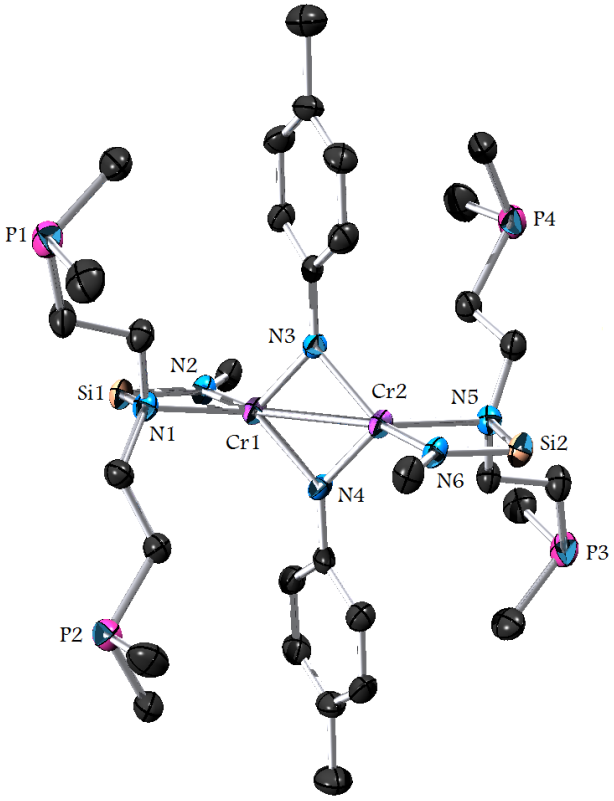

Figure 10: Thermal ellipsoid (50%) plot of **13**. Hydrogen atoms, methyl and iso-propyl groups have been omitted for clarity.

The synthesis of complex **13** highlights the ability of a transient Cr(I) species to undergo a two-electron oxidation process to produce a Cr(III) complex, and with the aim of directly probing specific intermediates in the catalytic oligomerization of ethylene to see if oxidative coupling occurred, we performed the reduction of **2** with KC_8 in the presence of ethylene. The reduction of **2** with KC_8 in THF at -78 °C under an atm of ethylene resulted in a green solution. Following the removal of the solvent under vacuum, extraction with hexane, and cooling at -40 °C, the metallacyclic complex $[N_2P_2]CrC_4H_8$ (**14**) was isolated as a green solid in 32% yield. An ORTEP diagram is provided in Figure 11, and selected bond distances and angles are shown in Table 3. The chromium atom lies in a distorted trigonal bipyramidal geometry with the $[N_2P_2]$ ligand bound κ^3-N_2P to the metal. As in the case of **4**, **5, 10,** and **12**, one of the phosphine arms is unbound to the metal center. All angles and distances are similar to those found in complexes **1** and **5**. The Cr1-C1 and Cr1-C2 distances (2.081(4) Å and 2.102(4) Å) are consistent with that found in **5** (2.067(5) Å) and with those reported in the only other structurally characterized metallacyclohexane $(Me_2NC_2H_4C_5Me_4)CrC_4H_8$ (2.103(1) Å and 2.080(1) Å).[20] The angles and distances about the carbon atoms in the metallacycle are consistent with sp^3 hybridization. The μ_{eff} was found to be 3.8 μ_B, in agreement with the presence of three unpaired electrons. To the best of our knowledge, this constitutes only the second example of a stable chromium metallacyclohexane formed by oxidative coupling of ethylene.[20]

The formation of the metallacycle **14** is in agreement with the mechanism proposed for ethylene trimerization by Bercaw and co-workers,[18] in which initial reduction of the metal center from Cr(II) to Cr(I) is followed by coordination of two ethylene molecules to the metal center leading to oxidative coupling and generation of the Cr(III) metallacycle. This reaction is thought to be a key step in the tri-, tetra- and oligomerization of ethylene by chromium catalysts.

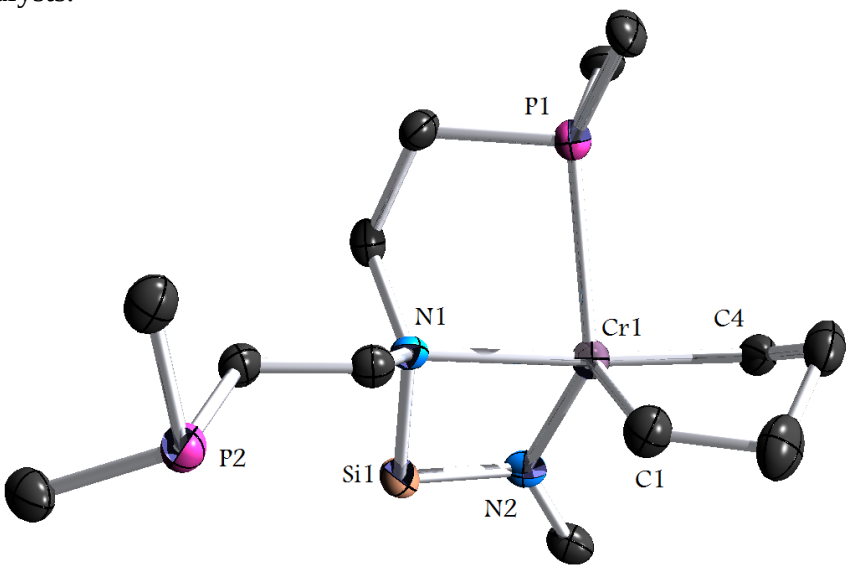

Figure 11: Thermal ellipsoid (50%) plot of **14**. Hydrogen atoms, methyl and iso-propyl groups have been omitted for clarity.

Cyclic voltammetry (CV) studies of **2**, **6**, **7**, **8**, **10** and **12** were carried out in THF with [*n*Bu_4N][PF_6] (0.1 M) as the supporting electrolyte. The CV of **2** shows one electrochemical process in the solvent window examined: a reversible one-electron oxidation for the Cr(II)/Cr(III) couple at 0.324 V vs Cp_2Fe/Cp_2Fe^+. No reduction process corresponding to the Cr(II)/Cr(I) couple was observed. The CV of **6** shows three processes, an irreversible oxidation at 1.12 V and two irreversible reductions at -1.37 and -1.87 V, while the CV of **1**[27] shows a one electron reversible reduction at -1.42 V.

The CVs of the cationic species **7** and **8** were very similar, showing two processes, a reversible reduction for Cr(III)/Cr(II) (at -1.28 V and -1.25 V, respectively) and an irreversible oxidation for Cr(III)/Cr(IV) at 0.471 V for **7** and 0.514 V for **8**.

The CV of **10** shows two reversible one electron oxidations in the same solvent window, at 0.071 V and 0.780 V. The first potential might indicate the oxidation of the Cr(II)-Cr(II) dimer to a Cr(II)-Cr(III) species, and the second electrochemical event might correspond to the Cr(II)-Cr(III)/Cr(III)-Cr(III) couple (Figure 12).

Finally the CV of **12** shows two reversible, one-electron oxidation processes at -0.637 and -0.025 V, followed by further electrochemical inseparable and unidentified events (Figure 20). The first oxidation was assigned to the Cr(I)/Cr(II) couple, and the second one to the Cr(II)/Cr(III) couple. The second oxidation potential is in agreement with the Cr(II)/Cr(III) potential found in **2** and the Cr(II)-Cr(II)/Cr(II)-Cr(III) potential for **10**.

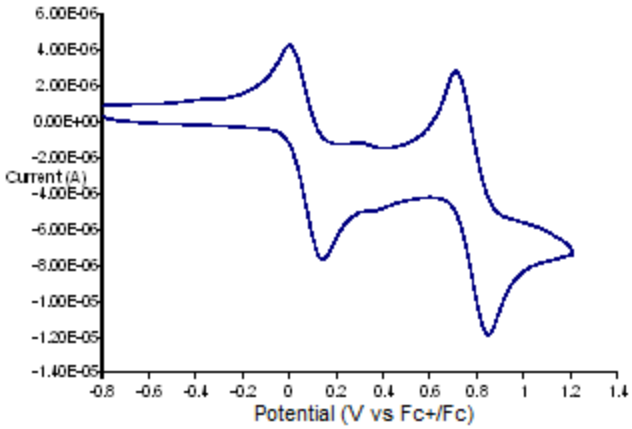

Figure 12: CV for **10** showing Cr(II)-Cr(II)/Cr(II)-Cr(III) and Cr(II)-Cr(III)/Cr(III)-Cr(III) oxidations. Carried out in THF with [*n*Bu$_4$N][PF$_6$] (0.1 M) as the supporting electrolyte.[41]

The CV experiments showed that under these conditions, the Cr(II)/Cr(III) redox process is straightforward in the halide species, but that upon alkylation the same redox processes becomes irreversible. The cationic species also showed an irreversible Cr(III)/Cr(IV) oxidation supporting the idea that the Cr(I)/Cr(III) couple is responsible for the formation of the metallacyclohexane. Only in the case of **12** were we able to observe the Cr(I)/Cr(II) couple in the window analyzed.

With the goal of understanding the differences in reactivity arising from different metal oxidation states, the activities of complexes **1** and **2** towards ethylene oligomerization were probed. The activity was screened at 1 and 10 atm of ethylene and at 25 °C and 80 °C with 30 μmol of precatalyst and 300 eq. of MAO as an activator. The results are summarized in Table 5.

A comparison of the activities of **1** and **2** show that the Cr(III) derivative **1** has a higher activity for ethylene polymerization; compound **1** produced almost 50% more polyethylene than **2** at 1 atm of ethylene at 25 °C and five times more polyethylene at 10 atm of ethylene pressure at 25 °C.

Compound **2**, however, did produce hexene and octene at 25 °C in a sufficient quantity to be detected by GC-MS. The presence of hexene, octene, decene and higher oligomers implies that under the reaction conditions tested, the Cr(II) derivative is capable of producing low weight oligomers. Under the same conditions using **1,** only polyethylene was observed.

Increasing the temperature to 80 °C while maintaining 10 atm of ethylene had a great influence on the amount of polyethylene obtained as well as on the distribution of products. At 80 °C, **1** produced 1.12 g of polyethylene, and the GC-MS trace showed the presence of C14 and higher oligomers in small quantities. Under the same conditions, 0.79 g of polyethylene insoluble in toluene and 2.39 g of soluble olefins were produced with **2**. Complex **2** gave a higher activity than complex **1** at 80 °C likely due to decomposition of the Cr(III) derivative. This phenomena has been observed with other Cr catalysts.[6] Our maximum production of polyethylene was with **2** which displayed an activity of 2.1×10^5 g polyethylene mol-Cr^{-1} h^{-1}, while running the reaction at 80 °C under 10 atm of ethylene

pressure. Other chromium catalysts for ethylene polymerization, like Cp*Cr(C_6F_5)(η^3-benzyl) or {2,6-bis[(2,4,6-trimethylphenyl)iminobenzyl]pyridine}$CrCl_3$, have shown activities of up to 1.56×10^8 g polyethylene mol Cr^{-1} h^{-1}.[42]

The activities of complexes **3, 4,** and **5** for ethylene oligomerization were tested without the use of an activator at 1 and 10 atm of ethylene at 25 °C. Under these conditions, none of the complexes were active for ethylene oligomerization. This observation suggests that MAO does more than just alkylate the metal center.

The activities of the cationic species **7**, **8** and **9** were also tested at 10 atm of ethylene at 25 ºC or at 80 ºC without an activator. None of these complexes were active catalysts for ethylene polymerization indicating that the active species formed upon addition of MAO to **1**-**3** is not a simple Cr(III) cationic alkyl derivative. The fact that the cationic alkyl complex **9** did not react with ethylene implies that MAO does not simply form a Cr(III) cationic alkyl complex as the active species.

We also tested complex **11** without adding MAO at 10 atm of ethylene and 25 ºC. Again, no reaction was observed, even with the reduced coordinating ability of the triflate in comparison to the chloride. Finally, we saw no reaction between **11** or **14** and ethylene (10 atm) at 25 °C, indicating that there is a large barrier to ethylene insertion for both complexes.

Table 5. Activity for ethylene polymerization of the synthesized complexes.

Precatalyst	Activator	Ethylene Pressure	Temperature (°C)	Polyethylene Yield (g)[a]	Productivity (g PE/mol Cr*h)
1	MAO, 300 eq.	1	25	0.064	4300
2	MAO, 300 eq.	1	25	0.044	2900
1[a]	MAO, 300 eq.	10	25	2.26	151000
2[a]	MAO, 300 eq.	10	25	0.47	31000
1[a]	MAO, 300 eq.	10	80	1.12	75000
2[a]	MAO, 300 eq.	10	80	3.18	212000
3[a]	none	10	25	0	0
3[a]	MAO, 300 eq.	1	25	0.119	7900
4[a]	none	10	25	0	0
5[a]	none	10	25	0	0
7[b]	none	10	25	0	0
8[b]	none	10	80	0	0
9[b]	none	10	25	0	0
10[b]	none	10	25	0	0
11[b]	none	10	25	0	0
14[b]	none	10	25	0	0

Conditions: a 0.03 mmol precatalyst, 40 mL toluene as solvent, 30 min run time. [b] 0.10 mmol precatalysts, 40 mL toluene as solvent, 1 h run time.

Conclusions

The [N_2P_2] ligand has the ability to stabilize reactive chromium complexes by changing its coordination mode, allowing for the synthesis and characterization of new Cr(II) and Cr(III) halide, alkyl, and hydride derivatives. Reaction of the chromium complexes with MAO gave active species for ethylene oligomerization/polymerization. However, these species were not selective for ethylene tri- or tetramerization. In order to gain insight into the ethylene oligomerization process with chromium catalysts, the alkyl species **3**, **4**, and **5**, and the cationic species **7**, **8**, and **9** were tested for ethylene polymerization without the use of an activator. These complexes did not catalyze the oligomerization/polymerization of ethylene, supporting the theory that the neutral alkyl derivatives, cationic Cr(III) derivatives, and cationic alkyl Cr(III) derivatives are not the active species formed after reaction with MAO.

The [N_2P_2] ligand also proved to be a useful supporting framework for studying the redox chemistry of chromium systems as a Phillips-type catalysis model. The reaction of **1** with 2 equivalents of MeLi resulted in reduction from Cr(III) to Cr(II), whereas the reaction of **10** with CO induced reduction of the metal to form the Cr(I) derivative **12**. Finally, we synthesized the chromium pentametallacycle **14** via reduction of **2** under an ethylene atm. Compounds similar to **14** have been proposed as intermediates for ethylene tri-, tetra- and oligomerization.

Table 6. **Con't**. Crystal data and structure refinement for **2**, **3**, **4**, **5**, **7**, **8**, **10**, **11**, **12**, **13** and **14**.

	2 [a]	**3**	**4**
Formula	$C_{22}H_{51}ClCrN_2P_2Si$	$C_{23}H_{54}CrN_2P_2Si$	$C_{26}H_{62}CrN_2P_2Si_2$
FW (g/mol)	521.13	500.71	572.90
T (K)	118(2)	143(2)	167(2)
Space group	$P2_1/c$	$P2_1/c$	$P2_1/c$
a (Å)	16.578(9)	16.718(4)	18.042(3)
b (Å)	11.973(7)	11.828(3)	10.1912(15)
c (Å)	14.632(8)	14.878(4)	19.639(3)
α (deg)	90.00	90.00	90.00
β (deg)	90.00[a]	91.894(3)	97.366(2)
γ (deg)	90.00	90.00	90.00
V (Å^3)	2904(3)	2940.4(12)	3581.2(10)
Z	4	4	4
λ (Å)	0.71073	0.71073	0.71073
μ (cm^{-1})	0.65	0.55	0.49
$R(F_0)$	0.0462	0.0430	0.0443
$R_w(F_0)$	0.0770	0.0939	0.1139

[a] The crystal was twinned and the angle was fixed to 90.00°.

Table 6. Crystal data and structure refinement for **2**, **3**, **4**, **5**, **7**, **8**, **10**, **11**, **12**, **13** and **14**.

	5	**7**
Formula	$4(C_{26}H_{62}ClCrN_2P_2Si_2)\cdot 2\,(C_4H_{10}O)$	$C_{22}H_{51}BClCrF_4N_2P_2Si\cdot C_4H_8O$
FW (g/mol)	2581.64	680.04
T (K)	135(2)	125(2)
Space group	$P2_1/c$	P-1
a (Å)	17.228(6)	11.570(6)
b (Å)	37.463(13)	11.938(7)
c (Å)	12.631(5)	13.261(7)
α (deg)	90.00	96.570(6)
β (deg)	102.621(4)	91.873(7)
γ (deg)	90.00	98.387(7)
V (Å^3)	7955(5)	1797.9(17)
Z	2	2
λ (Å)	0.71073	0.71073
μ (cm^{-1})	0.52	0.56
$R(F_0)$	0.0642	0.0416
$R_w(F_0)$	0.1531	0.1245

Table 6. Con't. Crystal data and structure refinement for **2**, **3**, **4**, **5**, **7**, **8**, **10**, **11**, **12**, **13** and **14**.

	8	**10**	**11**
Formula	$C_{46}H_{71}BClCrN_2P_2Si\cdot C_4H_8O$	$C_{44}H_{104}Cr_2N_4P_4Si_2$	$C_{23}H_{51}CrF_3N_2O_3P2SSi$
FW (g/mol)	912.44	973.39	634.76
T (K)	121(2)	144(2)	124(2)
Space group	$P2_1/c$	P-1	$P\,2_1\,2_1\,2_1$
a (Å)	13.935(17)	10.9976(16)	11.203(9)
b (Å)	35.24(4)	12.2720(18)	12.097(10)
c (Å)	10.647(13)	12.4998(19)	23.821(19)
α (deg)	90	114.965(2)	90
β (deg)	97.804(15)	108.976(2)	90
γ (deg)	90	90.341(2)	90
V (Å^3)	5180(11)	1426.0(4)	3228(4)
Z	4	1	4
λ (Å)	0.71073	0.71073	0.71073
μ (cm^{-1})	0.39	0.57	0.60
$R(F_0)$	0.0571	0.0358	0.0747
$R_w(F_0)$	0.1137	0.0745	0.1687

Table 6. Con't. Crystal data and structure refinement for **2**, **3**, **4**, **5**, **7**, **8**, **10**, **11**, **12**, **13** and **14**.

	12	**13**	**14**
Formula	$C_{24}H_{51}CrO_2N_2P_2Si$	$C_{58}H_{116}Cr_2N_6P_4Si_2$	$C_{26}H_{59}CrN_2P_2Si$
FW (g/mol)	541.70	1181.63	541.78
T (K)	133(2)	171(2)	137(2)
Space group	Pbcn	P-1	$P2_1/c$
a (Å)	33.381(4)	13.174(3)	17.623(6)
b (Å)	8.7353(11)	15.113(3)	10.722(4)
c (Å)	21.005(3)	17.002(4)	17.429(6)
α (deg)	90.00	89.222(3)	90.00
β (deg)	90.00	88.345(3)	102.428(5)
γ (deg)	90.00	84.857(3)	90.00
V (Å^3)	6124.9(14)	3369.8(13)	3216.0(19)
Z	8	2	4
λ (Å)	0.71073	0.71073	0.71073
μ (cm^{-1})	0.54	0.49	0.51
$R(F_0)$	0.0475	0.0444	0.0530
$R_w(F_0)$	0.1034	0.0933	0.0929

Experimental

General. Unless otherwise noted, all reactions were performed using standard Schlenk and N_2-atm glove box techniques. Solvents were dried by passing through a column of activated alumina and degassed with nitrogen.[43] C_6D_6 and $CDCl_3$ were dried over Na/benzophenone and vacuum transferred. All NMR spectra were obtained in C_6D_6 or $CDCl_3$ at ambient temperature using Bruker AV-300 or AVQ-400 spectrometers. ^{1}H NMR chemical shifts (δ) were calibrated relative to residual solvent peak. Magnetic susceptibility measurements were performed in C_6D_6 or $CDCl_3$ according to the Evans NMR method at 293 K.[44] Melting points were determined using sealed capillaries prepared under a nitrogen atm and are uncorrected. Infrared (IR) spectra were recorded with a Mattson Genesis Series FTIR spectrophotometer as Nujol mulls between KBr plates. UV-Vis spectra were determined with a Varian Cory 50 UV-Vis spectrophotometer using a 1 cm quartz cell. Elemental analyses were performed at the University of California, Berkeley Microanalytical Facility. X-ray crystal diffraction analyses were performed at the University of California, Berkeley CHEXRAY facility. $Li[N_2P_2]$,[27] $[N_2P_2]CrCl_2$ (**1**)[27] $CrCl_2(THF)$,[45] and $CrCl_3(THF)_3$ [46] were prepared according to literature procedures. The remaining starting materials were obtained from Aldrich and used without further purification.

$[N_2P_2]$CrCl (2). A solution of $Li[N_2P_2]$ (0.66 g, 1.5 mmol) in 10 mL of toluene was added dropwise to a suspension of $CrCl_2(THF)$ (0.29 g, 1.5 mmol) in 20 mL of toluene at room temperature. The solution turned from yellow to deep blue in five minutes. The solution was stirred overnight, filtered, concentrated and cooled to -40 °C, resulting in the formation of light blue, needle-like crystals (0.45 g, 58%). ^{1}H NMR (C_6D_6) 3.31 (br), 1.73(br), 1.15 (br), 1.08 (br), 0.88 (br), 0.32(br). IR (cm^{-1}) 1248 (m), 1219 (m), 1088 (s), 1021 (s), 936 (w), 854

(s), 802 (m), 731(w), 608 (w). UV-Vis (nm) 625, 815. Anal. Calc: C, 50.70; H, 9.86; N, 5.38. Observed C, 50.71; H, 10.23; N, 5.74. mp 172-175 °C. $\mu_{eff} = 4.7\ \mu_B$.

$[N_2P_2]$CrMe (3). Method A) A 1.6 M solution of MeLi (0.44 mL, 0.70 mmol) in diethyl ether was added to a solution of $[N_2P_2]$CrCl (0.34 g, 0.64 mmol) in 15 mL of THF at -78 °C. The solution immediately turned from blue to brown. The reaction mixture was allowed to warm to room temperature and was stirred for one hour. The solvent was removed under vacuum, and the product was extracted with hexane (2 x 10 mL). The solution was concentrated and cooled to -40 °C to give purple, block-like crystals (0.124 g, 38%).

Method B) A 1.6 M solution of MeLi (1.0 mL, 1.6 mmol) in diethyl ether was added to a suspension of $[N_2P_2]CrCl_2$ (0.40 g, 0.72 mmol) in 25 mL of diethyl ether at -78 °C. The solution immediately turned brown. The reaction mixture was allowed to warm to room temperature and was stirred for 10 h. The solvent was removed under vacuum, and the product was extracted with hexane (2 x 10 mL) and crystallized from hexane to -40 °C to give block-like purple crystals (0.17 g, 29%).

Method C) A suspension of KC_8 (0.11 g, 0.81 mmol) in 15 mL THF was added to a solution of **2** (0.40 g, 0.77 mmol) in 20 mL THF at -78 ºC. A solution of $AlMe_3$ in hexanes (1.2 mL, 2.0 M) was added while keeping the temperature at -78 ºC. The mixture was warmed to room temperature and was stirred 1 h. The solvent was removed under vacuum, and the product was extracted with hexane (2 x 10 mL) and crystallized at -40 °C to give block-like purple crystals (0.11 g, 47%). ^{1}H NMR (C_6D_6) 3.30 (br), 1.74 (br), 1.25 (br), 1.15 (br), 0.71 (br), 0.31 (br). IR (cm^{-1}) 1259 (m), 1092 (m), 1016 (m), 800 (m), 720 (w). UV-Vis (nm) 400, 620. MS *m/z* 500 (M^+). Anal. Calc: C, 55.17; H, 10.87; N, 5.59. Observed C, 54.81; H, 11.22; N, 5.77. mp 93-94 °C. $\mu_{eff} = 4.5\ \mu_B$.

$[N_2P_2]CrCH_2SiMe_3$ (4). A solution of $LiCH_2SiMe_3$ (0.13 g, 1.4 mmol) in 10 mL of toluene was added to a solution of $[N_2P_2]$CrCl (0.52 g, 1.0 mmol) in 20 mL of toluene at room temperature. The solution immediately turned from blue to purple, and the reaction mixture was stirred overnight. The solvent was removed under vacuum, and the product was extracted with hexane (2 x 10 mL). The solution was concentrated and cooled to -40 °C to give purple, block-like crystals (0.24 g, 53%). ^{1}H NMR (C_6D_6) 9.07 (br), 3.31 (br), 1.73 (br), 1.25 (br), 1.16 (br), 0.36 (br), 0.21 (br). IR (cm^{-1}) 1246 (m), 1211 (m), 1087 (m), 1048 (w), 1019 (m), 850 (s), 794 (m), 735 (w). Anal. Calc: C, 54.51; H, 10.91; N, 4.89; Observed C, 54.44; H, 11.23; N, 4.92. mp 65-68 °C. $\mu_{eff} = 4.4\ \mu_B$.

$[N_2P_2]CrClCH_2SiMe_3$ (5). A solution of $LiCH_2SiMe_3$ (0.06 g, 0.63 mmol) in 10 mL of toluene was added to a solution of $[N_2P_2]CrCl_2$ (0.35 g, 0.63 mmol) in 15 mL of toluene at room temperature. The solution immediately turned from purple to dark blue and the reaction mixture was stirred overnight. The solvent was removed under vacuum, and the product was extracted with hexane (2 x 10 mL). The solution was concentrated and cooled to -40 °C to give purple, block-like, crystals (0.22 g, 57%). ^{1}H NMR (C_6D_6) 3.21(br), 1.64 (br), 1.18 (br), 1.07 (br), 0.97 (br), 0.30 (s), 0.24 (s). IR (cm^{-1}) 1259 (m), 1089 (w), 1050 (w), 1019 (m), 842 (w), 799 (m). Anal. Calc: C, 51.33; H, 10.27; N, 4.60. Observed C, 51.31; H, 10.02; N, 4.42. mp 96-99 °C. $\mu_{eff} = 3.9\ \mu_B$.

$[N_2P_2]$Cr(Cl)Me (6). A 1.6 M solution of MeLi in diethyl ether (0.85 mL, 1.4 mmol) was added to a solution of $[N_2P_2]CrCl_2$ (0.75 g, 1.3 mmol) in 40 mL of THF at -78 °C. The solution was allowed to warm up at room temperature, giving a deep purple solution. After stirring overnight, the solvent was removed under vacuum, and the product was extracted

with diethyl ether (2 x 10 mL). Cooling to -40 °C gave the product as purple crystals (0.49 g, 68%). ^{1}H NMR (C_6D_6) 10.45 (br), 3.26 (br), 1.62 (br), 0.99 (br), -1.15 (br), -8.44 (br). IR (cm^{-1}) 1259 (s), 1087 (s), 1061 (s), 1016 (s), 885 (w), 850 (w), 800 (s), 605 (m). Anal. Calc: C, 51.52; H, 10.15; N, 5.22. Observed C, 51.60; H, 10.08; N, 5.49. mp 128-130 °C. μ_{eff} = 3.8 μ_B.

{[N_2P_2]CrCl}BF_4 (7). A solution of $AgBF_4$ (0.24 g, 1.2 mmol) in 20 mL of THF was added to a solution of **2** (0.60 g, 1.2 mmol) in 25 mL of THF at room temperature. The solution was stirred overnight, resulting in a blue to green color change and precipitation of a gray solid. The solvent was removed under vacuum. The solid was washed with ether and the product was extracted with THF (3 x 10 mL). The solution was concentrated and cooled to -40 °C to give green, block-like, crystals (0.44 g, 64%). ^{1}H NMR ($CDCl_3$) 22.2 (br), 15.9 (br), 9.66 (br), 3.77 (br), 1.86 (br), 1.16 (br), 0.08 (br), -11.3 (br). IR (cm^{-1}) 1261 (m), 1191 (w), 1061 (s), 1014 (m), 852 (m), 756 (m), 722 (w). Anal. Calc: C, 43.46; H, 8.46; N, 4.61. Observed C, 43.84; H, 8.39; N, 4.24. mp 188 - 191 °C. μ_{eff} = 3.8 μ_B.

{[N_2P_2]CrCl}BPh_4 (8). The synthesis was carried out analogously to that of **7** starting with $AgBPh_4$ (0.33 g, 0.77 mmol) and **2** (0.40 g, 0.77 mmol), to yield dark green, block-like crystals (0.19 g, 29%). ^{1}H NMR ($CDCl_3$) 22.4 (br), 16.5 (br), 7.44 (br), 7.08 (br), 3.76 (br), 3.18 (br), 1.88 (br), 1.18 (br), 0.18 (br), -12.9 (br). IR (cm^{-1}) 1578 (m), 1256 (s), 1185 (m), 1091 (m), 1021 (s), 886 (m), 851 (s), 799 (m), 759 (m), 731 (s), 705 (s), 611 (m). Anal. Calc: C, 65.74; H, 8.52; N, 3.33. Observed C, 65.55; H, 8.30; N, 3.65. mp 213 - 214 °C. μ_{eff} = 3.9 μ_B.

{[N_2P_2]CrCH_2SiMe_3}BF_4 (9). The synthesis was carried out analogously to that of **7** starting with $AgBF_4$ (0.15 g, 0.77 mmol) and **4** (0.42 g, 0.73 mmol), to yield purple, block-like crystals (0.32 g, 60%). ^{1}H NMR (C_6D_6) 13.8 (br), 3.26 (br), 1.65 (br), 1.39 (br), 1.17 (br), 1.08 (br), 0.30 (br), -5.28 (br). IR (cm^{-1}) 1260 (s), 1093 (s), 1053 (s), 1020 (s), 929 (w), 859 (m), 799 (m), 759 (m), 721 (m). Anal. Calc: C, 47.34; H, 9.47; N, 4.25. Observed C, 47.02; H, 9.43; N, 4.13. mp 76 - 80 °C. μ_{eff} = 3.7 μ_B.

([N_2P_2]Cr)$_2$(μ-H)$_2$ (10). A solution of $NaAlH_2(OCH_2CH_2OMe)_2$ (Red-Al®, 3.5 M in toluene, 0.36 g, 1.2 mmol) was added to a solution of [N_2P_2]CrCl (0.60 g, 1.1 mmol) in 25 mL of THF at -78 °C. The solution turned from purple to dark brown. The reaction mixture was warmed to room temperature and stirred for 1 h, after which the solvent was removed under vacuum. The crude product was extracted with hexane (2 x 10 mL), and the solution was concentrated and cooled to -40 °C to give brown, block-like, crystals (0.47 g, 84%). ^{1}H NMR 4.11 (br), 3.54 (br), 3.27 (br), 3.21 (br), 2.52 (br), 1.67 (br), 1.41 (br), 0.87 (br), 0.29 (s). IR (cm^{-1}) 1347 (m), 1259 (m), 1208 (m), 1083 (s), 1033 (m), 1015 (s), 919 (w), 848 (m), 796 (m), 755 (w), 728 (m). Anal. Calc: C, 54.29; H, 10.77; N, 5.76. Observed C, 52.50; H, 10.83; N, 5.49. mp 88-90 °C. μ_{eff} = 2.2 μ_B.

[N_2P_2]CrOSO_2CF_3 (11). A solution of $AgOSO_2CF_3$ (0.19 g, 0.74 mmol) in 15 mL of toluene was added to a solution of **10** (0.35 g, 0.36 mmol) in 25 mL of THF at room temperature. The solution was refluxed overnight, the solvent was removed under vacuum, and the product was extracted with toluene (3 x 10 mL). The solution was concentrated and cooled to -40 °C to give blue, needle-like, crystals (0.18 g, 39%). ^{1}H NMR (C_6D_6) 14.9 (br), 3.26 (br), 1.64 (br), 1.18 (br), 1.11 (br), 0.24 (br), -1.21 (br). IR (cm^{-1}) 1318 (s), 1235 (s), 1214 (s), 1171 (m), 1159 (w), 1098 (w), 1032 (s), 912 (w), 855 (m), 734 (w), 634 (s). Anal. Calc: C,

43.52; H, 8.10; N, 4.41: S, 5.05. Observed C, 43.23; H, 7.89; N, 4.19: S, 5.23. mp 155 - 157 °C. $\mu_{eff} = 4.6\ \mu_B$.

$[N_2P_2]Cr(CO)_2$ (12). Carbon monoxide was added into a solution of $([N_2P_2]Cr)_2(\mu\text{-}H)_2$ (**7**) (0.30 g, 0.31 mmol) in 25 mL of hexane at -78 °C. The reaction mixture was allowed to warm to room temperature and was stirred overnight resulting in a color change from brown to dark red. The solvent was removed under vacuum, and the product was extracted with diethyl ether (2 x 10 mL). The solution was concentrated and cooled to -40 °C to give brown, block-like, crystals (0.18 g, 53%). ^{1}H NMR 3.26 (s), 2.28 (br), 1.17 (br), 1.12 (br), 0.82 (br), 0.29 (br). IR (cm^{-1}) 1872 (vs), 1742 (vs), 1352 (s), 1248 (s), 1200 (s), 1045 (s), 1018 (s), 890 (m), 845 (s), 746 (m), 670 (w). Anal. Calc: C, 53.21; H, 9.49; N, 5.17. Observed C, 53.05; H, 9.84; N, 5.44. mp 123-124 °C. $\mu_{eff} = 1.8\ \mu_B$.

$([N_2P_2]Cr)_2(\mu\text{-}NC_7H_7)_2$ (13). A solution of *p*-tolyl azide (0.14 g, 1.1 mmol) dissolved in 10 mL THF and a suspension of KC_8 (0.15 g, 1.1 mmol) in 10 mL THF were added to a solution of $[N_2P_2]CrCl$ (0.60 g, 1.1 mmol) in 30 mL of THF at -78 °C. The solution turned from blue to dark brown and gas evolution was observed. The reaction mixture was warmed to room temperature and was stirred for 2 h. The solvent was removed under vacuum, and the product was extracted with hexane (2 x 10 mL). The solution was concentrated and cooled to -40 °C to give brown, block-like, crystals (0.30 g, 44%). ^{1}H NMR 7.09 (s) 3.22 (m), 2.89 (s), 1.65 (br), 1.55 (br), 1.40 (br), 1.17 (s), 1.08 (m), 0.94 (s), 0.29 (s), 0.17 (br). ^{31}P NMR 4.76 (s). IR (cm^{-1}) 1595 (w), 1487 (s), 1266 (s), 1209 (s), 1101 (w), 1060 (m), 1047 (m), 903 (w), 847 (s), 814 (s), 777 (m), 756 (m). Anal. Calc: C, 58.95; H, 9.89; N, 7.11. Observed C, 58.70; H, 9.80; N, 6.95. mp 173-177 °C. $\mu_{eff} = 0\ \mu_B$.

$[N_2P_2]CrC_4H_8$ (14). A suspension of KC_8 in THF was added by cannula to a solution of $[N_2P_2]CrCl$ (0.80 g, 1.5 mmol) in 25 mL of THF at -78 °C, while maintaining 1 atm of ethylene pressure. The solution turned from blue to dark brown, and a dark gray precipitate was observed. The reaction mixture was warmed to room temperature and stirred for 1 h. The solvent was removed under vacuum, and the product was extracted with hexane (2 x 10 mL) to give a green solution. Concentration and cooling to -40 °C gave green, block-like, crystals (0.24 g, 32%). ^{1}H NMR 3.24 (br), 1.66 (br), 1.17 (br), 1.09 (br), 0.29 (br). IR (cm^{-1}) 1350 (w), 1248 (m), 1203 (m), 1068 (s), 1051 (s), 1019 (s), 894 (w), 845 (m), 797 (s), 769 (w), 735 (m), 611 (w). MS *m/z* 485 ($[N_2P_2]Cr^+$), 56 ($C_4H_8^+$). Anal. Calc: C, 57.64; H, 10.98; N, 5.17. Observed C, 55.95; H, 11.11; N, 5.17. mp 113-115 °C. $\mu_{eff} = 3.8\ \mu_B$.

Ethylene polymerization experiments at 1 atm of ethylene. The precatalyst (0.03 mmol) was dissolved in 10 mL of toluene and added to 30 mL of toluene with the requisite amount of MAO (0.52 g, 300 eq. Al, if used). The flask was purged with ethylene and then pressurized to 1 atm of ethylene. The reaction was run for 30 min before being quenched with 120 mL of a solution of 5% HCl/ethanol. The solid product was washed with ethanol and dried under vacuum overnight, affording a white powder. A 10 mL aliquot of the liquid was analyzed by GC-MS.

Ethylene polymerization experiments at 10 atm of ethylene. A Fisher-Porter tube was filled with 30 mL of toluene and MAO (0.52 g, 300 eq. Al). A solution of precatalyst (0.03 mmol) dissolved in 10 mL of toluene was then added. The tube was purged with ethylene, then pressurized to 10 atm The reaction was allowed to run for 30 min, keeping the pressure at 8-10 atm. After quenching with 120 mL of a solution of 5% HCl/ethanol, the resulting

solid was filtered, washed with ethanol and dried under vacuum overnight. A 10 mL aliquot of the filtrate was analyzed by GC-MS.

Characterization of the products by GC-MS. A 10 mL aliquot of the reaction filtrate was washed with 15 mL of deionized water, dried over anhydrous magnesium sulfate and analyzed by GC-MS using a Agilent 6890N GC with a High Resolution Gas Chromatography Column (30 m length, 25 mm diameter) capillary column and a Agilent 5973N mass selective detector, adding mesitylene (25 μL/mL) as internal standard. Working conditions were 35 °C (10 min) with temperature increases of 10 °C/min to 280 °C (10 min).

Crystallographic Analysis. Single crystals of **2**, **3**, **4**, **5**, **7, 8, 10, 11, 12, 13** and **10** were coated in Paratone-N oil, mounted on a Kaptan loop, transferred to a Siemens SMART diffractometer CCD area detector[47] centered in the beam, and cooled by a nitrogen flow low-temperature apparatus that has been previously calibrated by a thermocouple placed at the same position as the crystal. Preliminary orientation matrices and cell constants were determined by collection of 60 30-second frames, followed by spot integration and least-squares refinement. An arbitrary hemisphere of data was collected and the raw data were integrated using SAINT.[48] Cell dimensions reported were calculated from all reflections with $I > 10$. The data were corrected for Lorentz and polarization effects, but no correction for crystal decay was applied. Data were analyzed for agreement and possible absorption using XPREP.[49] An empirical absorption correction based on comparison of redundant and equivalent reflections was applied using SADABS.[50] The structures were solved using SHELXS[51] and refined on all data by full-matrix least squares with SHELXL-97.[52] Thermal parameters for all non-hydrogen atoms were refined anisotropically. ORTEP diagrams were created using ORTEP-3.[53]

References

1. Groppo, E.; Lamberti, C.; Bordiga, S.; Spoto, G.; Zecchina, A. *Chem. Rev.* **2005,** *105*, 115-183.
2. McDaniel, M. P. *Adv. Catal.* **1985,** *33*, 47-98.
3. Bowen, L. E.; Charernsuk, M.; Wass, D. F. *Chem. Commun.* **2007**, 2835-2837.
4. Briggs, J. R. *J. Chem. Soc. Chem. Comm.* **1989**, 674-675.
5. Crewdson, P.; Gambarotta, S.; Djoman, M. C.; Korobkov, I.; Duchateau, R. *Organometallics* **2005,** *24*, 5214-5216.
6. Dixon, J. T.; Green, M. J.; Hess, F. M.; Morgan, D. H. *J. Organomet. Chem.* **2004,** *689*, 3641-3668.
7. Freeman, J. W. B., J. L.; Knudsen, R. D. US 5856257 (Phillips Petroleum Company) 1999. US 5856257 (Phillips Petroleum Company)
8. Lashier, M. E. EP 0780353A1, (Phillips Petroleum Company) 1997. EP 0780353A1, (Phillips Petroleum Company)
9. Manyik, R. M. W., W. E.; Wilson, T. P. US 3300458 (Union Carbide Corporation) 1967. US 3300458 (Union Carbide Corporation)
10. McGuinness, D. S.; Brown, D. B.; Tooze, R. P.; Hess, F. M.; Dixon, J. T.; Slawin, A. M. Z. *Organometallics* **2006,** *25*, 3605-3610.
11. McGuinness, D. S.; Wasserscheid, P.; Keim, W.; Hu, C. H.; Englert, U.; Dixon, J. T.; Grove, C. *Chem. Commun.* **2003**, 334-335.

12. van Rensburg, W. J.; Grove, C.; Steynberg, J. P.; Stark, K. B.; Huyser, J. J.; Steynberg, P. J. *Organometallics* **2004,** *23*, 1207-1222.
13. Jabri, A.; Crewdson, P.; Gambarotta, S.; Korobkov, I.; Duchateau, R. *Organometallics* **2006,** *25*, 715-718.
14. Andes, C.; Harkins, S. B.; Murtuza, S.; Oyler, K.; Sen, A. *J. Am. Chem. Soc.* **2001,** *123*, 7423-7424.
15. Deckers, P. J. W.; Hessen, B.; Teuben, J. H. *Angew. Chem. Int. Edit.* **2001,** *40*, 2516-+.
16. Santi, R. R., A. M.; Grande, M.; Sommazzi, A.; Masi, F.; Proto, A. WO 0168572, (ENICHEM S.P.A.). 2001. WO 0168572, (ENICHEM S.P.A.).
17. Agapie, T.; Day, M. W.; Henling, L. M.; Labinger, J. A.; Bercaw, J. E. *Organometallics* **2006,** *25*, 2733-2742.
18. Agapie, T.; Labinger, J. A.; Bercaw, J. E. *J. Am. Chem. Soc.* **2007,** *129*, 14281-14295.
19. Agapie, T.; Schofer, S. J.; Labinger, J. A.; Bercaw, J. E. *J. Am. Chem. Soc.* **2004,** *126*, 1304-1305.
20. Emrich, R.; Heinemann, O.; Jolly, P. W.; Kruger, C.; Verhovnik, G. P. J. *Organometallics* **1997,** *16*, 1511-1513.
21. Bollmann, A.; Blann, K.; Dixon, J. T.; Hess, F. M.; Killian, E.; Maumela, H.; McGuinness, D. S.; Morgan, D. H.; Neveling, A.; Otto, S.; Overett, M.; Slawin, A. M. Z.; Wasserscheid, P.; Kuhlmann, S. *J. Am. Chem. Soc.* **2004,** *126*, 14712-14713.
22. Tomov, A. K.; Chirinos, J. J.; Jones, D. J.; Long, R. J.; Gibson, V. C. *J. Am. Chem. Soc.* **2005,** *127*, 10166-10167.
23. McGuinness, D. S.; Wasserscheid, P.; Morgan, D. H.; Dixon, J. T. *Organometallics* **2005,** *24*, 552-556.
24. Chomitz, W. A.; Arnold, J. *Chem. Commun.* **2007**, 4797-4799.
25. Chomitz, W. A.; Arnold, J. *Dalton Trans.* **2009**, 1714-1720.
26. Chomitz, W. A.; Arnold, J. *Inorg. Chem.* **2009,** *48*, 3274-3286.
27. Chomitz, W. A.; Mickenberg, S. F.; Arnold, J. *Inorg. Chem.* **2008,** *47*, 373-380.
28. Chomitz, W. A.; Sutton, A. D.; Krinsky, J. L.; Arnold, J. *Organometallics* **2009,** *28*, 3338-3349.
29. Chomitz, W. A.; Arnold, J. *Chem-Eur. J.* **2009,** *15*, 2020-2030.
30. Chomitz, W. A.; Arnold, J. *Chem. Commun.* **2008**, 3648-3650.
31. Hermes, A. R.; Morris, R. J.; Girolami, G. S. *Organometallics* **1988,** *7*, 2372-2379.
32. Fryzuk, M. D.; Leznoff, D. B.; Rettig, S. J.; Young, V. G. *J. Chem. Soc. Dalton.* **1999**, 147-154.
33. Kohn, R. D.; Kociokkohn, G. *Angew. Chem. Int. Edit.* **1994,** *33*, 1877-1878.
34. Alsoudani, A. R. H.; Batsanov, A. S.; Edwards, P. G.; Howard, J. A. K. *J. Chem. Soc. Dalton.* **1994**, 987-995.
35. Overett, M. J.; Blann, K.; Bollmann, A.; Dixon, J. T.; Haasbroek, D.; Killian, E.; Maumela, H.; McGuinness, D. S.; Morgan, D. H. *J. Am. Chem. Soc.* **2005,** *127*, 10723-10730.
36. MacAdams, L. A.; Buffone, G. P.; Incarvito, C. D.; Golen, J. A.; Rheingold, A. L.; Theopold, K. H. *Chem. Commun.* **2003**, 1164-1165.
37. Fryzuk, M. D.; Leznoff, D. B.; Rettig, S. J.; Thompson, R. C. *Inorg. Chem.* **1994,** *33*, 5528-5534.

38. Legzdins, P.; Rettig, S. J.; Smith, K. M.; Tong, V.; Young, V. G. *J. Chem. Soc. Dalton.* **1997**, 3269-3276.
39. Cooley, N. A.; Watson, K. A.; Fortier, S.; Baird, M. C. *Organometallics* **1986,** *5*, 2563-2565.
40. Danopoulos, A. A.; Wilkinson, G.; Sweet, T. K. N.; Hursthouse, M. B. *J. Chem. Soc. Dalton.* **1996**, 271-281.
41. Under these conditions, the peak to peak separation of the Co(II)/Co(III) couple in cobaltocene (used as reference) was 0.16 mV.
42. Esteruelas, M. A.; Lopez, A. M.; Mendez, L.; Olivan, M.; Onate, E. *Organometallics* **2003,** *22*, 395-406.
43. Alaimo, P. J.; Peters, D. W.; Arnold, J.; Bergman, R. G. *J. Chem. Educ.* **2001,** *78*, 64-64.
44. Piguet, C. *J. Chem. Educ.* **1997,** *74*, 815-816.
45. Kohler, F. H.; Prossdorf, W. *Z. Naturforsch. B.* **1977,** *32*, 1026-1029.
46. Kern, R. J. *J. Inorg. Nucl. Chem.* **1962,** *24*, 1105-1109.
47. SMART *Area-Detector Software Package, Bruker Analytical X-ray Systems, Inc.: Madison, WI, (2001-2003).* 2001-2003.
48. SAINT *SAX Area-Detector Integration Program, V6.40; Bruker Analytical X-ray Systems Inc.: Madison, WI, (2003).* 2003.
49. PREP *(v 6.12) Part of the SHELXTL Crystal Structure Determination Package, Bruker Analytical X-ray Systems, Inc.: Madison, WI, (2001).* 2001.
50. SADABS *Bruker-Nonius Area Detector Scaling and Absorption v. 2.05 Bruker Analytical X-ray Systems, Inc.: Madison, WI (2003).* 2003.
51. SHELXS *Program for the Refinement of X-ray Crystal Structures, Part of the SHELXTL Crystal Structure Determination Package, Bruker Analytical X-ray Systems Inc.: Madison, WI, (1995-99).* 1995-1999.
52. SHELXL *Program for the Refinement of X-ray Crystal Structures, Part of the SHELXT Crystal Structure Determination Package, Bruker Analytical Systems Inc.: Madison, WI, (1995-99).* 1995-1999.
53. Farrugia, L. *J. Appl. Cryst.* **1997,** *30*, 565.

Chapter 2:

Metal complexes of Co, Ni and Cu with the pincer ligand $HN(CH_2CH_2P^iPr_2)_2$: preparation, characterization and electrochemistry

Introduction

Mixed hard/soft donor pincer ligands have been extensively studied in recent decades due to their ability to stabilize metal complexes in a wide variety of important stoichiometric and catalytic reactions.[1-5] Of the plethora of pincer ligands found in the literature, we were attracted to the $HN(CH_2CH_2PR_2)_2$ $H(NP^R_2)$ (R= alkyl) scaffold, first synthesis by Edwards and co-workers,[6-8] as a mimic model for the ligand $HN(Si(Me)_2CH_2PR)_2$ developed by Fryzuk,[9] the $H(NP^R_2)$ ligand. This general framework has the ability to form complexes acting as an amide, a secondary amine, a tertiary amine, or as a tetradentate ligand by adding an extra coordination group at the amine site.[10-13] The ligand form complexes with early and late transition metals,[10-16] as well as actinides.[17, 18]

The $H(NP^R_2)$ ligand set has a rich coordination chemistry. Edwards and co-workers have shown that by varying the ligand to metal ratio and the size of the alkyl groups on the phosphines, $(NP^R_2)M$, $(NP^R_2)_2M$, and $\{(NP^R_2)M\}_2$ species can be formed.[19] It also stabilizes reactive species and unusual electronic structures. Gusev and co-workers have used it to isolate *trans*-dihydride species,[14] and Schneider *et. al*. to prepare a square-planar, low spin $(NP^R_2)Ru(II)$ complex.[20] The latter group has also shown that the complex $(H(NP^R_2))RuCl_2PMe_3$ is capable of heterolytic splitting of H_2 after treatment with KO^tBu.[21, 22] The $(NP^R_2)Ir$ derivative activates two C-H bonds in THF to give the Fisher-carbene species $[PN(H)PIr(H)_2(=CO(CH_2)_3]BPh_4$.[15]

The $H(NP^R_2)$ scaffold has been also applied to carry out a wide variety of catalytic transformations. McGuinness and co-workers have shown that the PN(H)P-Cr(III) derivative is an active catalyst for ethylene trimerization after activation with MAO, giving 1-hexene with high activity and selectivity; by substituting H of the N*H* moiety for an alkyl or aryl group, the selectivity of the system is lost.[12, 23] It has been also used for transfer hydrogenation of ketones,[24] the dehydrogenation of ammonia-borane and *N*-methylamine-borane with high turnover numbers,[21, 25] and for the synthesis of high molecular weight polyaminoboranes.[26]

The ability of the $H(NP^R_2)$ ligand sets to stabilize different metal centers and oxidation states make them good candidates for the study of electrocatalytic transformations. In particular, our group is interested in the electrocatalytic dehydrogenation of organic molecules with first row transition metals, targeting transformations producing protons and electrons for fuel-cell applications. With this in mind, we prepared a series of Ni complexes with the ligand $HN(CH_2CH_2P^iPr_2)_2$ (HPNP) to study their electrochemical proprieties through cyclic voltammetry. Co and Cu derivatives were synthesized for comparison purposes.[27] The ligand was chosen due its known chemistry and previous experience with this scaffold.[10, 28-31] During the course of this investigation, we found interesting reactivity of the $[HPNPNiNCCH_3]^{2+}$ species with piperidine, giving rise to the formation of the complex $(HPNPNiN(H)C(CH_3)NC_5H_{10})(BF_4)_2$ in good yield.

Results and Discussion

The reaction of the ligand HPNP with $NiBr_2$ in THF, followed by evaporation of the solvent, and crystallization from CH_2Cl_2/diethyl ether solution yields the complex (HPNPNiBr)Br (**1**) in 77%. The ^1H NMR spectrum of **1** shows all the peaks corresponding to the HPNP ligand in a rigid conformation where the axial and equatorial protons in the backbone are inequivalent and the CH_3 protons in the isopropyl groups are not related by a symmetry plane. In solution, the phosphorous atoms are equivalent, showing one signal at 56.9 ppm in the ^{31}P NMR spectrum.

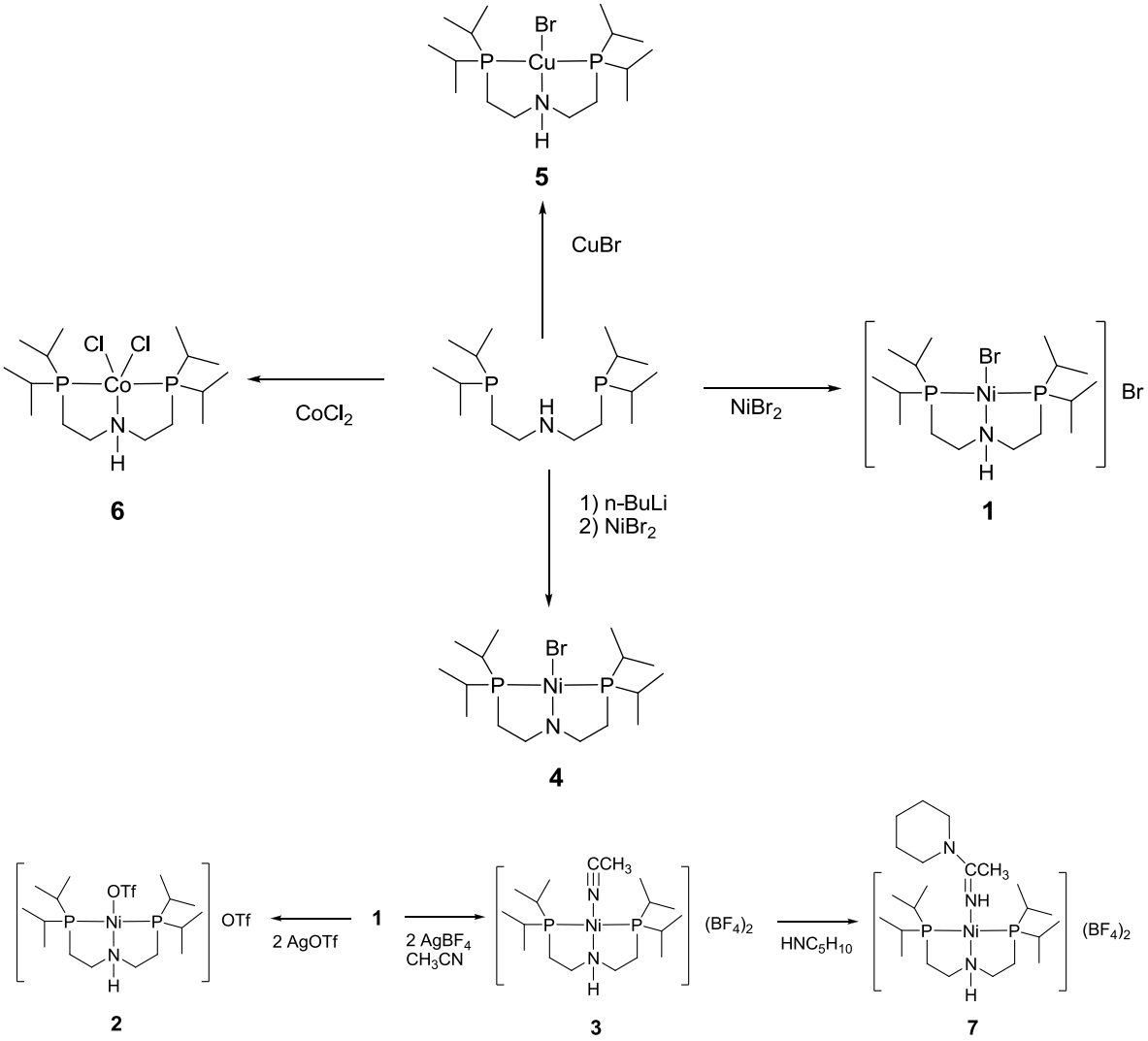

Scheme 1. Synthesis of HPNP metal complexes.

Crystals suitable for an X-ray diffraction study were grown from a concentrated solution of **1** in CH_2Cl_2 layered with diethyl ether. Unfortunately, twinning problems and disorder in the molecule did not allow us to refine the structure within acceptable values. However, the connectivity found indicates a Ni metal center in a square planar environment, with one bromide coordinated to the metal center and one unbound.

We targeted the synthesis of the triflate derivative of the HPNPNi complex as a mimic for the fuel cell membrane environment (e.g. Nafion® features perfluorinated sulfonic groups). Complex **1** reacts with two equivalents of AgOTf in CH_2Cl_2 to produce an orange solution and white precipitate (AgBr). After filtration trough Celite®, (HPNPNiOTf)OTf (**2**) was obtained in 79% yield from a CH_2Cl_2/diethyl ether solution. The ^{1}H NMR spectrum for **2** resembles that observed for **1**, showing two multiplets each for the NC*H*$_2$ and the PC*H*$_2$ protons, four multiplets for the C*H*$_3$ protons, and one singlet for the phosphorous atoms, indicating the same geometry around the metal observed in **1**. The ^{19}F NMR spectrum shows two singlets, at 76.39 and -77.39 ppm, in a 1:1 ratio, the last one corresponds well with the peak observed for the unbound triflate anion. The signal corresponding to the N*H* proton appears at 5.36 ppm, while in **1** it is at 7.09 ppm.

Table 1: Selected bond distances and angles for HPNP complexes **3-7**.

	3 [a]	**4** [b]	**5** [b]	**6** [c]	**7** [a]
M – N1	1.920(2) Å	1.874(2) Å	2.1744(15) Å	2.336(2) Å	1.950(3) Å
M – P1	2.2319(7) Å	2.1741(9) Å	2.2448(6) Å	2.3968(10) Å	2.2403(12) Å
M - P2	2.2166(7)) Å	2.1739(9) Å	2.2470(6) Å	2.4215(10) Å	2.2297(12) Å
M – X1	-	2.3472(6) Å	2.4432(4) Å	2.3097(9) Å	-
M – X2	1.845(2) Å	-	-	2.3246(9) Å	1.894(3) Å
N2-C17	1.135(3) Å	-	-	-	1.316(4) Å
X1 – M – N1	177.42(10)°	170,07(7)°	105.68(4)°	173.16(6)°	178.52(13)°
P1 – M – P2	171.70(3)°	171.34(3)°	125.39(2)°	125.67(3)°	167.50(4)°
P1 – M – N1	86.11(6)°	86.39(8)°	86.18(4)°	78.24(6)°	85.89(8)°

[a] X = N, [b] X = Br, [c] X = Cl.

Reaction of **1** with $AgBF_4$ (instead of AgOTf) under in the similar conditions produced an intractable mixture of products. When the reaction with $AgBF_4$ is performed in CH_2Cl_2 in the presence of excess acetonitrile, complex $(HPNPNiNCCH_3)(BF_4)_2$ (**3**) is obtained as yellow, rod-like crystals, in 88% yield. The ^{1}H NMR spectrum of **3** resembles that observed for **2**, with a similar splitting pattern for the peaks corresponding to the HPNP ligand. A singlet at 1.96 ppm for the CH_3CN protons (3 H) is observed. The presence of acetonitrile bound to the metal center was confirmed by IR spectroscopy (strong absorption at 2301 cm^{-1} corresponding to the C-N stretch, free CH_3CN stretch is 2252 cm^{-1}). As in **1**, the ^{31}P NMR shows only one singlet (69.37 ppm). Interestingly, the ^{19}F NMR displays two singlets with relative integrations 3 to 1 (-150.53 and -150.60 ppm respectively), attributed to H-F interactions between the H_{amine} and the fluorine atoms in the BF_4^- anions. Similar interactions have been observed for related systems.[24]

The structure of **3** was confirmed by X-ray crystallography (Figure 3). The geometry around the metal center is square planar (N1-Ni1-N2 177.53(15)°, N2-Ni1-P1 94.20(5)°, P1-Ni1-P1 171.71(4)°, N1-Ni1-P1 86.17(9)°). The distances around the metal center and the HPNP ligand were Ni1-N1: 1.917(3) Å, Ni1-P1 2.2325(11) Å and Ni1-P2 2.2161(11) Å, in

agreement with those observed in related systems,[32] while the Ni-NC and N-C distances (1.847(3) Å and 1.130(5) Å respectively) show a small degree of activation of the nitrile group (free CH_3CN 1.1571 Å). These distances are consistent with other Ni-acetonitrile complexes found in the literature.[32, 33] There is a short H_{amine}-F contact in the solid state (2.081 Å), smaller than the sum of the Van der Waals radii (2.67 Å), supporting the idea that H-F interactions are present.

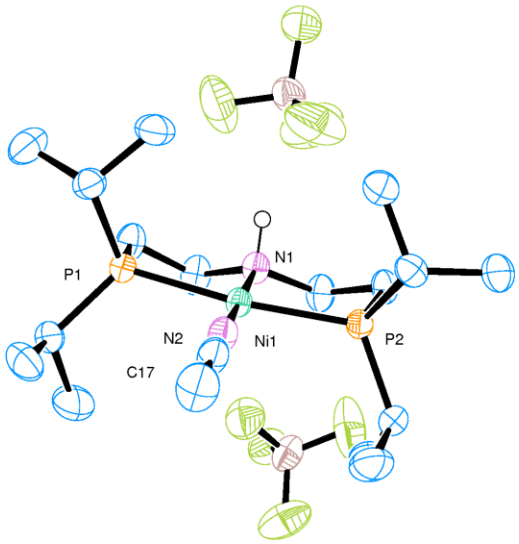

Figure 1: Thermal ellipsoid (50%) plot of **3**. Hydrogen atoms bound to carbon have been omitted for clarity.

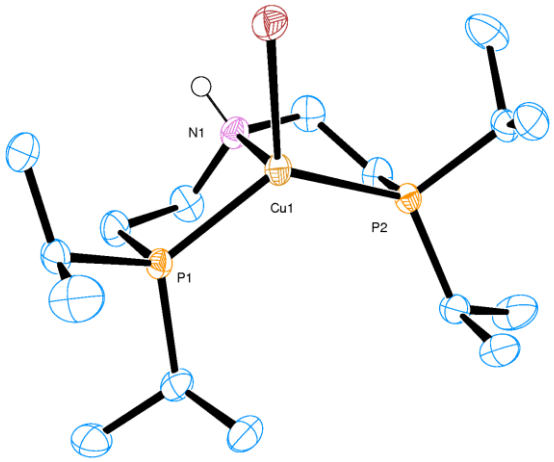

Figure 3: Thermal ellipsoid (50%) plot of **5**. Hydrogen atoms bound to carbon have been omitted for clarity.

With a Noyori-Morris-type mechanism in mind, where a concerted transfer of proton and hydride from the substrate to the catalyst occurs,[34, 35] we aimed for the synthesis of the Ni-amide derivative. The HPNP ligand can be deprotonated with n-BuLi to give LiPNP.[10] The reaction with $NiBr_2$ in THF forms PNPNiBr (**4**) in moderate yield (47%), after

crystallization from hexane. The NMR spectra for **4** shows higher symmetry than the one observed for **1-3**, with only one multiplet for each of the NC*H*$_2$, PC*H*(CH$_3$)$_2$), and PC*H*$_2$ protons, a singlet for the phosphorous atoms, and two sets of signals for the methyl groups. Recrystallization of **4** from hexane afforded crystals suitable for an X-ray diffraction study (Table 1, Figure 4). Complex **4** displays a square planar geometry, and a constriction in the Ni1-N1, Ni1-P1 and Ni1-P2 distances (1.873(2) Å, 2.1741(10) Å and 2.1738(10) Å respectively) compared with **3**. The Ni1-N1-C1 and Ni1-N1-C2 angles (120.56(19)° and 120.5(2)°) are consistent with an amide donor.

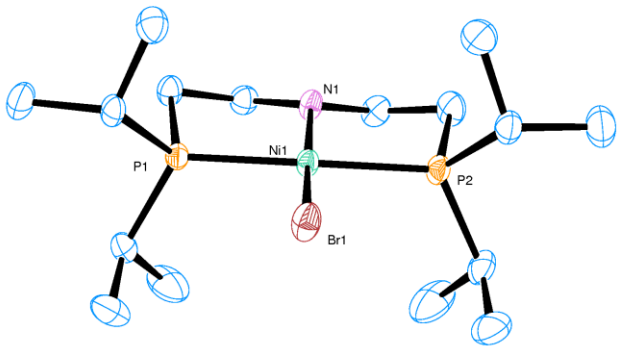

Figure 2: Thermal ellipsoid (50%) plot of **4**. Hydrogen atoms have been omitted for clarity.

Complex HPNPCuBr (**5**) was synthesized by reaction of HPNP with CuBr in THF and was purified by crystallization from a concentrated solution in toluene cooled to -40 °C. The product was obtained as colorless, block-like crystals, in 61% yield and fully characterized by ^{1}H NMR, ^{31}P NMR, and X-ray crystallography. Selected bond lengths and angles are provided in Table 1, and an ORTEP diagram is shown in Figure 5. Complex **5** displays a distorted tetrahedral geometry around the metal center. The Cu1-Br1, Cu1-N1, Cu1-P1, and Cu-P2 distances are in accordance with those found in related Cu(I) complexes.[36, 37] In solution, four multiplets assigned to the NC*H*$_2$, PC*H*(CH$_3$)$_2$), PC*H*$_2$ and C*H*$_3$ protons are observed.

Under the same reaction conditions and work-up used for **1**, the cobalt complex HPNPCoCl$_2$ (**6**) is obtained in 86% yield as pink needles. Complex **6** is paramagnetic, displaying broad signals in the ^{1}H NMR and ^{31}P NMR (27.8 ppm) spectra. The magnetic moment for the complex, calculated by the Evans method in solution, was 4.0 μ_B at 293 K, consistent with a d^7 metal center having three unpaired electrons. Crystals suitable for an X-ray diffraction study were grown from a concentrated solution of **6** in CH$_2$Cl$_2$/diethyl ether (Table 1). **6** displays a distorted trigonal bipyramidal geometry with the amine and a chlorine atom in the axial positions (N1-Co-Cl1 173.16(6)°) and the phosphines and a chloride ligand in the equatorial positions.

The electrochemical properties of the complexes synthesized were studied using cyclic voltammetry (CV) in acetonitrile as the solvent. Complexes **1-3**, **5** are water and

moisture stable enough to perform the CV experiments outside the glovebox. The potentials were referenced to the ferrocene/ferrocinium redox couple.

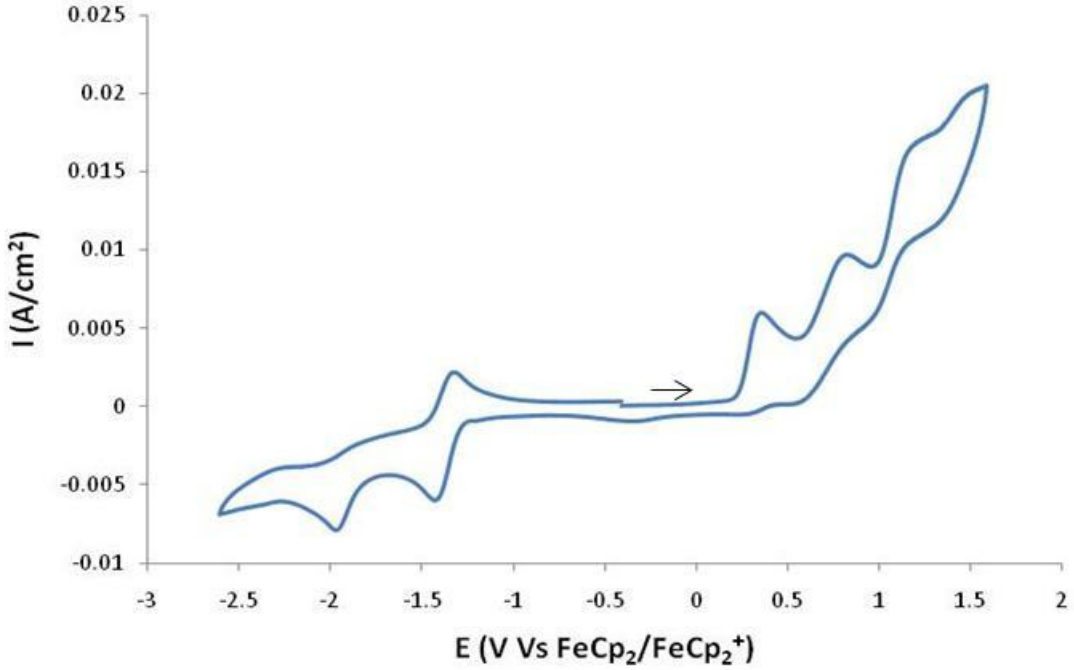

Figure 4: CV for **1**. Conditions: 15 mL CH_3CN, 2 mM complex, 0.1 M Et_4NBF_4. Scan rate: 100 mV/s.

The cyclic voltammogram of **1** (Figure 4) shows two oxidations at 0.34 V and 0.82 V corresponding to the oxidation of the bromide anion (compared with the CV of LiBr under the same conditions). These oxidations are followed by a series of irreversible oxidations that could not be assigned. On the reductive portion of the voltammogram, two waves were observed: a quasi-reversible one electron reduction at -1.38 V corresponding to the HPNPNi(II)Br/HPNPNi(I)Br redox pair, and an irreversible reduction at -1.95 V that we assigned to a Ni(I)→Ni(0) process. The loss of a ligand or rearrangement of the complex coordination sphere could account for the irreversibility of the process. Similar behavior has been previously observed for Ni complexes.[38-42]

For complex **2**, the CV shows oxidation processes above 1.0 V, similar to those observed for **1**. These processes could not be assigned. The reduction part of the voltammogram displays a reversible reduction at -1.09 V, followed by an irreversible reduction at -1.95 V (the latter is in good agreement with the process observed for **1** at -1.96 V). We assigned the reversible wave to the HPNPNi(II)/HPNPNi(I) redox pair (Figure 5). In this case the wave is completely reversible. Complex **3** also displays a one electron reversible reduction, an irreversible reduction, and several irreversible oxidations that were not assigned. Although the irreversible processes observed match those found in **1** and **2**, the reversible wave, assigned to the Ni(II)/Ni(I) redox pair, occurs at the same potential than the one observed in **2** (-1.09 V, Figure 6), indicating that in acetonitrile solution complex **2** exists as $(HPNPNiNCCH_3)(OTf)_2$.

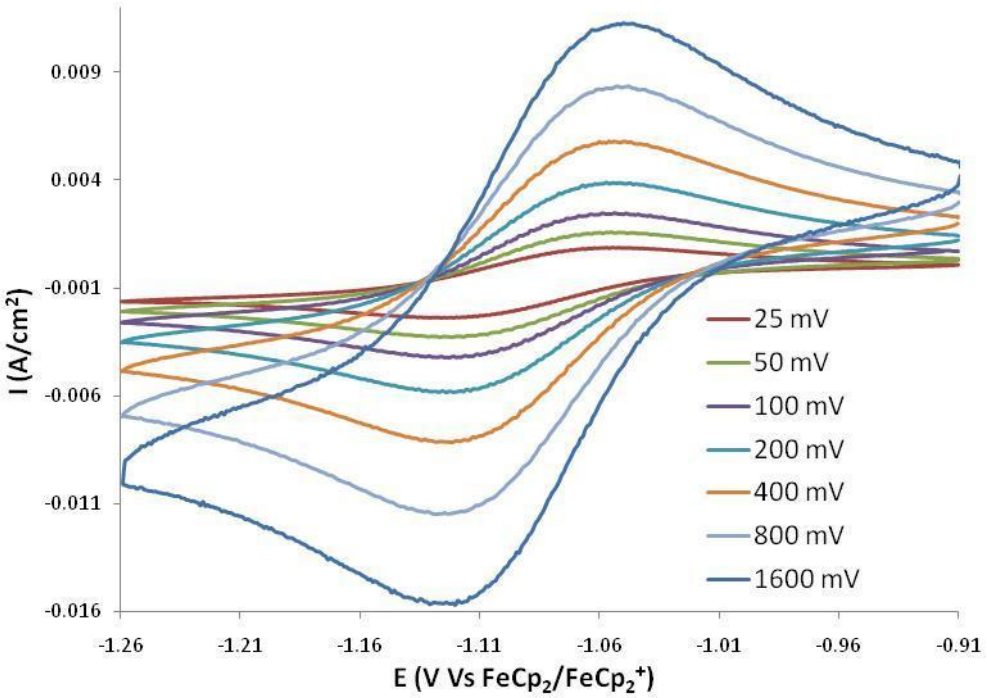

Figure 5: Reversible reduction for **2** at multiple scan rates. Conditions: 15 mL CH_3CN, 2 mM complex, 0.1 M Et_4NBF_4.

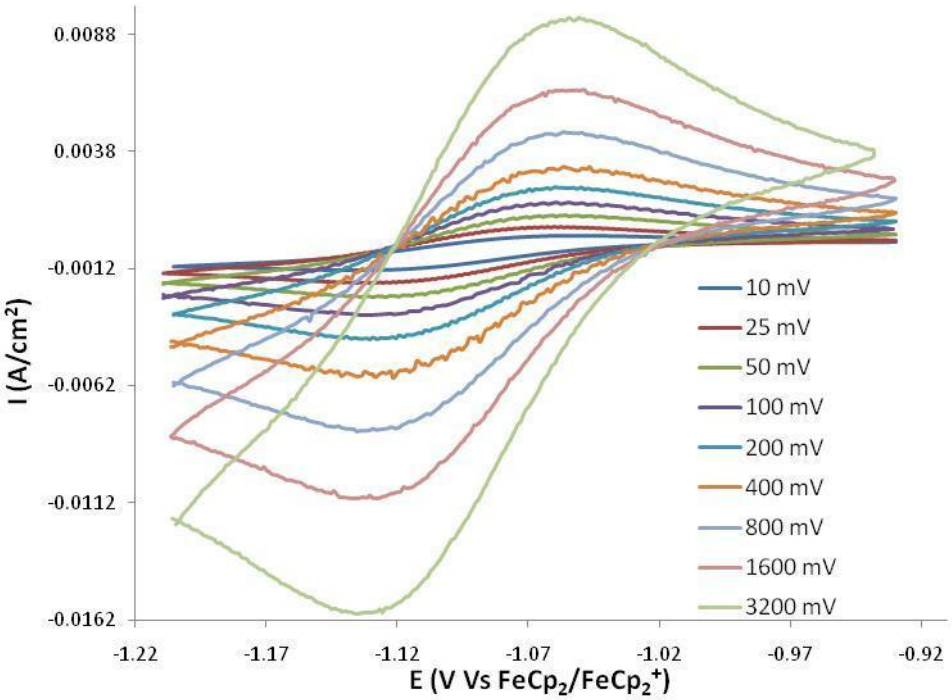

Figure 6: Reversible reduction for **3** at multiple scan rates. Conditions: 15 mL CH_3CN, 2 mM complex, 0.1 M Et_4NBF_4.

Complex **4** changes color from green to purple by dissolution it in acetonitrile. The CV shows at least four irreversible oxidations starting at -0.37 V. In the reduction section of the voltammogram, two processes were observed: a reversible reduction at -1.38 V and an irreversible reduction at -1.99 V (Figure 7). The most striking feature of the voltammogram is the low current density observed for the process at -1.38 V (1.4 A/cm^2 at 100mV/s) sweeping from -1.2 to -1.8 V. If the CV is run to oxidation potentials first (above -0.37 V), the reversible peak shows a 2.5 fold increase in the current density. If the CV of **4** is run in THF instead of CH_3CN, the same phenomenon is observed, with a 3.5 fold increase in the current density. No change of color is observed in this solvent. We envisioned that an equilibrium between the species PNPNiBr and $[PNPNiL]^+$ (L = solvent) is established in solution. The oxidation processes result in the irreversible decoordination of the bromide ligand, giving rise to the acetonitrile bound species that shows a reversible peak at -1.38 V. The second reduction (Ni(I)→Ni(0)) occurs at the same potential than previously observed.[39]

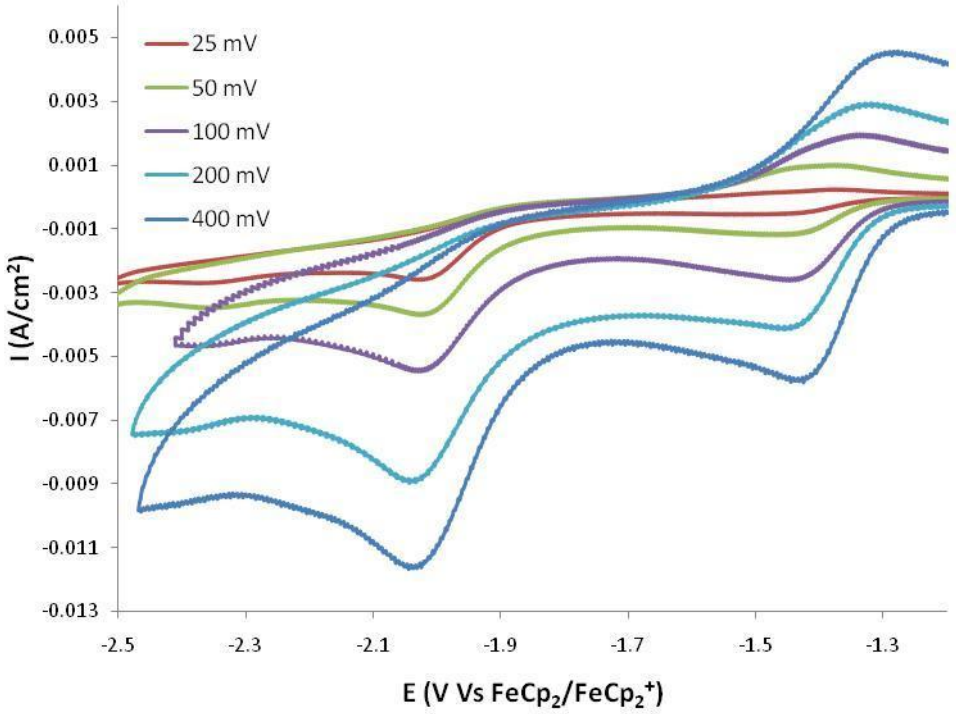

Figure 7. CV for **2** (reduction side) at different scan rates after sweeping to oxidation potentials. Conditions: 15 mL CH_3CN, 2 mM complex, 0.1 M Et_4NBF_4.

The copper complex **5** does not display any activity in the reduction region (as low potentials as -2.5 V), and the oxidation side shows a series of irreversible processes that were not assigned. The cobalt complex **6** shows two reversible curves at -1.39 V and -0.47 V. These processes were assigned to the Co(II)/Co(I) and Co(III)/Co(II) redox couples respectively (Figure 8).[38]

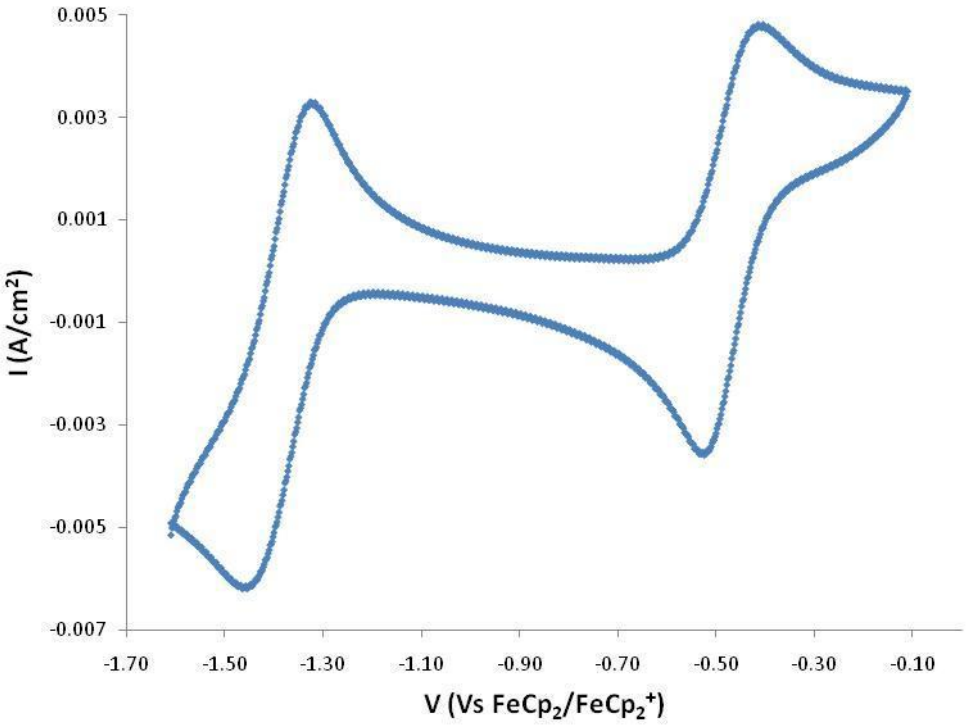

Figure 8: CV for **6**. Conditions: 15 mL CH_3CN, 2 mM complex, 0.1 M Et_4NBF_4. Scan rate: 100 mV/s.

With the goal of studying how organic substrates for dehydrogenation affect the electrochemical properties of our system, we aimed for the synthesis of a piperidine coordinated Ni species by displacing acetonitrile in **3**. The reaction was carried out in CH_2Cl_2, and a change of color from yellow to orange was observed after addition of piperidine. The reaction mixture was stirred overnight. Concentration of the solution and layering with diethyl ether produced an orange, crystalline product. The ^{1}H NMR spectrum of the reaction product shows sets of signals corresponding to the HPNP ligand and the piperidine moiety, as well as a broad singlet at 3.14 ppm (1 H), and a singlet at 3.37 ppm (3 H). The ^{31}P NMR and ^{19}F NMR spectra show that all the P and F atoms are equivalent in solution. . Two broad peaks were seen in the IR spectrum above 3000 cm^{-1}. These data are consistent with formation of a product containing a new ligand resulting from piperidine attack at the carbon atom of the acetonitrile, followed by proton transfer, producing $[(HPNP)Ni(N(H)C(CH_3)NC_5H_{10})](BF_4)_2$. Related reactivity has been observed for Al and Pt as well as other metals.[43, 44]

Confirmation of **7** came from an X-ray diffraction study with crystals grown from a CH_2Cl_2/diethyl ether solution (Table 1, Figure 9). As in **1-4**, complex **7** displays a square planar geometry around the metal center with the nitrogen atoms and phosphorous atoms trans to each other (N1-Ni1-N2 178.73(19)°, P1-Ni1-P2 167.47(5)°). The Ni-N2 and N2-C17 distances (1.892(4) Å and 1.308(6) Å, respectively) are longer than those observed in **3** (1.847(3) Å and 1.130(5) Å), in agreement with the change in hybridization from sp to sp^2. An *E* conformation for the imino product is observed. Short H-F distances are observed

between the HPNP-amine and the imine protons with the BF_4 anions (2.063 and 2.274 Å respectively).

To explore this reactivity further, we targeted the catalytic formation of $HN=C(CH_3)NC_5H_{10}$ using complex **3** as the catalyst. To the best of our knowledge, the addition of amines to nitriles without electron withdrawing groups has only been achieved catalytically with lanthanides.[45, 46] Otherwise the reaction must be carried out with stoichimetric amounts,[47, 48] or under harsh conditions in the presence of a Lewis acid.[49] After 24 h at room temperature in acetonitrile as the solvent using 5% load of **3** to piperidine, the desired imine was obtained in 47% yield determined by ^1H NMR. The synthesis of the product was confirmed by GC-MS.

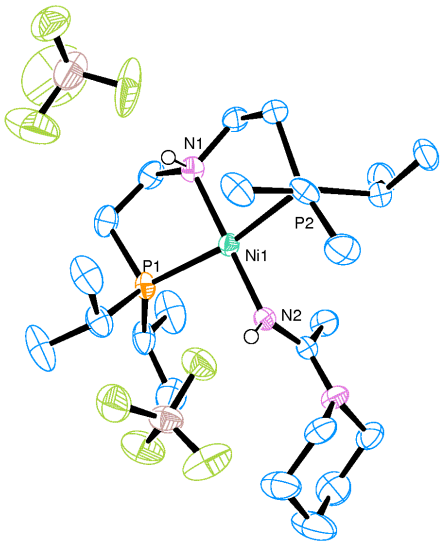

Figure 9: Thermal ellipsoid (50%) plot of **7**. Hydrogen atoms bound to carbon have been omitted for clarity.

Conclusions

A series of Ni complexes were synthesized and fully characterized by NMR techniques and X-ray diffraction studies. Their electrochemical behavior was analyzed by cyclic voltammetry. In this context, the HPNP ligand was shown to be a good scaffold to study the reductive properties of different transition metal complexes. The voltammograms of the Ni species showed that the anions used affect both the redox potential and the reversibility of the Ni(II)/Ni(I) redox pair. Finally, interesting reactivity between piperidine and acetonitrile bound to a nickel metal center was observed. The piperidine attacks the carbon atom of the nitrile group to form the amidine $HN=C(CH_3)NC_5H_{10}$ complex with an *E* configuration. The synthesis of the amidine can be performed catalytically.

Table 2. Crystal data and structure refinement for **3-7**.

	3	**4**	**5**
Formula	$C_{18}H_{40}\ B_2F_8N_2NiP_2$	$C_{16}H_{36}BrNNiP_2$	$C_{16}H_{37}BrCuPNP$
FW (g/mol)	578.77	443.02	448.86
T (K)	124(2)	128(2)	127 (2)
Space group	Pca2(1)	P-1	P-1
a (Å)	15.647	7.6375(13)	10.9127(17)
b (Å)	12.136	13.287(2)	14.507(2)
c (Å)	14.337	21.376(4)	14.876(2)
α (deg)	90.00	80.639(2)	88.971(2)
β (deg)	90.00	79.962(2)	76.820(2)
γ (deg)	90.00	78.139(2)	70.614(2)
V (Å^3)	2722.5	2072.2(6)	2158.7(6)
Z	4	4	4
λ (Å)	0.71073	0.71073	0.71073
μ (mm^{-1})	0.894	3.014	3.007
$R(F_0)$	0.0266	0.0307	0.0211
$R_w(F_0)$	0.0716	0.0709	0.0527
G. of. F.	1.049	1.021	1.037

Table 2. **Con't**. Crystal data and structure refinement for **3-7**.

	6	**7**
Formula	$C_{16}H_{37}Cl_2CoPNP$	$C_{23}H_{51}B_2F_8N_3Ni\ P_2$
FW (g/mol)	435.23	663.94
T (K)	123(2)	151(2)
Space group	P-1	Cc
a (Å)	7.365(2)	15.302(8)
b (Å)	10.492(3)	16.458(8)
c (Å)	14.101(4)	13.709(6)
α (deg)	83.855(4)	90.00
β (deg)	88.517(3)	107.915(8)
γ (deg)	77.590(3)	90.00
V (Å^3)	1058.0(5)	3285(3)
Z	2	4
λ (Å)	0.71073	0.71073
μ (mm^{-1})	1.212	0.751
$R(F_0)$	0.0359	0.0348
$R_w(F_0)$	0.0870	0.0694
G. of. F.	1.032	1.013

Experimental

General. Unless otherwise noted, all reactions were performed using standard Schlenk techniques under N_2-atm or in an N_2-atm glove box. Solvents were dried by passing through a column of activated alumina and degassed with nitrogen.[50] C_6D_6 and $CDCl_3$ were dried over Na/benzophenone and CaH_2, respectively, and vacuum transferred. All NMR spectra were obtained in $CDCl_3$, C_6D_6 or CD_3CN at ambient temperature using Bruker AVQ-400 or AVB-400 spectrometer. ^1H NMR chemical shifts (δ) were calibrated relative to residual solvent peak. The assignments were confirmed by ^1H-^1H COSY, ^1H-^{13}C HSQC, and ^{13}C-DEPT135 NMR spectroscopy. Melting points were determined using sealed capillaries prepared under a nitrogen atm. Infrared (IR) spectra were recorded with a Thermo Scientific Nicolet iS10 series FTIR spectrophotometer as Nujol mulls between KBr plates. Elemental analyses were performed at the University of California, Berkeley Microanalytical Facility. X-ray crystal diffraction analyses were performed at the University of California, Berkeley CHEXRAY facility. Cyclic voltammograms were recorded with a Gamry Reference 600™ potentiostat, using a glassy carbon working electrode, with an area of 0.049 cm^2, a 'no leak' Ag/AgCl reference electrode, and a platinum counterelectode, and calibrated to the ferrocene/ferrocinium redox couple (at 0.00 V). Magnetic susceptibility measurements were performed in $CDCl_3$ according to the Evans NMR method at 293 K.[51] The ligand HPNP was prepared according to literature procedures[10]. The remaining starting materials were obtained from Aldrich and used without further purification.

[(HPNP)NiBr]Br. A solution of HPNP (0.30 g, 0.98 mmol) in 10 mL of THF was added to a suspension of $NiBr_2$ (0.21 g, 0.96 mmol) in 15 mL of THF. The reaction mixture was stirred overnight. The solvent was removed under vacuum and the solid extracted with CH_2Cl_2 (3 x 10 mL). Concentration of the solution and layering with diethyl ether produce orange, rod-like crystals (0.39 g, 77%). ^1H NMR {$CDCl_3$} 7.10 (s (br), 1H, N*H*), 3.09 (m, 2H, NCH_2), 2.37 (m, 2H, PC*H*$(CH_3)_2$), 2.22 (m, 6H, PCH_2 (2), NCH_2 (2), PC*H*$(CH_3)_2$ (2)), 1.69 (m, 2H, PCH_2), 1.55, 1.48, 1.42 and 1.35 (td, 24H, PCH(CH_3)$_2$). $^{31}P\{^1H\}$ NMR 56.9 (s). $^{13}C\{^1H\}$ NMR 54.63 (t, N*C*H_2), 24.89 (t, P*C*H$(CH_3)_2$), 24.19 (t, P*C*H$(CH_3)_2$), 21.25 (t, P*C*H_2), 19.61, 19.13, 18.19 and 17.99 (s, PCH(*C*H_3)$_2$). IR (cm^{-1}) 3122 (w), 2799 (s), 1365 (s), 1245 (m), 1116 (w), 1055 (m), 1031 (s), 880 (m), 832 (s), 775 (w), 719 (s), 669 (m). Anal. Calc: C, 36.68; H, 7.12; N, 2.67. Observed C, 36.95; H, 7.33; N, 2.79. Mp 292-294 °C.

[(HPNP)NiOTf]OTf. (HPNPNiOTf)OTf (2). A solution of AgOTf (0.30 g, 1.06 mmol) in 15 mL of CH_2Cl_2 was added dropwise to a solution of (HPNPNiBr)Br (0.30 g, 0.57 mmol) in 15 mL of CH_2Cl_2 at room temperature. A white precipitate immediately appeared, and a color change from orange to orange-yellow was observed. The reaction mixture was stirred overnight and filtered through Celite®. The orange solution was concentrated and layered with diethyl ether to give orange, needle-like crystals (0.30 g, 79%). ^1H NMR {$CDCl_3$} 5.36 (s (br), 1H, N*H*), 2.81 (m, 2H, NCH_2), 2.60 (m, 2H, PC*H*$(CH_3)_2$), 2.31 (m, 4H, NCH_2 (2), PCH(CH_3)$_2$ (2)), 2.02 (m, 2H, PCH_2), 1.71, 1.60, 1.44 and 1.37 (td, 24H, PCH(CH_3)$_2$), 1.19 (m, 2H, PCH_2). $^{31}P\{^1H\}$ NMR 58.08 (s). ^{19}F NMR -76.39 (s, 1F), -77.39 (s, 1F). $^{13}C\{^1H\}$ NMR 56.23 (t, N*C*H_2), 24.81 (m, P*C*H$(CH_3)_2$), 20.23, 18.77, 18.23 and 17.90 (s, PCH(*C*H_3)$_2$), 17.69 (m, P*C*H_2). IR (cm^{-1}) 3444 (w), 1294 (s), 1243 (s), 1224 (s), 1159 (s), 1029 (s), 880 (w), 828 (m), 723 (m), 637 (s), 517 (w). Anal. Calc: C, 32.65; H, 5.63; N, 2.12. Observed C, 32.83; H, 5.84; N, 2.29. Mp 214-215 °C.

[(HPNPNiNCCH$_3$](BF$_4$)$_2$. A solution of $AgBF_4$ (0.23 g, 1.2 mmol) in 15 mL of CH_2Cl_2 was added dropwise to a solution of [(HPNP)NiBr]Br (0.30 g, 0.57 mmol) in 15 mL of CH_2Cl_2 and 1.0 mL of acetonitrile. A white precipitate immediately appeared, and a color change from orange to yellow was observed. The reaction mixture was stirred for 1 h and filtered through Celite®. The yellow solution was concentrated to 5 mL and layered with diethyl ether to give yellow, rod-like crystals (0.29 g, 88%). Crystals suitable for an X-ray diffraction study were grown from a concentrated solution of CH_2Cl_2 layered with diethyl ether. ^{1}H NMR {CD_3CN} 4.74 (s (br), 1H, N*H*), 3.08 (m, 2H, NCH_2), 2.79 (m, 2H, NCH_2), 2.63 (m, 2H, PC*H*(CH_3)$_2$), 2.54 (m, 2H, PC*H*(CH_3)$_2$), 2.19 (m, 2H, PCH_2), 2.09 (m, 2H, PCH_2), 2.06 (s, 3H, CNCH_3), 1.56, 1.54, 1.46 and 1.44 (m, 24H, PCH(CH_3)$_2$). ^{31}P{^{1}H} NMR 69.37 (s). ^{19}F NMR -150.53 (s, 1F), -150.60 (s, 3F). ^{13}C{^{1}H} NMR 55.00 (s, N*C*H_2), 24.89 (m, P*C*H(CH_3)$_2$), 23.49 (m, P*C*H(CH_3)$_2$), 19.52 (m, P*C*H_2), 18.21, 18.19, 17.35 and 17.04 (s, PCH(*C*H_3)$_2$). IR (cm^{-1}) 3180 (s), 2333 (m), 2301 (s, C-N), 1393 (s), 1282 (m), 1249 (s), 1217 (m), 1057 (s, br), 882 (m), 832 (s), 787 (w), 723 (s), 659 (m), 633 (s), 520 (m). Anal. Calc: C, 37.35; H, 6.97; N, 4.84. Observed C, 37.60; H, 7.04; N, 4.89. Mp 277-281 (d).

(PNP)NiBr. A solution of LiPNP (0.30 g, 0.96 mmol) in 10 mL of THF was added dropwise to a suspension of $NiBr_2$ (0.21 g, 0.96 mmol) in 15 mL of THF. The reaction mixture changed from an orange suspension to a dark green solution. After stirring the mixture overnight the solvent was removed under vacuum and the residue extracted with hexane (3 x 10 mL). Concentration of the solution and crystallization to -40 °C produced dark green, block-like crystals (0.20 g, 47%). Crystals suitable for an X-ray diffraction study were grown from a concentrated solution in hexane cooled at -40 °C. ^{1}H NMR {C_6D_6} 2.57 (m, 4H, NCH_2), 2.11 (m, 4H, PC*H*(CH_3)$_2$), 1.51 (td, 12H, PCH(CH_3)$_2$), 1.38 (m, 4H, PCH_2), 1.12 (td, 12H, PCH(CH_3)$_2$). ^{31}P{^{1}H} NMR 67.22 (s). ^{13}C{^{1}H} NMR 61.17 (t, N*C*H_2), 24.47 (t, P*C*H(CH_3)$_2$), 22.88 (t, P*C*H_2), 19.74 and 18.16 (s, *C*H_3). IR (cm^{-1}) 2767 (s), 2694 (m), 2622 (w), 1531 (w), 1459 (w), 1364 (s), 1318 (m), 1212 (w), 1153 (w), 1096 (s), 1069 (m), 1026 (s), 969 (m), 882 (s), 826 (s), 722 (s), 653 (m), 632 (s), 465 (m). Anal. Calc: C, 43.38; H, 8.19; N, 3.16. Observed C, 43.02; H, 8.28; N, 2.92. Mp 113-114 °C.

(HPNP)CuBr. A solution of HPNP (0.30 g, 0.98 mmol) in 10 mL of THF was added to a suspension of CuBr (0.14 g, 0.97 mmol) in 15 mL of THF. The reaction mixture changed from a pale green suspension to colorless after finishing the addition. The reaction mixture was stirred overnight. The solvent was removed under vacuum and the solid extracted with toluene (3 x 10 mL). Concentration of the solution and crystallization at -40 °C produced colorless, block-like crystals (0.27 g, 61%). Crystals suitable for an X-ray diffraction study were grown from a concentrated solution in toluene cooled to -40 °C. ^{1}H NMR {C_6D_6} 2.67 (s (br), 1H, N*H*), 2.40 (m, 4H, NCH_2), 1.83 (m, 4H, PC*H*(CH_3)$_2$), 1.34 (m, 4H, PCH_2), 1.16 (m, 24H, PCH(CH_3)$_2$). ^{31}P{^{1}H} NMR 2.91 (s). ^{13}C{^{1}H} NMR 45.00 (m, N*C*H_2), 24.14 (t, P*C*H(CH_3)$_2$), 23.82 (t, P*C*H_2), 19.40 (dt, *C*H_3). IR (cm^{-1}) 3227 (m), 2866 (s), 1380 (w), 1259 (m), 1229 (m), 1186 (w), 1102 (s), 1053 (s), 1040 (s), 1022 (s), 930 (w), 881 (s), 817 (s), 799 (s), 765 (m), 684 (s). Anal. Calc: C, 42.81; H, 8.31; N, 3.12. Observed C, 43.13; H, 8.46; N, 3.29. Mp 158-160 °C.

(HPNP)CoCl$_2$. The reaction was carried out analogously to that of the copper complex, starting with HPNP (0.31 g, 1.01 mmol) and $CoCl_2$ (0.13 g, 1.00 mmol) to give pink, needle-like crystals (0.37 g, 86%). Crystals suitable for an X-ray diffraction study were grown from a concentrated solution of CH_2Cl_2 layered with diethyl ether. ^{1}H NMR {$CDCl_3$} 38.8 (br),

3.85 (br), 3.25 (br), 2.36 (br), 2.10 (br), 1.94 (br), 1.74 (br), 0.63 (br), 0.14 (br). $^{31}P\{^{1}H\}$ NMR 27.8 (br). IR (cm^{-1}) 3244 (m), 1391 (m), 1242 (s), 1218 (m), 1182 (m), 1095 (s), 1043 (s), 896 (s), 829 (m), 769 (w), 698 (s), 669 (m). μ_{eff}: 4.0 μ_B. Anal. Calc: C, 44.15; H, 8.57; N, 3.22. Observed C, 44.14; H, 8.59; N, 3.43. Mp 234-235 °C.

[(HPNP)NiN(H)C(CH_3)NC_5H_{10}](BF_4)$_2$. A solution of piperidine (0.035 mL, 0.48 mmol) in 10 mL of THF was added dropwise to a solution of [(HPNP)NiBr]Br (0.20 g, 0.35 mmol) in 15 mL of THF at room temperature. A color change from orange to dark orange was observed. The reaction mixture was stirred overnight. The solution was filtered, concentrated and layered with diethyl ether to give orange, block-like, crystals (0.16 g, 76%). ^{1}H NMR {$CDCl_3$} 4.50 (s (br), 1H, N*H*), 3.56 (br, 1H, PC*H*(CH_3)$_2$), 3.37 (s, 3H, CC*H*$_3$), 3.14 (s (br) 1H, *H*N=C), 2.96 (m, 2H, NC*H*$_2$), 2.77 (s (br), 2H, *p*-NC_5H_{10}), 2.64 (m, 2H, NC*H*$_2$), 2.51 (m, 2H, PC*H*$_2$), 2.34 (m, 1H, PC*H*(CH_3)$_2$), 2.25 (m, 2H, PC*H*$_2$), 2.11 (m, 2H, PC*H*(CH_3)$_2$), 1.78 (m, 4H, *m*-NC_5H_{10}), 1.65 – 1.10 (m, 28 H, PCH(C*H*$_3$)$_2$ (24) and *o*-NC_5H_{10} (4)). ^{31}P-NMR$\{^{1}H\}$ 47.77 (s). ^{19}F NMR$\{^{1}H\}$ 152.14 (s). ^{13}C NMR$\{^{1}H\}$ 54.31 (m, *o*-N*C*$_5H_{10}$), 54.25 (m, N*C*H$_2$), 25.86 (s, N=C*C*H$_3$), 24.05 (m, P*C*H(CH_3)$_2$), 23.46 (m, P*C*H$_2$), 23.22 (m, P*C*H(CH_3)$_2$), 19.51 (m, *m*-NC_5H_{10} and *p*-NC_5H_{10}), 18.97 (s, *C*H$_3$), 18.30 (s, *C*H$_3$) 17.38 (m, *C*H$_3$). IR (cm^{-1}) 3330 (m), 3190 (m), 1596 (s), 1243 (w), 1055 (s), 1027 (s), 881 (w), 721 (m). Anal. Calc: C, 41.61; H, 7.74; N, 6.33. Observed C, 41.65; H, 7.96; N, 6.34. Mp 129-133 °C (d).

Catalysis experiment. Piperidine (0.10 mL, 1.0 mmol) was added via syringe to a solution of **3** (29 mg, 0.05 mmol) in 5.0 mL of CH_3CN and the reaction mixture was stirred for 24 h. A solution of trimethoxybenzene (23 mg, 0.14 mmol, internal standard) in 25 mL diethyl ether was added. The reaction mixture was washed with a concentrated solution of NaOH (2 x 2 mL). The organic phase was separated, dried over sodium sulfate and analyzed by ^{1}H NMR spectroscopy. An aliquot was analyzed by GC-MS and compared to reported values.[48]

Crystallographic Analyses.

Single crystals of the compounds were coated in Paratone-N oil, mounted on a Kaptan loop, transferred to a Siemens SMART, SMART APEX or SMART QUAZAR diffractometer CCD area detector[52] centered in the beam, and cooled by a nitrogen flow low-temperature apparatus that has been previously calibrated by a thermocouple placed at the same position as the crystal. Preliminary orientation matrixes and cell constants were determined by collection of 60 30-s frames, followed by spot integration and least-squares refinement. An arbitrary hemisphere of data was collected and the raw data were integrated using SAINT.[53] Cell dimensions reported were calculated from all reflections with I>10. The data were corrected for Lorentz and polarization effects, but no correction for crystal decay was applied. Data were analyzed for agreement and possible absorption using XPREP.[54] An empirical absorption correction based on comparison of redundant and equivalent reflections was applied using SADABS.[55] The structures were solved using SHELXS[56] and refined on all data by full-matrix least-squares with SHELXL-97.[57] Thermal parameters for all non-hydrogen atoms were refined anisotropically. ORTEP diagrams were created using ORTEP-32.[58]

References.

1. Albrecht, M.; van Koten, G. *Angew. Chem. Int. Ed.* **2001,** *40*, 3750-3781.
2. Gibson, V. C.; Spitzmesser, S. K. *Chem. Rev.* **2003,** *103*, 283-315.

3. van der Boom, M. E.; Milstein, D. *Chem. Rev.* **2003,** *103*, 1759-1792.
4. Chomitz, W. A.; Arnold, J. *Chem-Eur. J.* **2009,** *15*, 2020-2030.
5. Liang, L. C. *Coordin. Chem. Rev.* **2006,** *250*, 1152-1177.
6. Danopoulos, A. A.; Edwards, P. G. *Polyhedron.* **1989,** *8*, 1339-1344.
7. Danopoulos, A. A.; Edwards, P. G.; Parry, J. S.; Wills, A. R. *Polyhedron.* **1989,** *8*, 1767-1769.
8. Danopoulos, A. A.; Wills, A. R.; Edwards, P. G. *Polyhedron.* **1990,** *9*, 2413-2418.
9. Fryzuk, M. D.; Macneil, P. A. *J. Am. Chem. Soc.* **1981,** *103*, 3592-3593.
10. Chomitz, W. A.; Mickenberg, S. F.; Arnold, J. *Inorg. Chem.* **2008,** *47*, 373-380.
11. Friedrich, A.; Drees, M.; Kass, M.; Herdtweck, E.; Schneider, S. *Inorg. Chem.* **2010,** *49*, 5482-5494.
12. McGuinness, D. S.; Wasserscheid, P.; Morgan, D. H.; Dixon, J. T. *Organometallics.* **2005,** *24*, 552-556.
13. Wills, A. R.; Edwards, P. G. *J. Chem. Soc. Dalton Trans.* **1989**, 1253-1257.
14. Choualeb, A.; Lough, A. J.; Gusev, D. G. *Organometallics.* **2007,** *26*, 3509-3515.
15. Friedrich, A.; Ghosh, R.; Kolb, R.; Herdtweck, E.; Schneider, S. *Organometallics.* **2009,** *28*, 708-718.
16. Marziale, A. N.; Herdtweck, E.; Eppinger, J.; Schneider, S. *Inorg. Chem.* **2009,** *48*, 3699-3709.
17. Coles, S. J.; Danopoulos, A. A.; Edwards, P. G.; Hursthouse, M. B.; Read, P. W. *J. Chem. Soc. Dalton Trans.* **1995**, 3401-3408.
18. Coles, S. J.; Edwards, P. G.; Hursthouse, M. B.; Read, P. W. *J. Chem. Soc. Chem. Comm.* **1994**, 1967-1968.
19. Alsoudani, A. R. H.; Batsanov, A. S.; Edwards, P. G.; Howard, J. A. K. *J. Chem. Soc. Dalton Trans.* **1994**, 987-995.
20. Askevold, B.; Khusniyarov, M. M.; Herdtweck, E.; Meyer, K.; Schneider, S. *Angew. Chem. Int. Ed.* **2010,** *49*, 7566-7569.
21. Kass, M.; Friedrich, A.; Drees, M.; Schneider, S. *Angew. Chem. Int. Ed.* **2009,** *48*, 905-907.
22. Friedrich, A.; Drees, M.; auf der Gunne, J. S.; Schneider, S. *J. Am. Chem. Soc.* **2009,** *131*, 17552-17553.
23. McGuinness, D. S.; Wasserscheid, P.; Keim, W.; Hu, C. H.; Englert, U.; Dixon, J. T.; Grove, C. *Chem. Commun.* **2003**, 334-335.
24. Clarke, Z. E.; Maragh, P. T.; Dasgupta, T. P.; Gusev, D. G.; Lough, A. J.; Abdur-Rashid, K. *Organometallics.* **2006,** *25*, 4113-4117.
25. Friedrich, A.; Drees, M.; Schneider, S. *Chem-Eur. J.* **2009,** *15*, 10339-10342.
26. Staubitz, A.; Sloan, M. E.; Robertson, A. P. M.; Friedrich, A.; Schneider, S.; Gates, P. J.; Gunne, J.; Manners, I. *J. Am. Chem. Soc.* **2010,** *132*, 13332-13345.
27. Abdur-Rashid, K.; Graham, T.; Tsang, C.-W.; Chen, X.; Guo, R.; Jia, W.; Amoroso, D.; Sui-Seng, C. WO2008/141439. 2008. The complexes HNP2NiCl2, HNP2CuCl and HNP2CoCl2 have been reported in this patent but not fully characterized.
28. Chomitz, W. A.; Arnold, J. *Chem. Commun.* **2007**, 4797-4799.
29. Chomitz, W. A.; Arnold, J. *Dalton Trans.* **2009**, 1714-1720.
30. Chomitz, W. A.; Arnold, J. *Inorg. Chem.* **2009,** *48*, 3274-3286.
31. Rozenel, S. S.; Chomitz, W. A.; Arnold, J. *Organometallics.* **2009,** *28*, 6243-6253.

32. van der Vlugt, J. I.; Lutz, M.; Pidko, E. A.; Vogt, D.; Spek, A. L. *Dalton Trans.* **2009**, 1016-1023.
33. Pandarus, V.; Zargarian, D. *Organometallics.* **2007,** *26*, 4321-4334.
34. Noyori, R.; Ohkuma, T. *Angew. Chem. Int. Ed.* **2001,** *40*, 40-73.
35. Clapham, S. E.; Hadzovic, A.; Morris, R. H. *Coordin. Chem. Rev.* **2004,** *248*, 2201-2237.
36. Khan, M. M. T.; Paul, P.; Venkatasubramanian, K.; Purohit, S. *J. Chem. Soc. Dalton Trans.* **1991**, 3405-3412.
37. van der Vlugt, J. I.; Pidko, E. A.; Vogt, D.; Lutz, M.; Spek, A. L.; Meetsma, A. *Inorg. Chem.* **2008,** *47*, 4442-4444.
38. Wiedner, E. S.; Yang, J. Y.; Dougherty, W. G.; Kassel, W. S.; Bullock, R. M.; DuBois, M. R.; DuBois, D. L. *Organometallics.* **2010,** *29*, 5390-5401.
39. Wilson, A. D.; Newell, R. H.; McNevin, M. J.; Muckerman, J. T.; DuBois, M. R.; DuBois, D. L. *J. Am. Chem. Soc.* **2006,** *128*, 358-366.
40. Bhattacharya, D.; Samide, M. J.; Peters, D. G. *J. Electroanal. Chem.* **1998,** *441*, 103-107.
41. Whyte, T.; Casey, A. T.; Williams, G. A. *Inorg. Chem.* **1995,** *34*, 2781-2787.
42. Bontempelli, G.; Peccolo, R.; Daniele, S.; Ugo, P. *Inorg. Chim. Acta.* **1985,** *99*, 43-47.
43. Belluco, U.; Benetollo, F.; Bertani, R.; Bombieri, G.; Michelin, R. A.; Mozzon, M.; Pombeiro, A. J. L.; da Silva, F. C. G. *Inorg. Chim. Acta.* **2002,** *330*, 229-239.
44. Engelhardt, L. M.; Junk, P. C.; Raston, C. L.; Skelton, B. W.; White, A. H. *J. Chem. Soc. Dalton Trans.* **1996**, 3297-3301.
45. Forsberg, J. H.; Spaziano, V. T.; Balasubramanian, T. M.; Liu, G. K.; Kinsley, S. A.; Duckworth, C. A.; Poteruca, J. J.; Brown, P. S.; Miller, J. L. *J. Org. Chem.* **1987,** *52*, 1017-1021.
46. Wang, J. F.; Xu, F.; Cai, T.; Shen, Q. *Org. Lett.* **2008,** *10*, 445-448.
47. Garigipati, R. S. *Tetrahedron Lett.* **1990,** *31*, 1969-1972.
48. Rousselet, G.; Capdevielle, P.; Maumy, M. *Tetrahedron Lett.* **1993,** *34*, 6395-6398.
49. Oxley, P.; Partridge, M. W.; Short, W. F. *J. Chem. Soc.* **1947**, 1110-1116.
50. Alaimo, P. J.; Peters, D. W.; Arnold, J.; Bergman, R. G. *J. Chem. Edu.* **2001,** *78*, 64-64.
51. Piguet, C. *J. Chem. Educ.* **1997,** *74*, 815-816.
52. SMART *Area-Detector Software Package, Bruker Analytical X-ray Systems, Inc.: Madison, WI, (2001-2003).* 2001-2003.
53. SAINT *SAX Area-Detector Integration Program, V6.40; Bruker Analytical X-ray Systems Inc.: Madison, WI, (2003).* 2003.
54. PREP *(v 6.12) Part of the SHELXTL Crystal Structure Determination Package, Bruker Analytical X-ray Systems, Inc.: Madison, WI, (2001).* 2001.
55. SADABS *Bruker-Nonius Area Detector Scaling and Absorption v. 2.05 Bruker Analytical X-ray Systems, Inc.: Madison, WI (2003).* 2003.
56. SHELXS *Program for the Refinement of X-ray Crystal Structures, Part of the SHELXTL Crystal Structure Determination Package, Bruker Analytical X-ray Systems Inc.: Madison, WI, (1995-99).* 1995-1999.
57. SHELXL *Program for the Refinement of X-ray Crystal Structures, Part of the SHELXT Crystal Structure Determination Package, Bruker Analytical Systems Inc.: Madison, WI, (1995-99).* 1995-1999.
58. Farrugia, L. *J. Appl. Cryst.* **1997,** *30*, 565.

Chapter 3:

A bimetallic ruthenium complex acts as a platform to support proposed intermediates in dinitrogen reduction to ammonia

Introduction

Atmospheric nitrogen fixation to produce ammonia efficiently is one of the most challenging problems in chemistry.[1-5] Two processes account for the majority of NH_3 synthesized: the Haber and Bosch process and the biological fixation of dinitrogen.[1-4, 6-10] The former yields ammonia from dinitrogen and dihydrogen, employing an iron catalyst at high temperatures and pressures, whereas the latter occurs at ambient temperature and pressure. The most common enzyme to perform this transformation has an iron-molybdenum-sulfur cluster (the Fe-Mo cofactor) as the catalytic agent.[11, 12] Efforts have been made to explain the mechanism of nitrogen fixation via transition metal complexes.[13] The most successful experimental approaches for nitrogen reduction thus far involve a Chatt-type mechanism, in which one transition metal atom coordinates N_2, and reduction of which generates ammonia.[14, 15] Important examples of dinitrogen reactivity include the direct hydrogenation of N_2 with zirconium,[16] the reduction of hydrazine to ammonia with Fe/Mo/S cubanes[17-23] and $[Cp^*WMe_3]^+$,[24, 25] the oxidation of ammonia to N_2 via bridging species with Ru cofacial metalloporphyrins,[26] and the catalytic reduction of N_2 to ammonia at a single Mo center.[15] Recently, Schneider and coworkers have been able to stabilize a Ru(IV) nitrido complex with a PNP type ligand that undergoes hydrogenolysis at room temperature to produce ammonia in high yield.[27] While using a related pincer ligand, Nashibayashi showed that dimolybdenum dinitrogen complexes are effective catalysts for the formation of ammonia.[14]

In the nitrogenase synthesis of ammonia, it is likely than the Fe-Mo cofactor plays a bigger role in the activation of N_2 than acting solely as a single metal binding site.[11, 28] Evidence indicates than the cluster acts as the binding and reducing site for N_2, as well as the intermediates hydrazine and diazene.[9, 12, 29-32] Theoretical models suggest that N_2 binds to iron,[28, 33] whereas recent experimental work indicates that N_2 and the hydrazine intermediate formed interact with a common 4Fe-4S face in the waist region of the cluster.[9, 29, 31]

By continuing our work on the use of multidentate ligands to stabilize reactive metal centers,[34, 35] we explore the chemistry of a bimetallic ruthenium system capable of supporting a series of complexes with $(N_2)_2$, $(H_2)_2$, mixed N_2/H_2, diazene, and hydrazine ligands.[36] The system is capable of producing ammonia from N_2 in low yields and it catalytically decomposes hydrazine to produce NH_3.

Results and Discussion

The reaction of $[HPNPRuCl]_2(\mu\text{-}Cl)_2$[37] (**1**) (HPNP = $HN(CH_2CH_2P^iPr_2)_2$)[38] with two equivalents of $AgBF_4$ in THF at room temperature under nitrogen generates the complex $[HPNPRu(N_2)]_2(\mu\text{-}Cl)_2](BF_4)_2$ (**2**) as yellow needles in 74% yield. The ^1H NMR spectrum of **2** showed all the signals for the HPNP ligand, with a broad singlet at 5.76 ppm corresponding to the NH protons.

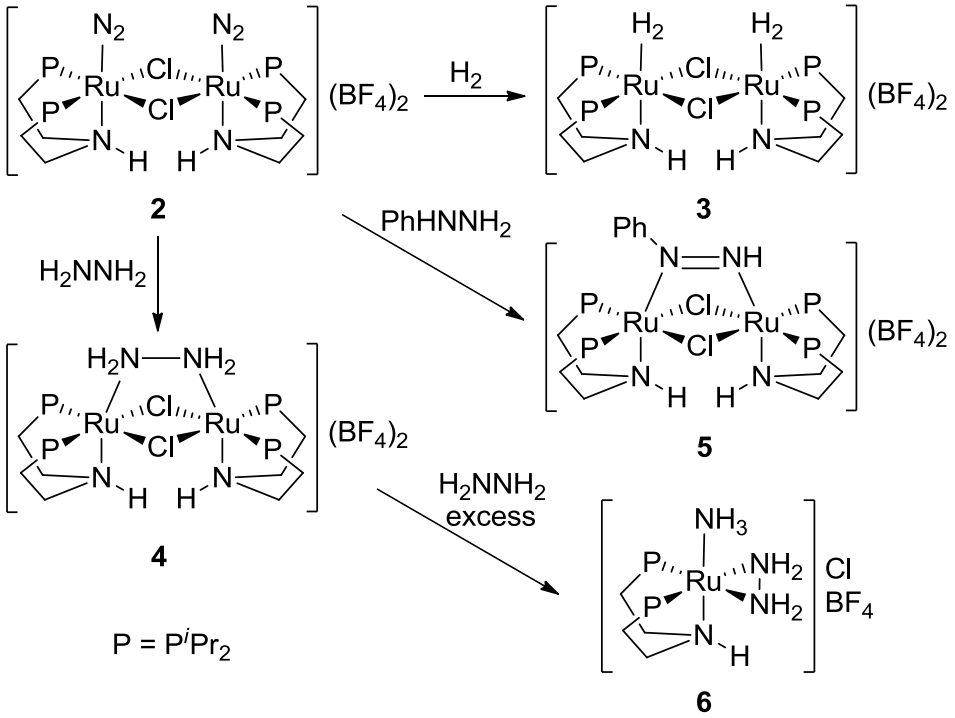

Scheme 1. Synthesis of ruthenium bimetallic complexes.

The structure of **2**, determined by X-ray diffraction, is shown in Figure 1. It consists of two ruthenium atoms bridged by two chlorides, with one N_2 molecule bound end-on to each metal center. The Ru-Ru separation is 3.8329(3) Å, the N-N bond length of 1.103(3) Å indicates a low degree of activation. The IR spectrum shows a strong absorption band at 2161 cm^{-1} for the N-N stretch. In this complex, the dinitrogen molecules display a parallel configuration, with a small dihedral angle for N2-Ru1-Ru2-N4 of 4.3(1)°. We believe that the geometry displayed by **2** is influenced by formation of hydrogen bonds between the BF_4 anion and the amine N-H. In the solid state, H_{amine}-F distances found were 2.066(9) and 2.068(8) Å, considerably shorter than the sum of the van der Waals radii (2.67 Å). The parallel geometry observed in **2** remains in solution: only one sharp signal at 72.01 ppm is seen in the ^{31}P NMR, while the ^{19}F NMR showed two signals very close to each other, at -151.41 and -151.47 ppm, consistent with the presence of H-F interactions.

Further confirmation came from an ESI-MS experiment in acetonitrile, where the molecular ion corresponding to the protonated cation $\{[(HPNPRu(\mu\text{-}Cl)_2(HPNPRu(N_2))](BF_4)\}^+$ (i.e., from loss of one N_2 ligand and one BF_4 anion bound) was detected at 1001 m/z.

Both dinitrogen ligands are displaced by H_2 to produce the complex $[(HPNPRu(H_2)Cl)_2(\mu\text{-}Cl)_2](BF_4)_2$ (**3**) as yellow needles in 74% yield. A broad singlet is observed in the ^1H NMR spectrum at -7.49 ppm, corresponding to two H_2 molecules bound in the complex, whereas the ^{31}P NMR shows a singlet at 84.09 ppm.

An X-ray analysis of **3** shows distances and angles around the metal center close to those found in **2** (Figure 1). The dihydrogen atoms were found in the Fourier map and refined isotropically after fixing one Ru–H distance to 1.69 Å. When the reaction was performed with D_2 and HD, the corresponding complexes $[(HPNPRu(D_2))_2(\mu\text{-}Cl)_2](BF_4)_2$ (**3b**) and $[(HPNPRu(HD)Cl)_2(\mu\text{-}Cl)_2](BF_4)_2$ (**3c**) were observed. For **3c** the signal appears as a 1,1,1 triplet of triplets at -7.56 ppm in the ^1H NMR due to H–D coupling and P–H coupling. The $J_{H\text{-}D}$ coupling constant was 30.4 Hz, consistent with an H–H distance of 0.91 Å.[39]

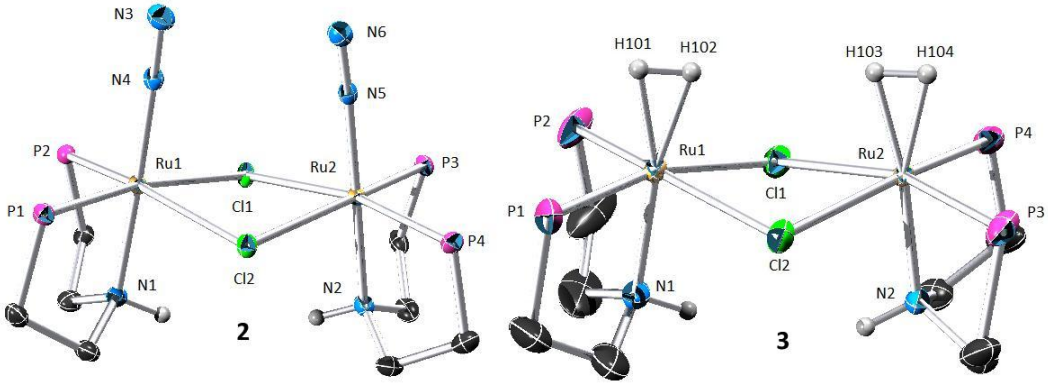

Figure 1: Thermal ellipsoid (50%) plot of the bimetallic complexes **2** and **3**. Carbon atoms of the isopropyl group, BF_4 anions, solvent molecules and hydrogen atoms have been omitted for clarity.

Species **3** reacts with N_2 to regenerate **2** after 6 days. These reactions can be followed by ^1H NMR and ^{31}P NMR (Figure 2). The two reactions proceed through the same intermediate, assigned as the mixed species $[(HPNPRu(H_2))(\mu\text{-}Cl)_2(HPNPRu(N_2))](BF_4)_2$ (**2b**). The latter shows a broad singlet at -7.41 ppm in the ^1H NMR spectrum for the H_2 protons, and two singlets in ^{31}P NMR spectrum, at 84.69 ppm and 71.95 ppm, due to the two different Ru centers. The reversible binding of H_2 was investigated by DFT calculations,[40] which show that the dinitrogen complex **2** is more stable than both the mixed dihydrogen/dinitrogen (**2b**) and the bis dihydrogen complexes (**3**) by 4.5 kcal/mol and 10.2 kcal/mol respectively.

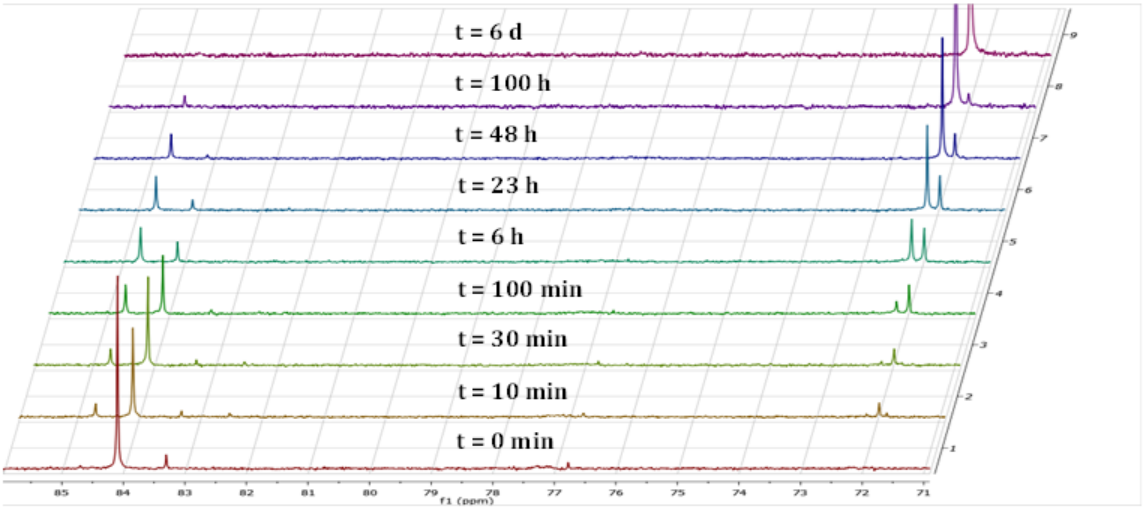

Figure 2. Reaction of **3** with excess N_2 followed by ^{31}P NMR.

Table 1: Selected bond distances and angles for Ru complexes **2**, **3** and **4a**.

	2	**3**	**4a**
Ru1 – Ru2	3.8329(3) Å	3.8078(5) Å	3.5556(9) Å
Ru1 – N3	1.950(2) Å	-	2.149(9) Å
Ru2 – N4	1.944(2) Å	-	2.138(7) Å
N3 – N4	1.103(3) Å	-	1.435(9) Å
N1 – Ru1 – N3	177.33(9)°	177.81° [a]	170.8(3)°
N2 – Ru2 – N5	178.1(1)°	171.29° [a]	171.8(3)°
N3 – Ru1 – Ru2 – N5	4.3(1)°	4.41° [b]	-12.3(3) °

[a] $N\text{-}Ru\text{-}H2_{centroid}$ angle. [b] $H2_{centroid}\text{-}Ru1\text{-}Ru2\text{-}H2_{centroid}$ torsion angle.

Reaction of **2** with one equivalent of hydrazine in THF generates the complex $[(HPNPRu)_2(\mu\text{-}H_2NNH_2)(\mu\text{-}Cl)_2](BF_4)_2$ (**4**), obtained in 58% yield as yellow crystals after work up of the reaction mixture. Complex **4** crystallizes in two conformations: from chloroform it has the same geometry observed for **2** and **3** (**4a**); from DCM/diethyl ether we see the HPNP ligands at an approximate 100º angle from each other (**4b**) (Figure 3). The parallel conformation (**4a**) shows Ru-N distances of 2.149(9) and 2.138(7) Å, a Ru-Ru distance of 3.5556(9) Å and a N-N distance of 1.435(9) Å, whereas the conformation in **4b** displays Ru1-N3 2.246(7), Ru2-N4 2.125(7) Å, Ru1-Ru2 3.525(1) and N3-N4 1.472(9) Å distances. The major crystallographic difference is in one Ru-N distance, due to the change in the atom *trans* to the nitrogen in the hydrazine (i.e. from nitrogen to phosphorus).

The ^1H NMR and ^{31}P NMR spectra show that **4a** is more stable in solution than **4b**. The ^1H NMR spectrum taken 20 min after dissolving **4b** in CD_2Cl_2 shows the presence of the two conformations: six peaks in the region between 4.5 and 6.5 ppm for **4b**, and a singlet at 5.78 ppm for **4a** in the same region. The ^{31}P NMR also shows two sets of signals, two doublets of doublets for the configuration in **4b**, and one singlet at 68.53 ppm for the one in **4a**. After 24 h, the ^1H NMR and ^{31}P NMR spectra show complete conversion to **4a**. The fact that only one signal is observed for the protons attached to nitrogen atoms in **4a** indicates fast exchange of

the NH_2 protons of the hydrazine and the NH proton in the ligand. At low temperatures (-50 °C) the singlet splits into two broad singlets, integrating 2:1. A mechanism involving reversible η^2/η^1 binding of the hydrazine, from bridging ligand to terminal, followed by hydrogen transfer from another Ru dimer accounts for the fast exchange as well as for the interconversion between the parallel and the staggered conformations. The proposed mechanism is supported by DFT: **4a** and the η^1 bound species $Ru(NH_2NH_2)/Ru(N_2)$ have the same energy (within 0.4 kcal/mol), whereas the conformation observed in **4b** is 4.5 kcal/mol less stable than that in **4a**. The complex formed by proton transfer from the ligand to the hydrazine to give the species $\{[PNPRu(NH_3)]_2(\mu\text{-}Cl)_2\}^{2+}$ requires 17.1 kcal/mol

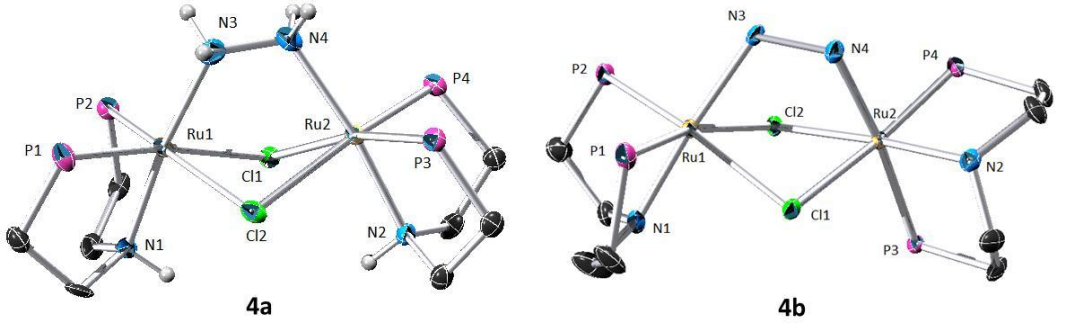

Figure 3: Thermal ellipsoid (50%) plot of the bimetallic complexes **4a** and **4b**. Carbon atoms of the isopropyl group, BF_4 anions, solvent molecules and hydrogen atoms have been omitted for clarity.

Table 2: Selected bond distances and angles for Ru complexes **4a**, **5** and **6**.

	4b	**5**	**6**
Ru1 – Ru2	3.525(1) Å	3.4121(4) Å	-
Ru1 – N3	2.246(7) Å	1.983(3) Å	2.159(2) Å [a]
Ru2 – N4	2.125(7) Å	2.084(3) Å	-
N3 – N4	1.472(9) Å	1.289(5) Å	1.436(3) Å
N1 – Ru1 – N3	90.4(2)°	172.4(1)°	175.69(8)°
N2 – Ru2 – N5	174.7(3)°	168.7(1)°	70.9(1)° [b]
N3 – Ru1 – Ru2 – N5	16.0(3)°	-1.0(1)°	-

[a] Ru-NH_3 distance. [b] $N_{hydazine}$-Ru1-$N_{hydrazine}$ angle.

Treatment of **2** with H_2NNHPh instead of hydrazine gave a purple solid in low yield (13%). After crystallization, an X-ray structure analysis showed the formation of the diazene complex $[(HPNPRu)_2(\mu\text{-}Cl)_2(\mu\text{-}HNNPh)](BF_4)_2$ (**5**) via oxidation of phenylhydrazine (Figure 4). The N-N distance is 1.289(5) Å and the Ru-N-N-Ru dihedral angle is almost planar compared to **4a,** which has a zigzag conformation (Figure 3). The ^1H NMR reveals a singlet at 15.5 ppm (1 H), consistent with the NH proton in the phenyldiazene ligand.

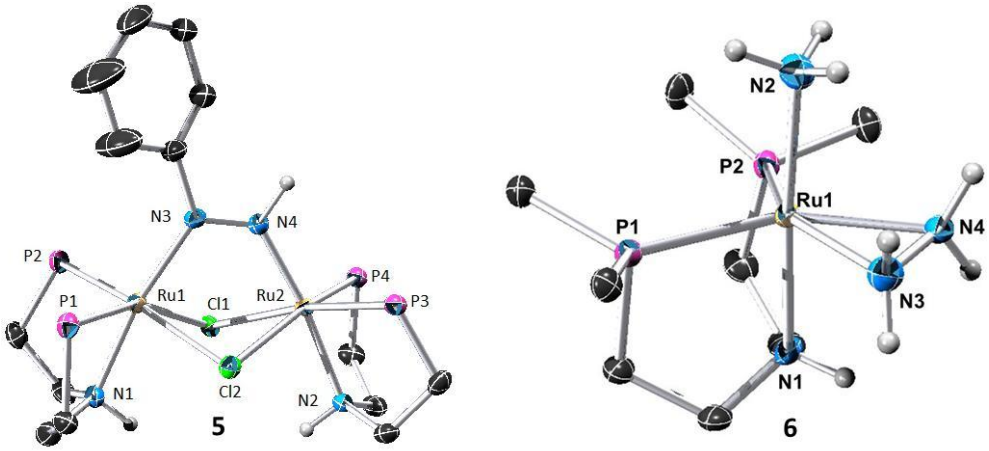

Figure 4: Thermal ellipsoid (50%) plot of complexes **5** and **6**. Carbon atoms of the isopropyl group, BF_4 anions, solvent molecules and hydrogen atoms have been omitted for clarity.

Complex **4** reacts with HCl, hydrazine, and $Cp_2Co/HLuBF_4$ to produce ammonia (Table 2). Close to 100% production of ammonia is achieved by treatment of **4** with HCl/H_2O. Ammonia is also produced by reaction with HCl/Et_2O (no hydrazine is observed in any case), and by disproportionation, with 26% yield based on hydrazine. The same yield was obtained with $Cp_2Co/HLuBF_4$, indicating that the later combination is not effective in promoting this reaction. When $HBF_4{\cdot}Et_2O$ was added to **4** under nitrogen atmosphere, we observed the production of ammonia and compound **2**, which was recovered by crystallization. Starting from the dinitrogen complex **2**, addition of Cp_2Co as the reducing agent and $LuHBF_4$ as the proton source in THF produced trace amounts of ammonia, quantified by the indophenol test.[41] No hydrazine was detected in this reaction.[42]

Table 3: Ammonia synthesis results.

Catalyst	mmol cmpd	Eq. N_2H_4	Eq. Cp_2Co	Eq. $HLuBF_4$	T.O.N.[a]	Yield NH_3[b]
4	0.011	1.0	No	No	1.93	96%
4	0.010	12.3	No	No	5.90	26%
4	0.010	11.5	85	164	5.38	26%
2	0.045	0	16	32	0.03	-

Reaction conditions: 10 mL THF, room temperature, 16 h. [a] T.O.N. per Ru dimer molecule; [b] Yield calculated based on hydrazine. Ammonia was quantified by the indophenol test.[41]

To explore further the disproportionation process, we reacted **4** with excess of hydrazine. After work up of the product, the crystal structure analysis showed the formation of the monometallic species $[HPNPRu(NH_3)(\eta^2\text{-}N_2H_4)](BF_4)Cl$ (**6**) (Figure 4). The Ru-N bond distances for hydrazine, ammonia and the ligand are very similar (2.157(2) Å, 2.159(2) Å, 2.149(3) Å and 2.136(2) Å respectively), whereas the N-N bond distance (1.436(3) Å) is practically the same as in free hydrazine. The ^1H NMR spectrum is consistent with the proposed formula; the ammonia ligand appears as a singlet at 2.06 ppm and the hydrazine as a doublet at 6.38 ppm. Formation of **6** confirms the synthesis of ammonia by a disproportionation mechanism. When the reaction is performed on an NMR scale, evolution of H_2 was observed.

The transformation of N_2 into ammonia in this system was studied by DFT to evaluate whether **2**, **3**, **4a**, and **5*** (the analogue of **5** with the phenyl replaced with H) are valid intermediates in this reaction. After optimization, their energies were compared, as shown in Figure 5. This study shows that after displacement of one dinitrogen molecule to generate the **2b**, the formation of the bridging diazene species **5*** lies at 16.4 kcal/mol higher in energy. In comparison, diazene formation from N_2 and H_2 in absence of the bimetallic ruthenium complex was 43.2 kcal/mol uphill. Complex **5*** is also more stable than the species $Ru(NNH_2)/RuN_2$ (**5b**) expected from a Chatt-type mechanism by 13.0 kcal/mol. The hydrazine complex **4a**, formed by addition of another H_2 molecule to **5***, is favored by 7.2 kcal/mol. This complex was more stable than the mixed species $Ru(=NH)/Ru(NH_3)$ (**4c**), formed by the splitting of the N-N bond (13.3 kcal/mol) by almost 22 kcal/mol in comparison with the species $Ru(NHNH_3)/Ru(N_2)$ (**4d**). The last step of the transformation – the addition of a third H_2 molecule to generate two molecules of ammonia and re-form the di-dinitrogen species – liberates 35.8 kcal/mol of energy. This DFT study indicates that the four complexes **2**, **2b**, **4a** and **5*** are valid intermediates for the transformation of N_2 to ammonia within this system.

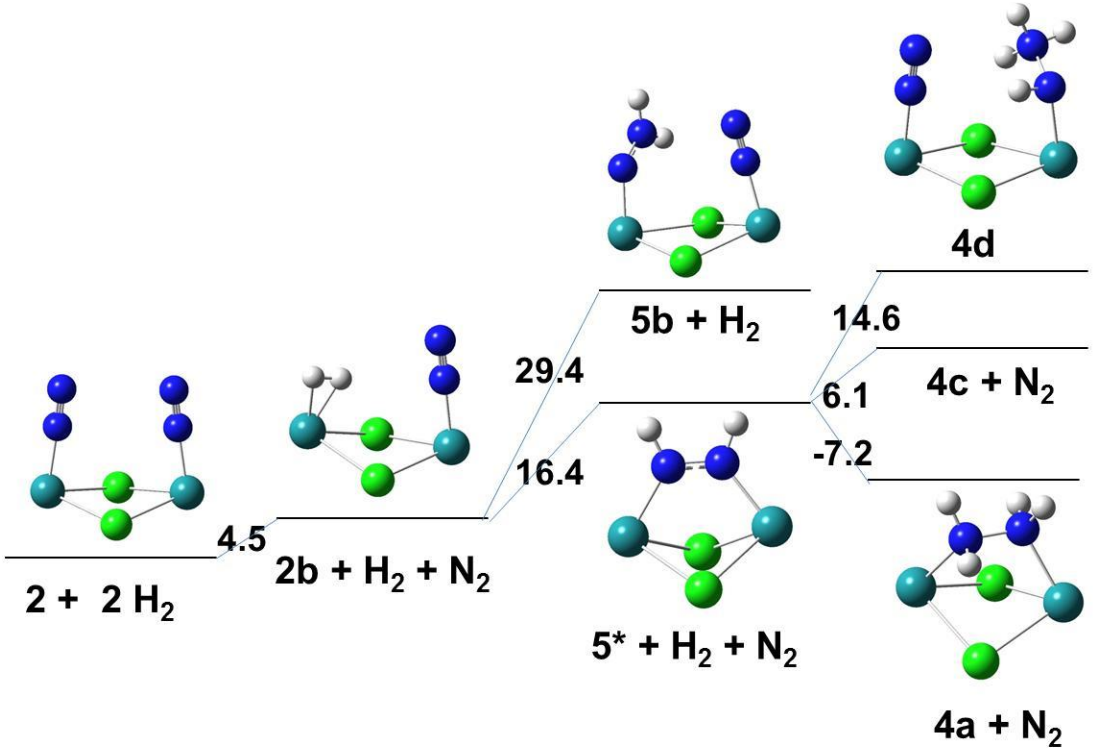

Figure 5. Zero-point energy calculations for the hydrogenation of dinitrogen with HPNPRu complexes.

We decided to synthesize the analogous ruthenium complexes with triflate and tetraphenylborate anions. Reaction of **1** with $AgOSO_2CF_3$ generates the complex $\{[HPNPRu]_2(\mu\text{-}OSO_2CF_3)(\mu\text{-}Cl)_2]\}OSO_2CF_3$ (**7**) as orange, block-like crystals in 84% yield. The ^1H NMR and ^{13}C NMR spectra show all the peaks corresponding to the HPNP ligand. The ^{31}P-NMR spectrum shows two doublets at 70.83 and 70.43 ppm with an AB pattern and

a $J_{P\text{-}P}$ coupling of 32.4 Hz. The crystal structure analysis of **7** showed one triflate coordinated to both metal centers via two oxygen atoms (Figure 6).

When the analogous reaction was carried out with two equivalents of $AgBPh_4$, complex $[(HNP_2Ru)_2(\mu\text{-}Cl)_3]BPh_4$ (**8**) was isolated as orange, block like crystals, in 67% yield. The ^{31}P-NMR spectrum shows two doublets at 76.75 ppm and 67.92 ppm, with an AX pattern and a $J_{P\text{-}P}$ coupling of 32.4 Hz. The X-ray crystallographic analysis confirmed the presence of three bridging chloride ligands. Attempts to abstract a second chloride (e. g. refluxing **8** in THF with excess of $AgBPh_4$) failed, indicating that the H-F interactions are necessary for the coordination of nitrogen.

Complex **2** reacted with two equivalents of Cp_2Co at room temperature in THF to give a yellow-orange suspension. After work up of the reaction mixture, $[(HNP_2Ru)_2(\mu\text{-}Cl)_3]BF_4$ (**9**) was obtained as an orange powder in 63% yield. The X-ray diffraction analysis of **9** shows an almost identical structure to **8** (Figure 6).

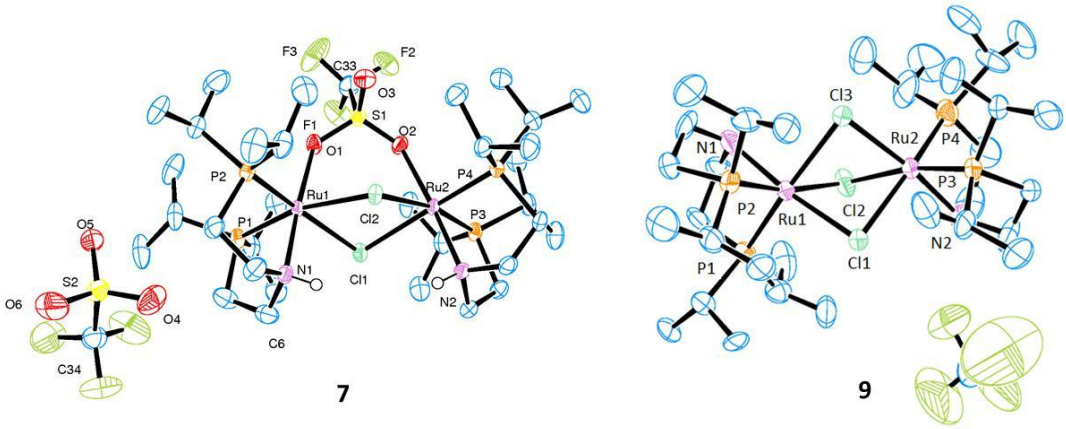

Figure 6: Thermal ellipsoid (50%) plot of the bimetallic complexes **7** and **9**. Hydrogen atoms have been omitted for clarity.

Reaction of **2** with CO in CH_2Cl_2 formed the monomeric complex $[HNP_2RuCl(CO)_2]BF_4$ (**10**) as colorless, block like crystals, in 30% yield, fully characterized by NMR spectroscopy and X-ray crystallography (Figure 7). Starting material or an intractable mixture of products resulted for the reaction of **2** with HBF_4, P_4, (thianthrene)BF_4, O_2, and N_2O.

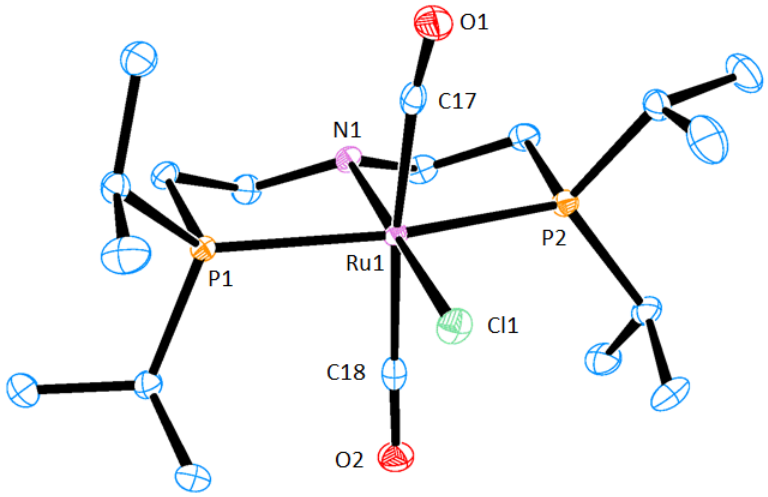

Figure 7: Thermal ellipsoid (50%) plot of **10**. BF_4 anion and hydrogen atoms have been omitted for clarity.

Conclusions

The HPNP ligand is a good a scaffold to study the chemistry of bimetallic ruthenium complexes. A series of complexes with N_2, H_2, N_2/H_2, bridging diazene, and hydrazine ligands were synthesized and characterized. For these complexes a parallel conformation is observed. The unusual geometry is due the formation of hydrogen bonds between the protons in the amine and the BF_4 anion.

The system allows study of interconversion reactions proposed as important steps for the nitrogen reduction to ammonia by the nitrogenase enzyme. When **2** is reacted with hydrazine, a dimeric complex with the hydrazine ligand bridging the two metal centers is formed (**4**). This complex further reacts with hydrazine to produce **6**, with ammonia and hydrazine bound to the Ru atom. The reaction of **2** with phenylhydrazine generates the diazene species **5**. Complex **2** also promotes the formation of ammonia from dinitrogen in the presence of protons and a reducing agent, or the catalytic formation of ammonia from hydrazine. DFT calculations support the idea that the complexes synthesized are valid intermediates for reduction of nitrogen to ammonia.

Table 4. Crystal data and structure refinement for structures **2 - 10**.

	2	**3**	**4a**
Formula	$C_{32}H_{74}B_2Cl_2F_8N_6P_4Ru_2 \cdot CH_2Cl_2$	$C_{32}H_{78}B_2Cl_2F_8N_2P_4Ru_2 \cdot CH_2Cl_2$	$C_{32}H_{78}B_2Cl_2F_8N_4P_4Ru_2 \cdot 4CHCl_3$
FW (g/mol)	1198.44	1146.43	1567.00
T (K)	113(2)	100(2)	100(2)
Space group	$P2_1/c$	$P\ 2_1\ 2_1\ 2_1$	P-1
a (Å)	15.7122(5)	16.2143(6)	11.8002(4)
b (Å)	14.9191(5)	16.7728(7)	13.2180(4)
c (Å)	22.5318(8)	18.0133(7)	22.3853(7)
α (deg)	90	90	83.049(2)
β (deg)	104.3220(10)	90	80.921(2)
γ (deg)	90	90	67.533(2)
V ($Å^3$)	5117.6(3)	4898.9(3)	3179.06(18)
Z	4	4	2
λ (Å)	0.71073	0.71073	0.71073
μ (mm^{-1})	0.985	1.023	1.219
# unique reflections	9460	8983	11647
R_{int}	0.0249	0.0318	0.0674
R [I > 2sigma(I)]	0.0267	0.0405	0.0625
$R(F_0)$*	0.0347	0.0437	0.1079
$R_w(F_0)$*	0.0853	0.1058	0.1725
G. of. F.	1.131	1.103	1.061

Table 4. **Con't.** Crystal data and structure refinement for structures **2 - 10**.

	4b	**5**	**6**
Formula	$C_{32}H_{78}B_2Cl_2F_8N_4P_4Ru_2$	$C_{38}H_{80}B_2Cl_2F_8N_4P_4Ru_2$	$C_{16}H_{45}BClF_4N_4P_2Ru\cdot CH_2Cl_2$
FW (g/mol)	1089.52	1163.60	662.75
T (K)	100(2)	100(2)	100(2)
Space group	P b c a	Cc	P 2_1 2_1 2_1
a (Å)	13.171(5)	10.1804(6)	9.2003(2)
b (Å)	18.485(5)	27.0385(18)	15.0373(4)
c (Å)	40.465(5)	19.0234(11)	20.8396(5)
α (deg)	90	90	90
β (deg)	90	93.132(3)	90
γ (deg)	90	90	90
V (Å^3)	9852(5)	4953.8(5)	2883.11(12)
Z	8	4	4
λ (Å)	0.71073	0.71073	0.71073
μ (mm^{-1})	0.909	0.910	0.972
# unique reflections	9153	4623	5317
R_{int}	0.0874	0.0281	0.0300
R [I > 2sigma(I)]	0.0760	0.0285	0.0199
$R(F_0)$*	0.0980	0.0310	0.0200
$R_w(F_0)$*	0.1707	0.0706	0.0466
G. of. F.	1.192	1.054	1.204

Table 4. Con't. Crystal data and structure refinement for structures **2 - 10**.

	7	**8**
Formula	$C_{33}H_{74}B_2Cl_2F_3N_2P_4Ru_2S\cdot CF_3O_3S$	$C_{32}H_{74}Cl_3N_2P_4Ru_2 \cdot BC_{24}H_{20}$
FW (g/mol)	1182.01	1238.36
T (K)	144(2)	109(2)
Space group	$P2_1/n$	$P2_1/c$
a (Å)	10.242(2)	15.8755(14)
b (Å)	34.018(8)	19.2248(17)
c (Å)	14.882(3)	19.4072(17)
α (deg)	90	90
β (deg)	103.049(4)	95.7450(10)
γ (deg)	90	90
V (Å^3)	5051.2(19)	5893.4(9)
Z	4	4
λ (Å)	0.71073	0.71073
μ (mm^{-1})	0.976	0.794
# unique reflections	9286	10878
R_{int}	0.0500	0.0458
R [I > 2sigma(I)]	0.0317	0.0826
$R(F_0)$*	0.0409	0.0971
$R_w(F_0)$*	0.0770	0.1871
G. of. F.	1.050	1.365

Table 4. Con't. Crystal data and structure refinement for structures **2 - 10**.

	9	**10**
Formula	$C_{32}H_{78}Cl_3N_2P_4Ru_2 \cdot BF_4 \cdot C_4H_{10}O$	$C_{18}H_{37}ClNO_2P_2Ru_2 \cdot BF_4$
FW (g/mol)	1080.26	584.76
T (K)	100(2)	100(2)
Space group	P-42$_1$c	P 2$_1$ 2$_1$ 2$_1$
a (Å)	25.3447(9)	11.7009(5)
b (Å)	25.3447(9)	12.2407(5)
c (Å)	14.4707(6)	17.5457(7)
α (deg)	90	90
β (deg)	90	90
γ (deg)	90	90
V (Å^3)	9295.3(6)	2513.02(18)
Z	2	4
λ (Å)	0.71073	0.71073
μ (mm^{-1})	1.003	0.902
# unique reflections	8224	4550
R_{int}	0.0432	0.0250
R [I > 2sigma(I)]	0.0308	0.0164
$R(F_0)$*	0.0398	0.0175
$R_w(F_0)$*	0.0752	0.377
G. of. F.	1.119	1.080

Experimental.

General considerations. Unless otherwise noted, all reactions were performed using standard Schlenk techniques under N_2-atm or in a N_2-atm glove box. Solvents were dried by passing through a column of activated alumina and degassed with nitrogen[43]. $CDCl_3$ and CD_2Cl_2 were dried over CaH_2 and vacuum transferred. All NMR spectra were obtained in $CDCl_3$ or CD_2Cl_2 at ambient temperature using Bruker AVQ-400, AV-500, DRX-500 or AV-600 spectrometers. ^{1}H NMR chemical shifts (δ) were calibrated relative to residual solvent peak. The assignments were confirmed by ^{1}H-^{1}H COSY, ^{1}H-^{13}C HSQC, and ^{13}C-DEPT135 NMR spectroscopy. Melting points were determined using sealed capillaries prepared under a nitrogen atm. Infrared (IR) spectra were recorded with a Thermo Scientific Nicolet iS10 series FTIR spectrophotometer as a powder or Nujol mulls between KBr plates or in solution with a CsF cell. Elemental analyses were performed at the University of California, Berkeley Microanalytical Facility. X-ray crystal diffraction analyses were performed at the University of California, Berkeley CHEXRAY facility. $(HNP_2RuCl)_2(\mu\text{-}Cl_2)_2$ was prepared by a modified procedure from literature.[37] The remaining starting materials were obtained from Aldrich and used without further purification.

$(HPNPRuCl)_2(\mu\text{-}Cl)_2$ (1). A solution of HPNP (1.3 g, 4.3 mmol, HPNP = $(^iPr_2PCH_2CH_2)_2NH$) in 20 mL of ethanol was added to a suspension of $[(COD)RuCl]_2(\mu\text{-}Cl)_2$ (1.2 g, 2.1 mmol) in 80 mL of ethanol. The reaction mixture was refluxed 16 h. The solution turned from brown to orange. The solvent was removed under vacuum and the solid

extracted with CH_2Cl_2. Concentration of the solution and precipitation with hexane gave an orange powder (1.6 g, 78%). ^{1}H NMR, ^{31}P-NMR matched reported literature values.[37]

{[HPNPRu(N_2)]$_2$(μ-Cl)$_2$}(BF_4)$_2$ (2). A solution of $AgBF_4$ (0.15 g, 0.77 mmol) in 10 mL of THF was added dropwise to a suspension of **1** (0.35 g, 0.37 mmol) in 15 mL of THF at room temperature and nitrogen atm. A white precipitate immediately appears, and a color change from orange to yellow was observed. The reaction mixture was stirred overnight. The solvent was removed under vacuum, and the product extracted with CH_2Cl_2 (3 x 20 mL) and filter through celite. The solution was concentrated and layered with hexane to give yellow, needle-like crystals (0.31 g, 74%). Crystals suitable for an X-ray diffraction study were grown from a concentrated solution of CH_2Cl_2 layered with diethyl ether. ^{1}H NMR ($CDCl_3$) 5.76 (s (br), 2H, N*H*), 3.21 (m, 4H, NCH_2), 2.94 (m, 4H, NCH_2), 2.58 (m, 4H, PC*H*(CH_3)$_2$), 2.14 (m, 8H, PC*H*(CH_3)$_2$ (4) and PCH_2 (4)), 1.96 (m, 4H, PCH_2), 1.49 – 1.26 (m, 48H, PCH(CH_3)$_2$) ^{31}P-NMR 72.01 (s, 4P). ^{19}F NMR -151.41 (s), -151.47 (s). ^{13}C-NMR 51.3 (s, NCH_2), 30.1 (t, P*C*H(CH_3)$_2$), 25.9 (dt, *C*H_2P), 25.0 (dt, P*C*H(CH_3)$_2$), 20.5 – 18.6 (m, *C*H_3). IR (cm^{-1}, Nujol mull) 3257 (m), 2161 (s, N_2), 1283 (w), 1259 (m), 1244 (m), 1061 (s), 959 (m), 929 (w), 906 (m), 827 (m), 818 (w), 791 (w), 729 (m), 698 (m), 665 (w), 607 (w), 520 (w). Anal. Calc: C, 34.52; H, 6.70; N, 7.55. Observed C, 34.49; H, 6.62; N, 7.32. Mp 140-143 °C (d).

{[HPNPRu(H_2)]$_2$(μ-Cl)$_2$}(BF_4)$_2$ (3a). A solution of **2** (0.30 g, 0.27 mmol) in 20 mL of CH_2Cl_2 was saturated with H_2 at room temperature and stirred for 2 days. No change of color is observed. The solution was concentrated and, keeping the H_2 atm, layered with hexane to yield yellow, block-like crystals (0.21 g, 74%). Crystals suitable for an X-ray diffraction study were grown from a concentrated solution of CH_2Cl_2 layered with diethyl ether. ^{1}H NMR ($CDCl_3$) 6.33 (s (br), 2H, N*H*), 3.50 (m, 4H, NCH_2), 3.01 and 2.89 (m, 4H, NCH_2), 2.33 (m, 4H, PC*H*(CH_3)$_2$), 2.18 (m, 4H, PC*H*(CH_3)$_2$), 1.96 (m, 4H, PCH_2), 1.86 (m, 4H, PCH_2), 1.51 – 1.05 (m, 48H, PCH(CH_3)$_2$), -7.49 (s (br), 4H, H_2). ^{31}P-NMR 83.98 (s). ^{19}F NMR -151.71 (s), -151.75 (s). ^{13}C-NMR 50.4 (s, NCH_2), 29.1 (m, P*C*H(CH_3)$_2$), 25.9 (m, *C*H_2P), 23.9 (m, P*C*H(CH_3)$_2$), 21.0- 18.0 (m, *C*H_3). IR (cm^{-1}, Nujol mull) 3259 (w), 1260 (m), 1259 (m), 1056 (s), 1061 (s), 800 (m), 668 (w). Anal. Calc: C, 36.21; H, 7.41; N, 2.64. Observed C, 35.74; H, 7.34; N, 2.61 (N_2 readily displaces H_2). Mp 161-164 °C (d).

{[HPNPRu(D_2)]$_2$(μ-Cl)$_2$}(BF_4)$_2$ (3b). A solution of **2** (30 mg, 0.027 mmol) in 0.5 mL $CDCl_3$ was placed in a J. Young NMR tube. The solution was evacuated on liquid nitrogen and the J. Young tube was filled with D_2 and warmed up to room temperature (the procedure was repeated 3 times). The reaction was monitored by ^{31}P-NMR, after 4 days the reaction was more than 90% complete. The presence of the mix species {[HPNPRu(H_2)](*μ*-Cl)$_2$[HPNPRu(N_2)]}(BF_4)$_2$ was still observed. ^{2}H NMR ($CDCl_3$) -7.55 (s). ^{31}P NMR 83.98 (s).

{[HPNPRu(HD)]$_2$(μ-Cl)$_2$}(BF_4)$_2$ (3c). The reaction was carried out analogously to that of **5b** with HD. ^{1}H NMR ($CDCl_3$) -7.56 (tt, HD), $J_{H\text{-}D}$ 30.4 Hz, $J_{H\text{-}P}$ 5.6 Hz. ^{31}P NMR{^{1}H} 83.95 (s).

[(HPNPRu)$_2$(μ-Cl)$_2$(μ-H_2NNH_2)](BF_4)$_2$ (4). Dry hydrazine (9 μL, 0.32 mmol) was added via syringe to a suspension of **2** (0.32 g, 0.29 mmol) in 25 mL of THF at room temperature and stirred overnight. The reaction goes from yellow suspension to a yellow-orange suspension. The solution was filtered over celite and the remaining solid washed with THF (2 x 5 mL). The solution was evaporated to dryness and the yellow solid formed redisolved in

CH_2Cl_2. After filtration, the solution was concentrated and layered with diethyl ether, to yield rod-like, yellow crystals (0.18 g, 58%). (**4a**) Crystals suitable for an X-ray diffraction study were grown from a concentrated solution of $CHCl_3$ slowly evaporated; (**4b**) crystals suitable for an X-ray diffraction study were grown from a concentrated solution of CH_2Cl_2 layered with diethyl ether. ^{1}H NMR (CD_2Cl_2) 5.77 (s, 6H, N*H*$_2$ and N*H*), 3.00 (m, 8H, NC*H*$_2$ (4) and PC*H*$_2$ (4)), 2.50 (m, 4H, NC*H*$_2$), 2.19 (m, 4H, PC*H*(CH_3)$_2$), 1.86 (m, 4H, PC*H*$_2$), 1.48 (m, 4H, PC*H*(CH_3)$_2$), 1.41-1.20 (m, 48 H, PCH(C*H*$_3$)$_2$). ^{31}P-NMR 68.61 (s). ^{19}F NMR -151.21 (s). ^{13}C-NMR 51.43 (N*C*H$_2$), 30.01 (t, P*C*H(CH_3)$_2$), 28.13 (m, P*C*H$_2$), 25.30 (t, P*C*H(CH_3)$_2$), 20.20 (s, *C*H$_3$), 20.06 (s, *C*H$_3$), 19.87 (s, *C*H$_3$), 18.64 (s, *C*H$_3$). IR (cm^{-1}, Nujol mull) 3331 (m, NH_2), 3273 (m NH_2)), 1598 (m, NH_2)), 1051 (s), 1335 (w), 1256 (w), 1051 (s), 998 (s), 882 (s), 826 (s), 763 (m), 700 (m). Anal. Calc: C, 35.28; H, 7.22; N, 5.14. Observed C, 35.02; H, 7.02; N, 5.02. Mp 188-188 °C (d).

[(HPNPRu)$_2$(μ-Cl)$_2$(μ-HNNPh)](BF$_4$)$_2$ (5). Dry H_2NNHPh (27 μL, 0.27 mmol) was added via syringe to a suspension of **2** (0.30 g, 0.27 mmol) in 25 mL of THF at room temperature and stirred overnight. The reaction goes from yellow suspension to a purple suspension. The solution was filtered of and the remaining purple solid washed with THF (2 x 5 mL). The solid was dissolved in CH_2Cl_2 and filtered over celite. The solution was concentrated and layered with diethyl ether, to yield plate-like, dark red crystals (0.04 g, 13%). Crystals suitable for an X-ray diffraction study were grown from a concentrated solution of CH_2Cl_2 layered with diethyl ether. ^{1}H NMR (CD_2Cl_2) 15.55 (s, 1H, PhNN*H*), 7.71 (d, 2H, *o*-C_6H_5), 7.63 (7, 1H, *p*-C_6H_5), 7.55 (t, 2H, *m*-C_6H_5), 6.31 (m, 1H, NH), 6.27 (m, H, NH), 3.26 (m, 4H, N*H*$_2$), 2.88 (m, 2H, N*H*$_2$), 2.69 (m, 2H, N*H*$_2$), 2.58 (m, 2H, PC*H*(CH_3)$_2$), 2.47 (m, 2H, PC*H*(CH_3)$_2$), 2.25 (m, 8H, PC*H*(CH_3)$_2$ (4) and PC*H*$_2$ (4)), 2.05 (m, 2H, PC*H*$_2$), 1.98 (m, 2H, PC*H*$_2$), 1.50-0.88 (m, 48 H, PCH(C*H*$_3$)$_2$). ^{31}P-NMR 63.60 (s), 56.55 (s). ^{19}F NMR -152.01 (s). ^{13}C-NMR 156.56 (*i-C*), 130.02 (*m-C*), 128.53 (*p-C*), 121.63 (*m-C*), 50.30 and 50.03 (s, N*C*H$_2$), 37.34 (m, P*C*H(CH_3)$_2$), 31.51 and 29.26 (m, *C*H$_2$P), 26.87 and 24.92 (m, P*C*H(CH_3)$_2$), 21.25-19.02 (m, *C*H$_3$). IR (cm^{-1}, Nujol mull) 3259 (w, NH), 3160 (w, NH)), 1260 (s, N=N)), 1021 (s),800 (m), 720 (w), 689 (w). Anal. Calc: C, 39.22; H, 6.93; N, 4.81. Observed C, 38.86; H, 6.82; N, 4.67. Mp 245-249 °C (d).

[HPNPRu(NH$_3$)(η^2-N$_2$H$_4$)](BF$_4$)Cl (6). Dry hydrazine (36 μL, 1.1 mmol) was added via syringe to a solution of **4** (0.05 g, 0.046 mmol) in 5 mL of CH_2Cl_2 at room temperature under Ar atm. The reaction solution goes from yellow to light yellow. After 48 h the solution was layered with diethyl ether to yield rod-like, colorless crystals (0.03 g, 57%). Crystals suitable for an X-ray diffraction study were grown from a concentrated solution of CH_2Cl_2 layered with diethyl ether. ^{1}H NMR (CD_2Cl_2) 6.38 (d, 4 H, N_2H_4), 5.93 (s, 1H, NH), 2.77 (m, 2H, PC*H*(CH_3)$_2$), 2.65 (m, 2H, N*H*$_2$), 2.58 (m, 2H, N*H*$_2$), 2.47 (m, 2H, PC*H*$_2$), 2.15 (m, 2H, PC*H*$_2$), 2.06 (s, 3H, N*H*$_3$), 1.91 (m, 2H, PC*H*(CH_3)$_2$), 1.39-1.11 (m, 24H, PCH(C*H*$_3$)$_2$). ^{31}P-NMR 80.19 (s). ^{19}F NMR -149.24 (s), 149.29 (s). IR (cm^{-1}, Nujol mull) 3287 (m, NH), 3110 (m, NH_2)), 1614 (m), 1574 (m), 1427 (m), 1300 (m), 1251 (w), 1150 (m), 1030 (s), 1003 (s), 926 (m), 880 (s), 818 (s), 727 (s), 698 (s). $C_{16}H_{44}BClF_4N_4P_2Ru{\cdot}CH_2Cl_2$ Anal. Calc: C, 30.78; H, 7.00; N, 8.45. Observed C, 30.69; H, 7.14; N, 8.84. Mp 97-100 °C (d).

[(HNP$_2$Ru)$_2$(μ-Cl)$_2$(μ-OSO$_2$CF$_3$)]OSO$_2$CF$_3$ (7). A solution of $AgOSO_2CF_3$ (0.16 g, 0.62 mmol) in 10 mL of THF was added dropwise to a suspension of (HNP$_2$RuCl)$_2$(μ-Cl)$_2$ (0.30 g, 0.31 mmol) in 15 mL of THF at room temperature. A white precipitate appears and a color change from orange to yellow was observed. The reaction mixture was stirred overnight. The

solvent was removed under vacuum, the product was extracted with CH_2Cl_2 (3 x 20 mL) and filter through celite. The solution was concentrated and layered with hexane to give orange, block-like crystals (0.31 g, 84%). Crystals suitable for an X-ray diffraction study were grown from a concentrated solution of CH_2Cl_2 layered with diethyl ether. ^{1}H NMR 5.94 (s (br), 2H, N*H*), 3.26 (m, 2H, PC*H*$(CH_3)_2$), 2.95 (m, 4H, PC*H*$(CH_3)_2$ (2), NC*H*$_2$ (2)), 2.73 (m, 2H, NC*H*$_2$), 2.45 (m, 2H, NC*H*$_2$), 2.33 (m, 2H, NC*H*$_2$), 2.11 (m, 2H, PC*H*$(CH_3)_2$), 2.00 (m, 4H, PC*H*$_2$), 1.93 (m, 2H, PC*H*$(CH_3)_2$), 1.6-1.2 (m, 48, PCH(C*H*$_3)_2$), 1.10 (m, 4H, PC*H*$_2$). ^{31}P-NMR 70.83 (d, 2P), 70.43 (d, 2P). ^{19}F-NMR -77.26 (s, 3F), -77.67 (s, 3F). ^{13}C-NMR 54.8 (d, NC*H*$_2$), 31.1 (d, P*C*H$(CH_3)_2$), 30.2 (d, P*C*H$(CH_3)_2$), 29.5 (d, P*C*H$_2$), 27.3 (d, P*C*H$_2$), 25.0 (m, P*C*H$(CH_3)_2$), 19.7-19.1(m, *C*H$_3$). IR (cm^{-1}, Nujol mull) 3444 (w), 1295 (s), 1243 (s) 1224 (s), 1159 (s), 1029 (s), 880 (w), 828 (w), 723 (m), 637 (w), 574 (w), 517 (w). Anal. Calc: C, 34.55; H, 6.31; N, 2.37; S, 5.43. Observed C, 34.67; H, 6.24; N, 2.52; S, 5.83. Mp > 300 °C.

[(HNP$_2$Ru)$_2$(μ-Cl)$_3$]BPh$_4$ (8). A solution of AgBPh$_4$ (0.34 g, 0.79 mmol) in 10 mL of THF was added dropwise to a suspension of (HNP$_2$RuCl)$_2$(μ-Cl)$_2$ (0.30 g, 0.31 mmol) in 15 mL of THF at room temperature. A white precipitate appears and a color change from orange to yellow-orange was observed. The reaction mixture was stirred overnight, and then refluxed 24 h. The solvent was removed under vacuum, the product was extracted with CH_2Cl_2 (3 x 20 mL) and filter through celite. The solution was concentrated and layered with diethyl ether to yield orange, block-like crystals (0.26 g, 67%). Crystals suitable for an X-ray diffraction study were grown from a concentrated solution of CH_2Cl_2 layered with diethyl ether. ^{1}H NMR 7.44 (m (br), 8H, *m-H*, BPh$_4$), 7.03 (t, 8H, *o-H*, BPh$_4$), 6.88 (t, 4H, *p-H*, BPh$_4$), 3.96 (s (br), 2H, N*H*), 3.10 (m, 2H, PC*H*$(CH_3)_2$), 2.82 (m, 2H, PC*H*$(CH_3)_2$), 2.54 (m, 2H, NC*H*$_2$), 2.15 (m, 2H, NC*H*$_2$), 2.09 (m, 2H, NC*H*$_2$), 1.83 (m, 6H, NC*H*$_2$ (2), PC*H*$_2$ (4)), 1.72 (m, 2H, PC*H*$(CH_3)_2$), 1.55 – 1.14 (m, 52H, PC*H*$(CH_3)_2$ (2), PC*H*$_2$ (2), PCH(C*H*$_3)_2$ (48)), 0.89 (m, 2H, PC*H*$_2$). ^{31}P-NMR 76.75 (d, 2P), 67.92 (d, 2P). ^{13}C-NMR 136.6 (*i-C*, BPh$_4$), 125.9 (*o-C*, *m-C*, BPh$_4$), 122.0 (*p-C*, BPh$_4$), 51.9 (d, NC*H*$_2$), 31.3 (d, P*C*H$(CH_3)_2$), 29.5 (d, P*C*H$_2$), 29.2 (t, PCH(CH3)2), 20.7-18.8 (m, *C*H$_3$). IR (cm^{-1}, powder) 3249 (w), 3053 (w), 2954 (m), 2928 (m), 2869 (m), 1580 (w), 1458 (s), 1427 (m), 1404 (w), 1388 (m), 1368 (m), 1252 (w), 1183 (w), 1087 (s), 1053 (m), 1031 (m), 883 (s), 816 (s). Anal. Calc: C, 54.30; H, 7.65; N, 2.26. Observed C, 54.57; H, 7.73; N, 2.38. Mp 285-288 °C.

[(HNP$_2$Ru)$_2$(μ-Cl)$_3$]BF$_4$ (9). A solution of cobaltocene (0.10 g, 0.54 mmol) in 10 mL of THF was added dropwise to a suspension of **2** (0.30 g, 0.27 mmol) in 15 mL of THF at room temperature under nitrogen atm. A color change from a yellow suspension to a yellow-orange suspension was observed. The reaction mixture was stirred overnight. The solvent was removed under vacuum, and the product washed with diethyl ether (2 x 5 mL) and THF (3 x 5 mL). The analytically pure product was obtained as an orange powder (0.17 g, 63%). Crystals suitable for an X-ray diffraction study were grown from a concentrated solution of CH_2Cl_2 layered with diethyl ether. ^{1}H NMR 4.30 (s (br), 2H, N*H*), 3.15 (m, 2H, PC*H*$(CH_3)_2$), 2.86 (m, 4H, NC*H*$_2$), 2.75 (m, 2H, PC*H*$(CH_3)_2$), 2.07 (m, 4H, NC*H*$_2$), 2.04 (m, 2H, PC*H*$(CH_3)_2$), 1.91 (m, 4H, PC*H*$_2$), 1.72 (m, 2H, PC*H*$(CH_3)_2$), 1.51 – 1.08 (m, 52H, PCH(C*H*$_3)_2$ (48) and PC*H*$_2$ (4)) ^{31}P-NMR 77.14 (d, 2P), 68.0 (d, 2P). ^{19}F NMR -152.29 (s), -152.34 (s). ^{13}C-NMR 53.5 (s, NC*H*$_2$), 51.8 (s, NC*H*$_2$), 31.2 (d, PC*H*$(CH_3)_2$), 29.6 (d, *C*H$_2$P), 29.3 (t, P*C*H$(CH_3)_2$), 26.4 (d, *C*H$_2$P), 26.4 (d, P*C*H$(CH_3)_2$), 20.9- 18.8 (m, *C*H$_3$). IR (cm^{-1}, Nujol mull) 3118 (m), 1377 (m), 1325 (w), 1260 (m), 1040 (s), 687 (m), 834 (m), 801 (s),

494 (w). Anal. Calc: C, 38.20; H, 7.41; N, 2.78. Observed C, 38.50; H, 7.24; N, 2.63. Mp 282-284 °C.

[$HNP_2RuCl(CO)_2$]BF_4 (10). A solution of **2** (0.25 g, 0.22 mmol) in 15 mL of CH_2Cl_2 was saturated with CO at room temperature and stirred overnight. The reaction goes from yellow to pale yellow (almost colorless) solution. The solution was concentrated and layered with diethyl ether, to yield block-like, colorless crystals (0.08 g, 30%). Crystals suitable for an X-ray diffraction study were grown from a concentrated solution of CH_2Cl_2 layered with diethyl ether. ^{1}H NMR 4.70 (s (br), 1H, N*H*), 3.36 (m, 2H, PCH_2), 2.66 (m, 4H, PC*H*$(CH_3)_2$), 2.28 (m, 2H, PCH_2), 2.03 (m, 4H, NCH_2), 1.61 – 1.32 (m, 24H, PCH(C$H_3)_2$). ^{31}P-NMR 49.79 (s). ^{19}F NMR -150.08 (s), -150.13 (s). ^{13}C-NMR 199.8 (s, *C*O), 194.2 (s,*C*O), 57.7 (s, N*C*H_2), 31.8 (t, P*C*H$(CH_3)_2$), 27.4 (t, *C*H_2P), 26.6 (t, P*C*H$(CH_3)_2$), 19.9 (s, *C*H_3), 19.2 (s, *C*H_3), 19.2 (s, *C*H_3), 19.0 (s, *C*H_3). IR (cm^{-1}, Nujol mull) 3264 (m), 2090 (m), 2008 (s, CO), 1991 (s, CO), 1377 (m), 1104 (s), 1059 (s), 834 (m), 788 (w), 707 (w), 669 (w), 585 (s). Anal. Calc: C, 36.97; H, 6.33; N, 2.40. Observed C, 36.71; H, 6.33; N, 2.33. Mp 301-304 °C (d).

Ammonia synthesis by disproportionation of hydrazine.[18] In a typical experiment, 5 µL hydrazine (0.16 mmol) were added to a suspension of **4** (11.0 mg, 0.010 mmol) in 10 mL THF. The reaction mixture was stirred for 16 h and 0.2 mL concentrated HCl were added via syringe. The volatiles were removed under vacuum and 15 mL of a 4 M NaOH/water solution were added under Ar atm. Between 10 – 12 mL of the solution were distilled to 12 mL of H_2SO_4 (0.5 M) and the volume was taken to 25 mL with distil water. The amount of ammonia produced was analyzed by the indophenol test.[41] Additionally, the reaction mixture was treated with HCl/Et_2O (1M) and the formation of ammonia confirmed by ^{1}H NMR in d^6-dmso.

Ammonia synthesis by reaction of 4 with hydrazine, cobaltocene and lutidinium tetrafluoroborate.[25] In a typical experiment **4** (11.0 mg, 0.010 mmol)), cobaltocene (160 mg, 0.85 mmol) and lutidinium were placed in a Schlenk tube. THF (10 mL) and 5 µL hydrazine (0.16 mmol) were added via syringe at -78ºC. The reaction mixture was warmed up to room temperature, stirred for 16 h and worked up as for the disproportionation reaction.

Ammonia synthesis by disproportionation of 4. The same procedure mention before was followed without the addition of hydrazine. The formation of ammonia was quantified by the indophenol test and confirmed by ^{1}H NMR. Hydrazine presence was analyzed by the p-(dimethylamino) benzaldehyde test.[42]

Ammonia synthesis by reaction of 2 with cobaltocene and lutidinium tetrafluoroborate.[25] In a typical experiment **2** (50.0 mg, 0.045 mmol), cobaltocene (140 mg, 0.74 mmol) and lutidinium were placed in a Schlenk tube. THF (20 mL) was added at -78 °C via syringe. The reaction mixture was warmed up at room temperature and stirred for 48 h. Concentrated HCl (0.2 mL) was added via syringe. The volatiles were removed under vacuum and 15 mL of a 4 M NaOH/water solution were added under Ar atm. Between 10 – 12 mL of the solution were distilled to 12 mL of H_2SO_4 (0.5 M) and the volume was taken to 25 mL with distil water. The amount of ammonia produced was analyzed by the indophenol test[41] and hydrazine presence was analyzed by the p-(dimethylamino) benzaldehyde test.[42] Additionally, the reaction mixture was distilled to 12 mL HCl/water (1M). The solution was dried under vacuum at 80 °C for 20 h and the ammonia formation was confirmed by ^{1}H NMR. Ammonia was also confirmed by ^{1}H NMR in d^6-dmso after treating the reaction mixture with HCl/Et_2O (1M).

Crystallographic Analyses. Single crystals of **2** to **10** were coated in Paratone-N oil, mounted on a Kaptan loop, transferred to a Bruker SMART APEX or APEX II QUAZAR diffractometer with CCD area detector,[44] centered in the beam, and cooled by a nitrogen flow low-temperature apparatus that has been previously calibrated by a thermocouple placed at the same position as the crystal. Preliminary orientation matrixes and cell constants were determined by collection of 60 30-s frames, followed by spot integration and least-squares refinement. A data collection strategy was computed with COSMO to ensure a redundant and complete data set, and the raw data were integrated using SAINT.[45] The data were corrected for Lorentz and polarization effects, but no correction for crystal decay was applied. An empirical absorption correction based on comparison of redundant and equivalent reflections was applied using SADABS.[46] XPREP[47] was used to determinate the space group. The structures were solved using SHELXS[48] and refined on all data by full-matrix least-squares with SHELXL-97.[49] Thermal parameters for all non-hydrogen atoms were refined anisotropically. ORTEP diagrams were created using ORTEP-32.[50]

Computational Details. All structures and energies were calculated using the Gaussian09 suite of programs.[51] Self-consistent field computations were performed with tight convergence criteria on ultrafine grids, while geometry optimizations were converged to tight geometric convergence criteria for all compounds. Spin expectation values <S>2 indicated that spin contamination was not significant in any result. Frequencies were calculated analytically at 298.15 K and 1 atm. Structures were considered true minima if they did not exhibit imaginary vibration modes. Optimized geometries were compared using the sum of their electronic and zero-point energies. In order to reduce the computational time, the isopropyl groups attached to phosphorous were substituted for methyl groups.

The B3LYP hybrid functional was used throughout this computational study.[52, 53] For geometry optimizations and frequency calculations, the light atoms were treated with 6-31++G(d,p) basis set,[51] whereas the Ru atoms were treated with ECP28MWB[54] Stuttgart-type basis set.[54, 55]

References

1. Hidai, M.; Mizobe, Y. *Chem. Rev.* **1995,** *95*, 1115-1133.
2. Howard, J. B.; Rees, D. C. *Chem. Rev.* **1996,** *96*, 2965-2982.
3. MacKay, B. A.; Fryzuk, M. D. *Chem. Rev.* **2004,** *104*, 385-401.
4. Hazari, N. *Chem. Soc. Rev.* **2010,** *39*, 4044-4056.
5. Rodriguez, M. M.; Bill, E.; Brennessel, W. W.; Holland, P. L. *Science* **2011,** *334*, 780-783.
6. Somorjai, G. A. *Chem. Rev.* **1996,** *96*, 1223-1235.
7. Crossland, J. L.; Tyler, D. R. *Coordin. Chem. Rev.* **2010,** *254*, 1883-1894.
8. Tuczek, F.; Horn, K. H.; Lehnert, N. *Coordin. Chem. Rev.* **2003,** *245*, 107-120.
9. Barney, B. M.; Lee, H. I.; Dos Santos, P. C.; Hoffmann, B. M.; Dean, D. R.; Seefeldt, L. C. *Dalton Trans.* **2006**, 2277-2284.
10. Hendrich, M. P.; Gunderson, W.; Behan, R. K.; Green, M. T.; Mehn, M. P.; Betley, T. A.; Lu, C. C.; Peters, J. C. *Proc. Natl. Acad. Sci. U.S.A.* **2006,** *103*, 17107-17112.
11. Howard, J. B.; Rees, D. C. *Proc. Natl. Acad, Sci. U.S.A.* **2006,** *103*, 17088-17093.
12. Einsle, O.; Tezcan, F. A.; Andrade, S. L. A.; Schmid, B.; Yoshida, M.; Howard, J. B.; Rees, D. C. *Science* **2002,** *297*, 1696-1700.
13. Leigh, G. J. *Science* **2003,** *301*, 55-56.
14. Arashiba, K.; Miyake, Y.; Nishibayashi, Y. *Nat. Chem.* **2011,** *3*, 120-125.
15. Yandulov, D. V.; Schrock, R. R. *Science* **2003,** *301*, 76-78.
16. Pool, J. A.; Lobkovsky, E.; Chirik, P. J. *Nature* **2004,** *427*, 527-530.
17. Demadis, K. D.; Coucouvanis, D. *Inorg. Chem.* **1994,** *33*, 4195-4197.
18. Demadis, K. D.; Malinak, S. M.; Coucouvanis, D. *Inorg. Chem.* **1996,** *35*, 4038-4046.
19. Takei, L.; Dohki, K.; Kobayashi, K.; Suzuki, T.; Hidai, M. *Inorg. Chem.* **2005,** *44*, 3768-3770.
20. Coucouvanis, D.; Demadis, K. D.; Malinak, S. M.; Mosier, P. E.; Tyson, M. A.; Laughlin, L. J. *J. Mol. Catal. A: Chem.* **1996,** *107*, 123-135.
21. Coucouvanis, D.; Mosier, P. E.; Demadis, K. D.; Patton, S.; Malinak, S. M.; Kim, C. G.; Tyson, M. A. *J. Am. Chem. Soc.* **1993,** *115*, 12193-12194.
22. Challen, P. R.; Koo, S. M.; Kim, C. G.; Dunham, W. R.; Coucouvanis, D. *J. Am. Chem. Soc.* **1990,** *112*, 8606-8607.
23. Malinak, S. M.; Demadis, K. D.; Coucouvanis, D. *J. Am. Chem. Soc.* **1995,** *117*, 3126-3133.
24. Schrock, R. R.; Glassman, T. E.; Vale, M. G. *J. Am. Chem. Soc.* **1991,** *113*, 725-726.
25. Schrock, R. R.; Glassman, T. E.; Vale, M. G.; Kol, M. *J. Am. Chem. Soc.* **1993,** *115*, 1760-1772.
26. Collman, J. P.; Hutchison, J. E.; Ennis, M. S.; Lopez, M. A.; Guilard, R. *J. Am. Chem. Soc.* **1992,** *114*, 8074-8080.
27. Askevold, B.; Nieto, J. T.; Tussupbayev, S.; Diefenbach, M.; Herdtweck, E.; Holthausen, M. C.; Schneider, S. *Nat. Chem.* **2011,** *3*, 532-537.
28. Smith, B. E. *Science* **2002,** *297*, 1654-1655.
29. Dos Santos, P. C.; Igarashi, R. Y.; Lee, H. I.; Hoffman, B. M.; Seefeldt, L. C.; Dean, D. R. *Accounts Chem. Res.* **2005,** *38*, 208-214.
30. Zdilla, M. J.; Verma, A. K.; Lee, S. C. *Inorg. Chem.* **2008,** *47*, 11382-11390.

31. Barney, B. M.; Igarashi, R. Y.; Dos Santos, P. C.; Dean, D. R.; Seefeldt, L. C. *J. Biol. Chem.* **2004,** *279*, 53621-53624.
32. Barney, B. M.; Yang, T. C.; Igarashi, R. Y.; Dos Santos, P. C.; Laryukhin, M.; Lee, H. I.; Hoffman, B. M.; Dean, D. R.; Seefeldt, L. C. *J. Am. Chem. Soc.* **2005,** *127*, 14960-14961.
33. Lovell, T.; Li, J.; Liu, T. Q.; Case, D. A.; Noodleman, L. *J. Am. Chem. Soc.* **2001,** *123*, 12392-12410.
34. Chomitz, W. A.; Arnold, J. *Chem-Eur. J.* **2009,** *15*, 2020-2030.
35. Rozenel, S. S.; Kerr, J. B.; Arnold, J. *40*, 10397-10405.
36. Two papers have recently appeared showing the ability of monometallic Fe(II) species to stabilize ammonia, hydrazine and diazene complexes: Saouma, C. T.; Moore, C. E.; Rheingold, A. L.; Peters, J. C. *Inorg. Chem.* **2011,** *50*, 11285-11287; Crossland, J. L.; Balesdent, C. G.; Tyler, D. R. *Inorg. Chem.* **2011,** 10.1021/ic201873a.
37. Kaess, M.; Friedrich, A.; Drees, M.; Schneider, S. *Angew. Chem., Int. Ed.* **2009,** *48*, 905-907.
38. Details of experimental procedures are provided in the SI. We note that while our studies were in progress, Schneider et al published the same compound using a very similar procedure. See: Kaess, M.; Friedrich, A.; Drees, M.; Schneider, S. *Angew. Chem., Int. Ed.* **2009**, *48*, 905-907.
39. Gelabert, R.; Moreno, M.; Lluch, J. M.; Lledos, A.; Pons, V.; Heinekey, D. M. *J. Am. Chem. Soc.* **2004,** *126*, 8813-8822.
40. DFT calculations were performed using B3LYP with 6-31++G(d,p) basis set for all atoms except Ru (Stuttgart-type small core ECPs and their appropriate valence basis sets were used for this atom). In order to reduce the computational time, the isopropyl groups attached to phosphorous were substituted for methyl groups.
41. Chaney, A. L.; Marbach, E. P. *Clin. Chem.* **1962,** *8*, 130-132.
42. Watt, G. W.; Chrisp, J. D. *Anal. Chem.* **1952,** *24*, 2006-2008.
43. Alaimo, P. J.; Peters, D. W.; Arnold, J.; Bergman, R. G. *J. Chem. Educ.* **2001,** *78*, 64-64.
44. SMART *Area-Detector Software Package, Bruker Analytical X-ray Systems, Inc.: Madison, WI, (2001-2003).* 2001-2003.
45. SAINT *SAX Area-Detector Integration Program, V6.40; Bruker Analytical X-ray Systems Inc.: Madison, WI, (2003).* 2003.
46. SADABS *Bruker-Nonius Area Detector Scaling and Absorption v. 2.05 Bruker Analytical X-ray Systems, Inc.: Madison, WI (2003).* 2003.
47. PREP *(v 6.12) Part of the SHELXTL Crystal Structure Determination Package, Bruker Analytical X-ray Systems, Inc.: Madison, WI, (2001).* 2001.
48. SHELXL *Program for the Refinement of X-ray Crystal Structures, Part of the SHELXT Crystal Structure Determination Package, Bruker Analytical Systems Inc.: Madison, WI, (1995-99).* 1995-1999.
49. SHELXS *Program for the Refinement of X-ray Crystal Structures, Part of the SHELXTL Crystal Structure Determination Package, Bruker Analytical X-ray Systems Inc.: Madison, WI, (1995-99).* 1995-1999.
50. Farrugia, L. *J. Appl. Crystallogr.* **1997,** *30*, 565.
51. Frisch, M. J. T., G. W.; Schlegel, H. B.; Scuseria, G. E.; Robb, M. A.; Cheeseman, J.; R.; Scalmani, G. B., V.; Mennucci, B.; Petersson, G. A.; Nakatsuji, H.; Caricato, M.; Li,; X.; Hratchian, H. P. I., A. F.; Bloino, J.; Zheng, G.; Sonnenberg, J. L.; Hada, M.; Ehara,; M.;

Toyota, K. F., R.; Hasegawa, J.; Ishida, M.; Nakajima, T.; Honda, Y.; Kitao, O.;; Nakai, H. V., T.; J. A. Montgomery, J.; Peralta, J. E.; Ogliaro, F.; Bearpark, M.; Heyd, J. J.;; Brothers, E. K., K. N.; Staroverov, V. N.; Kobayashi, R.; Normand, J.; Raghavachari, K.;; Rendell, A. B., J. C.; Iyengar, S. S.; Tomasi, J.; Cossi, M.; Rega, N.; Millam, J. M.; Klene,; M.; Knox, J. E. C., J. B.; Bakken, V.; Adamo, C.; Jaramillo, J.; Gomperts, R.; Stratmann, R.; E.; Yazyev, O. A., A. J.; Cammi, R.; Pomelli, C.; Ochterski, J. W.; Martin, R. L.;; Morokuma, K. Z., V. G.; Voth, G. A.; Salvador, P.; Dannenberg, J. J.; Dapprich, S.;; Daniels, A. D. F., Ö.; Foresman, J. B.; Ortiz, J. V.; Cioslowski, J.; Fox, D. J. *Gaussian09, Revision B.01; Gaussian, Inc.: Wallingford, CT, 2010.*, 2010.
52. Becke, A. D. *Phys. Rev. A* **1988,** *38*, 3098-3100.
53. Lee, C. T.; Yang, W. T.; Parr, R. G. *Phys. Rev. B* **1988,** *37*, 785-789.
54. Andrae, D.; Haussermann, U.; Dolg, M.; Stoll, H.; Preuss, H. *Theor. Chim. Acta* **1990,** *77*, 123-141.
55. Martin, J. M. L.; Sundermann, A. *J. Chem. Phys.* **2001,** *114*, 3408-3420.

Chapter 4:

Reduction chemistry of cobalt complexes with the ligand $HN(CH_2CH_2PiPr_2)_2$: Reactivity with nitrogen, hydrogen and phenylsilane.

Introduction

Transition metal complexes with low oxidation states and coordination numbers are inherently reactive, offering the opportunity to observe unusual reactivity and to study novel transformations.[1] Cobalt complexes in low oxidation states can polymerize olefins,[2] catalyze the hydrogenation and hydrosilation of 1-hexene,[3] and reduce protons to generate hydrogen by electrocatalysis[4-6] and photocatalysis.[5] Dubois and co-workers studying the series of hydride complexes $[H_2Co(L)_2]^+$, $HCoL_2$, $[HCoL_2(CH_3CN)]^+$, and $[CoL_2(CH_3CN)]^{2+}$ (L= dppe) w obtained thermodynamic values for one hydride- and two proton-transfer reactions between these species.[7]

Cobalt complexes also have also form dimeric and trimeric species. Stuart and co-workers synthesized a Co(I) dimer with a planar Co_2P_2 core, capable of coordinate two N_2 molecules to generate the species $[Co(\mu\text{-}t\text{-}Bu_2P)(PMe_3)(N_2)]_2$, as well as the mixed Co(I)/Co(II) species $Co_2(\mu\text{-}t\text{-}Bu_2P)_2(PMe_3)_2$.[8] The trimer $[Cp^*_3Co_3(\mu^2\text{-}H)_3(\mu^3\text{-}H)]$ has also been obtained.[9, 10] Mindiola and co-workers isolated a $[(PNP)Co]_2$ dimer that behaves as a three coordinate Co(I) synthon when treated with substrates such as CO or N_2.[1] The Co_2N_2 core in this complex resembles that observed by Harkins and Peters for related dinuclear Cu(I) systems.[11, 12]

Low coordination numbers have been observed for cobalt centers using chelating ligands. Holland isolated three coordinate Co complexes with nacnac type ligands,[13] including a tricoordinate Co(I) hydride in a high spin conformation.[14, 15] With PNP type ligands, Caulton characterized a three coordinate (PNP)Co complex that reversible binds N_2, and reacts with hydrogen to produce a species formulated as $(PNP)Co(H)_2$, capable of hydrogenating ethane quantitatively.[16] Caulton's three coordinate complex also reacts with CO to generate (PNP)CoCO,[17] with I_2 to form (PNP)CoI,[17] and with H_3SiPh to generate a product where the ligand has been rearranged with 3 or 4 hydrides bound to the metal center.[16] Because the (PNP)Co complex has a triplet ground state, all of its redox reactivity involves a change in spin state.[18]

Pincer ligands also stabilize a wide variety of oxidation states. Chirik synthesized a series of anionic, neutral, and cationic Co bis(imino)pyridine species bound to N_2, showing by DFT calculations on the series that all the compounds are Co(I) centers with the chelating ligand being reduced.[19] This group observed C-H activation in the ligand via a cobalt azide complex.[20] Using the ligand N_2P_2, our group synthesized the species $[N_2P_2]Co$ and $[N_2P_2]CoH$. The former reacts with aryl azides at low temperatures, generating a species whose reactivity is consistent with an imido Co=NR character.[21, 22]

Recently, Heinekey and co-workers have explored the reactivity of cobalt with the pocop ligand (pocop = κ^3-C_6H_3-1,3-$[OP(t\text{Bu})_2]_2$) toward amino borane dehydrogenation.[23-25] The complexes $[(pocop)Co(H_2)]$ and $[(pocop)Co(H_2)(H)_2]$ were obtained in these studies.[25] Prior to this work, Brookhart reported the cationic complex $[Cp^*Co(PMe_3)(H)(H_2)]^+$, which has a hydride ligand that exchanges with the hydrogen ligand;[26] the only other examples of H_2 bound to Co were prepared by photoextrusion of a CO and were characterized by IR spectroscopy.[27, 28]

As mention in Chapter 2, the $HN(CH_2CH_2PR_2)_2$ $H(NP^R_2)$ (R= alkyl) scaffold,[29-31] has the potential to stabilize reduced species. Tto gain insight into the stability of metal complexes in low oxidation states with this ligand, we explored the reduction chemistry of the $HPNPCoCl_2$ complex (**1**).

Results and discussion

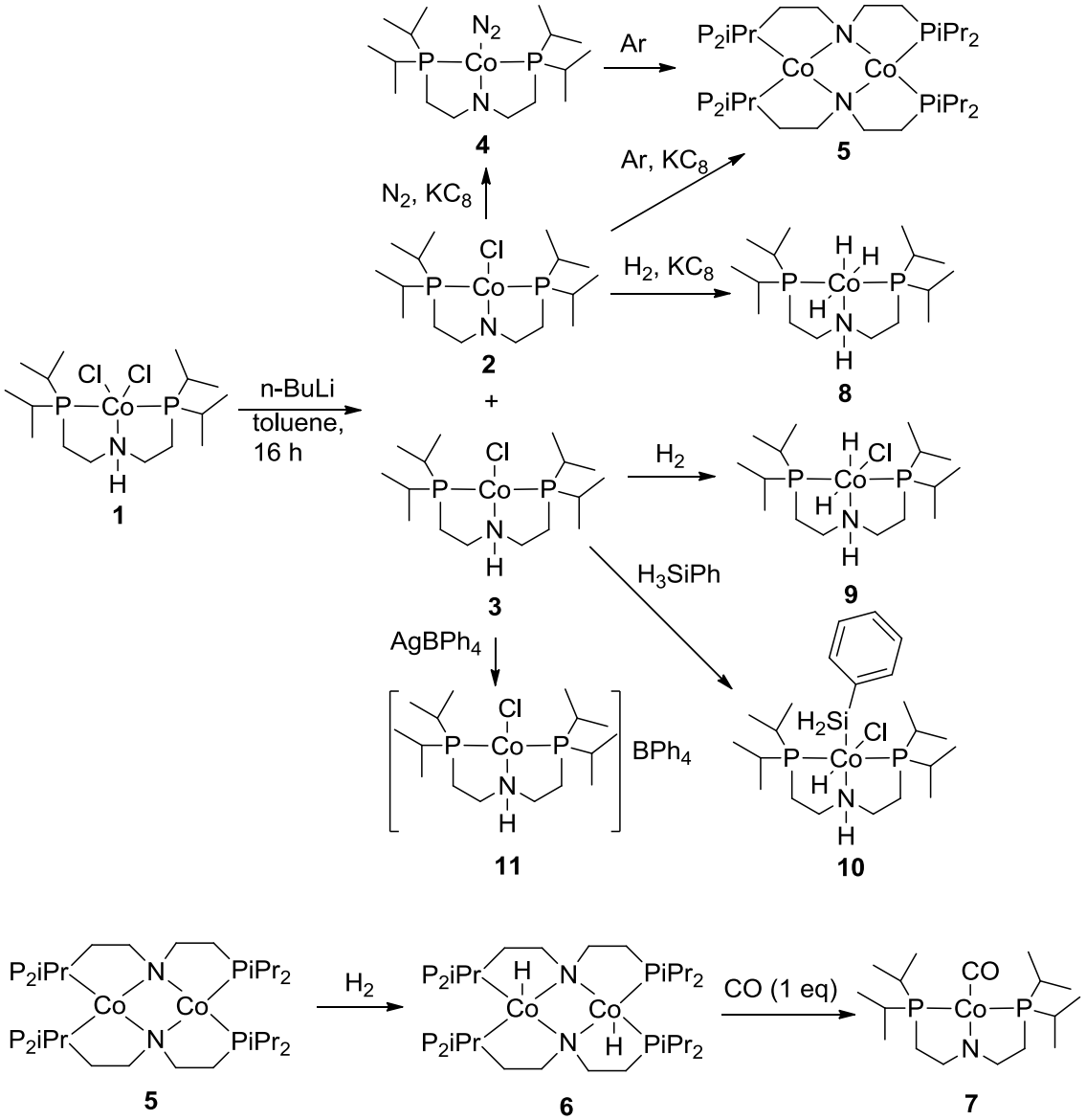

Scheme 1. Synthesis of cobalt complexes.

The reaction of (HPNP)$CoCl_2$ (**1**)[32] with *n*-BuLi produced two complexes: the deprotonated Co(II) product (PNP)CoCl (**2**),which crystallized from hexane as brown blocks in 42% yield, and the Co(I) reduced species (HPNP)CoCl (**3**), obtained as blue crystals from toluene in 18% yield. Crystals suitable for an X-ray diffraction study for complexes **2** and **3** were grown from concentrated solutions of hexanes and toluene cooled to -40 ˚C, respectively (Figure 1, Table 1). Complex **2** displays a square planar geometry, with the phosphine ligands *trans* to each other (171.99(7)˚) and the chloride ligand trans to the nitrogen atom (178.6(1)˚). The distances around the metal center (Co1 – N1: 1.833(4) Å, Co1 – P1: 2.186(1) Å, Co1 – P2: 2.200 (1) Å, and Co1 – Cl1: 2.215 Å) are in agreement with

those found in related cobalt complexes.[1, 16, 17] The angles around the nitrogen atom (124.8(3)˚ and 123.9(3)˚) are consistent with an amido ligand. The magnetic moment for **2** in solution was found to be 1.8 μ_B by the Evans method,[33] and is consistent with one unpaired electron.

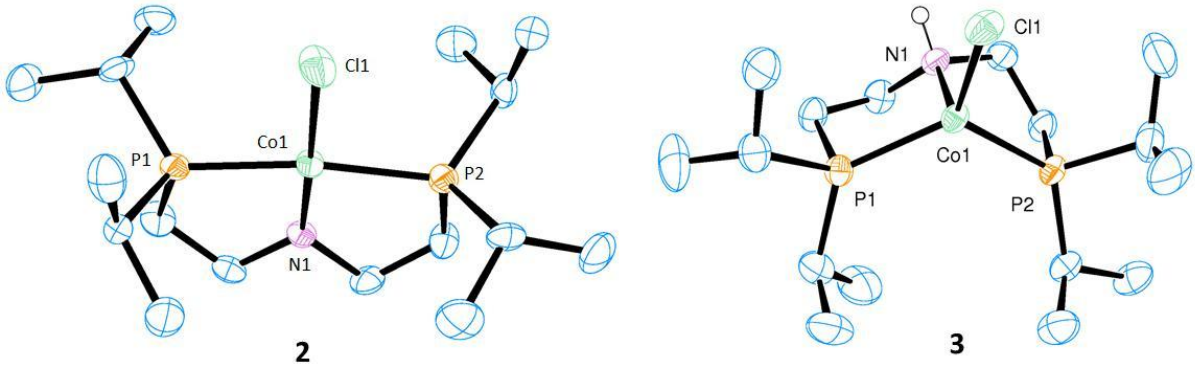

Figure 1: Thermal ellipsoid (50%) plot of **2** and **3**. Hydrogen atoms bonded to carbon have been omitted for clarity.

Complex **3** is also paramagnetic with a magnetic moment (μ_{eff} = 2.6 μ_B) consistent with two unpaired electrons. The geometry around the metal center is distorted from tetrahedral (Cl1 – Co1 – N1: 110.38(4)˚, Cl1 – Co1 – P1: 123.54(2)˚, and Cl1 – Co1 – P2: 116.35(2)˚) due the inability of the amine moiety to π bond to the metal center. The N1 – Co1 distance (2.152(2) Å), and the angles around the amine confirm the sp^3 hybridization of the nitrogen atom. A small elongation in the distances around the cobalt center is observed in comparison with **2**, due the change in the oxidation state of the metal from Co(II) to Co(I) (Figure 1, Table 1).

Table 1: Selected bond distances and angles for Co complexes **2** – **4**.

	2 [a]	**3** [a]	**4** [b]
Co1 – X	2.215(1) Å	2.2566(6) Å	1.740(1) Å
Co1 - P1	2.186(1) Å	2.2550(6) Å	2.1737(4) Å
Co1 - P2	2.200(1) Å	2.2521(6) Å	2.1638(4) Å
Co1 – N1	2.5253(17) Å	2.152(2) Å	1.856(1) Å
X – Co– P1	92.45(5)°	123.54(2)°	94.88(5)°
X – Co – P2	95.31(6)°	116.35(2)°	94.66(5)°
X – Co – N1	177.9(1)°	110.39(4)°	171.49(6)°
P1 – Co – P2	171.51(6)°	118.38(2)°	168.54(2)°

[a] X = Cl; [b] X = N2.

Complex **2** is reduced by KC_8 under N_2 to produce the species (PNP)CoN_2 (**4**), obtained as brown block-like crystals in 77% yield. Species **4** is diamagnetic and displays the signals expected for the PNP ligand, with the methyl groups appearing as two multiplets. The structure of **4** was determined by X-ray diffraction (Figure 2, Table 1). It displays a square-planar geometry with distances and angles around the metal center closely related to those

observed for **2**. The N – N distance in the dinitrogen ligand was 1.124(2) Å. A strong absorption at 1999 cm^{-1} is observed in the IR for the N – N stretch, indicating a small degree of activation for the N –N bond. Complex **4** is unstable and decomposes in the solid-state in a nitrogen-filled glove box within days, as seen by the disappearance of the peak at 1999 cm^{-1} in the IR spectrum.

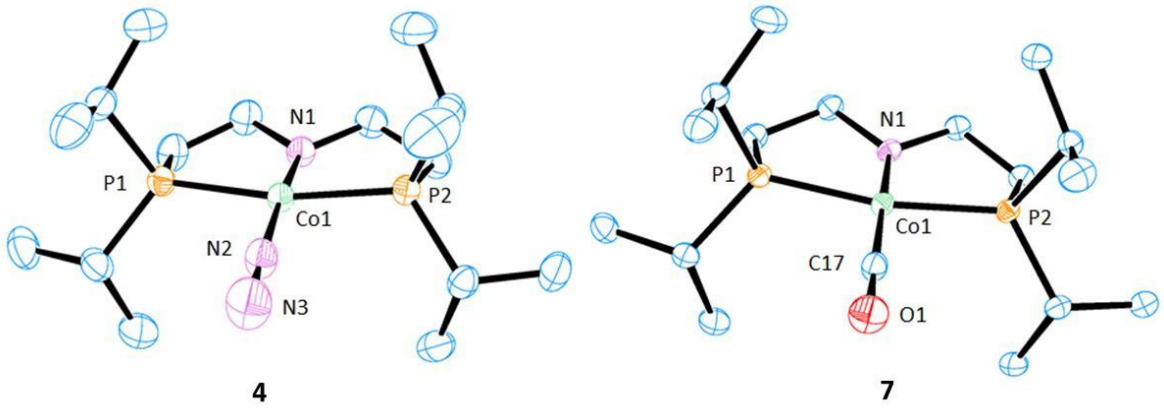

Figure 2: Thermal ellipsoid (50%) plot of **4** and **7**. Hydrogen atoms have been omitted for clarity.

When the reduction of **2** was performed in Ar atm instead of in N_2, the bimetallic complex $[(PNP)Co]_2$ (**5**) was formed in 50% yield. The identity of **5** was elucidated by X-ray crystallography. Complex **5** crystallizes in two conformations: from diethyl ether with three independent molecules per unit cell, showing different degrees of disorder, but distances and angles almost identical (**5a**), and from toluene with only one independent molecule per unit cell (Figure 3). The structure observed for **5a** shows a Co_2N_2 core related to that observed by Mindiola and co-workers,[1] with the amido ligand bridging the two metal centers (each one in a distorted tetrahedral environment) and the phosphines of each PNP ligands attached to different Co atoms. The Co – Co distance (2.4224(6) Å) is consistent with a double bond between the atoms.[8, 34] The Co1 – N1 – Co2 and Co1 – N2 – Co2 angles present in the Co_2N_2 core are 73.33(9)˚ and 73.59(9)˚, while the torsion angle N1 - Co1 - Co2 - N2 is 125.80(9)˚, with the nitrogen in the ligand 1.243 Å above the Co1 – N1 – Co2 plane. There is a small elongation in the Co – N and P – Co distances in comparison to **4**, due to the new geometry around the metal center.

The geometry observed for complex **5b** is very similar to that for **5a**. Besides the different space group and unit cell parameters, the major difference is a close contact between one of the cobalt atoms and a carbon adjacent to the amide. The Co1 – C1 distance observed is 2.014(4) Å, and is within the values for Co – C bonds (e.g $N_2P_2CoCH_3$: 1.995(5) Å, $N_2P_2CoCH_2Si(CH_3)_3$: 2.033(2) Å[35]). All C1 – Co1 distances in **5a** are longer than 2.8 Å. The distances and angles around Co2 (not bound to carbon) are nearly the same as those for **5a** (within 0.023 Å); in the case of Co1, a contraction of the Co – N distance is observed (close to 0.09 Å) while the P1 – Co1 – P3 angle is almost 4˚ larger. A closer look at the structure showed that two positions for C1 are present in the structure (bound and unbound) in a 8:1 ratio favoring the Co – C bond. We propose that **5b** is formed by C – H bond

activation at the carbon adjacent to N, forming the species [Co(H)(μ-PNP)(μ-$PCH_2CH_2NCHCH_2P$)Co] (**5b**). The hydride ligand was observed in the Fourier map and refined isotropically. Related C - H activation has been observed by Schneider[36] and Chirik.[20]

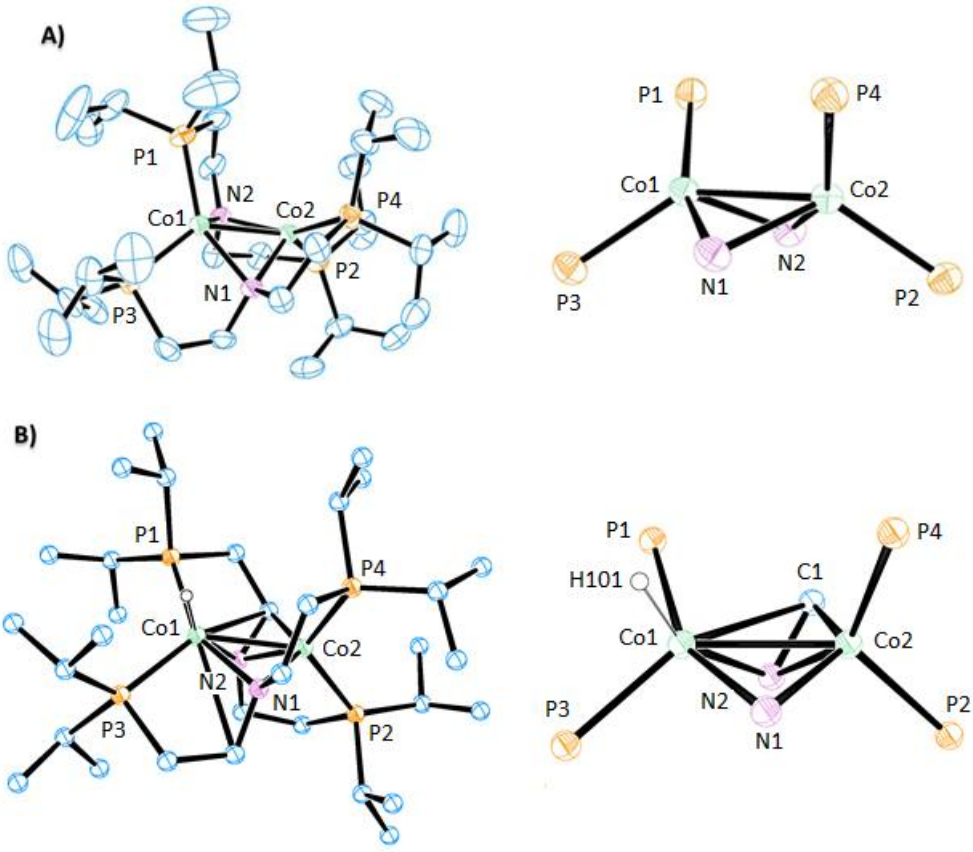

Figure 3: A) Thermal ellipsoid (50%) plot of **5** (A) and **5b** (B). Hydrogen atoms have been omitted for clarity (left). Close up of the Co_2N_2 core (right).

We investigated this hypothesis by NMR spectroscopy. The ^{1}H NMR spectrum of **5** showed two species in solution, in agreement with the presence of conformations **5a** and **5b**. They appear in an approximate ratio of 10 to 1, with all the signals observed appeared as broad peaks. The major product was assigned to **5a**; it displays all the peaks corresponding to the PNP ligand with the methyl groups appearing as four peaks integrating to 12 protons each. In the ^{31}P NMR spectrum, **5a** shows a broad signal at 85.71 ppm. The peaks observed in the ^{1}H NMR for the minor product (**5b**) are closely related to those in **5a**, but not all the peaks for the ligand were observed due to overlap. Species **5b** shows a peak at 87.4 ppm in the ^{31}P NMR spectrum. A low temperature ^{1}H NMR study was performed to determine the identity of **5b**. At -60 °C, the **5a**:**5b** ratio is close to 1 to 1. At this temperature the peaks are very broad and overlapping of the signal is observed, making the assignments impossible. The magnetic moment of the complex was determined to be 0.8 μ_B per cobalt atom using the Evans method. At this point we cannot determine the origin of the magnetic moment.

Table 2: Selected bond distances and angles for Co complexes **5**, **5b** and **6**.

	5	**5b**	**6**
Co1 – Co2	2.4216(6) Å	2.4150(4) Å	2.240(1) Å
Co1 - P1	2.2268(9) Å	2.2177(7) Å	2.170(2) Å
Co1 - P2	2.1881(7) Å	2.1770(5) Å	2.193(2) Å
Co1 – N1	1.998(3) Å	1.909(2) Å	2.009(3) Å
Co2 – Co1– P1	139.08(3)°	136.07(2)°	117.00(4)°
Co2 – Co1 – P2	104.97(3)°	102.11(2)°	125.77(4)°
Co2 – Co1 – N1	52.12(7)°	52.25(5)°	55.7(1)°
P1 – Co1 – P2	114.94(3)°	119.00(2)°	117.23(5)°
N1 – Co1 – N2	91.3(1)°	92.35(7)°	111.7(1)°

Based on the NMR spectroscopy and X-ray crystallography results, we believe that **5a** and **5b** are at equilibrium in solution. At high temperature **5a** is favored over **5b**. At low temperature both species are present in similar concentrations. Crystallization from diethyl ether occurred faster, favoring the formation of **5a**, whereas a slower crystallization from toluene allowed the formation of **5b**.Further experiments are necessary to ensure that the different conformations are not due packing effects in the crystal lattice.

We investigated the reaction of **5** with N_2 to ascertain whether it acts as a synthon for the monomeric (PNP)Co(I) complex.[1] After stirring **5** in diethyl ether for 48 h at room temperature under an N_2 atmosphere, **5** was recovered as the only product as determined by ^{1}H NMR and X-ray crystallography. Stirring **4** under Ar generates **5** as the major product (also characterized by ^{1}H NMR and X-ray crystallography), indicating that this conformation is more stable..

Complex **5** reacts with hydrogen in toluene over the course of two days. Crystallization from diethyl ether gave a new product, obtained in 53% yield. The ^{1}H NMR spectrum indicates the formation of a paramagnetic species, with peaks at 18.18 (br), 11.06 (br), -9.22 (br), -12.15 (br), -13.56 (br), and -22.04 (d) ppm. The later peak was observed as a pseudodoublet of triplets, coupled to two different phosphorous atoms, one of them with a $J_{H\text{-}P}$: 87 Hz. In the ^{31}P NMR spectrum, two peaks are observed, indicating different P environments. We assigned the new complex as the species[(PNP)CoH]$_2$ (**6**). An X-ray diffraction study confirmed the dimeric structure, with distances and angles closely related to those in **5** (Figure 4, Table 2). Major differences were observed for the Co1 – Co2 (2.240(1) Å) and N1 – N2 (3.308(4) Å) distances at the Co_2N_2 core, that deviate significantly from those in **5** (by 0.18 Å and 0.40 Å respectively), and for the torsion angle N1 - Co1 - Co2 - N2 (171.5(2)˚) indicating an almost planar conformation with the N2 atom laying only 0.244 Å above the Co1 – N1 – Co2 plane.

Although it has been reported that the cobalt dimeric complex $Co_2(\mu\text{-}PPh_2)_2(CO)_6$ can crystallize in two conformation, one bent and one planar,[37] the experimental evidence in our case indicates two different species. We propose the addition of H_2 along the Co – Co bond to form a Co(II) dimer, with a hydride attached to each metal center. To confirm this hypothesis we performed the hydrogenation reaction with D_2 to generate [(PNP)CoD]$_2$ (**6b**). The ^{2}H NMR spectrum only shows one peak, a doublet at -21.88 ppm, by decoupling ^{31}P, the signal became a singlet. The IR analysis also agrees with the proposed addition of hydrogen. Complex **6** shows a sharp peak at 1883 cm^{-1}, assigned to the Co – H stretch; **6b** shows the

peak at 1548 cm^{-1}, and the rest of the IR spectra are almost identical. The difference between the two peaks does not correspond to the value expected by the reduced mass, which may indicate tunneling effects or exchange processes in the molecule,[38] or the hydride coupled to other atoms. Interactions between the metal centers are present, as can be inferred by the magnetic moment of the molecule (μ_{eff} = 0.7 μ_B/Co), which indicates antiferromagnetic coupling. Finally, **6** reacts with CCl_4 to produce $CHCl_3$, as observed by ^{1}H-NMR spectroscopy.

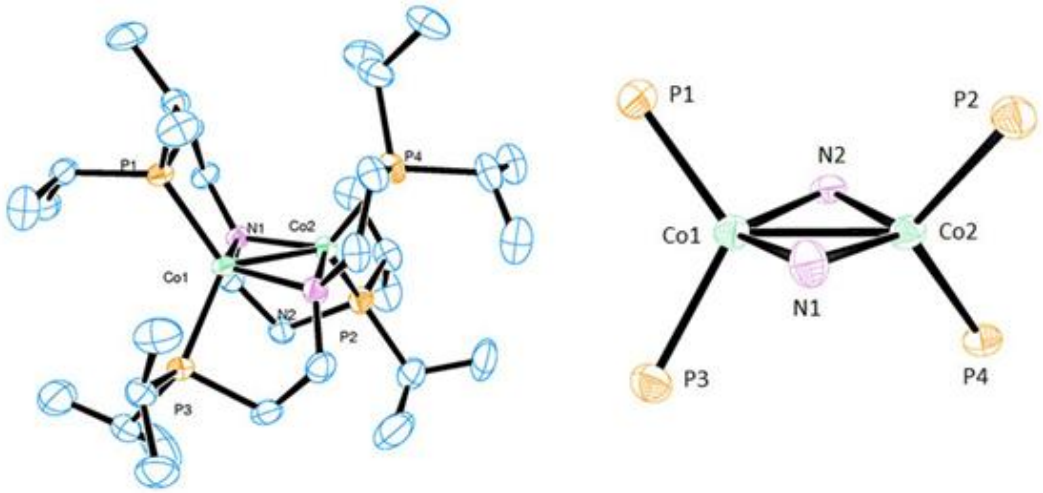

Figure 4: A) Thermal ellipsoid (50%) plot of **6**. Hydrogen atoms have been omitted for clarity (left). Close up of the Co_2N_2 core (right).

Adding of one equivalent of CO to **6** in hexane generated the monomeric square planar species (PNP)CoCO (**7**). The ^{1}H NMR spectrum is very similar to that for **4**, with one peak for each of the NCH_2, PCH_2, and PCH protons, and two peaks for the methyl groups. In the ^{31}P NMR spectrum, P atoms appear as a peak at 102.52 ppm. X-ray diffraction confirmed that **7** is analogous to **4**, with the N_2 ligand replaced by CO (Figure 2, Table 1). The C-O distance (1.172(2) Å) and the IR stretch (1882 cm^{-1}) indicate a considerable degree of π back donation. The values are very close to those found by Caulton and co-workers for their related PNP system.[17]

To explore further the electronic structure of **5**, DFT calculations were performed using B3LYP and the pure DFT function TPSS, with 6-31++G(d,p) basis set for all atoms.[47, 50] To reduce the computational time, the isopropyl groups attached to phosphorous were replaced by methyl groups (Figure 5). Complex **5** was modeled as a singlet and as a triplet using B3LYP. The results showed that the triplet electronic state is more stable by 20.9 kcal/mol. Also, the triplet has a bent Co_2N_2 core, with a N1 - Co1 - Co2 - N2 torsion angle of 123.07°, while the singlet displays an almost planar conformation (with the same torsion angle being 172.98°). Complex **5** (as a triplet) has a lower energy than the combination of two monomeric complexes ($P^{Me}NP^{Me}$)Co (where the isopropyl groups attached to phosphorous were replaced with methyl groups) in a triplet electronic state by 9.1 kcal/mol. The calculations showed consistent distances and angles between the experimental and theoretical values for the triplet electronic state (Table 2).

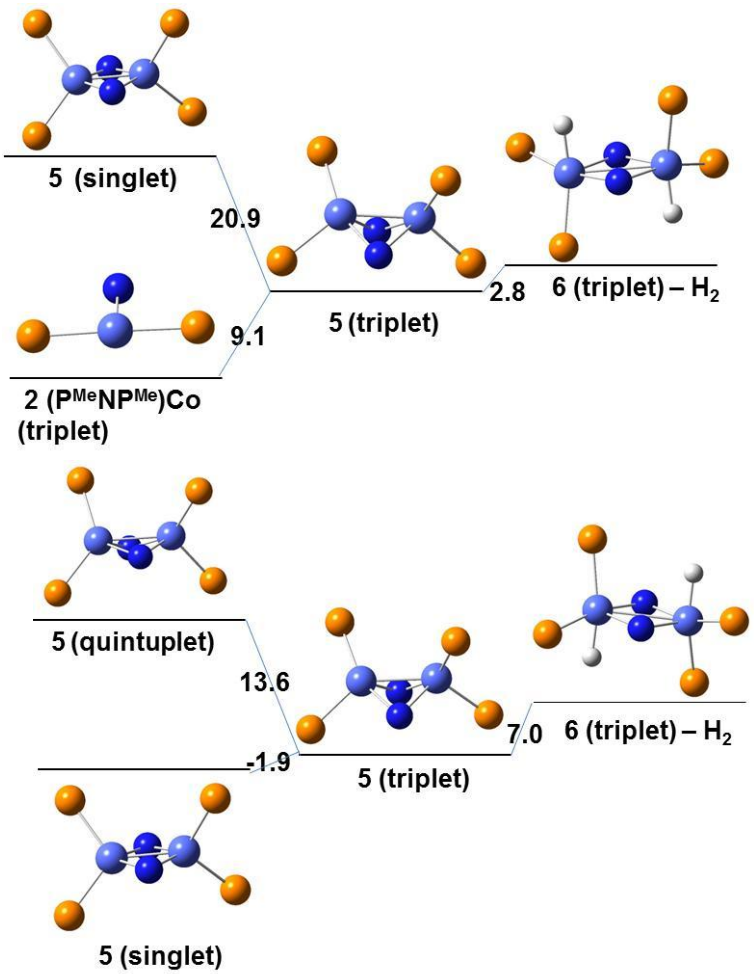

Figure 5. Zero-point energy calculations for **5** and **6** with B3LYP functional (top), and TPSS functional (bottom).

The calculations with TPSS show related geometries for the Co_2N_2 core of **5**, almost planar in the case of the singlet and the quintuplet, and bent for the triplet (torsion angle N1 - Co1 - Co2 - N2: 124.79°). In this case, the singlet and triplet have almost the same energy (the triplet is 1.9 kcal/mol less stable), whereas the quintuplet has a higher energy by 15.6 kcal/mol.

We also attempted to model the energies for **6** as both a singlet and a triplet, but the singlet state did not converge in either of the calculations (B3LYP and TPSS). Although the distances and angles for the Co_2N_2 core did not match the experimental values (Table 4), analysis of the calculations showed interesting features. The structure optimization indicates that terminal hydrides are favored over bridging hydrides (starting with bridging hydrides, the geometry optimization favored terminal ones). Also, the Co_2N_2 core for this species is planar instead of bent (the torsion angle N1 - Co1 - Co2 - N2 obtained was 179.97° with B3LYP and 179.95° with TPSS). The zero-point energies observed for **6** were higher by 2.8 kcal/mol with B3LYP and 7.0 kcal/mol with TPSS in comparison with **5**.

Table 3: Experimental and calculated values for **5** with B3LYP and TPSS.

$(NP2Co)_2$	**Experimental**	**B3LYP singlet**	**B3LYP triplet**	**TPSS singlet**	**TPSS triplet**	**TPSS quintuplet**
Co1 – Co2	2.4216(6) Å	2.100 Å	2.343 Å	2.130 Å	2.327 Å	2.421 Å
N 1– N2	2.909(4) Å	3.375 Å	3.023 Å	3.310 Å	2.930 Å	3.139 Å
Co1 –N1	1.998(3) Å	1.988 Å	1.987 Å	1.968 Å	1.964 Å	2.001 Å
Co1 – N2	2.067(3) Å	1.992 Å	2.171 Å	1.973 Å	2.076 Å	2.004 Å
N1 – Co1 – N2	91.4(1) °	115.94 °	93.37 °	114.25 °	92.94 °	101.82 °
Co1-N1-Co2	73.17(9) °	63.69 °	68.41 °	65.42 °	70.26 °	72.47 °
N1-Co1-Co2-N2	125.8(1) °	172.98 °	123.07 °	173.04 °	124.79 °	147.31 °

Table 4: Experimental and calculated values for **6** with B3LYP and TPSS.

$(NP2CoH)_2$	**Experimental**	**B3LYP triplet**	**TPSS triplet**
Co1 – Co2	2.240(1) Å	2.950 Å	2.807 Å
N 1– N2	3.307(4) Å	3.018 Å	2.996 Å
Co1 –N1	1.997 Å	2.060 Å	2.030 Å
Co1 – N2	2.009(3) Å	2.162 Å	2.076 Å
Co - H	-	1.522 Å	1.525 Å
N1 – Co1 – N2	111.7(1)°	91.22°	93.72°
Co1-N1-Co2	68.0(1) °	91.49°	87.48°
N1-Co1-Co2-N2	171.5(2) °	179.97 °	179.95 °

DFT indicates that the triplet electronic state is favorable on these systems. Although a higher level of theory is needed for the complete analysis of the electronic proprieties, the current model correctly describes the geometry observed for the Co_2N_2 core in **5**, and shows a good approximation in the case of **6**. The calculations also indicate that the formation of **6** with terminal hydrides is favored over bridging ones.

The reduction of **2** with KC_8 was also performed under a hydrogen atm. This reaction generates the complex (HPNP)Co$(H)_3$ (**8**) in 29% yield after crystallization from hexane. The structure of **8**, determined by X-ray diffraction, shows that two H_2 molecules were added to the Co complex, one across the N – Co bond and the other oxidative added to the metal center, generating a hexacoordinate Co(III) species in an octahedral environment (Figure 6). The hydride ligands were found in the Fourier map and were refined isotropically with no constraints. The Co – P distances (2.1211(6) Å) are slightly shorter than those found in **2**, given the higher oxidation state of the metal center. Elongation of the Co1 – N1 distance (2.039(3) Å) in comparison to **2**, as well as the Co1 – N1 – C angles (111.5(5)˚ and 115.5(5)˚) confirmed the protonation of the amide. The H – Co distances found were 1.32(3) Å for the *trans* hydrides, and 1.37(4) Å for the one *trans* to nitrogen. These values are consistent with other Co – hydride species characterized by X-ray crystallography.[7]

Table 5: Selected bond distances and angles for Co complexes **5 - 11**.

	8 [a]	**9** [b]	**10** [c]	**11**
Co1 – Cl	1.50(4) Å	2.3238(9) Å	2.367(4) Å	2.179(1) Å
Co1 - P1	2.1211(6) Å	2.144(1) Å	2.184(4) Å	2.239(1) Å
Co1 - P2	2.1211(6) Å	2.145(1) Å	2.204(4) Å	2.239(1) Å
Co1 – N1	2.039(3) Å	2.040(3) Å	2.08(1) Å	1.975(2) Å
Co1 – H2	1.32(4) Å	1.44(4) Å	-	-
Co1 – X	1.37(4) Å	1.38(3) Å	2.225(4) Å	-
Cl – Co – P1	98(2)°	93.73(4)°	98.4(1)°	93.60(3)°
Cl – Co – P2	86(2)°	95.67(4)°	91.1(1)°	93.95(3)°
Cl – Co – N1	171(2)°	90.58(8)°	87.1(3)°	178.23(7)°
Cl – Co – H2	167(4)°	175(2)°	-	-
Cl – Co – X	91(4)°	97(1)°	111.4(1)°	-
P1 – Co – P2	175.45(7)°	169.36(4)°	166.8(2)°	172.34(3)°
X – Co – N2	180(2)°	173(1) °	161.3(3) °	-

[a] X = H2 and Cl replaced by H1; [b] X = Si; [c] X = H2.

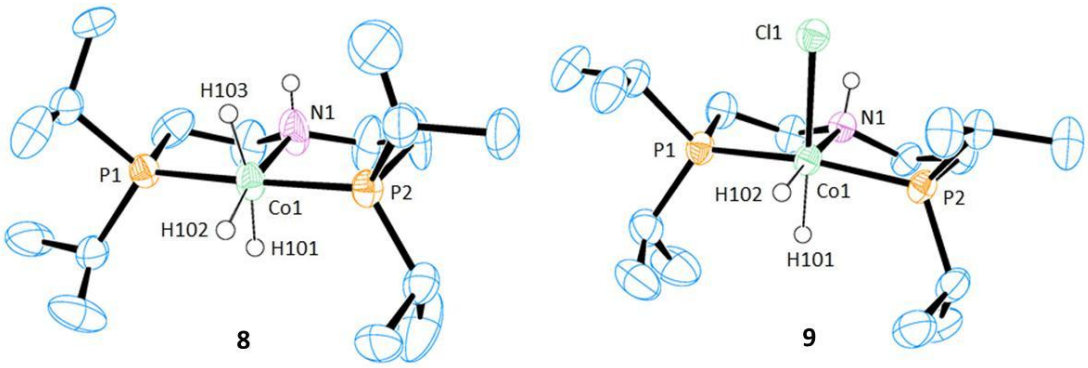

Figure 6: Thermal ellipsoid (50%) plot of **8** and **9**. Hydrogen atoms bonded to carbon have been omitted for clarity.

The behavior of **8** in solution was investigated by ^{1}H NMR spectroscopy (Figure 7). At room temperature, two species are present, along with a small amount of **6** (observed as a pseudodoublet of triplets at -22.09 ppm, $J_{H\text{-}P}$: 87 Hz). The species assigned to **8** showed broad peaks at -12.49 ppm and -26.25 ppm. A second species displayed broad peaks at -8.88, 11.93 and 19.14 ppm. This complex was assigned as the mixed hydride-hydrogen species (PNP)Co(H)$_2$(H$_2$) (**8b**) by comparison with Heinekey's work.[25] A low temperature ^{1}H NMR experiment showed that at -48 °C, the peak at -12.49 ppm splits in two triplets of doublets centered at -12.55 and -12.29 ppm. The broad peak at -26.25 ppm is as a triplet of triplets. Peaks at -12.55 and -12.29 ppm were assigned as the two *trans* hydride ligands, slightly different from each other due the amine proton ($J_{H\text{-}H}$: 19 Hz, $J_{P\text{-}H}$ 46 Hz). The signal at -26.25 ppm is coupled to the two *trans* hydrides ($J_{H\text{-}H}$: 19 Hz) and to two phosphorouses ($J_{H\text{-}P}$: 60 Hz), and was assigned to the *cis* hydride. At -48 °C, the peak for **8b** (-8.88 ppm) almost disappeared, as well as the peaks at 11.93 and 19.14 ppm, with new signals appearing as broad peaks of low intensity at -17.11, 15.36, and 25.95 ppm. We assigned these new signals

to the species (HPNP)CoH(H_2) (**8cH$_2$**), by comparison to the spectrum observed for **3**. Further experiments are necessary however to assign unequivocally these peaks (Figure 7).

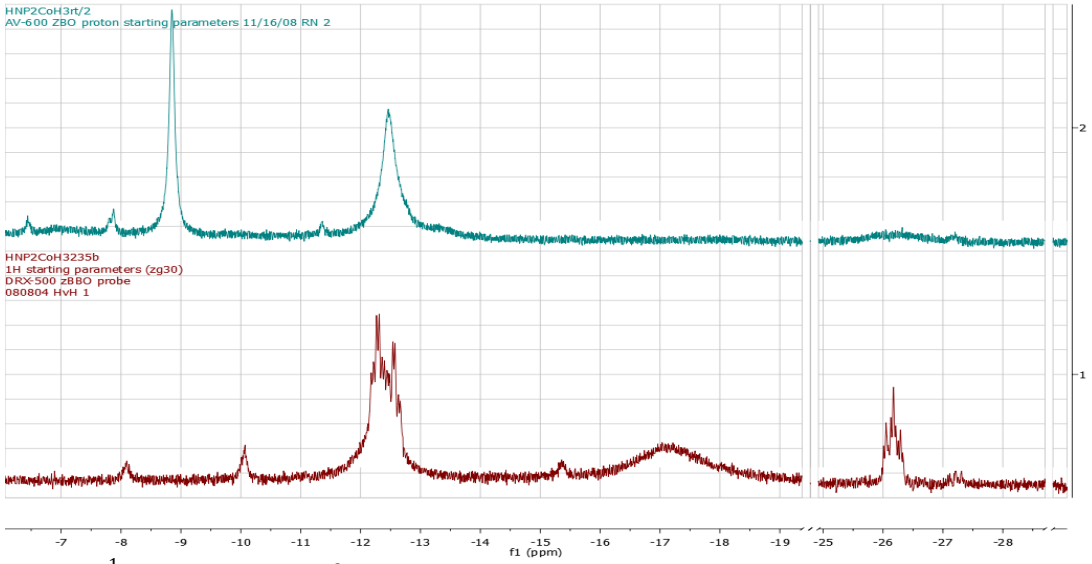

Figure 7: ^{1}H NMR spectra for **8** at 295 K (top), and 235 K (bottom).

We also investigated the chemistry of **8** via DFT calculations.[47] The zero-point energies for the species **8**, (PNP)Co(H_2) (**8b**), (PNP)Co(H_2)(H_2) (**8bH2**), (HPNP)Co(H) (**8c**), (HPNP)Co(H)(H_2) (**8cH2**), and (PNP)Co (the trigonal Co(I) complex analogous to the one observed by Caulton and co-workers[16]) were calculated using B3LYP with the 6-31++G(d,p) basis set (Figure 8). The complexes **8**, **8b** and **8bH2** were calculated with using a singlet electronic state while **8c** and **8cH2** were calculated as triplets. We attempted to calculate the energies for the complexes (PNP)Co(H_2) (singlet and triplet) and **8cH2** (singlet), but they either rearranged to generate **8b** or **8**, or did not converge. The calculations indicate that the cobalt species generated by oxidative addition of hydrogen to form **8b**, or by the addition of hydrogen through the Co – N bond to generate the Co(I) species **8c**, have almost the same energy within experimental error (2.5 kcal/mol downhill for **8b**). These species are less stable than the tricoordinate complex (PNP)Co in a triplet electronic state by 5.2 and 2.6 kcal/mol, respectively. Complex (PNP)Co is more stable as a triplet than as a singlet by 22.5 kcal/mol, but it is less favored energetically than the tetracoordinate complex **4** by 7.2 kcal/mol. When hydrogen coordinates to **8b** or **8c** to form **8bH2** and **8cH2**, the energy difference between them is 0.7 kcal/mol. Coordination of the hydrogen H_2 molecule to the cobalt metal center is uphill by 8.7 kcal/mol for the **8b** → **8bH2** reaction, and by 6.9 kcal/mol for the analogous reaction starting with **8c**. Once the hydride-dihydrogen species are formed, the oxidative addition of the dihydrogen molecule to generate **8** is favored by approximately 15 kcal/mol for both species. DFT calculations suggests that either **8b** or **8c** are valid intermediates formed by the addition of one hydrogen molecule after the reduction with KC_8 of **2**, and a second addition of a hydrogen molecule to generate **8** is energetically favorable. The values obtained for this system are in agreement with related calculations performed by Henekey[25] and Caulton groups.[16] The later one ruled out the formation of HPNPCo($H)_3$ in their system based on experimental data.[16]

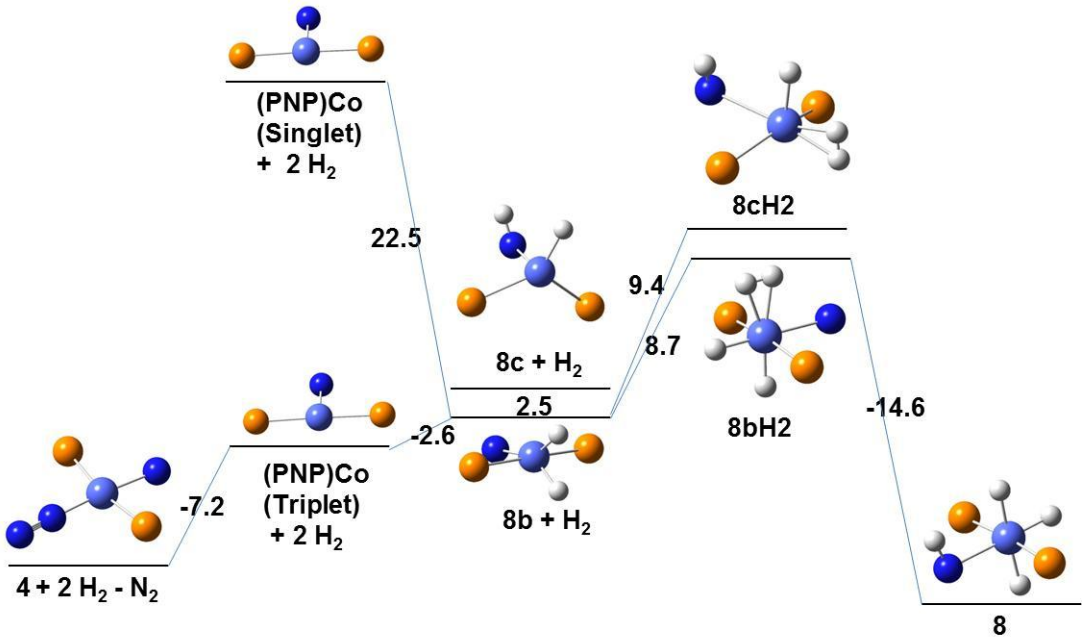

Figure 8. Zero-point energy calculations for the hydrogenation reaction proposed intermediates.

Complex **3** also reacts with hydrogen to generate (HPNP)CoCl(H)$_2$ (**9**), which is only stable at low temperatures under hydrogen; heating or removing the hydrogen quickly regenerates **3** even in the solid state. Crystals suitable for an X-ray diffraction study were grown from a concentrated solution of toluene cooled to -40 ºC under hydrogen. A crystal was placed immediately into the cold nitrogen stream of the diffractometer at 100 K (see Figure 6, Table 5). The high quality of the data allowed for the location of the hydrides, which were refined isotropically with no constraints. The study confirmed the oxidative addition of hydrogen to the Co(I) metal center to generate the Co(III), with the hydrides *cis* to each other. The *cis* addition is in agreement with calculations performed by Heinekey and co-workers in related systems.[25] Complex **9** crystallizes with two independent molecules per unit cell, with distances and angles comparable with those found in **8**. The hydride *trans* to the amino ligand has a slightly shorter Co – H distance (1.37(3) and 1.39(5) Å) than the one *trans* to the chlorine (1.43(4) and 1.48(4) Å). The H – Co – N and H – Co – Cl angles are close to the ideal 180˚ for an octahedral environment (between 173 and 178˚).

The equilibrium of **3** and **9** under hydrogen was monitored using ^{1}H NMR spectroscopy. At room temperature, two sets of signals were observed, one corresponding to paramagnetic **3**, and another for diamagnetic **9**; all the peaks corresponding to the HPNP ligand were located except for the NH proton. The two hydrides appeared as pseudoquartets at -23.54 and -30.03 ppm.

The equilibrium between **3** and **9** was followed by UV-Vis spectroscopy to determine the thermodynamic parameters for the reaction under one atm H_2. The concentration of **3** was used to generate a Van't Hoff plot, and the parameters found for the reaction at temperatures between 20 °C and 80 °C were ΔH° = -8.3 kcal/mol and ΔS° = -26.5 cal/mol. The entropy

difference is consistent with that of free hydrogen (31 cal/mol), and the values are in agreement with the equilibrium observed by NMR spectroscopy.

Complex (HPNP)CoCl(H)SiH_2Ph (**10**) was also obtained by oxidative addition of one H – Si bond of H_3SiPh to the cobalt center in **3**. The reaction was carried out in toluene, and the product was isolated in 66% yield as yellow crystals. An X-ray diffraction study of **10** showed two independent molecules per unit cell. Poor data and twinning problems did not allow refinement of the structure to acceptable values (Figure 9), but the study displayed the cobalt metal center to be in a square pyramidal environment (the hydride ligand was not observed), due to a H – Si *cis* addition, with the silane ligand *trans* to the amine. As in the case of **9**, complexes **3** and **10** are in equilibrium in solution. Complex **10** is diamagnetic, and the peaks for the HPNP ligand and the silane were observed in the spectrum. The SiH_2 protons appeared as a singlet at 4.69 ppm, while the CoH peak was observed as triplet at -28.78 ppm (J_{P-H}: 56Hz).

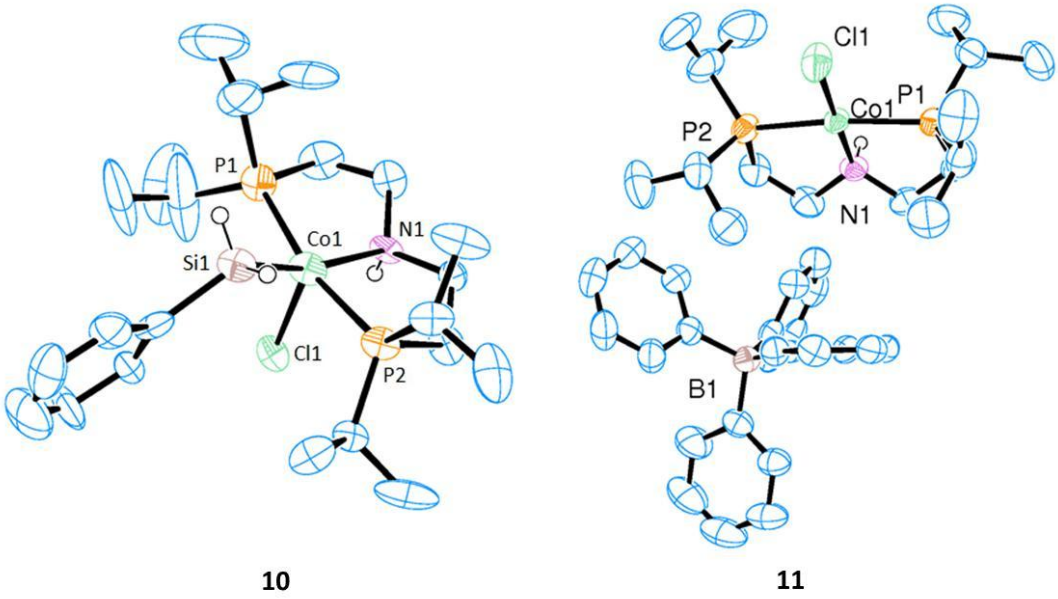

10 **11**

Figure 9: Thermal ellipsoid (50%) plot of **10** and **11**. Hydrogen atoms bonded to carbon have been omitted for clarity.

The formation of **9** and **10** was investigated by DFT calculations using B3LYP with the 6-31++G(d,p) basis set.[47] The addition of H_3SiPh and hydrogen to **3** to generate **9** and **10** was found to be uphill (3.8 and 6.7 kcal/mol respectively). These values are consistent with the fact that both species are present in solution (Figure 10).

Finally, **3** also reacts with $AgBPh_4$ in THF to generate {(HPNP)CoCl}BPh_4 (**11**) in 78% yield, characterized by an X-ray crystallography (Figure 9). Complex **11** displayed a square planar geometry around the cobalt atom, with angles and distances in agreement with those in **2** (within 0.05 Å). The N – Co distance showed an elongation of 0.14 Å, due the inability of the amine ligand to donate the lone pair to the metal center. The angles around the N ligand confirmed an sp^3 hybridization. The most interesting feature of **11** is its formal electron count of 15 electrons. .

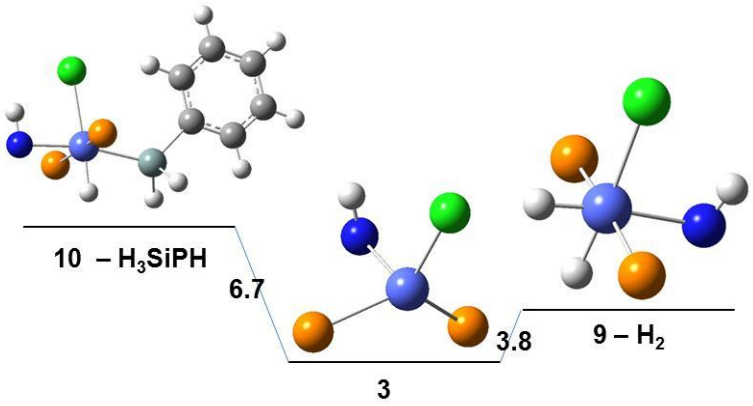

Figure 10. Zero-point energy calculations for **3**, **9** and **10**.

Conclusions.

A series of cobalt complexes with the ligand HPNP (or the deprotonated form PNP^-) were synthesized and characterized. These proved to be useful for studying the reduction chemistry for this system. The results obtained in this work were supported by X-ray crystallography, NMR spectroscopy, variable-temperature NMR, UV-Vis, IR, and DFT calculations.

The investigation showed that the treatment of the Co(II) precursor **1** with n-BuLi generates the deprotonated product **2**, as well as the reduced product **3**. Complex **2** reacts with KC_8 to generate different products depending upon the atmosphere under which the reduction is performed. The monomeric square planar N_2 complex **4** is obtained in N_2 atmosphere, and the dimeric species **5** is formed under Ar. Complex **8** is generated under an hydrogen atmosphere by the addition of two H_2 molecules, one across the N – Co bond.

Complex **5** also reacts with hydrogen to generate **6**, and, in this case H_2, is added to the Co – Co bond to give a dihydride species. We also observed the oxidative addition of H-H and H-Si bonds to complex **3**, to form the complexes **9** and **10**. In both cases, NMR experiments showed that species **3** and **9** (or **10**) are in equilibrium in solution. For the transformation of **3** with hydrogen to generate **9**, the thermodynamic parameters were obtained by following the reaction by UV-Vis spectroscopy. DFT calculations performed indicate that the formation of the nitrogen bound species **4** or the dimeric species **5a**, is favored over the tricoordinate (PNP)Co complex Addition of two hydrogen molecules to a reduced metal center to form **8** is also energetically favored.

Table 6. Crystal data and structure refinement for **2-11**.

	2	**3**	**4**
Formula	$C_{16}H_{36}ClCoNP_2$	$C_{16}H_{37}ClCoNP_2$	$C_{16}H_{36}CoN_3P_2$
FW (g/mol)	398.78	399.79	391.35
T (K)	104(2)	169(2)	159(2)
Space group	P 2_1 2_1 2_1	$P2_1/c$	P-1
a (Å)	13.319(3)	10.2394(11)	7.6183(7)
b (Å)	13.324(3)	13.5741(15)	8.5862(8)
c (Å)	23.314(6)	15.6167(17)	17.7206(16)
α (deg)	90	90	77.2980(10)
β (deg)	90	101.668(2)	84.3140(10)
γ (deg)	90	90	68.0490(10)
V (Å^3)	3137.4(17)	2125.7(4)	1048.62(17)
Z	8	4	2
λ (Å)	0.71073	0.71073	0.71073
μ (mm^{-1})	1.109	1.079	0.972
# unique reflections	7555	3895	3834
R_{int}	0.0488	0.0225	0.0188
R [I > 2sigma(I)]	0.0430	0.0275	0.0221
$R(F_0)$*	0.0515	0.0313	0.0234
$R_w(F_0)$*	0.0766	0.0693	0.0611
G. of. F.	1.099	1.089	1.090

Table 6. **Cont'd.** Crystal data and structure refinement for **2-11**.

	5	**5b**	**6**
Formula	$C_{96}H_{216}Co_6N_6P_{12}$	$C_{32}H_{72}Co_2N_2P_4$	$C_{32}H_{72}Co_2N_2P_4$
FW (g/mol)	2179.97	726.66	726.66
T (K)	141(2)	165(2)	163(2)
Space group	P-1	C 2/c	P-1
a (Å)	17.8232(14)	36.173(5)	9.7022(16)
b (Å)	18.3731(14)	10.119(5)	12.226(2)
c (Å)	19.2160(15)	21.802(5)	17.863(3)
α (deg)	94.2560(10)	90	108.791(2)
β (deg)	109.3530(10)	104.63(5)	95.504(2)
γ (deg)	97.7940(10)	90	102.746(2)
V (Å^3)	5834.2(8)	7722(4)	1924.4(6)
Z	2	8	2
λ (Å)	0.71073	0.71073	0.71073
μ (mm^{-1})	1.040	1.048	1.051
# unique reflections	21294	7109	7053
R_{int}	0.0259	0.0252	0.0608
R [I > 2sigma(I)]	0.0318	0.0302	0.0501
$R(F_0)$*	0.0388	0.0434	0.0972
$R_w(F_0)$*	0.0797	0.0770	0.1316
G. of. F.	1.042	1.040	1.020

Table 6. Cont'd. Crystal data and structure refinement for **2-11**.

	7	**8**	**9**
Formula	$C_{17}H_{36}CoNOP_2$	$C_{16}H_{40}CoNP_2$	$C_{16}H_{39}ClCoNP_2$
FW (g/mol)	391.34	367.36	401.80
T (K)	100(2)	100(2)	149(2)
Space group	P-1	C 2/c	P-1
a (Å)	7.6066(8)	19.9694(6)	10.526(6)
b (Å)	8.4996(9)	7.4326(3)	15.026(8)
c (Å)	17.1584(17)	13.6932(5)	15.316(8)
α (deg)	82.4060(10)	90	62.877(7)
β (deg)	82.8630(10)	98.0270(10)	86.128(8)
γ (deg)	69.2410(10)	90	85.906(8)
V (Å^3)	1024.63(18)	2012.50(13)	2149(2)
Z	2	4	4
λ (Å)	0.71073	0.71073	0.71073
μ (mm^{-1})	0.995	1.005	1.068
# unique reflections	3748	1833	7961
R_{int}	0.0241	0.0217	0.0363
R [I > 2sigma(I)]	0.0281	0.0336	0.0420
$R(F_0)$*	0.0332	0.0364	0.0516
$R_w(F_0)$*	0.0722	0.0886	0.1096
G. of F.	1.045	1.056	1.153

Table 6. Cont'd. Crystal data and structure refinement for **2**-**11**.

	10	**11**
Formula	$C_{22}H_{44}ClCoNP_2Si$	$C_{92}H_{130}Cl_2Co_2N_2O_3P_2$
FW (g/mol)	506.99	1646.24
T (K)	100(2)	129(2)
Space group	P 2_1	P-1
a (Å)	10.7291(18)	11.079(5)
b (Å)	20.878(4)	13.562(5)
c (Å)	12.305(2)	16.435(5)
α (deg)	90	100.691(5)
β (deg)	100.014(9)	97.532(5)
γ (deg)	90	100.824(5)
V (Å^3)	2714.3(6)	2347.9(15)
Z	4	1
λ (Å)	0.71073	0.71073
μ (mm^{-1})	0.902	0.524
# unique reflections	9894	8573
R_{int}	0.1755	0.0286
R [I > 2sigma(I)]	0.1026	0.0484
$R(F_0)$*	0.1903	0.0718
$R_w(F_0)$*	0.2855	0.1444
G. of. F.	1.052	1.044

Experimental.

General considerations. Unless otherwise noted, all reactions were performed using standard Schlenk techniques under an N_2-atm or in a N_2-atm glove box. Solvents were dried by passing through a column of activated alumina and degassed with nitrogen.[39] C_6D_6 was dried over Na/benzophenone and vacuum transferred. All NMR spectra were obtained in C_6D_6 or $C_6D_5CD_3$ at ambient temperature using Bruker AVQ-400, AV-500 or AV-600 spectrometers. ^{1}H NMR chemical shifts (δ) were calibrated relative to the residual solvent peak. Magnetic susceptibility measurements were performed in C_6D_6 according to the Evans NMR method at 293 K.[33] Melting points were determined using sealed capillaries prepared under a nitrogen atm. Infrared (IR) spectra were recorded with a Thermo Scientific Nicolet iS10 series FTIR spectrophotometer as a powder or a Nujol mull between KBr plates. UV-Vis spectra were determined with a Varian Cory 50 UV-Vis spectrophotometer using a 1 cm quartz cell. Elemental analyses were performed at the University of California, Berkeley Microanalytical Facility. X-ray crystal diffraction analyses were performed at the University of California, Berkeley CHEXRAY facility. (HPNP)$CoCl_2$ (**1**) was prepared according to literature procedure.[32] The remaining starting materials were obtained from Aldrich and used without further purification.

(PNP)CoCl (2). A 1.6 M solution of *n*-BuLi (0.90 mL, 1.4 mmol) in hexanes was added to a suspension of (HPNP)$CoCl_2$ (0.60 g, 1.4 mmol) in 25 mL of toluene at -78 °C. The suspension immediately turned from purple to red. The reaction mixture was allowed to warm to room temperature and was stirred for 3 h. The solvent was removed under vacuum, and the product was extracted with hexanes (3 x 15 mL). The solution was concentrated and cooled to -40 °C to give brown, block-like crystals (0.23 g, 42%). Crystals suitable for an X-ray diffraction study were grown from a concentrated solution of diethyl ether cooled to -40ºC. ^{1}H NMR 1.73 (br), 1.06 (br), 0.31 (br), -3.47 (br), -17.32 (br). ^{31}P NMR -1.83 (br). IR (cm^{-1}) 2816 (m), 2797 (s), 2708 (w), 2625 (w), 1404 (w), 1364 (s), 1318 (m), 1238 (s), 1208 (m), 1098 (s), 1024 (s), 882 (m), 723 (s), 632 (s). Anal. Calc: C, 48.19; H, 9.10; N, 3.51. Observed C, 48.17; H, 9.48; N, 3.50. Mp 60-63 °C. μ_{eff} = 1.8 μ_B.

(HPNP)CoCl (3). After the extraction of **2**, the remaining residue was extracted with toluene (4 x 15 mL) to give a blue solution. The solution was concentrated and cooled to -40 °C to give blue, block-like crystals (0.10 g, 18%). Crystals suitable for an X-ray diffraction study were grown from a concentrated solution of toluene cooled to -40ºC. ^{1}H NMR 64.76 (br), 29.22 (br), 20.10 (br), 17.84 (br), 11.70 (br), 10,26 (br), -0.20 (br), -1.76 (br), -13.57 (br). ^{31}P NMR 83.0 (br). IR (cm^{-1}) 3216 (s, N-H), 1408 (w), 1363 (s), 1244 (m), 1181 (m), 1157 (w), 1080 (s), 1044 (s), 1012 (s), 886 (m), 815 (s), 769 (m). 678 (s), 630 (m), 606 (s). Anal. Calc: C, 48.07; H, 9.33; N, 3.50. Observed C, 48.15; H, 9.48; N, 3.59. Mp 186-188 °C. μ_{eff} = 2.6 μ_B.

(PNP)CoN$_2$ (4). A solution of **2** (0.70 mL, 1.8 mmol) in 15 mL of THF was added to a suspension of KC_8 (0.31 g, 2.3 mmol) in 10 mL of THF at -78 °C under an N_2 atm. The suspension immediately turned from brown to red-brown. The reaction mixture was allowed to warm to room temperature and was stirred for 2 h. The solvent was removed under vacuum, and the product was extracted with hexane (3 x 15 mL). The solution was concentrated and cooled to -40 °C to give brown, block-like crystals (0.53 g, 77%). Crystals suitable for an X-ray diffraction study were grown from a concentrated solution of hexane cooled to -40ºC. ^{1}H NMR 2.98 (br, 4H, N*H*), 2.11 (br, 4H, PC*H*(CH_3)), 1.67 (br, 4H, PCH_2),

1.39 (br, 12H, CH_3), 1.15 (br, 12H, CH_3). ^{31}P NMR 92.54 (s). ^{13}C NMR 61.4 (m, NCH_2), 25.2 (m, P$CH(CH_3)$), 23.7 (m, PCH_2), 20.0 (s, CH_3), 18.6 (s, CH_3). IR (cm^{-1}) 2816 (m), 2783 (w), 2699 (m), 2621 (w), 1999 (s, N-N), 1402 (w), 1362 (s), 1317 (m), 1234 (s), 1206 (s), 1101 (s), 1065 (m), 1022 (s), 965 (m), 882 (m), 818 (s), 721 (s), 631 (s). Anal. Calc: C, 49.10; H, 9.27; N, 10.74. Observed C, 48.94; H, 9.19; N, 7.79. Complex **4** readily loses N_2. Mp 148-150 °C.

[**(PNP)Co]$_2$ (5).** The synthesis was carried out analogously to that of **4** under an Ar atm, starting with KC_8 (0.30 g, 2.2 mmol) and (PNP)CoCl (0.75 g, 1.9 mmol), to yield brown, block-like crystals (0.34 g, 50%) after crystallization from hexane. Crystals suitable for an X-ray diffraction study were grown from a concentrated solution of diethyl ether (**5**) or toluene (**5b**) cooled to -40ºC. ^{1}H NMR 4.87 (br, 4H, PC$H(CH_3)$), 3.10 (br, 4H, NCH_2), 2.76 (br, 4H, NCH_2), 2.24 (br, 12H, PC$H(CH_3)$ (4H) and PCH_2 (8H)), 1.90 (br, 12H, CH_3), 1.31 (br, 12H, CH_3), 0.89 (br, 12H, CH_3), 0.31 (br, 12H, CH_3). ^{31}P NMR 85.71 (br). ^{13}C NMR 61.4 (m, NCH_2), 25.2 (m, P$CH(CH_3)$), 23.7 (m, PCH_2), 20.0 (s, CH_3), 18.6 (s, CH_3). IR (cm^{-1}) 1260 (s), 1149(w), 1092 (s), 1025 (s), 880 (w), 799 (s), 668 (w), 607 (m). Anal. Calc: C, 52.89; H, 9.99; N, 3.85. Observed C, 52.87; H, 9.66; N, 3.90. Mp 113-116 °C. $\mu_{eff} = 0.8\ \mu_B$/Co.

[**(PNP)CoH]$_2$ (6).** Hydrogen was added into a solution of [(PNP)Co]$_2$ (0.15 g, 0.21 mmol) in 15 mL of toluene at room temperature. The reaction mixture was stirred for 48 h, resulting in a color change from brown to brown-yellow. The solvent was removed under vacuum, and the product was extracted with diethyl ether (3 x 10 mL). The solution was concentrated and cooled to -40 °C to give brown, block-like, crystals (0.80 g, 53%). Crystals suitable for an X-ray diffraction study were grown from a concentrated solution of diethyl ether cooled to -40ºC. ^{1}H NMR (C_6D_6) 18.18 (br), 11.06 (br), 4.87 (br), 3.10 (br), 2.77 (br), 1.90 (br), 1.54 (br), 1.32 (br), 1.02 (br), 0.90 (br), 0.31 (br), -9.22 (br), -12.15 (br), -13.56 (br), -22.04 (d). ^{31}P NMR 77.88 (br), 55.84 (br). IR (cm^{-1}) 1883 (s, Co-H), 1361 (m), 1260 (m), 1236 (w), 1026 (s), 880 (m), 812 (m), 640 (w), 607 (w). Anal. Calc: C, 52.74; H, 10.24; N, 3.84. Observed C, 52.74; H, 10.21; N, 3.87. Mp 159-161 °C (d). $\mu_{eff} = 0.7\ \mu_B$/Co.

[**(PNP)CoD]$_2$ (6b).** The synthesis was carried out analogously to that of **6** in D_2 atm, starting with (PNP)CoCl (0.50 g, 0.69 mmol), to yield brown, block-like crystals (0.15 g, 30%) after crystallization from hexane. ^{2}H NMR -21.88 (d). ^{31}P NMR 78.34 (br), 55.38 (br). IR (cm^{-1}) 2803 (s), 1548 (s, D-Co), 1356 (s) 1261 (m), 1235 (m), 1179 (w), 1151 (m), 1026 (s), 881 (s), 811 (m), 700 (w), 666 (w), 641 (m), 606 (m).

(PNP)CoCO (**7**)**.** Carbon monoxide (16.5 mL, 0.68 mmol) was added via syringe into a solution of **6** (0.25 g, 0.34 mmol) in 15 mL of hexane at room temperature. The reaction mixture was stirred overnight and no color change is observed. The solution was concentrated and cooled to -40 °C to give brown, block-like, crystals (0.80 g, 53%). Crystals suitable for an X-ray diffraction study were grown from a concentrated solution of hexane cooled to -40ºC. ^{1}H NMR 3.33 (m, 4H, NH), 2.18 (m, 4H, PC$H(CH_3)$), 1.89 (m, 4H, PCH_2), 1.39 (m, 12H, CH_3), 1.16 (m, 12H, CH_3). ^{31}P NMR 102.52 (s). ^{13}C NMR 60.5 (t, NCH_2), 25.4 (t, P$CH(CH_3)$), 24.4 (t, PCH_2), 19.1 (s, CH_3), 17.7 (s, CH_3). IR (cm^{-1}) 2815 (m), 2782 (s), 1882 (s, C-O), 1104 (s), 1023 (s), 882 (s), 814 (s), 718 (s), 657 (s), 633 (s). Anal. Calc: C, 52.17; H, 9.27; N, 3.58. Observed C, 52.31; H, 9.14; N, 3.60. Mp 154-156 °C.

(HPNP)Co(H)$_3$ (8). A solution of **2** (0.30 mL, 0.75 mmol) in 10 mL of diethyl ether was added to a suspension of KC_8 (0.13 g, 0.96 mmol) in 10 mL of diethyl ether at -78 °C under a hydrogen atm. The reaction mixture was allowed to warm to room temperature and was

stirred for 48 h. Graphite is formed and no color change is observed. The solvent was removed under vacuum, and the product was extracted with hexane (3 x 10 mL) keeping the hydrogen atm. The solution was concentrated and cooled to -40 °C to give brown, block-like crystals (0.80 g, 29%). Crystals suitable for an X-ray diffraction study were grown from a concentrated solution of diethyl ether cooled to -40ºC under hydrogen atm. ^{1}H NMR 18.62 (br), 11.17 (br), 2.98 (br), 2.84 (m), 2.28 (m), 1.98 (br), 1.63 (m), 1.59 (m), 1.32 (m), 1.05 (m), 0.87 (m), -9.52 (br), -12.36 (br). ^{31}P NMR 111.9 (br), 78.2 (br), 55.1 (br). IR (cm^{-1}) 3381 (w), 1915 (w), 1883 (w), 1811 (w), 1548 (m), 1362 (m), 1260 (m), 1236 (w), 1174 (s), 1151 (m), 1025 (s), 881 (s), 812 (s), 721 (w), 667 (m), 607 (m). Anal. Calc: C, 52.31; H, 10.97; N, 3.81. Observed C, 51.01; H, 10.81; N, 3.59. Multiple attempts gave low carbon values. Mp 118-120 °C.

(HPNP)CoCl(H)$_2$ (9). A J. Young NMR tube was filled with 0.5 mL of a $C_6D_5CD_3$ solution of **3** (11 mg, 0.03 mmol). The solution was freeze-pump evacuated three times and filled with hydrogen. The reaction goes from blue to green. Crystals suitable for an X-ray diffraction study were grown from a concentrated solution of toluene cooled to -40ºC under hydrogen atm, to give yellow, block-like crystals, which were immediately transferred to the diffractometer. ^{1}H NMR ($C_6D_5CD_3$) 2.73 (br, 2H, NC*H*$_2$), 2.66 (br, 2H, NC*H*$_2$), 1.93 (br, 2H, PC*H*(CH$_3$)$_2$), 1.81 (br, 2H, PC*H*(CH$_3$)$_2$), 1.66 (br, 2H, PC*H*$_2$), 1.54 (br, 2H, PC*H*$_2$), 1.45 (s, 6H, C*H*$_3$), 1.22 (s, 6H, C*H*$_3$), 1.03 (s, 6H, C*H*$_3$), 0.77 (s, 6H, C*H*$_3$), -23.53 (q, 1H, CoH), -30.01 (m, 1H, CoH). ^{31}P NMR 52.4 (br).

(HPNP)CoCl(H)SiH$_2$Ph (10). H_3SiPh (0.10 mL, 0.81 mmol) was added via syringe to a solution of (HPNP)CoCl (0.30 g, 0.75 mmol) in 5 mL of toluene at room temperature. The solution was stirred for 1 h. A color change from blue to yellow was observed. The solution was cooled to -40 °C to give yellow, rod-like crystals (0.25 g, 66%). Crystals suitable for an X-ray diffraction study were grown from a concentrated solution of toluene cooled to -40ºC. ^{1}H NMR ($C_6D_5CD_3$) 8.25 (d, 2H, *o*-C_6H_5), 7.21 (m, 3H, *m*-C_6H_5 and *p*-C_6H_5), 6.20 (br, 1H, N*H*), 4.69 (s, 2H, Si*H*$_2$), 2.87 (br, 2H, NC*H*$_2$), 2.64 (br, 2H, NC*H*$_2$), 2.11 (br, 4H, PC*H*(CH$_3$)$_2$), 1.61 (br, 4H, PC*H*$_2$), 1.25 – 0.70 (m, 24H, C*H*$_3$), -28.78 (m, 1H, CoH, $J_{H\text{-}P}$: 55 Hz). ^{31}P NMR 87.42 (br), 66.16 (br). IR (cm^{-1}) 3179 (w), 2037 (w), 1260 (s), 1084 (s), 1019 (s), 936 (w), 843 (m), 799 (s), 724 (w), 698 (w). Anal. Calc: C, 52.01; H, 8.93; N, 2.76. Observed C, 51.82; H, 9.11; N, 2.68. Mp 87-91 °C (d).

[(HPNP)CoCl](BF$_4$) (11). A suspension of $AgBPh_4$ (0.22 mL, 0.52 mmol) in 15 mL of THF was added via cannula to a solution of (HPNP)CoCl (0.20 g, 0.50 mmol) in 10 mL of THF at room temperature. The reaction mixture turned from a blue solution to a red suspension and the formation of Ag^0 is observed. After stirring for 1 h, the solvent was removed under vacuum, and the product was extracted with THF (3 x 10 mL). The solution was concentrated and cooled to -40 °C to give red, block-like crystals (0.28 g, 78%). Crystals suitable for an X-ray diffraction study were grown from a concentrated solution of THF cooled to -40ºC. ^{1}H NMR 6.23 (br), 5.05 (br), 3.62 (br), 1.48 (br), 0.96 (br), 0.38 (br). IR (cm^{-1}) 3182 (w), 1578 (m), 1424 (m), 1260 (s), 1085 (s), 1031 (s), 800 (s), 732 (s), 705 (s), 612 (m). Anal. Calc: C, 66.82; H, 7.99; N, 1.95. Observed C, 66.81; H, 8.16; N, 1.76. Mp 117-119 °C.

Crystallographic Analyses. Single crystals of **2** - **11** were coated in Paratone-N oil, mounted on a Kaptan loop, transferred to a Bruker SMART APEX or APEX II QUAZAR diffractometer with CCD area detector,[40] centered in the beam, and cooled by a nitrogen flow

low-temperature apparatus that has been previously calibrated by a thermocouple placed at the same position as the crystal. Preliminary orientation matrixes and cell constants were determined by collection of 60 30-s frames, followed by spot integration and least-squares refinement. A data collection strategy was computed with COSMO to ensure a redundant and complete data set, and the raw data were integrated using SAINT.[41] The data were corrected for Lorentz and polarization effects, but no correction for crystal decay was applied. An empirical absorption correction based on comparison of redundant and equivalent reflections was applied using SADABS.[42] XPREP[43] was used to determine the space group. The structures were solved using SHELXS[44] and refined on all data by full-matrix least-squares with SHELXL-97.[45] Thermal parameters for all non-hydrogen atoms were refined anisotropically. ORTEP diagrams were created using ORTEP-32.[46]

Computational Details. All structures and energies were calculated using the Gaussian09 suite of programs.[47] Self-consistent field computations were performed with tight convergence criteria on ultrafine grids, while geometry optimizations were converged to tight geometric convergence criteria for all compounds. Spin expectation values <S>2 indicated that spin contamination was not significant in any case. Frequencies were calculated analytically at 298.15 K and 1 atm. Structures were considered true minima if they did not exhibit imaginary vibration modes. Optimized geometries were compared using the sum of their electronic and zero-point energies. In order to reduce the computational time, the isopropyl groups attached to phosphorous were substituted for methyl groups for **5** and **6**. The B3LYP hybrid functional was used throughout this computational study.[48, 49] The TPSS functional was used to calculate **5** and **6**.[50] For geometry optimizations and frequency calculations all atoms were treated with 6-31++G(d,p) basis set.[47] A 5d diffusional function was used for all atoms except H, and no polarization functions were added for H.

References

1. Fout, A. R.; Basuli, F.; Fan, H. J.; Tomaszewski, J.; Huffman, J. C.; Baik, M. H.; Mindiola, D. J. *Angew. Chem. Int. Ed.* **2006,** *45*, 3291-3295.
2. Gibson, V. C.; Spitzmesser, S. K. *Chem. Rev.* **2003,** *103*, 283-315.
3. Brookhart, M.; Grant, B. E. *J. Am. Chem. Soc.* **1993,** *115*, 2151-2156.
4. Connolly, P.; Espenson, J. H. *Inorg. Chem.* **1986,** *25*, 2684-2688.
5. McNamara, W. R.; Han, Z. J.; Alperin, P. J.; Brennessel, W. W.; Holland, P. L.; Eisenberg, R. *J. Am. Chem. Soc.* **2010,** *133*, 15368-15371.
6. Wiedner, E. S.; Yang, J. Y.; Dougherty, W. G.; Kassel, W. S.; Bullock, R. M.; DuBois, M. R.; DuBois, D. L. *Organometallics* **2010,** *29*, 5390-5401.
7. Ciancanelli, R.; Noll, B. C.; DuBois, D. L.; DuBois, M. R. *J. Am. Chem. Soc.* **2002,** *124*, 2984-2992.
8. Jones, R. A.; Stuart, A. L.; Atwood, J. L.; Hunter, W. E. *Organometallics* **1983,** *2*, 1437-1441.
9. Kersten, J. L.; Rheingold, A. L.; Theopold, K. H.; Casey, C. P.; Widenhoefer, R. A.; Hop, C. *Angew. Chem. Int. Ed.* **1992,** *31*, 1341-1343.
10. Casey, C. P.; Hallenbeck, S. L.; Widenhoefer, R. A. *J. Am. Chem. Soc.* **1995,** *117*, 4607-4622.
11. Harkins, S. B.; Peters, J. C. *J. Am. Chem. Soc.* **2005,** *127*, 2030-2031.

12. Mankad, N. P.; Rivard, E.; Harkins, S. B.; Peters, J. C. *J. Am. Chem. Soc.* **2005,** *127*, 16032-16033.
13. Holland, P. L.; Cundari, T. R.; Perez, L. L.; Eckert, N. A.; Lachicotte, R. J. *J. Am. Chem. Soc.* **2002,** *124*, 14416-14424.
14. Ding, K. Y.; Brennessel, W. W.; Holland, P. L. *J. Am. Chem. Soc.* **2009,** *131*, 10804-10805.
15. Ding, K. Y.; Pierpont, A. W.; Brennessel, W. W.; Lukat-Rodgers, G.; Rodgers, K. R.; Cundari, T. R.; Bill, E.; Holland, P. L. *J. Am. Chem. Soc.* **2009,** *131*, 9471-9472.
16. Ingleson, M.; Fan, H. J.; Pink, M.; Tomaszewski, J.; Caulton, K. G. *J. Am. Chem. Soc.* **2006,** *128*, 1804-1805.
17. Ingleson, M. J.; Pink, M.; Caulton, K. G. *J. Am. Chem. Soc.* **2006,** *128*, 4248-4249.
18. Ingleson, M. J.; Pink, M.; Fan, H.; Caulton, K. G. *J. Am. Chem. Soc.* **2008,** *130*, 4262-4276.
19. Bowman, A. C.; Milsmann, C.; Atienza, C. C. H.; Lobkovsky, E.; Wieghardt, K.; Chirik, P. J. *J. Am. Chem. Soc.* **2010,** *132*, 1676-1684.
20. Atienza, C. C. H.; Bowman, A. C.; Lobkovsky, E.; Chirik, P. J. *J. Am. Chem. Soc.* **2010,** *132*, 16343-16345.
21. Chomitz, W. A.; Arnold, J. *Chem. Commun.* **2008**, 3648-3650.
22. Chomitz, W. A.; Mickenberg, S. F.; Arnold, J. *Inorg. Chem.* **2008,** *47*, 373-380.
23. Marder, T. B. *Angew. Chem. Int. Ed.* **2007,** *46*, 8116-8118.
24. Bullock, R. M. *Angew. Chem. Int. Ed.* **2011,** *50*, 4050-4052.
25. Hebden, T. J.; St John, A. J.; Gusev, D. G.; Kaminsky, W.; Goldberg, K. I.; Heinekey, D. M. *Angew. Chem. Int. Ed.* **2011,** *50*, 1873-1876.
26. Doherty, M. D.; Grant, B.; White, P. S.; Brookhart, M. *Organometallics* **2007,** *26*, 5950-5960.
27. Gadd, G. E.; Upmacis, R. K.; Poliakoff, M.; Turner, J. J. *J. Am. Chem. Soc.* **1986,** *108*, 2547-2552.
28. Sweany, R. L.; Russell, F. N. *Organometallics* **1988,** *7*, 719-727.
29. Fryzuk, M. D.; Macneil, P. A. *J. Am. Chem. Soc.* **1981,** *103*, 3592-3593.
30. Danopoulos, A. A.; Edwards, P. G. *Polyhedron.* **1989,** *8*, 1339-1344.
31. Danopoulos, A. A.; Edwards, P. G.; Parry, J. S.; Wills, A. R. *Polyhedron.* **1989,** *8*, 1767-1769.
32. Rozenel, S. S.; Kerr, J. B.; Arnold, J. *Dalton Trans.* **2011,** *40*, 10397-10405.
33. Piguet, C. *J. Chem. Educ.* **1997,** *74*, 815-816.
34. Harley, A. D.; Guskey, G. J.; Geoffroy, G. L. **1983,** *2*, 53-59.
35. Chomitz, W. A.; Arnold, J. *Inorg. Chem.* **2009,** *48*, 3274-3286.
36. Kass, M.; Friedrich, A.; Drees, M.; Schneider, S. *Angew. Chem. Int. Ed.* **2009,** *48*, 905-907.
37. Harley, A. D.; Whittle, R. R.; Geoffroy, G. L. **1983,** *2*, 383-387.
38. Limbach, H. H.; Scherer, G.; Maurer, M.; Chaudret, B. **1992,** *31*, 1369-1372.
39. Alaimo, P. J.; Peters, D. W.; Arnold, J.; Bergman, R. G. *J. Chem. Educ.* **2001,** *78*, 64-64.
40. SMART *Area-Detector Software Package, Bruker Analytical X-ray Systems, Inc.: Madison, WI, (2001-2003).* 2001-2003.
41. SAINT *SAX Area-Detector Integration Program, V6.40; Bruker Analytical X-ray Systems Inc.: Madison, WI, (2003).* 2003.

42. SADABS *Bruker-Nonius Area Detector Scaling and Absorption v. 2.05 Bruker Analytical X-ray Systems, Inc.: Madison, WI (2003).* 2003.
43. PREP *(v 6.12) Part of the SHELXTL Crystal Structure Determination Package, Bruker Analytical X-ray Systems, Inc.: Madison, WI, (2001).* 2001.
44. SHELXL *Program for the Refinement of X-ray Crystal Structures, Part of the SHELXT Crystal Structure Determination Package, Bruker Analytical Systems Inc.: Madison, WI, (1995-99).* 1995-1999.
45. SHELXS *Program for the Refinement of X-ray Crystal Structures, Part of the SHELXTL Crystal Structure Determination Package, Bruker Analytical X-ray Systems Inc.: Madison, WI, (1995-99).* 1995-1999.
46. Farrugia, L. *J. Appl. Crystallogr.* **1997,** *30*, 565.
47. Frisch, M. J. T., G. W.; Schlegel, H. B.; Scuseria, G. E.; Robb, M. A.; Cheeseman, J.; R.; Scalmani, G. B., V.; Mennucci, B.; Petersson, G. A.; Nakatsuji, H.; Caricato, M.; Li,; X.; Hratchian, H. P. I., A. F.; Bloino, J.; Zheng, G.; Sonnenberg, J. L.; Hada, M.; Ehara,; M.; Toyota, K. F., R.; Hasegawa, J.; Ishida, M.; Nakajima, T.; Honda, Y.; Kitao, O.;; Nakai, H. V., T.; J. A. Montgomery, J.; Peralta, J. E.; Ogliaro, F.; Bearpark, M.; Heyd, J. J.;; Brothers, E. K., K. N.; Staroverov, V. N.; Kobayashi, R.; Normand, J.; Raghavachari, K.;; Rendell, A. B., J. C.; Iyengar, S. S.; Tomasi, J.; Cossi, M.; Rega, N.; Millam, J. M.; Klene,; M.; Knox, J. E. C., J. B.; Bakken, V.; Adamo, C.; Jaramillo, J.; Gomperts, R.; Stratmann, R.; E.; Yazyev, O. A., A. J.; Cammi, R.; Pomelli, C.; Ochterski, J. W.; Martin, R. L.;; Morokuma, K. Z., V. G.; Voth, G. A.; Salvador, P.; Dannenberg, J. J.; Dapprich, S.;; Daniels, A. D. F., Ö.; Foresman, J. B.; Ortiz, J. V.; Cioslowski, J.; Fox, D. J. *Gaussian09, Revision B.01; Gaussian, Inc.: Wallingford, CT, 2010.*, 2010.
48. Becke, A. D. *Phys. Rev. A* **1988,** *38*, 3098-3100.
49. Lee, C. T.; Yang, W. T.; Parr, R. G. *Phys. Rev. B* **1988,** *37*, 785-789.
50. Frisch, M. J. T., G. W.; Schlegel, H. B.; Scuseria, G. E.; Robb, M. A.; Cheeseman, J.; R.; Scalmani, G. B., V.; Mennucci, B.; Petersson, G. A.; Nakatsuji, H.; Caricato, M.; Li,; X.; Hratchian, H. P. I., A. F.; Bloino, J.; Zheng, G.; Sonnenberg, J. L.; Hada, M.; Ehara,; M.; Toyota, K. F., R.; Hasegawa, J.; Ishida, M.; Nakajima, T.; Honda, Y.; Kitao, O.;; Nakai, H. V., T.; J. A. Montgomery, J.; Peralta, J. E.; Ogliaro, F.; Bearpark, M.; Heyd, J. J.;; Brothers, E. K., K. N.; Staroverov, V. N.; Kobayashi, R.; Normand, J.; Raghavachari, K.;; Rendell, A. B., J. C.; Iyengar, S. S.; Tomasi, J.; Cossi, M.; Rega, N.; Millam, J. M.; Klene,; M.; Knox, J. E. C., J. B.; Bakken, V.; Adamo, C.; Jaramillo, J.; Gomperts, R.; Stratmann, R.; E.; Yazyev, O. A., A. J.; Cammi, R.; Pomelli, C.; Ochterski, J. W.; Martin, R. L.;; Morokuma, K. Z., V. G.; Voth, G. A.; Salvador, P.; Dannenberg, J. J.; Dapprich, S.;; Daniels, A. D. F., Ö.; Foresman, J. B.; Ortiz, J. V.; Cioslowski, J.; Fox, D. J. *Gaussian09, Revision a.2; Gaussian, Inc.: Wallingford, CT, 2009.*, 2009.

Appendix A:

Positional coordinates for calculated structures in Chapter 3

Calculation coordinates and energies For Chapter 3 (Ru chemistry)

H_2
E (a.u.) = -1.168849
ZPE (a.u.) = 0.010125

H	0.000000344	0.000000000	0.000000000
H	-0.000000344	0.000000000	0.000000000

N_2
E (a.u.) = -109.521430ZPE
(a.u.) = 0.005591

N	-0.000000997	0.000000000	0.000000000
N	0.000000997	0.000000000	0.000000000

HNNH
E (a.u.) = -110.621419
ZPE (a.u.) = 0.028412

N	0.000010495	-0.000044701	0.000048892
H	-0.000008520	0.000036289	-0.000006528
N	-0.000010495	0.000044701	-0.000048892
H	0.000008520	-0.000036289	0.000006528

H_2NNH_2
E (a.u.) = -111.822025
ZPE (a.u.) = 0.052616

N	-0.000488579	0.000274662	0.000009513
H	0.000124489	-0.000164397	-0.000196340
H	0.000124494	-0.000177547	0.000184484
N	0.000488579	-0.000274659	-0.000009616
H	-0.000124489	0.000177657	-0.000184429
H	-0.000124494	0.000164283	0.000196388

NH_3
E (a.u.) = -56.531624
ZPE (a.u.) = 0.034385

N	0.000106604	-0.000000001	0.000000000
H	-0.000035535	0.000022703	0.000000000
H	-0.000035535	-0.000011351	-0.000019661
H	-0.000035535	-0.000011351	0.000019661

$\{[HNP_2Ru(N_2))_2(\mu\text{-}Cl)_2\}^{2+}$ (2)
E (a.u.) = -3438.583611
ZPE (a.u.) = 0.599711

Ru	-0.000002281	0.000009776	0.000010095
Ru	0.000002516	-0.000007250	-0.000000492
P	0.000001106	0.000004818	0.000006064
P	0.000004957	-0.000006928	0.000004759
P	0.000000813	0.000004587	-0.000007149
Cl	-0.000001270	0.000000769	-0.000003866
P	-0.000002640	0.000003353	-0.000007469
Cl	0.000003204	-0.000001265	0.000002226
N	0.000001869	0.000003541	-0.000002100
N	-0.000002740	-0.000006812	0.000003010
H	-0.000005171	-0.000001568	0.000001676
C	0.000005396	0.000004303	0.000003892
H	0.000004445	-0.000001830	0.000007142
N	0.000002632	-0.000002455	-0.000008479
N	0.000000502	-0.000002414	0.000003941
H	-0.000003537	-0.000003223	0.000001294
C	0.000002535	0.000004648	0.000002004
H	-0.000001823	0.000000101	-0.000004072
C	0.000009088	-0.000000493	0.000000070
H	-0.000005181	0.000001139	-0.000002966
N	0.000005952	0.000005796	-0.000001677
C	0.000000553	-0.000000310	-0.000001004
H	-0.000006084	-0.000000769	-0.000004066
H	-0.000003407	-0.000001280	-0.000002003
N	0.000004191	0.000004132	-0.000002270
C	0.000002902	-0.000003063	0.000002130
H	0.000001380	0.000000678	0.000000502
C	-0.000005451	-0.000003055	0.000002297
H	-0.000001864	-0.000003683	0.000002441
H	-0.000002489	-0.000003447	0.000004884
C	0.000003350	-0.000000250	0.000005608
H	-0.000002339	-0.000002548	0.000004885
H	0.000001921	-0.000002504	0.000005802
C	-0.000002781	-0.000000504	0.000001576
H	-0.000001763	-0.000002635	0.000002479
H	-0.000003508	-0.000003731	0.000003589
C	0.000010323	-0.000000614	0.000003241
H	0.000001867	0.000001438	0.000006631
C	-0.000004933	-0.000001038	0.000001526
H	-0.000006137	-0.000003566	-0.000001574
H	-0.000004473	-0.000002733	-0.000001635
C	-0.000004766	-0.000002939	0.000000363

H	-0.000004165	-0.000001904	-0.000002285
H	-0.000006540	-0.000002269	-0.000001164
C	-0.000000719	0.000002687	0.000004410
H	0.000000692	0.000001357	-0.000001084
C	0.000004156	-0.000003523	0.000006601
H	0.000000471	-0.000000870	0.000005566
H	-0.000000859	-0.000003014	0.000004917
C	0.000000097	-0.000001665	-0.000006536
H	-0.000005217	0.000004245	-0.000006817
C	-0.000002046	0.000002706	-0.000008621
H	-0.000002277	0.000000365	-0.000006622
C	-0.000002604	-0.000001727	-0.000001770
H	-0.000003686	0.000000368	-0.000000990
H	-0.000004721	-0.000000923	-0.000004447
H	0.000000236	0.000003103	-0.000006378
H	-0.000003807	0.000001290	-0.000006127
H	0.000000074	0.000003058	-0.000005215
H	-0.000001664	0.000001832	-0.000004083
H	0.000005134	0.000001731	0.000000487
H	0.000002972	0.000001217	0.000003304
H	0.000004913	0.000001628	0.000003113
H	0.000005200	0.000001391	0.000004091
H	0.000001243	0.000002255	-0.000005621
H	-0.000000268	0.000000837	-0.000004673
H	0.000000166	0.000004016	-0.000007386
H	-0.000003249	0.000000958	-0.000006710
H	0.000005447	0.000002358	0.000003339
H	0.000005799	0.000001038	0.000003423
H	0.000004430	-0.000000971	0.000002840
H	0.000003926	0.000002249	0.000001130

{[HPNPRu(H$_2$)](μ-Cl)$_2$[HPNPRu(N$_2$)]}$^{2+}$ (2b)

E (a.u.) = -3330.223934

ZPE (a.u.) = 0.607547

Ru	0.000001679	-0.000013665	0.000001822
Ru	0.000006729	-0.000017942	-0.000003044
P	0.000002439	0.000004591	0.000003284
P	0.000001104	0.000002463	0.000000748
P	0.000003826	0.000001418	0.000003992
Cl	-0.000007142	0.000008120	0.000004745
Cl	-0.000002957	0.000001490	-0.000003654
N	-0.000002710	-0.000000148	0.000001075
H	0.000000315	-0.000001124	0.000001393
N	-0.000000715	0.000000377	-0.000000093
H	0.000000242	-0.000000380	-0.000000066
C	0.000000031	0.000000212	0.000000216
H	0.000000588	0.000000688	-0.000000238
H	0.000000158	0.000001147	-0.000000024
C	0.000000467	0.000000208	-0.000000203
H	0.000000166	0.000000388	-0.000000238
H	0.000000076	0.000000618	0.000000045
C	0.000002944	0.000000427	0.000000865
H	0.000001152	-0.000001013	-0.000000237
H	-0.000000271	-0.000000649	-0.000000527
C	0.000000331	0.000002410	-0.000000279
H	-0.000000663	-0.000000304	-0.000000239
H	0.000000805	-0.000000200	-0.000000401
C	-0.000001303	-0.000002583	-0.000000544
H	0.000000806	-0.000000765	-0.000000614
H	0.000000706	0.000000081	-0.000000862
C	0.000001327	-0.000001645	-0.000001199
H	-0.000001521	0.000000920	-0.000000008
H	-0.000000828	0.000000883	0.000000258
P	-0.000002027	0.000002785	0.000000232
C	-0.000000606	0.000000203	0.000000342
H	-0.000000289	0.000000646	0.000000339
H	-0.000000240	0.000000405	0.000000176
C	0.000000158	0.000001107	0.000000180
H	-0.000000034	0.000000608	-0.000000048
H	-0.000000248	0.000000680	0.000000210
H	0.000001245	0.000004350	-0.000000530
H	0.000001243	0.000002269	0.000000118
C	-0.000002089	0.000000229	-0.000000456
H	0.000000744	-0.000000601	-0.000000182
H	0.000000720	-0.000000612	-0.000000831
H	0.000000577	-0.000000496	-0.000000322
C	-0.000001385	-0.000000435	-0.000001875
H	-0.000000055	-0.000001601	0.000000342
H	0.000000460	-0.000000822	-0.000000631
H	0.000000636	-0.000000677	0.000000584
C	-0.000000634	0.000000094	0.000000431
H	0.000000528	-0.000000331	0.000000306
H	-0.000000544	-0.000001096	0.000000774

H	0.000000370	-0.000001229	0.000000073
C	-0.000002072	0.000000537	-0.000000106
H	-0.000000821	0.000000451	0.000000127
H	0.000000210	-0.000000089	-0.000000090
H	-0.000001418	-0.000001579	0.000000233
C	-0.000000411	-0.000000139	0.000000351
H	-0.000000357	0.000000379	0.000000564
H	-0.000000495	0.000000278	0.000000119
H	-0.000000137	0.000000148	0.000000259
C	-0.000000330	-0.000000012	-0.000000471
H	-0.000000434	0.000000872	0.000000420
H	-0.000000107	0.000000586	0.000000176
H	-0.000000103	0.000000328	0.000000357
C	-0.000000059	0.000001107	-0.000000177
H	0.000000333	0.000000596	-0.000000462
H	-0.000000018	-0.000000003	-0.000000065
H	0.000000189	0.000000942	0.000000427
C	-0.000000078	0.000000380	-0.000000591
H	0.000000385	0.000000120	0.000000067
H	0.000000592	0.000000170	-0.000000137
H	0.000000584	0.000000407	-0.000000383
N	-0.000002745	0.000003790	-0.000009688
N	0.000000976	-0.000000767	0.000003863

{[HNP$_2$Ru(H$_2$)]$_2$(μ-Cl)$_2$}$^{2+}$ (3)
E (a.u.) = -3221.862253
ZPE (a.u.) = 0.615433

Ru	0.000017030	-0.000000298	-0.000016827
Ru	-0.000012966	-0.000009632	-0.000033554
P	-0.000000275	0.000003466	-0.000001139
P	0.000003731	-0.000000681	-0.000001592
P	-0.000001022	-0.000000085	0.000003825
Cl	-0.000000741	-0.000007395	-0.000001561
Cl	0.000003589	-0.000001733	0.000011301
N	0.000014085	0.000030103	0.000014529
H	-0.000005485	-0.000003364	0.000002071
N	-0.000018837	0.000000267	-0.000000726
H	0.000004621	-0.000000638	0.000002573
C	-0.000003613	0.000005331	-0.000002592
H	-0.000000255	0.000001186	0.000000677
H	0.000002548	-0.000001852	0.000000185
C	0.000009522	-0.000008378	0.000003852
H	0.000000343	-0.000000048	0.000000156
H	-0.000002051	0.000002755	-0.000001186
C	-0.000004809	-0.000008428	-0.000005940
H	0.000000324	-0.000000678	0.000002324
H	-0.000000457	0.000000460	0.000000154
C	0.000007732	0.000003010	0.000002719
H	-0.000002964	-0.000001914	-0.000000816
H	-0.000003100	-0.000000851	-0.000002095
C	0.000000042	-0.000000400	0.000000604
H	0.000002966	0.000000558	-0.000001111
H	0.000000290	-0.000000564	-0.000000054
C	-0.000002321	-0.000007579	-0.000003708
H	-0.000000001	0.000000448	-0.000001374
H	0.000001461	-0.000000661	0.000001462
P	-0.000004922	0.000003262	0.000003368
C	0.000007659	-0.000008805	-0.000003074
H	-0.000002456	0.000002240	-0.000000448
H	-0.000002036	0.000003763	-0.000001540
C	0.000000351	0.000008651	0.000004823
H	0.000000571	0.000000540	-0.000000034
H	0.000000579	-0.000000507	-0.000000961
H	-0.000006650	-0.000005759	0.000009799
H	0.000012514	0.000004781	0.000011687
H	-0.000009119	0.000010170	0.000000557
H	-0.000008612	-0.000012488	0.000003181
C	-0.000001675	-0.000000665	-0.000000081
H	0.000000302	-0.000001607	0.000000435
H	0.000001462	-0.000000344	0.000000363
H	0.000001535	0.000000258	-0.000000090
C	-0.000001339	-0.000002080	0.000002693
H	0.000000413	0.000000950	-0.000001059
H	-0.000000432	-0.000000433	0.000001256
H	0.000001135	-0.000000823	-0.000001541
C	0.000000807	0.000001178	0.000001559
H	0.000000318	-0.000004074	-0.000000749
H	-0.000000193	-0.000001757	-0.000001897
H	-0.000000372	-0.000000525	-0.000001367
C	-0.000001855	-0.000000172	-0.000000048
H	-0.000000441	-0.000000855	-0.000000235
H	0.000000416	0.000000759	-0.000000313
H	0.000000180	-0.000001304	-0.000000916
C	0.000002218	0.000003167	-0.000000623

H	-0.000001069	0.000000464	0.000001031
H	-0.000000974	-0.000000087	-0.000000927
H	-0.000000230	-0.000000561	-0.000000358
C	-0.000000029	0.000002788	0.000001775
H	0.000000935	-0.000000297	-0.000000234
H	-0.000001278	0.000000586	0.000000007
H	-0.000000465	0.000001786	-0.000000510
C	-0.000002825	-0.000001742	0.000001047
H	0.000000679	0.000001359	0.000000246
H	0.000001736	0.000002370	0.000000152
H	0.000001292	0.000001117	-0.000000748
C	0.000002072	0.000000493	0.000003889
H	-0.000000718	0.000001062	-0.000000521
H	0.000000854	0.000000321	0.000000039
H	0.000000276	0.000000418	-0.000001787

$[(HNP_2Ru)_2(\mu\text{-}Cl)_2(\mu\text{-}HNNH)]^{2+}$ (5*)

E (a.u.) = -3330.197750

ZPE (a.u.) = 0.616270

Ru	-0.000000099	0.000000675	-0.000000127
Ru	0.000002137	0.000020610	-0.000010234
Cl	-0.000001352	-0.000002600	0.000000022
Cl	-0.000002451	0.000006520	0.000005132
P	0.000001131	0.000002159	0.000002099
P	-0.000000020	-0.000008152	0.000003443
P	0.000000544	0.000006242	0.000002156
P	0.000003813	0.000003019	-0.000000717
C	-0.000000148	0.000005129	-0.000005441
H	-0.000000522	0.000001963	-0.000000902
H	0.000000268	-0.000000640	0.000000043
C	-0.000000364	-0.000007722	0.000001263
H	-0.000000892	0.000001868	-0.000000339
H	0.000000118	0.000002115	-0.000000463
N	0.000001998	-0.000010370	-0.000002655
H	-0.000000410	-0.000001703	0.000001240
N	0.000000882	-0.000005171	0.000000542
H	0.000001326	-0.000001013	0.000001127
C	-0.000000703	0.000000575	0.000000243
H	0.000000724	0.000000009	0.000000262
H	-0.000000588	0.000000899	0.000000153
C	-0.000002726	0.000000682	-0.000000256
H	-0.000000922	0.000000325	0.000001312
H	-0.000000232	0.000001017	0.000001536
C	-0.000008413	-0.000000244	-0.000004359
H	0.000000569	0.000002072	-0.000001379
H	-0.000000648	-0.000000104	-0.000003016
C	0.000000428	0.000002344	0.000002623
H	0.000001735	0.000000965	-0.000003697
H	-0.000001606	0.000000004	-0.000001464
C	-0.000000351	-0.000000763	-0.000000895
H	0.000000103	0.000000653	-0.000000315
H	-0.000000573	0.000000327	-0.000000734
C	0.000000718	0.000000434	-0.000000694
H	-0.000000429	-0.000000280	0.000001899
H	0.000000272	-0.000000011	0.000002484
C	-0.000005749	0.000006398	-0.000001154
H	-0.000002101	0.000001187	0.000000027
H	0.000004308	-0.000009490	0.000000984
H	0.000001486	-0.000001770	0.000002087
C	0.000000758	-0.000001581	0.000002318
H	0.000000680	-0.000000099	0.000000858
H	-0.000000910	-0.000000260	0.000000719
H	-0.000000219	-0.000000082	0.000000427
C	-0.000007695	-0.000001115	-0.000005311
H	0.000006402	0.000004634	-0.000001827
H	0.000001182	0.000000038	0.000000051
H	-0.000000611	-0.000000985	0.000000675
C	0.000002251	0.000002028	-0.000001068
H	-0.000000097	-0.000000842	-0.000000965
H	-0.000000285	-0.000000465	-0.000002222
H	0.000000811	0.000000522	-0.000002008
C	-0.000000804	-0.000002215	0.000001796
H	0.000000719	-0.000000161	0.000000944
H	0.000000093	-0.000000655	0.000001809
H	-0.000000250	-0.000001181	0.000001426
C	-0.000001605	-0.000000696	0.000001327
H	-0.000000047	-0.000001763	0.000001575
H	-0.000000344	-0.000000637	0.000001843
H	-0.000000277	0.000000442	0.000001767
C	-0.000000421	-0.000000945	0.000000417
H	-0.000000050	-0.000001187	0.000000148
H	0.000000870	-0.000001128	-0.000000636
H	0.000000124	-0.000001273	0.000000750
C	0.000002178	-0.000000617	-0.000001204

H	0.000000458	-0.000000542	-0.000001010
H	-0.000000764	-0.000000527	-0.000000379
H	-0.000000120	-0.000000779	-0.000000647
H	0.000002760	0.000001769	-0.000005298
N	0.000001416	-0.000007227	0.000009213
H	0.000001382	-0.000000017	0.000002203
N	0.000001157	-0.000000613	0.000000474

{[HPNPRu(NNH$_2$)](μ-Cl)$_2$ [HPNPRu(N$_2$)]}$^{2+}$ (5b)

E (a.u.) = -3439.698486

ZPE (a.u.) = 0.622190

Ru	0.000010157	-0.000001844	0.000013787
Ru	-0.000012488	0.000000585	0.000000576
P	0.000013832	0.000001271	0.000001287
P	-0.000012772	-0.000010374	0.000005086
P	0.000003189	0.000019350	-0.000003265
Cl	0.000004240	0.000006535	0.000004507
P	0.000007974	0.000005771	-0.000003096
Cl	-0.000001677	-0.000007255	0.000008821
N	0.000007307	-0.000001719	-0.000005614
N	0.000005438	-0.000020017	-0.000018942
H	-0.000010506	0.000008410	0.000006130
C	-0.000002018	-0.000005851	-0.000011377
H	0.000001489	0.000002512	0.000005114
N	0.000006767	0.000010522	0.000010654
N	-0.000002267	-0.000004639	0.000008953
H	0.000000708	-0.000004072	0.000000435
C	0.000002688	0.000010978	0.000010136
H	-0.000008118	-0.000005940	-0.000006414
C	0.000010171	-0.000008721	0.000003215
H	-0.000010119	-0.000000158	0.000000839
C	0.000001807	-0.000005080	0.000002614
H	0.000000870	0.000001132	-0.000002094
H	-0.000002158	0.000002433	0.000000085
N	0.000001938	0.000003408	-0.000002515
C	0.000001074	-0.000002115	0.000001596
H	0.000004917	0.000005430	0.000004356
C	-0.000005231	-0.000003559	-0.000000324
H	0.000002182	0.000004104	0.000002540
H	0.000000963	0.000002972	0.000001955
C	-0.000000695	0.000004330	0.000001147
H	-0.000002949	-0.000000545	0.000003884
H	0.000001840	-0.000001102	0.000000564
C	0.000004590	0.000018331	0.000006478
H	0.000003232	-0.000003040	-0.000002863
H	-0.000002734	-0.000003198	-0.000003632
C	0.000011561	-0.000001948	-0.000001521
H	-0.000006748	0.000004350	0.000002667
C	-0.000000290	0.000001826	-0.000002004
H	-0.000003913	-0.000000727	0.000000811
H	-0.000001991	-0.000000166	0.000000312
C	0.000001447	-0.000000446	0.000005353
H	0.000002522	-0.000001012	-0.000000486
H	-0.000002355	0.000001599	-0.000000678
C	-0.000007602	0.000005003	-0.000001708
H	-0.000001979	0.000003294	-0.000001035
C	0.000008591	-0.000008662	0.000006393
H	-0.000005160	0.000004371	-0.000000410
H	-0.000007227	-0.000000801	-0.000000829
C	-0.000006474	0.000004162	-0.000002243
H	0.000000460	-0.000002440	-0.000002598
C	0.000000724	-0.000000600	-0.000004905
H	0.000000792	0.000000640	0.000000449
C	-0.000009370	-0.000009294	-0.000007185
H	0.000000739	-0.000001048	0.000000951
H	-0.000001592	0.000001293	-0.000000585
H	0.000002763	0.000000350	-0.000001970
H	-0.000000647	-0.000000090	0.000001854
H	0.000002024	0.000000340	-0.000001497
H	0.000000797	0.000000270	0.000002017
H	0.000002073	0.000002128	0.000002384
H	0.000002813	0.000000267	0.000000357
H	0.000001428	0.000000833	0.000001806
H	0.000000076	-0.000000247	0.000002321
H	0.000002252	-0.000005411	-0.000007866
H	-0.000001564	-0.000000548	-0.000004828
H	-0.000000645	-0.000004820	-0.000001175
H	-0.000000328	-0.000002416	-0.000000997
H	0.000003792	0.000005724	0.000000467
H	0.000003213	0.000003382	-0.000000947
H	0.000002505	-0.000002431	-0.000002631
H	-0.000001166	-0.000001061	-0.000002284
N	-0.000020332	-0.000022131	-0.000024313

H	0.000003435	0.000001823	0.000001662
H	0.000001739	0.000005803	0.000000269

$[(HNP_2Ru)_2(\mu\text{-}Cl)_2(\mu\text{-}H_2NNH_2)]^{2+}$ (4a)

E (a.u.) = -3331.378060

ZPE (a.u.) = 0.641063

Ru	-0.000001162	0.000009607	0.000007328
Ru	0.000004235	-0.000012871	0.000008121
Cl	0.000003530	-0.000000157	-0.000002156
Cl	0.000000161	-0.000003102	-0.000001211
P	-0.000001553	-0.000003339	0.000002925
P	-0.000000766	0.000002845	-0.000001422
P	0.000000711	0.000004564	0.000001373
P	-0.000003308	-0.000000964	-0.000005150
C	-0.000000784	-0.000001026	-0.000000324
H	0.000000637	-0.000001730	-0.000000709
H	-0.000000323	-0.000000776	-0.000001198
C	-0.000002562	0.000000846	-0.000002838
H	0.000000011	0.000000709	-0.000001075
H	-0.000000705	0.000000796	-0.000001693
N	-0.000000354	0.000003966	-0.000000917
H	-0.000001478	0.000002040	0.000000935
H	0.000002403	0.000001290	0.000000601
N	-0.000003839	-0.000002364	-0.000002112
H	0.000001525	0.000002598	0.000000048
H	-0.000002505	0.000001130	-0.000000713
C	0.000001126	-0.000000931	-0.000000052
H	-0.000000251	-0.000003348	-0.000000304
H	0.000000896	-0.000004024	0.000000806
C	-0.000001969	0.000000897	0.000000390
H	0.000000357	-0.000003779	-0.000002253
H	-0.000000374	-0.000004683	-0.000001510
C	0.000000827	-0.000003291	0.000004145
H	0.000000726	-0.000001377	0.000002531
H	0.000000518	-0.000000916	0.000000797
C	0.000002522	0.000000082	-0.000000638
H	0.000000408	0.000000222	0.000002349
H	0.000000236	0.000000721	0.000001141
C	-0.000000679	0.000000436	0.000005738
H	0.000001424	-0.000001965	0.000001623
H	0.000002855	-0.000001907	0.000002409
C	0.000003388	0.000001365	-0.000000522
H	-0.000001702	-0.000002984	-0.000002049
H	-0.000000046	-0.000004551	-0.000002212
C	0.000002487	-0.000000574	-0.000002987
H	-0.000000606	0.000003060	-0.000001644
H	-0.000002820	0.000005464	0.000000639
H	-0.000001408	0.000004164	-0.000002322
C	-0.000001452	0.000001621	-0.000000075
H	-0.000001409	0.000002198	-0.000004217
H	-0.000000184	-0.000000402	-0.000004035
H	-0.000001480	0.000001432	-0.000002907
C	0.000003139	0.000001892	0.000003219
H	-0.000000209	0.000001355	0.000000399
H	0.000000520	0.000003815	0.000004141
H	-0.000000310	0.000004900	0.000000943
C	0.000002732	0.000000820	0.000002443
H	0.000000322	-0.000000035	0.000002344
H	-0.000000267	0.000002160	0.000002641
H	0.000000446	0.000001222	0.000003812
C	-0.000003098	-0.000001291	-0.000003925
H	0.000001792	0.000001387	0.000000135
H	-0.000001869	-0.000000690	-0.000002297
H	0.000000445	0.000002396	-0.000002308
C	0.000000213	-0.000000699	-0.000002535
H	-0.000000047	0.000001415	-0.000004274
H	-0.000002498	-0.000001628	-0.000003602
H	-0.000001204	0.000000118	-0.000003577
C	0.000000415	0.000000445	0.000001413
H	0.000000196	-0.000000677	0.000000457
H	-0.000000001	0.000000017	0.000002594
H	0.000000451	-0.000000410	-0.000000924
C	-0.000000723	0.000002880	0.000002141
H	0.000001154	0.000001755	0.000001454
H	0.000001710	-0.000000010	0.000001326
H	0.000002790	-0.000000825	0.000004536
H	-0.000000425	-0.000002682	-0.000001973
N	-0.000003270	0.000002721	0.000000588
H	-0.000000017	-0.000002847	-0.000001273
N	0.000000350	-0.000008497	-0.000002553

$[(HNP_2Ru)_2(\mu\text{-}Cl)_2(\mu\text{-}H_2NNH_2)]^{2+}$ (4b)

E (a.u.) = -3331.370923
ZPE (a.u.) = 0.640979

Ru	0.000021879	-0.000014986	0.000043255
Ru	0.000006731	0.000011544	-0.000005828
Cl	0.000002645	0.000000717	0.000010515
Cl	0.000000267	-0.000008312	-0.000013369
P	0.000007474	0.000003415	-0.000016206
P	0.000006720	-0.000003111	0.000001734
P	-0.000008230	-0.000002910	0.000015742
P	-0.000005351	0.000015383	0.000017027
N	-0.000011048	0.000018331	-0.000014618
H	-0.000002421	-0.000012179	0.000008449
H	0.000009109	0.000006538	-0.000004555
N	-0.000002248	-0.000018847	-0.000004481
H	0.000000808	0.000008939	0.000004503
H	-0.000000146	0.000000515	-0.000005545
C	-0.000014833	-0.000003078	-0.000014280
H	0.000003282	0.000000841	0.000000269
H	0.000001602	0.000004236	0.000003173
N	0.000000467	-0.000005131	-0.000003622
H	-0.000001585	-0.000000853	-0.000010424
N	-0.000003453	0.000018456	0.000003049
H	-0.000008000	-0.000006308	0.000005082
C	-0.000010871	-0.000016332	-0.000010000
H	0.000001588	-0.000000602	0.000004416
H	0.000000358	-0.000000307	0.000002697
C	0.000001815	0.000002090	0.000003329
H	-0.000001616	-0.000000401	-0.000002611
H	0.000000970	0.000000112	-0.000001082
C	-0.000000008	0.000012938	-0.000011226
H	0.000009952	0.000002282	-0.000001889
H	-0.000002016	0.000000792	-0.000001095
C	0.000006085	0.000000963	0.000002293
H	-0.000002888	-0.000001420	0.000001863
H	-0.000001708	0.000000655	0.000001661
C	0.000015220	0.000006234	-0.000007045
H	-0.000004078	-0.000001826	-0.000001497
H	-0.000002973	0.000001648	-0.000002617
C	0.000000128	-0.000012527	-0.000000775
H	-0.000002796	0.000000295	0.000000038
H	0.000003901	0.000000573	0.000001173
C	-0.000019538	0.000002993	-0.000004039
H	0.000001851	-0.000001351	0.000000316
H	0.000004144	-0.000007441	-0.000003222
C	0.000001728	-0.000009431	0.000001068
H	-0.000001961	0.000002592	0.000004364
H	0.000000440	0.000007166	0.000005232
H	0.000000421	0.000001094	0.000001616
C	-0.000002045	0.000002311	-0.000002422
H	-0.000001018	0.000000168	0.000004583
H	0.000001231	-0.000001040	0.000003536
H	-0.000000649	-0.000004080	0.000003607
C	0.000000494	-0.000007333	0.000002282
H	0.000001183	0.000002711	0.000000035
H	-0.000001918	0.000003449	0.000000027
H	0.000002620	0.000003911	-0.000003195
C	0.000007327	0.000003272	-0.000004942
H	-0.000002785	-0.000000451	0.000001206
H	0.000003782	0.000000560	0.000002900
H	0.000000032	-0.000002985	0.000003231
C	-0.000004039	-0.000000925	0.000001736
H	0.000000972	-0.000002117	-0.000004444
H	0.000001612	-0.000007665	0.000005695
H	0.000001013	-0.000001635	-0.000000547
C	-0.000004323	-0.000002005	-0.000010609
H	0.000004711	0.000003284	0.000000485
H	0.000001527	0.000003158	0.000002829
H	0.000003425	0.000000249	0.000003471
C	0.000002444	-0.000006793	0.000008940
H	-0.000004810	-0.000000422	-0.000005953
H	-0.000004483	0.000004015	-0.000006190
H	0.000002324	-0.000005054	-0.000002634
C	-0.000005115	0.000013991	-0.000000080
H	-0.000006030	0.000002327	-0.000008202
H	0.000001690	-0.000000913	0.000000197
H	-0.000000987	-0.000003976	0.000001625

{[HPNPRu(=NH))(μ-Cl)$_2$ (HPNPRu(NH$_3$)]}$^{2+}$ (4c)
E (a.u.) = -3331.356851
ZPE (a.u.) = 0.634876

Ru	-0.000000313	0.000006839	0.000003216
Ru	0.000008353	0.000006238	-0.000007016

P	0.000000412	0.000003397	-0.000000595
P	0.000009437	-0.000000673	-0.000002869
P	-0.000007512	-0.000010375	0.000003473
Cl	0.000000804	0.000001177	0.000015772
P	-0.000000838	0.000005768	0.000002172
Cl	-0.000008346	-0.000011824	-0.000006793
N	-0.000010376	0.000007168	0.000004844
H	0.000004287	-0.000001256	0.000002127
C	-0.000003065	-0.000002001	0.000001766
H	-0.000003556	-0.000002155	-0.000000141
N	-0.000000146	0.000006731	-0.000000836
H	-0.000001706	0.000001519	-0.000000474
C	0.000006524	0.000003141	-0.000001660
H	-0.000000922	-0.000000294	0.000005296
C	-0.000000847	-0.000000390	0.000000593
H	0.000001823	0.000000963	0.000000532
C	-0.000003894	0.000001695	-0.000000039
H	0.000001932	0.000001643	0.000003324
H	0.000002658	0.000003024	-0.000000189
C	-0.000005750	0.000001081	-0.000006765
H	-0.000001876	0.000000016	0.000002829
C	-0.000001523	0.000000662	-0.000003726
H	-0.000000757	0.000003256	-0.000001875
H	0.000000284	0.000003845	-0.000002107
C	-0.000001564	-0.000001054	-0.000004626
H	0.000001026	0.000003573	-0.000000349
H	-0.000000260	0.000001714	-0.000002682
C	0.000009585	-0.000003468	-0.000009377
H	-0.000001079	0.000000704	0.000000706
H	-0.000001005	0.000003421	0.000001898
C	-0.000006182	-0.000003056	0.000001971
H	0.000001557	0.000001864	-0.000004014
C	0.000003613	0.000006967	-0.000007969
H	-0.000001219	-0.000000917	0.000001660
H	0.000002996	0.000000566	0.000001983
C	0.000001370	0.000002485	-0.000004172
H	-0.000001108	0.000001686	0.000001367
H	0.000001273	0.000002666	0.000002551
C	0.000003258	-0.000001609	-0.000003447
H	0.000000987	-0.000003663	0.000001482
C	-0.000003142	0.000002862	-0.000003061
H	0.000000488	-0.000000057	-0.000000099
H	-0.000000685	-0.000000166	0.000000027
C	-0.000002628	0.000001206	0.000000348
H	0.000003798	-0.000000456	0.000005970
C	0.000002905	0.000000486	0.000002599
H	-0.000001705	0.000000340	0.000003325
C	0.000002014	0.000002887	0.000003440
H	0.000003292	-0.000001366	-0.000000735
H	0.000000555	-0.000001562	0.000005139
H	0.000001866	-0.000001040	0.000001679
H	0.000001801	0.000001587	0.000000897
H	0.000000378	-0.000001417	0.000001308
H	-0.000000472	-0.000000322	0.000000052
H	-0.000000530	0.000001007	-0.000000503
H	0.000001627	-0.000000190	-0.000002646
H	0.000001822	-0.000001905	-0.000001609
H	-0.000000437	-0.000003926	-0.000000817
H	-0.000000689	-0.000005038	0.000002741
H	0.000000813	-0.000004045	0.000001531
H	0.000000015	-0.000002394	0.000002946
H	0.000000732	-0.000001366	0.000001256
H	0.000000289	-0.000003219	-0.000003365
H	-0.000001385	-0.000000270	-0.000002539
H	-0.000002108	-0.000001959	-0.000001977
H	-0.000002003	-0.000001245	-0.000000542
H	-0.000002327	-0.000000114	0.000003229
H	-0.000001145	-0.000006123	-0.000006111
H	0.000006686	-0.000002526	0.000005306
N	-0.000008087	0.000000406	-0.000007087
N	0.000000929	-0.000011517	0.000004501
H	-0.000001000	0.000000367	-0.000003044

{[PNPRu(NH$_3$)]$_2$(μ-Cl)$_2$}$^{2+}$ (4f)

E (a.u.) = -3331.350761

ZPE (a.u.) = 0.632603

Ru	-0.000030484	0.000007643	0.000003503
Ru	0.000020945	-0.000006793	-0.000010921
P	0.000002279	0.000003519	0.000012941
P	-0.000005326	0.000001993	0.000015370
P	0.000019947	-0.000009964	-0.000004061
Cl	0.000004564	-0.000004652	0.000011567
P	-0.000015506	0.000000448	0.000001828
Cl	-0.000001201	0.000000532	-0.000005199

N	-0.000005696	0.000005981	0.000014441
C	0.000003796	0.000004141	0.000003915
H	-0.000000504	-0.000000962	-0.000000227
N	0.000003733	0.000003111	0.000016713
C	0.000004662	0.000005030	0.000000466
H	-0.000000551	0.000002675	0.000001806
C	-0.000003106	0.000004714	0.000000398
H	-0.000000442	-0.000002835	-0.000000397
C	0.000004975	0.000011929	0.000004051
H	-0.000002665	-0.000004151	-0.000001297
H	-0.000001255	-0.000003969	0.000001606
C	-0.000002506	-0.000004000	-0.000002480
H	-0.000000137	0.000001071	0.000000546
C	0.000016552	-0.000010328	-0.000008934
H	-0.000007046	0.000002472	-0.000000303
H	-0.000009297	0.000006902	0.000006328
C	-0.000007297	-0.000010513	-0.000011076
H	0.000004088	0.000000678	0.000000186
H	0.000000045	0.000003379	0.000003121
C	-0.000009468	-0.000011116	-0.000016782
H	0.000007541	-0.000000338	0.000000142
H	0.000012413	0.000004479	0.000009554
C	-0.000002155	0.000002602	0.000004693
H	-0.000000885	0.000000432	-0.000000356
C	-0.000007199	0.000015384	-0.000019658
H	0.000001057	-0.000003937	0.000002781
H	-0.000003043	-0.000003161	0.000001433
C	0.000003851	0.000015676	-0.000016874
H	0.000000504	-0.000005610	0.000000509
H	-0.000002632	-0.000003180	0.000002077
C	0.000000984	-0.000003730	-0.000003507
H	-0.000000146	-0.000001488	0.000001237
C	0.000008047	-0.000011779	-0.000010245
H	0.000001097	0.000002353	0.000003843
H	-0.000004083	0.000000878	-0.000001155
C	-0.000001400	-0.000001634	0.000000642
H	-0.000002424	0.000002053	-0.000000416
C	0.000003695	-0.000002003	0.000001662
H	0.000000516	0.000002409	-0.000000316
C	-0.000003753	0.000011657	0.000005237
H	0.000001045	-0.000003350	0.000000825
H	0.000002017	-0.000004738	-0.000001491
H	0.000001459	-0.000000642	0.000000297
H	-0.000001311	-0.000000868	0.000000222
H	0.000000061	-0.000000022	-0.000001407
H	0.000002266	-0.000001072	-0.000002788
H	-0.000000203	0.000002217	-0.000000687
H	0.000000738	0.000001105	0.000000446
H	0.000000980	-0.000000712	-0.000000078
H	0.000000379	-0.000001609	-0.000001461
H	0.000001216	0.000000201	-0.000001253
H	-0.000002826	-0.000001190	-0.000003020
H	-0.000001896	-0.000001032	0.000000609
H	0.000000554	-0.000000518	0.000000324
H	-0.000000811	-0.000001326	-0.000001715
H	0.000000358	-0.000000191	-0.000001719
H	-0.000000206	0.000000576	-0.000000318
H	-0.000000951	-0.000000513	-0.000000290
H	-0.000004668	-0.000002693	-0.000000945
H	0.000001973	0.000002857	0.000008697
H	0.000004323	0.000001601	0.000000113
H	-0.000001902	0.000002352	0.000009218
H	0.000003540	-0.000002373	0.000001721
H	-0.000005298	-0.000000202	-0.000002582
N	0.000004661	0.000000123	-0.000010137
N	-0.000000585	-0.000005982	-0.000010974

{[HPNPRu(NHNH$_3$)](*μ*-Cl)$_2$ [HPNPRu(N$_2$)]}$^{2+}$ (4d)

E (a.u.) = -3440.864688

ZPE (a.u.) = 0.647365

P	0.000001056	-0.000008203	0.000002141
P	0.000007822	-0.000003599	-0.000001583
P	-0.000005006	-0.000009012	-0.000012063
Cl	-0.000001567	0.000009388	0.000004984
P	0.000004364	-0.000004554	0.000011249
Cl	-0.000007960	-0.000007799	0.000003478
C	-0.000000849	-0.000001565	-0.000006829
H	-0.000002427	0.000001208	0.000002452
C	0.000001227	0.000003222	0.000007351
H	0.000001202	-0.000006459	0.000001500
C	0.000001602	0.000003064	0.000002082
H	0.000000258	0.000000097	0.000000356

C	-0.000000483	0.000007799	-0.000001253
H	-0.000002198	0.000000232	-0.000001244
H	0.000000855	0.000000279	-0.000000487
C	-0.000000925	0.000003125	0.000001647
H	-0.000000879	0.000000611	-0.000001029
C	-0.000000414	-0.000004011	-0.000004339
H	-0.000000390	0.000000154	0.000001035
H	-0.000001152	0.000000085	0.000001342
C	-0.000000470	0.000003137	-0.000005102
H	-0.000001886	0.000001607	-0.000001266
H	-0.000001335	0.000000331	0.000002419
C	0.000016463	-0.000018047	0.000008653
H	-0.000000396	0.000000215	-0.000001370
H	-0.000003140	0.000000659	0.000000112
C	-0.000001411	0.000001713	-0.000001706
H	-0.000001008	0.000001756	0.000000065
C	0.000005167	0.000013214	0.000003186
H	0.000001458	-0.000003743	-0.000000411
H	0.000001011	-0.000004393	0.000000248
C	-0.000007961	-0.000001404	-0.000000759
H	0.000000272	0.000000625	-0.000000271
H	0.000002831	-0.000000111	0.000001733
C	-0.000001639	0.000003392	0.000001839
H	-0.000002125	-0.000002303	0.000001045
C	-0.000008892	0.000012903	0.000000734
H	0.000000444	-0.000004269	0.000001443
H	0.000001017	-0.000001749	-0.000001568
C	-0.000001957	-0.000001774	-0.000001790
H	0.000000864	0.000000237	0.000000679
C	-0.000002101	0.000001367	0.000002115
H	0.000000275	0.000000839	-0.000001890
C	-0.000009460	-0.000012667	0.000012228
H	0.000002875	-0.000001417	0.000000831
H	-0.000000568	-0.000000678	-0.000001601
H	0.000000884	0.000000702	0.000000005
H	0.000001877	0.000001475	0.000000872
H	0.000002035	0.000000498	-0.000002018
H	-0.000001744	-0.000000032	-0.000003757
H	-0.000001434	-0.000000420	-0.000001760
H	-0.000000696	0.000000232	-0.000001896
H	0.000000966	0.000001689	-0.000000366
H	0.000001003	-0.000000255	-0.000002626
H	0.000001127	0.000000326	0.000000624
H	0.000001202	-0.000000708	0.000000099
H	-0.000000146	0.000002519	0.000000223
H	0.000001335	-0.000001660	-0.000000085
H	-0.000000080	-0.000000962	-0.000000414
H	-0.000004003	0.000006696	0.000002491
H	0.000002102	-0.000001612	0.000000265
H	-0.000002168	0.000000406	-0.000002411
Ru	0.000031768	0.000005197	0.000018138
H	-0.000004716	0.000004739	0.000001485
H	0.000005266	0.000007275	0.000005530
H	-0.000001424	-0.000001657	0.000006940
H	0.000015221	-0.000007062	-0.000005906
N	-0.000017339	-0.000004392	-0.000004666
N	0.000000648	-0.000006546	0.000000899
Ru	-0.000000047	0.000016241	-0.000000016
N	0.000010985	-0.000009587	-0.000029773
N	-0.000004452	0.000006919	0.000015289
H	-0.000000023	-0.000002789	0.000001361
H	0.000000520	-0.000001111	-0.000003136
N	-0.000026927	0.000012563	-0.000026697
N	0.000005797	-0.000002180	0.000000915

{[HPNPRu(NH_2NH_2)](μ-Cl)$_2$ [HPNPRu(N_2)]}$^{2+}$ (4e)

E (a.u.) = -3440.898844

ZPE (a.u.) = 0.647949

P	-0.000001153	0.000002481	0.000000799
P	0.000001181	-0.000000864	-0.000001376
P	-0.000001416	0.000001879	-0.000000321
Cl	-0.000002881	-0.000003408	-0.000001147
P	0.000003417	-0.000005338	0.000003041
Cl	0.000000648	-0.000001937	-0.000002518
C	0.000002092	0.000000038	-0.000001587
H	0.000000833	-0.000000027	-0.000000464
C	-0.000000841	-0.000001330	0.000001104
H	-0.000000194	-0.000000430	0.000000922
C	-0.000001780	-0.000000857	0.000001169
H	-0.000000834	-0.000000370	-0.000000375
C	-0.000001110	-0.000000742	-0.000003434
H	0.000000287	0.000000392	0.000001460

H	-0.000000311	0.000000435	0.000001273	H	-0.000000643	-0.000000847	0.000001054
C	-0.000001283	0.000000008	0.000000440	H	0.000000098	-0.000000505	0.000001707
H	0.000000201	-0.000000303	-0.000000857	H	-0.000000381	0.000000082	-0.000001817
C	0.000000471	0.000002858	0.000000261	H	-0.000001090	-0.000001489	-0.000000690
H	-0.000000389	0.000000893	-0.000000299	H	-0.000000250	0.000000203	-0.000001460
H	0.000000618	0.000001252	-0.000000298	H	0.000000185	-0.000001160	0.000000164
C	-0.000000179	-0.000000519	-0.000003248	Ru	0.000002456	0.000001930	0.000007382
H	-0.000000020	0.000001172	-0.000000978	H	-0.000000054	-0.000001521	0.000000241
H	0.000000039	0.000000264	-0.000001182	H	0.000000375	-0.000000284	-0.000000729
C	-0.000000125	0.000001094	-0.000001217	N	-0.000001695	-0.000002848	-0.000001943
H	0.000000058	0.000001033	-0.000000103	Ru	0.000009971	0.000019282	-0.000012620
H	0.000000356	0.000001566	-0.000000225	H	-0.000000270	0.000001709	-0.000000174
C	0.000000567	-0.000001386	-0.000001314	H	0.000002620	-0.000000044	0.000005083
H	0.000000064	-0.000000261	-0.000001626	N	-0.000001014	-0.000000518	0.000001767
C	0.000000351	0.000001711	0.000000857	N	-0.000008172	-0.000006203	-0.000002851
H	-0.000000084	0.000001457	0.000000750	H	0.000000142	-0.000000174	0.000000025
H	0.000000207	0.000000790	0.000000731	H	0.000000211	-0.000002275	0.000004518
C	0.000000183	-0.000000346	0.000001467	N	0.000000946	0.000000845	-0.000002898
H	-0.000000109	0.000000924	0.000000087	N	-0.000001534	-0.000001797	-0.000004733
H	0.000000297	0.000000993	0.000000313	N	0.000000249	-0.000007418	0.000010467
C	0.000000669	0.000000367	-0.000002985				
H	0.000000209	0.000000942	0.000000716				
C	-0.000000278	-0.000000125	-0.000000609				
H	0.000000058	0.000001334	-0.000001184				
H	-0.000000015	0.000000635	-0.000000635				
C	-0.000000177	-0.000000603	0.000001438				
H	-0.000000041	0.000000264	0.000001477				
C	-0.000001345	0.000000742	0.000002538				
H	0.000000049	-0.000000546	0.000000733				
C	-0.000000575	0.000001725	0.000001727				
H	-0.000000220	0.000000647	0.000000973				
H	0.000000324	0.000000914	0.000001121				
H	0.000000140	-0.000000966	0.000001020				
H	0.000000070	-0.000000595	0.000001762				
H	-0.000002076	-0.000001175	0.000000254				
H	0.000001615	0.000000247	0.000000197				
H	-0.000001504	-0.000000949	-0.000001513				
H	0.000001732	-0.000001105	-0.000001552				
H	0.000000124	-0.000000967	-0.000001272				
H	0.000000140	-0.000000079	-0.000001292				
H	-0.000000595	-0.000000479	0.000000959				
H	0.000000382	-0.000000321	0.000001532				

Appendix B:

Positional coordinates for calculated structures in Chapter 4

Calculation coordinates and energies For Chapter 4 (Co chemistry)

B3LYP

H2

E (a.u.) = -1.168849
ZPE (a.u.) = 0.010125

H	0.000000344	0.000000000	0.000000000
H	-0.000000344	0.000000000	0.000000000

N_2

E (a.u.) = -109.521430ZPE
(a.u.) = 0.005591

N	-0.000000997	0.000000000	0.000000000
N	0.000000997	0.000000000	0.000000000

H_3SiPh

E (a.u.) = -522.842654
ZPE (a.u.) = 0.115293

C	0.000041943	0.000077220	0.000012766
C	-0.000011771	0.000009709	-0.000022907
C	-0.000099907	0.000019515	0.000022598
C	0.000001443	-0.000025714	-0.000018745
C	0.000022375	-0.000089026	0.000010391
C	0.000001918	0.000011773	-0.000003855
H	0.000008314	-0.000037329	0.000002577
H	0.000022118	-0.000022885	0.000004694
H	0.000020123	0.000023738	0.000003562
H	0.000010630	0.000039020	0.000002732
H	-0.000016991	-0.000001352	-0.000008314
Si	0.000023568	-0.000005347	0.000047957
H	0.000006238	0.000000006	0.000026527
H	-0.000013588	-0.000004015	-0.000040635
H	-0.000016412	0.000004688	-0.000039348

$(P^{Me}NP^{Me})Co$ (singlet)

E (a.u.) = -2436.773899
ZPE (a.u.) = 0.271395

Co	0.000000001	0.000014010	-0.000015614
P	0.000002590	0.000005582	0.000001236
P	-0.000003103	0.000004085	0.000001430
N	0.000000889	-0.000011567	0.000012316
C	0.000004390	-0.000001210	0.000004793
H	-0.000000178	-0.000001941	-0.000002624
H	-0.000001726	-0.000001210	-0.000001798
C	0.000001617	-0.000003990	-0.000000215
H	-0.000001176	0.000001484	-0.000000018
H	0.000001649	0.000000724	0.000000211
C	-0.000003658	-0.000001526	0.000005286
H	0.000001776	-0.000001098	-0.000001660
H	0.000000134	-0.000001815	-0.000002714
C	-0.000002357	-0.000003929	0.000000339
H	-0.000001707	0.000000762	0.000000042
H	0.000001280	0.000001539	-0.000000035
C	-0.000007124	0.000000283	0.000002392
H	0.000003794	-0.000001139	-0.000000051
H	0.000002591	0.000001500	-0.000000938
H	0.000001928	0.000000185	-0.000000256
C	-0.000003084	-0.000000728	-0.000002923
H	0.000001415	0.000001074	0.000000622
H	-0.000001702	-0.000002206	-0.000000072
H	0.000002088	0.000000724	0.000000708
C	0.000006728	0.000001223	0.000001555
H	-0.000002317	-0.000000103	-0.000000229
H	-0.000002490	0.000001907	-0.000000446
H	-0.000003408	-0.000001622	0.000000125
C	0.000002503	-0.000001076	-0.000002125
H	0.000002197	-0.000001717	-0.000000250
H	-0.000001220	0.000000847	0.000000662
H	-0.000002320	0.000000946	0.000000252

$(P^{Me}NP^{Me})Co$ (triplet)

E (a.u.) = -2436.809775
ZPE (a.u.) = 0.270927

Co	-0.000000473	-0.000000208	0.000006045
P	-0.000002740	0.000002752	-0.000003616
P	-0.000000983	-0.000000067	-0.000007843
N	-0.000001573	0.000007657	0.000038384
C	-0.000000737	-0.000007576	-0.000002430
H	0.000003008	0.000000240	0.000000075
H	0.000000463	0.000000161	0.000001226
C	0.000027833	-0.000004556	-0.000020987
H	-0.000003123	0.000002707	0.000002959
H	-0.000001738	-0.000000438	0.000004269
C	-0.000002390	-0.000009513	-0.000004216

H	0.000000000	0.000000398	0.000000999
H	-0.000002598	0.000000801	0.000001259
C	-0.000024102	-0.000006944	-0.000020993
H	0.000001523	-0.000000425	0.000004451
H	0.000002460	0.000002841	0.000002963
C	-0.000000442	-0.000006423	-0.000007437
H	-0.000005387	0.000005802	0.000001992
H	-0.000003999	0.000004220	0.000004383
H	0.000002940	0.000001459	0.000005571
C	0.000016977	-0.000005905	-0.000002396
H	-0.000006348	0.000002403	-0.000000555
H	-0.000002507	0.000003788	-0.000002830
H	-0.000004975	-0.000000356	-0.000000495
C	0.000000486	-0.000006005	-0.000010712
H	-0.000000468	0.000002248	0.000007437
H	0.000004625	0.000003029	0.000002700
H	0.000003552	0.000007554	0.000002580
C	-0.000013067	-0.000006834	-0.000001084
H	0.000004172	0.000004325	-0.000002361
H	0.000004687	0.000003438	0.000002422
H	0.000004924	-0.000000574	-0.000001760

[($P^{Me}NP^{Me}$)Co]$_2$ (singlet)

E (a.u.) = -4873.600825

ZPE (a.u.) = 0.545658

Co	-0.000015229	0.000023950	0.000046719
Co	0.000025002	-0.000025507	0.000031378
P	-0.000004938	-0.000021557	-0.000025329
P	-0.000009427	-0.000008025	-0.000014555
P	-0.000020346	0.000005451	-0.000009136
P	0.000001625	-0.000001931	-0.000007339
N	-0.000004540	-0.000002534	-0.000031379
N	0.000005500	0.000009763	-0.000026223
C	-0.000008853	-0.000002282	-0.000000472
H	0.000001333	0.000002743	-0.000001555
H	0.000003202	0.000003886	-0.000001263
C	-0.000003123	0.000004208	0.000011149
H	0.000000341	0.000000581	-0.000001750
H	-0.000002927	0.000002667	-0.000003193
C	0.000005406	0.000003302	-0.000003399
H	-0.000002207	-0.000000597	0.000002318
H	0.000000032	-0.000004021	0.000003380
C	0.000025141	0.000005480	0.000001967
H	-0.000008421	0.000001480	-0.000004158
C	0.000004140	-0.000009042	0.000001496
H	-0.000002749	0.000006397	0.000000773
H	-0.000003974	0.000000379	0.000000233
C	-0.000001557	0.000006299	0.000007550
H	0.000000368	-0.000007442	-0.000001071
H	-0.000000955	-0.000001997	-0.000007322
C	0.000004418	0.000007952	0.000003381
H	0.000001955	-0.000005762	0.000005378
C	0.000000916	0.000000285	-0.000000022
H	0.000000103	-0.000002019	-0.000000277
C	-0.000000825	-0.000004889	-0.000005804
H	-0.000001047	0.000004061	0.000001852
C	0.000002246	-0.000001292	-0.000000014
H	-0.000001242	0.000000002	0.000002300
H	-0.000004370	0.000000320	0.000004033
C	0.000002217	0.000000114	0.000001657
H	0.000000022	-0.000000361	-0.000000003
C	0.000009602	0.000002422	0.000006147
H	-0.000003181	-0.000000620	0.000000815
H	-0.000003315	-0.000000851	-0.000001699
C	0.000009296	0.000006407	0.000012792
H	0.000002723	0.000005389	-0.000002686
H	0.000004114	0.000000405	-0.000006179
C	-0.000004619	-0.000010148	0.000000203
H	0.000002044	0.000005883	-0.000000770
C	0.000002953	-0.000001807	0.000003637
H	-0.000000440	0.000003263	-0.000000951
H	-0.000001063	0.000001526	0.000000267
H	-0.000000295	0.000003220	-0.000001133
C	0.000006319	0.000000656	0.000006386
H	-0.000002557	-0.000000100	-0.000002507
H	-0.000000291	0.000000673	0.000005518
H	-0.000002991	0.000001014	-0.000000594
H	-0.000000299	0.000002411	0.000000574
H	-0.000001010	-0.000000513	0.000004011
H	-0.000000398	0.000004495	0.000000160
H	-0.000000525	0.000003070	0.000002127
H	-0.000002421	-0.000000772	-0.000001867
H	-0.000000496	-0.000005738	-0.000001267
H	-0.000002286	-0.000002617	-0.000000645

H	-0.000001374	-0.000001833	-0.000002158
H	0.000000579	-0.000001672	-0.000000671
H	0.000002454	-0.000001347	-0.000000128
H	0.000000771	-0.000000987	-0.000000954
H	-0.000000529	-0.000001891	0.000000273

[($P^{Me}NP^{Me}$)Co]$_2$ (triplet)

E (a.u.) = -4873.634120

ZPE (a.u.) = 0.544614

Co	-0.000015229	0.00002395	0.000046719
Co	0.000025002	-0.000025507	0.000031378
P	-0.000004938	-0.000021557	0.000025329
P	-0.000009427	-0.000008025	0.000014555
P	-0.000020346	0.000005451	0.000009136
P	0.000001625	-0.000001931	0.000007339
N	-0.00000454	-0.000002534	0.000031379
N	0.0000055	0.000009763	0.000026223
C	-0.000008853	-0.000002282	0.000000472
H	0.000001333	0.000002743	0.000001555
H	0.000003202	0.000003886	0.000001263
C	-0.000003123	0.000004208	0.000011149
H	0.000000341	0.000000581	-0.00000175
H	-0.000002927	0.000002667	0.000003193
C	0.000005406	0.000003302	0.000003399
H	-0.000002207	-0.000000597	0.000002318
H	0.000000032	-0.000004021	0.00000338
C	0.000025141	0.00000548	0.000001967
H	-0.000008421	0.00000148	0.000004158
C	0.00000414	-0.000009042	0.000001496
H	-0.000002749	0.000006397	0.000000773
H	-0.000003974	0.000000379	0.000000233
C	-0.000001557	0.000006299	0.00000755
H	0.000000368	-0.000007442	0.000001071
H	-0.000000955	-0.000001997	0.000007322
C	0.000004418	0.000007952	0.000003381
H	0.000001955	-0.000005762	0.000005378
C	0.000000916	0.000000285	0.000000022
H	0.000000103	-0.000002019	0.000000277
C	-0.000000825	-0.000004889	0.000005804
H	-0.000001047	0.000004061	0.000001852
C	0.000002246	-0.000001292	0.000000014
H	-0.000001242	0.000000002	0.0000023
H	-0.00000437	0.00000032	0.000004033
C	0.000002217	0.000000114	0.000001657
H	0.000000022	-0.000000361	0.000000003
C	0.000009602	0.000002422	0.000006147
H	-0.000003181	-0.00000062	0.000000815
H	-0.000003315	-0.000000851	0.000001699
C	0.000009296	0.000006407	0.000012792
H	0.000002723	0.000005389	0.000002686
H	0.000004114	0.000000405	0.000006179
C	-0.000004619	-0.000010148	0.000000203
H	0.000002044	0.000005883	-0.00000077
C	0.000002953	-0.000001807	0.000003637
H	-0.00000044	0.000003263	0.000000951
H	-0.000001063	0.000001526	0.000000267
H	-0.000000295	0.00000322	0.000001133
C	0.000006319	0.000000656	0.000006386
H	-0.000002557	-0.0000001	0.000002507
H	-0.000000291	0.000000673	0.000005518
H	-0.000002991	0.000001014	0.000000594
H	-0.000000299	0.000002411	0.000000574
H	-0.00000101	-0.000000513	0.000004011
H	-0.000000398	0.000004495	0.00000016
H	-0.000000525	0.00000307	0.000002127
H	-0.000002421	-0.000000772	0.000001867
H	-0.000000496	-0.000005738	0.000001267
H	-0.000002286	-0.000002617	0.000000645
H	-0.000001374	-0.000001833	0.000002158
H	0.000000579	-0.000001672	0.000000671
H	0.000002454	-0.000001347	0.000000128

H	0.000000771	-0.000000987	-0.000000954
H	-0.000000529	-0.000001891	0.000000273

[($P^{Me}NP^{Me}$)CoH]$_2$ (triplet)
E (a.u.) = -4874.798505
ZPE (a.u.) = 0.560680

Co	0.000032939	-0.000012604	0.000047812
Co	-0.000034412	0.000021717	0.000040141
P	-0.000021453	-0.000001127	-0.000016227
P	0.000006746	0.000001921	0.000037632
P	0.000020381	0.000001558	-0.000012423
P	-0.000006982	-0.000003191	0.000034859
N	0.000003171	-0.000009810	-0.000025906
N	-0.000003102	0.000003168	-0.000033298
C	0.000000103	-0.000001220	0.000006086
H	0.000000819	-0.000003008	-0.000000845
C	0.000018663	0.000028724	0.000028207
H	-0.000001906	0.000000961	-0.000005644
H	0.000001781	-0.000004214	-0.000008217
C	-0.000022078	-0.000029595	0.000028927
H	0.000000906	-0.000001158	-0.000004533
H	-0.000002100	0.000002818	-0.000007896
C	0.000010222	-0.000004477	-0.000003741
H	0.000000357	0.000000710	0.000000883
C	0.000000525	-0.000001399	-0.000010480
H	0.000002032	-0.000000475	-0.000003528
C	-0.000002861	-0.000007926	-0.000006802
H	-0.000001645	-0.000001708	0.000001851
C	-0.000002060	-0.000017472	-0.000002771
H	-0.000001203	0.000000314	0.000001655
H	-0.000000829	0.000006806	0.000002013
C	-0.000000257	-0.000000974	0.000005545
H	-0.000001241	0.000003837	0.000000294
C	0.000003902	0.000015587	-0.000003769
H	0.000001151	-0.000000556	0.000001702
H	0.000000968	-0.000006492	0.000002562
C	0.000000064	0.000002231	-0.000010220
H	0.000004192	0.000004559	0.000000563
C	0.000003988	0.000008425	-0.000007237
H	0.000001441	0.000000286	0.000001331
C	-0.000002596	0.000007102	-0.000004345
H	0.000004784	-0.000000680	-0.000003932
H	-0.000002028	-0.000000315	0.000003159
C	0.000005369	-0.000003282	0.000000647
H	-0.000004980	0.000000800	-0.000003012
H	-0.000000181	0.000000090	0.000002749
C	-0.000022115	-0.000000551	-0.000009101
H	0.000001356	0.000001447	0.000003629
H	0.000004041	-0.000000678	-0.000001696
C	-0.000008240	0.000001468	-0.000002431
H	-0.000001465	0.000003392	0.000003028
C	0.000019781	0.000000351	-0.000009599
H	-0.000001193	-0.000001512	0.000003915
H	-0.000003898	0.000000524	-0.000001560
H	0.000000241	0.000003083	-0.000000899
H	-0.000000838	0.000003232	-0.000000673
H	-0.000000497	-0.000000572	0.000000828
H	0.000000772	-0.000000033	-0.000000945
H	0.000001066	0.000001818	0.000001802
H	0.000000286	0.000000494	0.000001354
H	-0.000002525	0.000000675	-0.000003896
H	0.000000510	0.000000906	-0.000000511
H	0.000001316	-0.000003626	0.000000841
H	-0.000000339	-0.000002785	-0.000000765
H	-0.000000657	0.000000840	-0.000000550
H	0.000001585	-0.000002924	0.000003015
H	-0.000000311	-0.000000708	0.000001336
H	-0.000001386	-0.000000722	0.000001298
H	-0.000000203	-0.000001075	-0.000001105
H	-0.000004285	-0.000004847	0.000000537
H	-0.000000865	0.000008639	-0.000033528
H	0.000005276	-0.000006768	-0.000028114

(PNP)CoN_2
E (a.u.) = -2860.630048
ZPE (a.u.) = 0.508308

Co	-0.000011450	0.000027761	0.000023414
P	-0.000000842	-0.000012677	-0.000006357
P	-0.000009525	-0.000010043	0.000005487
N	0.000038615	0.000007876	-0.000004871
C	0.000000614	-0.000001796	-0.000000483

H	0.000000938	0.000001382	-0.000000629
H	0.000000652	0.000001421	0.000001414
C	-0.000008332	-0.000003074	-0.000000520
H	0.000000598	0.000000929	-0.000000291
H	0.000001694	0.000000255	0.000000650
C	-0.000002114	0.000001727	0.000003775
H	0.000002402	0.000000589	-0.000000901
H	0.000002165	0.000001517	-0.000001944
C	-0.000007995	-0.000005975	-0.000003851
H	0.000001566	0.000000339	0.000001084
H	0.000000270	0.000001277	-0.000001009
C	-0.000000312	-0.000002337	-0.000004422
H	-0.000001082	0.000002375	-0.000000265
H	0.000000540	-0.000000245	-0.000000563
H	-0.000002089	0.000002228	0.000002248
C	-0.000000674	0.000004148	-0.000002479
H	-0.000000119	-0.000000579	0.000001315
C	-0.000001047	0.000000147	-0.000008645
H	-0.000000650	0.000000930	0.000002279
C	0.000001388	0.000001140	0.000001929
H	-0.000000687	0.000000198	-0.000000138
C	-0.000009263	0.000004180	0.000002361
H	0.000002504	-0.000001381	-0.000001382
C	-0.000001487	-0.000000145	0.000000289
H	-0.000001042	0.000001362	-0.000001052
H	-0.000000303	-0.000000716	0.000000306
H	0.000000729	0.000000286	-0.000000453
C	0.000000376	-0.000000213	0.000001010
H	-0.000000097	-0.000001656	0.000000334
H	-0.000000352	-0.000001385	0.000000290
H	-0.000000906	-0.000000795	0.000000875
C	0.000003055	-0.000002956	0.000002723
H	-0.000000028	-0.000000960	0.000000666
H	0.000000693	-0.000000880	-0.000000451
H	0.000000533	0.000001060	0.000000450
C	0.000001707	0.000000621	0.000002119
H	-0.000000391	-0.000001648	0.000000502
H	-0.000001003	-0.000002131	0.000000597
H	-0.000000734	-0.000001217	-0.000000479
C	-0.000000971	0.000003372	0.000000811
H	-0.000000817	0.000000785	-0.000001839
H	-0.000000409	-0.000000773	-0.000001702
H	-0.000000216	0.000000032	-0.000000631
N	-0.000001342	-0.000001036	-0.000000075
C	-0.000001955	0.000001082	-0.000001923
H	-0.000000207	0.000000775	-0.000001296
H	0.000001144	-0.000000516	0.000001018
H	0.000000082	0.000000211	0.000000012
C	0.000002825	-0.000001816	0.000003287
H	-0.000000415	-0.000000899	0.000000982
H	0.000001676	-0.000000327	-0.000000722
H	-0.000000254	0.000000177	0.000001072
N	0.000002343	-0.000012003	-0.000013925

(PNP)Co (singlet)

E (a.u.) = -2751.061184

ZPE (a.u.) = 0.498810

Co	-0.000000247	0.000019869	-0.000009192
P	0.000008184	-0.000010216	-0.000000549
P	-0.000008004	-0.000010290	-0.000000637
N	0.000000145	-0.000000281	-0.000005014
C	0.000008717	-0.000003671	0.000009447
H	-0.000000226	0.000001038	-0.000001916
H	-0.000000434	0.000000580	-0.000000631
C	0.000014639	0.000001266	0.000001942
H	-0.000003031	0.000002162	0.000000601
H	0.000000074	0.000001776	0.000000834
C	-0.000008883	-0.000003707	0.000009366
H	0.000000439	0.000000536	-0.000000719
H	0.000000252	0.000001295	-0.000001940
C	-0.000014780	0.000001377	0.000002067
H	-0.000000083	0.000001818	0.000000839
H	0.000003100	0.000002274	0.000000648
C	-0.000000248	-0.000002277	0.000000693
H	0.000000044	0.000000326	-0.000001865
H	-0.000000863	0.000000514	-0.000001377
H	0.000000602	0.000000078	-0.000001384
C	-0.000005307	0.000003619	-0.000002203
H	0.000001393	0.000000673	-0.000000015
C	0.000000470	-0.000002052	-0.000006486
H	0.000001210	0.000003657	0.000003597
C	0.000005056	0.000003425	-0.000002074
H	-0.000001384	0.000000627	-0.000000250
C	-0.000000400	-0.000001745	-0.000006647

H	-0.000000904	0.000003803	0.000003665
C	-0.000000384	-0.000001897	0.000001153
H	0.000000111	-0.000000159	-0.000001386
H	-0.000000020	-0.000000511	-0.000000789
H	0.000000671	0.000000801	-0.000001310
C	-0.000001352	-0.000003171	0.000004289
H	0.000000363	-0.000001357	0.000000723
H	-0.000000985	-0.000000750	-0.000000106
H	0.000000666	-0.000001436	0.000000044
C	0.000001060	0.000001722	0.000001026
H	0.000000193	-0.000000369	0.000001211
H	0.000000643	-0.000000172	0.000001529
H	-0.000000835	-0.000000153	0.000000620
C	0.000001485	-0.000003227	0.000004136
H	-0.000000471	-0.000001368	0.000000712
H	-0.000000680	-0.000001849	-0.000000022
H	0.000000959	-0.000000787	-0.000000208
C	0.000000264	-0.000002270	0.000000547
H	0.000000039	0.000000293	-0.000001856
H	-0.000000555	0.000000072	-0.000001436
H	0.000000770	0.000000665	-0.000001597
C	0.000000230	-0.000001788	0.000001043
H	-0.000000113	-0.000000144	-0.000001358
H	-0.000000643	0.000000768	-0.000001211
H	-0.000000045	-0.000000128	-0.000000756
C	-0.000000966	0.000001655	0.000001080
H	-0.000000107	-0.000000339	0.000001195
H	0.000000787	-0.000000257	0.000000436
H	-0.000000617	-0.000000317	0.000001490

(PNP)Co (triplet)

E (a.u.) = -2751.097103

ZPE (a.u.) = 0.498272

Co	0.000000270	-0.000015270	-0.000039115
P	-0.000006652	0.000007448	-0.000000567
P	0.000006479	0.000008120	-0.000000370
N	-0.000000237	-0.000042752	0.000076836
C	-0.000007039	0.000026795	-0.000027456
H	-0.000009990	-0.000008671	0.000011733
H	-0.000001345	-0.000007746	-0.000003954
C	-0.000053732	0.000001492	-0.000007436
H	0.000007098	-0.000003097	-0.000000645
H	0.000003827	0.000002039	0.000000870
C	0.000007018	0.000026739	-0.000027423
H	0.000001347	-0.000007751	-0.000003918
H	0.000009969	-0.000008683	0.000011736
C	0.000053931	0.000001370	-0.000007433
H	-0.000003840	0.000002041	0.000000875
H	-0.000007129	-0.000003105	-0.000000659
C	-0.000000010	0.000005028	-0.000004233
H	0.000000159	0.000001121	0.000003276
H	0.000002373	-0.000005703	0.000003932
H	0.000002298	0.000000791	0.000002558
C	0.000015130	0.000001789	0.000018226
H	-0.000001500	0.000003876	0.000002068
C	0.000005849	0.000001698	0.000012576
H	0.000004111	-0.000009490	-0.000008492
C	-0.000015310	0.000001746	0.000018256
H	0.000001476	0.000003884	0.000002086
C	-0.000005631	0.000001760	0.000012647
H	-0.000004160	-0.000009457	-0.000008467
C	-0.000013005	0.000004206	-0.000002842
H	0.000000665	0.000000813	0.000002287
H	0.000001985	0.000003537	0.000002294
H	0.000001176	-0.000001598	0.000001464
C	-0.000001028	-0.000002530	-0.000009763
H	-0.000000914	0.000001895	-0.000004786
H	-0.000001488	0.000002940	0.000003092
H	-0.000001021	-0.000002004	0.000000844
C	0.000008356	0.000006567	-0.000007802
H	-0.000001097	-0.000003903	-0.000002678
H	0.000001697	0.000002166	-0.000001439
H	-0.000000309	-0.000000650	-0.000002282
C	0.000001067	-0.000002558	-0.000009694
H	0.000000920	0.000001888	-0.000004793
H	0.000001007	-0.000001979	0.000000846
H	0.000001497	0.000002938	0.000003095
C	0.000000016	0.000004976	-0.000004202
H	-0.000000163	0.000001118	0.000003283
H	-0.000002319	0.000000790	0.000002551
H	-0.000002339	-0.000005698	0.000003947
C	0.000012991	0.000004137	-0.000002797
H	-0.000000653	0.000000811	0.000002265
H	-0.000001189	-0.000001585	0.000001450

H	-0.000001975	0.000003501	0.000002305
C	-0.000008349	0.000006563	-0.000007793
H	0.000001077	-0.000003889	-0.000002677
H	0.000000329	-0.000000634	-0.000002243
H	-0.000001695	0.000002171	-0.000001436

[(PNP)Co(H)$_2$ (singlet)
E (a.u.) = -2752.265827
ZPE (a.u.) = 0.515180

Co	-0.000001986	-0.000009339	0.000002325
P	-0.000007575	-0.000003098	0.000013499
P	-0.000005096	-0.000007745	0.000015745
N	0.000008760	0.000000068	-0.000006006
C	0.000007765	0.000000778	-0.000001434
H	-0.000002666	0.000000645	0.000001754
C	-0.000006452	-0.000005661	-0.000004201
H	0.000001296	0.000002367	-0.000003155
H	0.000001133	-0.000001909	0.000000002
C	-0.000000700	0.000010010	-0.000003905
H	0.000001607	0.000000230	0.000000010
H	0.000000649	-0.000002276	-0.000000115
C	0.000001128	0.000010681	-0.000001900
H	-0.000002883	0.000000008	0.000000255
C	0.000000249	0.000000108	0.000002061
H	0.000001021	-0.000001657	0.000000331
H	-0.000000021	-0.000001038	-0.000000868
H	0.000000752	-0.000002339	-0.000000008
C	0.000000661	-0.000000725	-0.000001125
H	0.000001574	0.000000460	-0.000000432
H	0.000000640	0.000000366	0.000000053
H	0.000000227	0.000000081	0.000003371
C	0.000002551	0.000002931	-0.000005660
H	-0.000000281	-0.000000057	0.000001110
H	-0.000002637	-0.000002564	0.000000042
C	-0.000005413	0.000000537	-0.000005215
H	-0.000000765	-0.000000785	-0.000001162
H	0.000000990	0.000002133	0.000000203
C	0.000000933	-0.000001271	-0.000001929
H	-0.000000165	-0.000003844	0.000000941
C	-0.000000917	-0.000003052	-0.000000295
H	-0.000000304	-0.000001342	0.000000591
H	0.000001690	-0.000001740	-0.000003142
H	-0.000001197	-0.000001086	0.000001305
C	0.000000044	-0.000001774	-0.000000412
H	-0.000000391	-0.000001561	0.000002342
H	-0.000000690	-0.000001430	0.000000246
H	0.000001161	-0.000000129	-0.000001332
C	0.000004634	0.000002841	-0.000001691
H	-0.000002146	0.000003222	-0.000001010
H	-0.000002106	0.000000134	0.000001672
H	-0.000000609	0.000001010	0.000000806
C	-0.000000358	-0.000006304	0.000002459
H	-0.000000060	0.000002182	0.000002663
H	0.000001381	0.000001411	-0.000000797
H	0.000000710	0.000002712	0.000000130
C	-0.000002484	-0.000000573	0.000003100
H	-0.000000036	0.000000585	-0.000002788
H	0.000000390	-0.000000145	-0.000000875
H	0.000000164	0.000001730	0.000000570
C	0.000003741	-0.000001880	0.000002782
H	-0.000000946	-0.000000871	0.000001434
H	0.000000099	-0.000001309	0.000001467
H	-0.000000293	0.000001331	0.000000524
C	-0.000002768	0.000003895	-0.000014976
H	0.000001104	0.000003058	0.000002425
H	-0.000004401	0.000010226	-0.000009226
H	0.000009292	0.000001765	0.000007443

[(PNP)Co(H)$_2$(H$_2$) (singlet)
E (a.u.) = -2753.420747
ZPE (a.u.) = 0.532475

Co	-0.000008003	-0.000011744	0.000009059
P	0.000002919	0.000004290	0.000011484
P	0.000000276	0.000011122	0.000005692
N	0.000006391	-0.000012539	0.000005221
C	0.000002750	-0.000001793	-0.000000484
H	0.000000058	0.000000005	0.000000380
C	0.000001899	-0.000003752	-0.000000676
H	-0.000000638	0.000001354	0.000001215
H	-0.000002041	0.000001448	0.000000123
C	-0.000005605	-0.000006345	0.000000914
H	0.000000696	0.000002054	-0.000000106
H	0.000001959	0.000002484	0.000000601
C	-0.000002211	-0.000001113	0.000000543

H	0.000001453	0.000000913	-0.000000857
C	0.000000007	-0.000002974	-0.000000035
H	0.000000602	-0.000002408	0.000000566
H	-0.000000272	-0.000002075	-0.000000040
H	0.000001147	-0.000002451	0.000000818
C	-0.000001065	0.000001173	-0.000001262
H	0.000001083	0.000001649	0.000002279
H	-0.000000462	0.000003909	0.000000741
H	0.000000273	0.000000454	0.000000309
C	-0.000006571	0.000008417	-0.000001900
H	-0.000001409	-0.000001652	-0.000002093
H	0.000000257	0.000001675	0.000000094
C	0.000007947	0.000004944	0.000002964
H	-0.000002259	0.000002849	-0.000000277
H	-0.000001096	-0.000001205	-0.000000680
C	0.000003472	0.000000213	0.000003030
H	0.000002148	-0.000000993	-0.000000119
C	0.000000689	-0.000002233	0.000001841
H	0.000000870	-0.000000691	0.000001939
H	0.000001449	-0.000000985	0.000001127
H	0.000000636	-0.000000346	0.000001513
C	0.000000852	0.000000262	0.000002135
H	0.000002184	-0.000000606	0.000002507
H	-0.000001027	0.000001343	0.000000368
H	0.000000091	0.000000058	0.000003470
C	0.000000834	0.000001908	-0.000000375
H	-0.000000355	0.000001750	-0.000001714
H	-0.000000964	0.000002276	-0.000001647
H	-0.000000054	-0.000000842	-0.000001773
C	-0.000001544	-0.000003996	-0.000000563
H	-0.000000505	-0.000002177	-0.000001084
H	-0.000000377	-0.000000392	-0.000000902
H	-0.000001118	-0.000000975	-0.000002288
C	-0.000001062	-0.000000418	0.000000185
H	-0.000000939	-0.000000972	-0.000001562
H	-0.000000717	-0.000000816	-0.000001644
H	0.000000188	-0.000002533	-0.000001761
C	0.000000037	-0.000002285	-0.000000065
H	-0.000000738	-0.000000453	-0.000000636
H	0.000000758	0.000000305	0.000000060
H	-0.000000811	0.000000229	-0.000001955
C	0.000002542	-0.000004317	-0.000005566
H	0.000000054	-0.000000185	-0.000001025
H	-0.000003303	0.000009751	0.000000144
H	-0.000001750	-0.000001624	-0.000033426
H	0.000001467	0.000006002	0.000011886
H	-0.000001090	0.000005052	-0.000006692

[(HPNP)CoH (triplet)

E (a.u.) = -2752.261774

ZPE (a.u.) = 0.517548

Co	-0.000025205	-0.000055926	0.000005146
P	0.000027749	-0.000001913	-0.000018947
P	-0.000008165	0.000068210	-0.000013440
N	0.000000701	0.000009394	-0.000006330
H	0.000003271	-0.000000560	-0.000008031
C	-0.000001718	-0.000003370	0.000000813
H	0.000000686	0.000001701	-0.000000106
H	-0.000001709	0.000000990	0.000002251
C	0.000012697	-0.000015095	0.000011431
H	0.000001934	0.000002030	0.000001696
C	0.000002276	0.000001643	-0.000004233
H	0.000000296	-0.000001171	-0.000002009
H	0.000000938	-0.000002455	-0.000000078
C	0.000003095	-0.000004269	-0.000000532
H	0.000001586	-0.000003287	0.000003858
H	-0.000002443	-0.000002908	-0.000000385
C	0.000004031	-0.000015165	-0.000007452
H	-0.000002350	0.000000554	0.000002110
C	-0.000004758	-0.000012381	0.000004493
H	0.000001851	-0.000002067	-0.000002771
H	0.000002098	-0.000000959	-0.000000484
C	-0.000009495	0.000010207	-0.000001582
H	0.000003171	0.000002454	-0.000001777
C	-0.000003756	0.000000762	0.000008137
H	-0.000000223	-0.000001255	0.000001915
C	-0.000000359	0.000001877	-0.000002849
H	0.000000183	0.000000198	0.000000981
H	0.000001040	0.000000856	0.000000280
H	-0.000000545	0.000000589	-0.000000089
C	-0.000000209	-0.000000644	0.000003994
H	-0.000000111	0.000001816	-0.000000836
H	-0.000000825	0.000000240	0.000000053
H	-0.000000180	0.000002244	-0.000002256

C	0.000005294	0.000002651	0.000000275
H	-0.000001826	-0.000001750	0.000000225
H	-0.000000337	0.000000084	0.000000138
H	-0.000000353	-0.000002054	-0.000000127
C	0.000001411	-0.000002275	-0.000000751
H	0.000000488	0.000000958	0.000000756
H	0.000000654	0.000000995	0.000001315
H	-0.000001045	0.000001165	0.000002699
C	-0.000000564	0.000000930	0.000008705
H	-0.000001699	0.000000591	-0.000002425
H	-0.000001595	0.000000429	-0.000003567
H	-0.000001542	0.000001140	-0.000003887
C	-0.000000474	0.000001616	-0.000001255
H	0.000000250	0.000000038	0.000002438
H	-0.000000530	-0.000000196	0.000001843
H	0.000002172	0.000000313	0.000000798
C	-0.000000048	0.000001271	-0.000002276
H	0.000002043	0.000001684	-0.000003785
H	-0.000000457	0.000002233	0.000001261
H	-0.000000934	-0.000002499	-0.000002596
C	-0.000002604	0.000005354	0.000009035
H	0.000000632	0.000002135	0.000001089
H	0.000000586	0.000001363	0.000000671
H	-0.000000386	0.000001131	0.000000451
H	-0.000004686	0.000000353	0.000016000

[(HPNP)CoH(H_2) (triplet)

E (a.u.) = -2753.419603

ZPE (a.u.) = 0.531796

Co	0.000001507	0.000004064	0.000000666
P	-0.000004507	-0.000000751	0.000003649
P	0.000001245	-0.000000051	-0.000009727
N	0.000005662	-0.000001612	-0.000007071
H	-0.000000408	-0.000003695	0.000001061
C	-0.000002986	-0.000002538	-0.000003207
H	0.000000520	-0.000000384	-0.000000203
H	-0.000000562	-0.000000405	0.000000163
C	0.000001574	0.000000334	0.000001814
H	-0.000000391	-0.000000318	-0.000000950
C	0.000005393	-0.000003479	0.000001810
H	0.000000608	-0.000000487	-0.000000912
H	0.000000813	-0.000001187	-0.000000654
C	-0.000002200	0.000006631	0.000005932
H	-0.000001365	0.000000982	0.000000597
H	0.000001445	-0.000000893	-0.000003265
C	-0.000000886	-0.000007033	0.000003074
H	-0.000001308	0.000000323	-0.000001680
C	-0.000003540	-0.000002163	0.000004025
H	0.000000060	0.000000192	-0.000000826
H	-0.000000946	-0.000000759	-0.000001123
C	-0.000001718	0.000002794	0.000000621
H	-0.000000163	-0.000000430	0.000001246
C	0.000003309	-0.000001632	0.000010059
H	0.000000443	0.000000765	0.000002457
C	0.000000125	0.000001343	-0.000000498
H	-0.000000266	0.000000504	0.000001125
H	-0.000000167	0.000000827	0.000001513
H	0.000000262	-0.000000037	0.000000042
C	-0.000000998	-0.000000396	-0.000000680
H	-0.000000011	0.000001011	-0.000000442
H	0.000000736	0.000000647	-0.000000483
H	-0.000000375	-0.000000276	-0.000000800
C	-0.000001871	-0.000000567	-0.000000752
H	0.000000950	-0.000000317	0.000000359
H	0.000000114	0.000000787	0.000000017
H	0.000000991	0.000000255	-0.000000869
C	-0.000000953	-0.000000599	-0.000000089
H	-0.000000181	0.000000143	0.000000686
H	-0.000000592	-0.000001249	0.000000525
H	0.000000966	-0.000000080	0.000000322
C	-0.000001023	0.000003539	-0.000003852
H	-0.000000632	0.000000819	-0.000001214
H	-0.000000164	0.000001494	-0.000000028
H	-0.000000380	0.000000425	-0.000000258
C	-0.000003108	-0.000000390	-0.000000068
H	0.000000028	-0.000001030	0.000001026
H	0.000000736	0.000001143	0.000001189
H	0.000000975	-0.000002995	0.000002300
C	0.000003447	0.000003009	-0.000003181
H	-0.000000063	0.000000001	-0.000001739
H	-0.000000137	0.000001343	-0.000000275
H	-0.000000281	-0.000001549	-0.000002242
C	0.000001696	0.000001920	-0.000006271
H	-0.000000704	-0.000000887	0.000002362

H	-0.000000205	0.000001344	0.000001840
H	0.000000169	-0.000000404	0.000001963
H	0.000000730	0.000000135	0.000001377
H	-0.000000558	-0.000008154	-0.000000953
H	-0.000000856	0.000009973	0.000000494

[(HPNP)CoH$_3$ (singlet)
E (a.u.) = -2753.444041
ZPE (a.u.) = 0.537061

Co	-0.000002970	-0.000008043	0.000000699
P	0.000003045	0.000002241	0.000008448
P	0.000002893	0.000002452	-0.000007604
N	-0.000003490	0.000010663	0.000000184
H	0.000000929	0.000000764	0.000001841
C	-0.000001007	0.000000663	-0.000004336
H	0.000000094	0.000001416	-0.000001233
C	0.000000754	-0.000001228	0.000003099
H	0.000001008	0.000002495	-0.000000380
H	0.000001517	0.000000696	0.000000054
C	-0.000000761	-0.000000116	0.000002530
H	-0.000000336	-0.000000506	-0.000001612
H	0.000000787	-0.000000982	-0.000000748
C	0.000000630	0.000000568	0.000002460
H	0.000000384	-0.000002007	-0.000000736
C	0.000000216	0.000002393	0.000000542
H	-0.000000766	0.000001561	0.000000087
H	0.000000842	0.000000449	-0.000000672
H	-0.000003154	0.000001267	-0.000000730
C	-0.000001579	0.000000693	-0.000003142
H	0.000001216	-0.000000117	0.000000154
H	0.000000674	-0.000003019	0.000001320
H	0.000000249	0.000000588	0.000000267
C	0.000002044	0.000002695	-0.000001606
H	0.000001012	-0.000001522	0.000000609
H	0.000001182	-0.000000171	0.000001564
C	0.000000332	-0.000003995	0.000000050
H	0.000000626	0.000000800	0.000001593
H	0.000002124	-0.000000563	0.000001219
C	-0.000001451	-0.000002601	-0.000000017
H	-0.000000114	-0.000000399	0.000000248
C	-0.000000292	0.000003419	0.000004746
H	-0.000000905	0.000001078	-0.000002429
H	-0.000001403	0.000001936	0.000001086
H	0.000002347	0.000000189	-0.000002241
C	-0.000000700	-0.000000361	-0.000003021
H	-0.000000303	0.000000518	0.000000312
H	0.000000253	0.000000621	0.000000536
H	0.000000861	0.000000322	0.000000839
C	0.000000608	0.000000321	0.000000087
H	-0.000001044	-0.000002233	0.000000356
H	0.000001551	-0.000001564	-0.000001061
H	-0.000001426	-0.000002830	0.000001164
C	0.000002666	-0.000005760	0.000001195
H	-0.000003148	0.000000945	0.000001553
H	-0.000000954	-0.000000969	-0.000001631
H	0.000000939	0.000000902	-0.000000339
C	0.000001745	-0.000000754	0.000000771
H	-0.000000119	-0.000000585	-0.000001246
H	0.000000319	0.000001663	0.000000555
H	-0.000000677	0.000000390	-0.000000802
C	-0.000001364	-0.000001149	0.000001063
H	-0.000001182	-0.000000941	-0.000000718
H	-0.000000951	-0.000001655	-0.000002645
H	-0.000000293	-0.000001656	-0.000000745
C	-0.000003563	0.000002590	-0.000005667
H	-0.000000105	0.000000772	0.000001244
H	-0.000000892	-0.000001273	0.000003034
H	-0.000000662	-0.000006492	0.000002639
H	0.000001764	0.000005422	-0.000002784

[(HPNP)CoCl (triplet)
E (a.u.) = -3211.962882
ZPE (a.u.) = 0.514200

Co	0.000006010	0.000001527	0.000013229
P	-0.000002812	-0.000001949	-0.000001318
Cl	-0.000001933	-0.000001119	-0.000003952
P	0.000003265	0.000002416	-0.000005230
N	-0.000001002	-0.000001345	0.000000413
H	0.000002019	0.000000807	-0.000002548
C	0.000001813	0.000001014	0.000000041
H	0.000000846	-0.000001865	0.000003026
H	0.000000302	-0.000001692	0.000000786
C	0.000004461	0.000004014	-0.000001526
H	-0.000001725	-0.000000485	0.000000353

C	0.000002480	0.000001560	-0.000003526
H	0.000002292	-0.000001133	-0.000001458
H	0.000002206	-0.000000965	-0.000000958
C	0.000000838	-0.000002874	-0.000002016
H	0.000001301	-0.000000480	0.000000371
H	0.000002365	-0.000001604	0.000000579
C	-0.000002593	-0.000000725	-0.000003596
H	0.000001038	0.000002795	-0.000002651
C	-0.000001340	-0.000005080	-0.000001328
H	0.000001010	0.000000000	0.000000314
H	0.000000420	0.000000614	-0.000002185
C	-0.000004350	-0.000002159	0.000002892
H	0.000001122	0.000000406	0.000001080
C	0.000003288	-0.000000081	0.000001802
H	0.000000137	-0.000000323	0.000003224
C	-0.000000358	-0.000002754	0.000003936
H	-0.000001290	0.000001402	-0.000000594
H	-0.000001525	0.000000885	0.000000157
H	-0.000001413	0.000001324	-0.000001049
C	0.000000922	0.000002513	-0.000001739
H	-0.000001704	0.000000076	0.000001831
H	0.000001579	-0.000001508	0.000001089
H	-0.000000859	0.000000967	0.000001274
C	-0.000004918	-0.000001558	-0.000001786
H	0.000000264	0.000000729	-0.000000120
H	-0.000000300	0.000000434	-0.000001981
H	0.000000870	0.000000005	-0.000001205
C	0.000002945	-0.000001670	-0.000000395
H	-0.000000960	0.000000019	0.000002239
H	-0.000001535	-0.000000294	0.000003370
H	0.000001013	-0.000001638	0.000002552
C	-0.000002733	0.000000426	-0.000001336
H	-0.000000412	0.000001663	-0.000002942
H	-0.000001376	0.000002874	-0.000001826
H	-0.000000678	0.000001662	-0.000002001
C	-0.000004272	-0.000002579	0.000000385
H	0.000000065	0.000000388	0.000002503
H	0.000000256	0.000000388	0.000001166
H	0.000001159	-0.000000217	0.000002597
C	-0.000000116	0.000003069	-0.000002805
H	-0.000000132	0.000000140	-0.000003734
H	-0.000000007	0.000000101	-0.000003287
H	0.000000425	-0.000000031	-0.000002249
C	-0.000001637	0.000000178	0.000004562
H	-0.000001604	0.000000824	0.000002179
H	-0.000001889	0.000000467	0.000001423
H	-0.000001241	0.000000444	0.000001966

[(HPNP)CoCl(H)$_2$ (singlet)

E (a.u.) = -3213.125691

ZPE (a.u.) = 0.532286

Co	-0.000047194	-0.000078972	-0.000068351
P	-0.000012420	0.000032851	0.000008988
Cl	-0.000003756	0.000007117	0.000003087
P	0.000002675	0.000024984	0.000009592
N	0.000017164	-0.000004327	0.000036591
H	0.000002312	0.000004521	-0.000003268
C	-0.000003002	-0.000001129	-0.000008149
H	-0.000000975	-0.000001436	0.000004053
H	-0.000000652	-0.000003684	0.000000825
C	-0.000000146	0.000003894	0.000004678
H	-0.000002014	-0.000003529	0.000000764
H	-0.000000659	-0.000002937	0.000001031
C	-0.000003683	0.000002998	-0.000003343
H	-0.000001569	-0.000000551	0.000001950
H	0.000003206	-0.000002936	0.000002372
C	0.000002325	0.000011318	-0.000001293
H	-0.000001734	-0.000002548	-0.000001405
C	-0.000013486	0.000008727	0.000000255
H	0.000002045	-0.000003239	0.000003259
C	0.000009876	-0.000001838	-0.000000500
H	0.000000381	-0.000002733	-0.000000011
H	-0.000004357	-0.000001935	0.000003078
C	0.000005866	0.000003329	0.000007077
H	-0.000003338	-0.000003166	-0.000001027
C	-0.000001938	0.000003828	-0.000003293
H	-0.000001253	0.000001685	0.000002260
H	0.000000622	0.000002739	0.000001186
H	0.000000533	0.000002609	0.000000046
C	-0.000002643	0.000008032	-0.000000908
H	0.000003234	-0.000002433	0.000001364
C	0.000004016	0.000000420	0.000005837
H	-0.000002225	0.000000434	0.000000574
H	-0.000000713	-0.000000570	-0.000000621

H	-0.000001007	0.000001739	0.000000256
C	0.000003356	-0.000002109	-0.000003479
H	0.000001488	0.000001595	-0.000002600
H	0.000000787	0.000001597	-0.000001510
H	0.000000823	0.000000961	-0.000002035
C	-0.000007083	0.000000650	-0.000002142
H	-0.000000017	0.000001730	0.000000320
H	0.000000112	-0.000000520	0.000000965
H	0.000000086	0.000000809	0.000002678
C	0.000003998	0.000003666	0.000000715
H	-0.000000570	0.000002436	-0.000000383
H	-0.000001570	0.000002411	-0.000000376
H	-0.000002195	0.000001871	0.000001819
C	-0.000002088	-0.000003490	0.000002119
H	0.000001387	-0.000001371	-0.000001705
H	0.000000772	-0.000002171	-0.000003086
H	0.000003441	-0.000000581	-0.000001849
C	-0.000002129	-0.000004801	0.000001947
H	0.000001035	-0.000000447	-0.000003265
H	0.000001895	-0.000002485	-0.000001539
H	0.000001464	-0.000000464	-0.000001705
C	0.000004028	-0.000002145	-0.000003834
H	0.000000545	0.000000800	-0.000002019
H	0.000001582	0.000002004	-0.000001002
H	0.000001211	0.000001716	-0.000002703
H	0.000030079	0.000000944	0.000036136
H	0.000012072	-0.000005866	-0.000018424

[(HPNP)CoCl(H)SiH$_2$Ph (singlet)

E (a.u.) = -3734.794851

ZPE (a.u.) = 0.634012

P	-0.000002124	0.000002439	-0.000007352
P	-0.000002070	0.000001719	-0.000004878
Cl	0.000000262	-0.000001923	0.000000508
H	-0.000000648	-0.000001384	0.000001206
H	0.000000006	0.000002386	0.000001792
N	-0.000018463	0.000000075	0.000006088
H	0.000003100	-0.000005226	-0.000003140
C	0.000000572	-0.000000609	-0.000000162
H	-0.000001028	0.000001049	-0.000000090
C	-0.000000618	-0.000000123	-0.000001393
H	0.000000816	-0.000000365	-0.000001203
H	0.000000094	-0.000000825	-0.000001230
C	-0.000001944	0.000003050	0.000001833
H	-0.000000042	0.000001223	-0.000001093
H	-0.000001189	0.000001429	-0.000000906
H	-0.000000704	-0.000000301	-0.000000915
C	0.000000161	-0.000000746	-0.000001236
H	-0.000000599	0.000000172	-0.000001845
H	0.000000607	-0.000000141	-0.000001478
C	-0.000000742	0.000001828	0.000000278
H	-0.000000989	0.000000810	-0.000000431
H	0.000000052	0.000000044	-0.000000130
H	-0.000000027	-0.000000346	-0.000000766
C	-0.000001579	0.000001096	-0.000000010
H	-0.000000769	0.000000889	-0.000001133
H	-0.000000911	0.000001194	-0.000000561
H	-0.000001374	0.000001284	-0.000000682
C	0.000000593	-0.000002294	-0.000002263
H	0.000000516	-0.000000917	0.000001139
C	0.000002218	-0.000001416	-0.000000338
H	-0.000000504	-0.000000994	0.000001960
H	-0.000000393	0.000000381	0.000000360
H	0.000000501	0.000000217	0.000001433
C	0.000002098	0.000001654	0.000000569
H	0.000000815	-0.000001066	0.000000294
H	0.000000845	-0.000001283	-0.000000857
H	-0.000000486	-0.000001324	-0.000001146
C	-0.000002883	0.000000621	0.000001772
H	0.000000690	-0.000000854	-0.000000976
C	-0.000000171	0.000000269	-0.000000104
H	0.000000215	0.000000021	-0.000000642
H	0.000001327	-0.000000825	-0.000000866
H	0.000000832	-0.000001011	0.000000514
C	-0.000002180	-0.000000401	-0.000000475
H	-0.000000297	0.000000629	0.000000259
H	-0.000000650	0.000001175	-0.000000659
H	-0.000000133	0.000000688	-0.000000898
C	0.000001344	0.000000792	-0.000002865
H	-0.000001660	0.000000719	0.000000903
C	0.000000572	-0.000001469	0.000002642
H	-0.000000074	-0.000000721	0.000000961
H	-0.000000715	0.000000527	0.000000604
H	0.000001579	0.000000482	-0.000000381

C	0.000006541	0.000000764	-0.000004294
H	0.000000357	-0.000001331	-0.000001222
H	-0.000000617	0.000000779	-0.000000026
C	0.000000817	0.000000670	-0.000006468
H	-0.000000604	0.000001194	-0.000000798
H	-0.000000045	-0.000000191	-0.000002043
C	0.000000242	-0.000000659	0.000002108
C	-0.000000027	-0.000000382	0.000001798
C	0.000000724	0.000000236	0.000001453
C	0.000000389	0.000000177	0.000002657
H	-0.000000717	0.000000275	0.000002168
C	0.000000962	-0.000001069	0.000002019
H	0.000000580	-0.000001481	0.000001001
C	0.000000534	-0.000000744	0.000002612
H	0.000000020	-0.000000173	0.000003120
H	0.000001214	-0.000001296	0.000001942
H	0.000000943	-0.000000971	0.000003104
Si	-0.000009726	-0.000007341	-0.000000900
Co	0.000025881	0.000009631	0.000010484
H	-0.000001315	-0.000000385	-0.000000726

TPSS

H2

E (a.u.) = -1.168293
ZPE (a.u.) = 0.010182

H	0.000000290	0.000000000	0.000000000
H	-0.000000290	0.000000000	0.000000000

$[(P^{Me}NP^{Me})Co]_2$ (singlet)

E (a.u.) = -4873.910549
ZPE (a.u.) = 0.539323

Co	0.000005300	0.000003563	0.000013376
Co	0.000022937	-0.000005029	0.000014893
P	0.000008239	0.000011918	-0.000003372
P	-0.000001427	0.000007034	-0.000007326
P	-0.000020738	0.000003301	-0.000002657
P	-0.000005723	-0.000004061	-0.000009614
N	-0.000017680	-0.000002503	-0.000010809
N	-0.000014390	-0.000006350	-0.000028666
C	0.000002112	0.000003031	0.000000692
H	0.000000990	0.000002844	-0.000000936
H	-0.000000648	0.000002165	-0.000000277
C	-0.000005251	0.000002184	-0.000011708
H	0.000002248	0.000000736	0.000000912
H	0.000003953	-0.000003638	0.000000864
C	-0.000001022	-0.000002855	0.000002860
H	0.000000531	-0.000002462	0.000001028
H	-0.000000303	-0.000002378	-0.000001282
C	-0.000004403	-0.000007873	-0.000004092
H	0.000006387	-0.000001391	-0.000001820
C	0.000010042	-0.000001847	0.000011862
H	-0.000000838	-0.000001998	0.000000531
H	-0.000003007	-0.000003989	0.000000296
C	0.000008466	0.000004241	0.000006444
H	0.000000619	0.000002705	-0.000001420
H	0.000001029	0.000002656	-0.000002754
C	-0.000004507	-0.000009300	0.000006237
H	-0.000000858	0.000002485	-0.000003089
C	0.000006095	-0.000003289	-0.000003768
H	0.000001489	-0.000002036	0.000001356
C	-0.000003508	-0.000001704	0.000004143
H	-0.000002502	0.000001706	0.000002482
C	-0.000000392	0.000001149	0.000015297
H	-0.000002419	-0.000002557	0.000000390
H	0.000000003	-0.000002858	-0.000000894
C	0.000003706	-0.000005463	0.000000591
H	0.000002963	-0.000002499	-0.000002081
C	-0.000008088	-0.000004535	-0.000003456
H	0.000000381	0.000000395	0.000002066
H	-0.000001766	0.000002083	0.000001965
C	0.000011162	0.000002646	0.000001825
H	0.000000566	0.000001206	-0.000002227
H	-0.000000326	0.000002456	-0.000000291
C	0.000002038	0.000002971	0.000006583
H	-0.000001270	0.000000546	0.000002173
C	-0.000000984	0.000006113	0.000000146
H	-0.000000277	0.000003342	0.000003237
H	-0.000001635	0.000001374	0.000000790
H	-0.000002044	0.000004956	0.000000557
C	-0.000003786	0.000004520	0.000002564
H	-0.000000187	0.000002497	0.000001319
H	-0.000003121	0.000002817	0.000002636
H	-0.000001929	0.000001055	0.000000625

H	0.000000211	0.000000156	0.000000960
H	-0.000003449	-0.000001259	0.000003109
H	-0.000001320	0.000001689	0.000000633
H	-0.000001986	0.000000157	-0.000001541
H	0.000002630	-0.000000609	-0.000001384
H	0.000003084	-0.000001550	-0.000000138
H	0.000004793	0.000000914	-0.000003661
H	0.000004863	-0.000000856	-0.000002056
H	0.000000357	-0.000000076	-0.000000157
H	0.000000925	-0.000000783	-0.000002205
H	0.000002270	-0.000003556	-0.000001275
H	0.000001399	-0.000004306	-0.000000488

[($P^{Me}NP^{Me}$)Co]$_2$ (triplet)
E (a.u.) = -4873.907484
ZPE (a.u.) = 0.538573

Co	0.000010580	-0.000009071	-0.000018525
Co	-0.000004911	0.000003962	0.000004543
P	0.000006348	0.000000229	0.000003710
P	-0.000002938	0.000003572	0.000002229
P	-0.000004821	0.000000191	-0.000003938
P	0.000000054	0.000002962	-0.000009924
N	-0.000006635	-0.000002638	0.000009275
N	-0.000003402	0.000000677	0.000002957
C	-0.000001855	-0.000002126	0.000002185
H	-0.000000016	-0.000002116	0.000000235
H	0.000000131	-0.000002274	0.000000419
C	0.000000380	0.000000067	0.000002006
H	-0.000002139	-0.000001997	0.000000594
H	-0.000000804	-0.000001454	0.000000275
C	0.000001517	0.000001851	-0.000001579
H	0.000000278	0.000001938	-0.000000529
H	-0.000000558	0.000001928	-0.000000253
C	-0.000006026	-0.000000116	0.000000350
H	0.000000271	-0.000001094	0.000002744
C	-0.000000757	0.000000636	0.000002382
H	0.000001133	0.000000726	-0.000001485
H	0.000000159	0.000000657	0.000000018
C	0.000001343	0.000003750	-0.000000929
H	-0.000000536	-0.000002063	0.000001286
H	0.000000113	-0.000001305	-0.000000676
C	-0.000000809	-0.000000780	0.000001535
H	-0.000000500	0.000002016	-0.000001007
C	-0.000001904	-0.000000878	-0.000000271
H	-0.000001584	0.000002120	0.000001665
C	0.000001268	0.000001060	0.000004310
H	0.000001999	-0.000000901	-0.000002089
C	0.000006692	-0.000000089	-0.000001819
H	0.000001412	0.000001962	-0.000001064
H	-0.000000336	0.000002154	0.000000155
C	-0.000002753	0.000005532	0.000002986
H	-0.000002136	0.000002360	0.000001724
C	-0.000002168	-0.000000337	-0.000002126
H	0.000003099	0.000000735	-0.000002061
H	0.000000177	0.000002508	0.000000597
C	0.000000023	0.000000512	0.000000404
H	-0.000000968	-0.000001177	0.000001500
H	-0.000000930	-0.000002079	0.000001542
C	0.000003573	0.000000166	-0.000001388
H	0.000001069	-0.000000416	0.000001405
C	0.000001410	-0.000005422	-0.000000332
H	0.000002361	-0.000002784	-0.000001088
H	0.000001081	-0.000003307	0.000000436
H	0.000001304	-0.000002887	0.000000091
C	0.000000188	-0.000001398	-0.000001711
H	0.000001315	-0.000001150	-0.000000695
H	0.000001837	0.000000666	-0.000001342
H	0.000002279	-0.000000881	-0.000001241
H	0.000000664	-0.000001464	-0.000001293
H	0.000002037	-0.000002599	-0.000001255
H	0.000000881	-0.000001416	-0.000000900
H	0.000001443	-0.000000623	-0.000002036
H	-0.000000798	-0.000000106	0.000001385
H	-0.000001786	0.000001265	-0.000000439
H	-0.000001818	0.000000759	0.000001862
H	-0.000001304	0.000001560	0.000001800
H	-0.000001060	0.000000670	0.000001208
H	-0.000002085	0.000001542	0.000001249
H	0.000000779	0.000003699	0.000000214
H	-0.000000863	0.000002519	0.000000719

[($P^{Me}NP^{Me}$)Co]$_2$ (quintuplet)
E (a.u.) = -4873.885742
ZPE (a.u.) = 0.536445

Co	-0.000006603	0.000004226	0.000001934
Co	-0.000011246	0.000019356	-0.000017842
P	0.000000562	-0.000014645	-0.000010136
P	0.000004111	0.000013472	0.000006069
P	0.000014178	-0.000014490	0.000004744
P	0.000004011	0.000004677	0.000015437
N	0.000007265	-0.000004891	-0.000007523
N	-0.000015247	-0.000015509	0.000009042
C	0.000001259	-0.000006447	-0.000000690
H	-0.000000666	-0.000001140	-0.000000210
H	-0.000001020	-0.000000461	-0.000001452
C	-0.000000970	-0.000000209	0.000005503
H	-0.000001761	-0.000000057	0.000000180
H	-0.000002275	-0.000001007	0.000000214
C	0.000001473	0.000008729	0.000000387
H	0.000001567	0.000000913	0.000000172
H	0.000001038	-0.000001609	-0.000000454
C	-0.000000973	0.000004565	0.000006806
H	-0.000006973	0.000000914	-0.000002117
C	0.000001347	0.000004464	-0.000003968
H	0.000002679	-0.000000823	-0.000000770
H	0.000003585	-0.000000590	0.000000577
C	-0.000001912	0.000001196	-0.000005605
H	0.000000228	-0.000002896	0.000000745
H	0.000001517	0.000000254	0.000001376
C	0.000005610	0.000007457	0.000001493
H	-0.000002057	-0.000002031	0.000002544
C	0.000000001	0.000006294	0.000005290
H	0.000000197	0.000000569	-0.000002204
C	0.000000493	-0.000004468	-0.000008036
H	0.000002892	0.000001612	-0.000000128
C	0.000004725	-0.000001868	-0.000001595
H	0.000001978	0.000003538	0.000000465
H	-0.000001777	0.000000920	0.000002400
C	-0.000000569	0.000001443	0.000000562
H	-0.000000700	0.000002831	0.000001691
C	0.000004888	0.000007539	-0.000003264
H	0.000000602	-0.000000292	0.000002259
H	-0.000000867	-0.000003655	-0.000000879
C	-0.000003719	0.000004247	0.000004657
H	-0.000000303	-0.000003452	0.000000329
H	-0.000001072	-0.000001568	-0.000002384
C	-0.000005157	-0.000009474	0.000003921
H	0.000000245	0.000003853	0.000001303
C	-0.000004345	-0.000003547	-0.000004073
H	0.000001685	-0.000002178	-0.000002033
H	0.000000292	-0.000003469	-0.000002538
H	-0.000001378	-0.000002032	-0.000001523
C	0.000007143	0.000002119	-0.000000446
H	0.000000528	-0.000002308	-0.000002514
H	0.000001099	-0.000001590	-0.000000661
H	0.000001677	-0.000002032	-0.000002190
H	0.000001419	-0.000001820	-0.000002007
H	0.000001750	-0.000000157	-0.000000133
H	-0.000001567	-0.000000272	-0.000000536
H	-0.000000683	0.000000730	-0.000000014
H	-0.000003964	0.000001137	0.000000730
H	-0.000001718	0.000001109	0.000002416
H	-0.000002372	-0.000001520	0.000001641
H	-0.000002055	0.000002132	0.000001145
H	0.000000433	-0.000000968	0.000000106
H	0.000000202	-0.000000810	0.000000504
H	0.000000360	0.000001672	0.000000818
H	0.000000910	0.000002318	0.000000471

[($P^{Me}NP^{Me}$)CoH]$_2$ (triplet)

E (a.u.) = -4875.064671

ZPE (a.u.) = 0.554572

Co	0.000025194	-0.000033119	-0.000003145
Co	-0.000028739	0.000034216	0.000003743
P	-0.000006397	-0.000008205	0.000006369
P	0.000006568	0.000000452	0.000012963
P	0.000005341	0.000007505	0.000005777
P	-0.000003868	-0.000000070	0.000011165
N	0.000002408	0.000000067	0.000010662
N	0.000000897	-0.000000705	-0.000018132
C	0.000004770	0.000000329	-0.000003765
H	0.000000210	-0.000001577	-0.000000291
C	-0.000001248	-0.000005287	-0.000018442
H	0.000003520	0.000002500	0.000004579
H	-0.000000090	0.000002316	0.000001809

C	0.000003308	0.000004279	-0.000020804	H	-0.000003282	0.000003521	-0.000000559
H	-0.000003516	-0.000002917	0.000003496	H	0.000002706	-0.000003221	-0.000000136
H	0.000000300	-0.000002420	0.000003237	H	0.000001742	-0.000003323	0.000000898
C	-0.000005658	0.000000433	-0.000000696	H	0.000004326	-0.000005214	0.000000442
H	0.000005353	0.000000489	-0.000002077	H	0.000003332	-0.000002255	0.000001141
C	-0.000009337	0.000001701	-0.000006169	H	-0.000001073	-0.000003392	0.000000397
H	0.000001992	-0.000006359	0.000000707	H	-0.000004060	-0.000002680	0.000000565
C	0.000000599	0.000002499	-0.000000035	H	0.000002939	-0.000003365	-0.000000226
H	-0.000001932	-0.000005358	-0.000000217	H	-0.000002314	-0.000005832	-0.000000800
C	0.000008331	0.000002920	0.000014758	H	-0.000025589	0.000012488	-0.000005158
H	-0.000002079	0.000000915	-0.000004862	H	0.000026966	-0.000010069	-0.000003895
H	-0.000004211	0.000000281	-0.000003414				
C	-0.000004532	-0.000000832	-0.000003677				
H	-0.000002482	0.000003161	-0.000000203				
C	-0.000008688	-0.000004004	0.000013601				
H	0.000002763	-0.000001038	-0.000005204				
H	0.000004139	-0.000000196	-0.000003339				
C	0.000009901	-0.000002138	-0.000006594				
H	0.000002206	0.000005779	-0.000001010				
C	-0.000001163	-0.000002879	0.000000208				
H	0.000004130	0.000002514	0.000000404				
C	-0.000010952	-0.000004229	0.000003294				
H	0.000006508	-0.000001697	0.000000615				
H	0.000004441	0.000004301	0.000002937				
C	0.000007631	0.000003590	0.000005992				
H	-0.000007613	0.000001115	0.000001366				
H	-0.000005385	-0.000002912	0.000004293				
C	-0.000010141	0.000002917	-0.000001447				
H	0.000000553	-0.000002580	-0.000002331				
H	-0.000001807	-0.000003946	0.000002038				
C	0.000005422	-0.000000174	-0.000000787				
H	-0.000003397	0.000002301	0.000001267				
C	0.000010370	-0.000001761	-0.000001129				
H	0.000000004	0.000002924	-0.000002255				
H	0.000001600	0.000003990	0.000001907				
H	-0.000001864	0.000003420	0.000000918				
H	-0.000000232	0.000001603	-0.000000340				
H	-0.000005786	-0.000000660	-0.000001735				
H	-0.000004234	0.000004917	0.000000691				
H	0.000001966	0.000005332	-0.000000301				
H	0.000001045	0.000003469	0.000000263				
H	-0.000001815	0.000006167	0.000000672				